

**NOVEL PROCESS DESIGNS TO IMPROVE THE EFFICIENCY  
OF POSTCOMBUSTION CARBON DIOXIDE CAPTURE**

**Eva Sanchez Fernandez**



# **NOVEL PROCESS DESIGNS TO IMPROVE THE EFFICIENCY OF POSTCOMBUSTION CARBON DIOXIDE CAPTURE**

## **PROEFSCHRIFT**

ter verkrijging van de graad van doctor  
aan de Technische Universiteit Delft,  
op gezag van de Rector Magnificus Prof.ir. K.C.A.M. Luyben  
voorzitter van het College voor Promoties,  
in het openbaar te verdedigen op 3 december 2013 om 15:00 uur

door

**Eva Sanchez Fernandez**

Ingeniero Químico, Universidad Complutense de Madrid

geboren te Madrid, Spain

Dit proefschrift is goedgekeurd door de promotor:

Prof. Dr. Ir. T. J.H. Vlugt

Samenstelling promotiecommissie:

Rector Magnificus	Voorzitter
Prof. Dr. Ir. T.J.H. Vlugt	Technische Universiteit Delft, promotor
Prof. Dr. S. Calero	U-Pablo de Olavide
Prof. Dr. H.F. Svendsen	NTNU, Noorwegen
Prof. Dr. S.H. Kjelstrup	Technische Universiteit Delft
Prof. Dr. Ir. A.H.M. Verkooijen	Technische Universiteit Delft
Dr. K. Damen	Nuon Energy
Dr. Ir. E.L.V. Goetheer	TNO Science and Industry

Dr. Ir. E. Goetheer heeft als begeleider in belangrijke mate aan de totstandkoming van het proefschrift bijgedragen.

Dit onderzoek werd financieel ondersteund door Nederlandse Organisatie voor Toegepast Natuurwetenschappelijk Onderzoek (TNO, Department Gas Treatment). Dit werk is mede uitgevoerd binnen Europese (CESAR) en nationale projecten (CATO-2).

Copyright © 2013 by E. Sanchez Fernandez

ISBN 978-94-6186-236-5

Printed by Ipskamp Drukkers BV

All rights reserved. NO part of the material protected by this copyright notice may be reproduced or utilised in any form or by means, electronic or mechanical, including photocopy, recording or by any information storage and retrieval system, without written permission from the publisher.

# Contents

---

<b>1</b>	<b>Introduction</b>	<b>1</b>
1.1	Carbon Capture and Storage: An option to mitigate global climate change	2
1.2	Post-Combustion Capture: Overview of technologies based on absorption	5
1.3	Precipitating systems with amino acid salts	7
1.4	Scope and organisation of this thesis	9
<b>2</b>	<b>Emissions of substances other than CO<sub>2</sub> from power plants with CCS technologies</b>	<b>11</b>
2.1	Introduction	12
2.2	Literature review	13
2.3	Reference cases description	16
2.4	Methodology	18
2.5	Results	20
2.6	Discussion	27
2.7	Conclusions	31
<b>3</b>	<b>Thermodynamic assessment of novel amine based CO<sub>2</sub> capture technologies in power plants based on EBTF methodology</b>	<b>33</b>
3.1	Introduction	34
3.2	Plant description of the selected reference cases (ASC PC and NGCC)	35
3.3	Capture plant description of the selected reference cases (MEA and AMP/PZ)	36
3.4	Methodology	41
3.5	Results and discussion	42
3.6	Conclusions	47
<b>4</b>	<b>Economic assessment of novel amine based CO<sub>2</sub> capture technologies in power plants based on EBTF methodology</b>	<b>49</b>
4.1	Introduction	50
4.2	The economic assessment methodology	51
4.3	Total cost assessment of ASC PC and NGCC power plants with CO <sub>2</sub> capture based on MEA and AMP/PZ	54
4.4	Economic assessment and sensitivity analysis of the selected case studies	63
4.5	Conclusions	68

<b>5</b>	<b>Optimisation of lean vapour compression based on net present value maximisation</b>	<b>71</b>
5.1	Introduction	72
5.2	Methodology	73
5.3	Results	78
5.4	Discussion	83
5.5	Conclusions	84
<b>6</b>	<b>Novel CO<sub>2</sub> capture process based on precipitating amino acid solvents</b>	<b>85</b>
6.1	Introduction	86
6.2	Conceptual process design	87
6.3	Solvent properties	92
6.4	Model development	98
6.5	Results and Discussion	99
6.6	Conclusions	105
<b>7</b>	<b>Analysis of process configurations for carbon dioxide capture by precipitating amino acid solvents</b>	<b>107</b>
7.1	Introduction	108
7.2	Baseline configuration (DECAB and DECAB Plus)	109
7.3	Alternative process configurations for DECAB and DECAB Plus	111
7.4	Model development	115
7.5	Results and Discussion	119
7.6	Conclusions	130
<b>8</b>	<b>The potential of precipitating amino acids for CO<sub>2</sub> capture</b>	<b>131</b>
8.1	Introduction	132
8.2	Potential of amino acid salts as solvents for CO <sub>2</sub> capture	133
8.3	Risks associated with precipitating amino acid solvent processes	137
8.4	Alternative process concepts	142
8.5	Future research	143
<b>9</b>	<b>Appendix</b>	<b>145</b>
9.1	EBTF summary of assumptions	146
9.2	Emission factors for air pollutants based on primary energy	149
9.3	Experimental data and procedures	152
9.4	VLEMS model basic calculations	166

<b>Nomenclature</b>	<b>171</b>
<b>References</b>	<b>176</b>
<b>Summary</b>	<b>191</b>
<b>Samenvatting</b>	<b>195</b>
<b>Acknowledgements</b>	<b>199</b>
<b>Curriculum Vitae</b>	<b>200</b>



---

## INTRODUCTION

### **ABSTRACT**

*The term carbon dioxide capture and storage (CCS) refers to a range of technologies that can reduce CO<sub>2</sub> emissions from fossil fuels enabling the continued use of this fuel type without compromising the security of electricity supply. The technologies applicable to CCS differ in many key aspects; the stage of the electricity generation process at which the CO<sub>2</sub> is captured, the CO<sub>2</sub> capture process, efficiency, availability and maturity of the technology. The integration of these technologies into power plants results in a reduction in power generation efficiency, which remains one of the major issues for the commercial implementation of CCS. Among the possible technologies, the focus of this thesis is on post-combustion capture as it is a known technology, is readily available and it can be retrofitted to existing power plants. This thesis is concerned with the development of new carbon capture processes that require less energy for CO<sub>2</sub> separation and are, at the same time, more environmentally friendly.*

*Prior to the development of any new process, the current state of the art needs to be analysed and updated in order to set realistic targets for the new technology and benchmark the potential of the newly developed processes. Therefore, part of the work of this thesis is a thorough benchmarking exercise in which updated baselines for the performance of conventional post-combustion capture processes are given.*

*The new process concepts developed in this thesis are based on the combination of enhanced absorption and enhanced desorption, two effects encountered in capture processes that are based on precipitating amino acid solvents. For this purpose, the conceptual design methodology has been followed with a specific target of energy reduction set to (at least) 30% of a conventional MEA process.*

## 1.1 Carbon Capture and Storage: An option to mitigate global climate change

The mitigation of CO<sub>2</sub> emissions is a matter of urgency and concern worldwide since it has been linked to global warming and climate change [1, 2]. The energy generation sector, from which 85% of the overall world energy usage depends on fossil fuels, accounts for 41% of global carbon emissions [3]. Although there is significant concern about the increasing amount of CO<sub>2</sub> that will be emitted, fossil fuels are foreseen to remain the dominant energy source for the largest part of the 21<sup>st</sup> century [4]. CO<sub>2</sub> emissions from fossil fuels are directly linked to the efficiency of energy conversion. This efficiency is improving with the development of advanced combustion and gasification technologies [5-8]. However, the potential improvements are not sufficient to abate CO<sub>2</sub> emissions drastically. On the other hand, alternative or renewable energy sources still have fundamental hurdles to overcome, such as providing sufficient amounts of base-load electricity generation, in order to displace fossil-fuel power.

The term Carbon dioxide Capture and Storage (CCS) refers to a range of technologies that can reduce CO<sub>2</sub> emissions from fossil fuels in order to bridge the gap presented by switching from our current fossil-fuel dependency to a low-carbon energy generation. For instance, a recent study states that the application of CCS technologies in Europe could abate 47% of total European CO<sub>2</sub> emissions (2 Gt CO<sub>2</sub> in 2007) by 2030 [4]. Therefore, applying CCS is considered a promising strategy to reduce CO<sub>2</sub> emissions while enabling the continued use of fossil fuels and without compromising the security of electricity supply. Within the European Union, it is foreseen that CCS will be implemented, along with high use of renewable energy, in order to achieve the long term target of greenhouse gas emissions reduction of 80-95% by 2050 [9].

CCS requires the formation of a pure CO<sub>2</sub> stream (CO<sub>2</sub> separation), transportation and long term storage in deep reservoirs underground. The characteristics of each of these steps and interconnections between them can be found in reference books [10-12]. The multiple technology options applicable to CCS have also been extensively documented in technical and economical reviews [13-15]. The technology options, illustrated in Figure 1.1, are generally grouped under three different capture strategies: post-combustion capture, pre-combustion capture and oxyfuel combustion.

Post-combustion capture (PCC) refers to the partial removal of CO<sub>2</sub> from flue gases produced by combustion of fossil fuels in boilers (in the case of coal fired stations) or in gas turbines (in the case of gas fired stations). The books by Woodhead Publishing Ltd [11] and Rackley [10] present a concise overview of the technology options for PCC. Their future implementation is related to efficiency and state of technology development. The reviews of Wang [16] and Olajire [17] summarise the options, developments and progress in PCC. Absorption processes with chemical solvents are currently the most used technology. These processes are efficient compared to other PCC processes, have been proven at commercial stage for CO<sub>2</sub> separation from natural gas and offer the possibility to retrofit existing coal power plants without severe modifications in their configuration. Other post combustion capture processes that are under development are based on membrane separation [18] or adsorption [19]. These technologies have not yet reached the same commercial stage as absorption processes. However, several demonstration processes are under way [20].

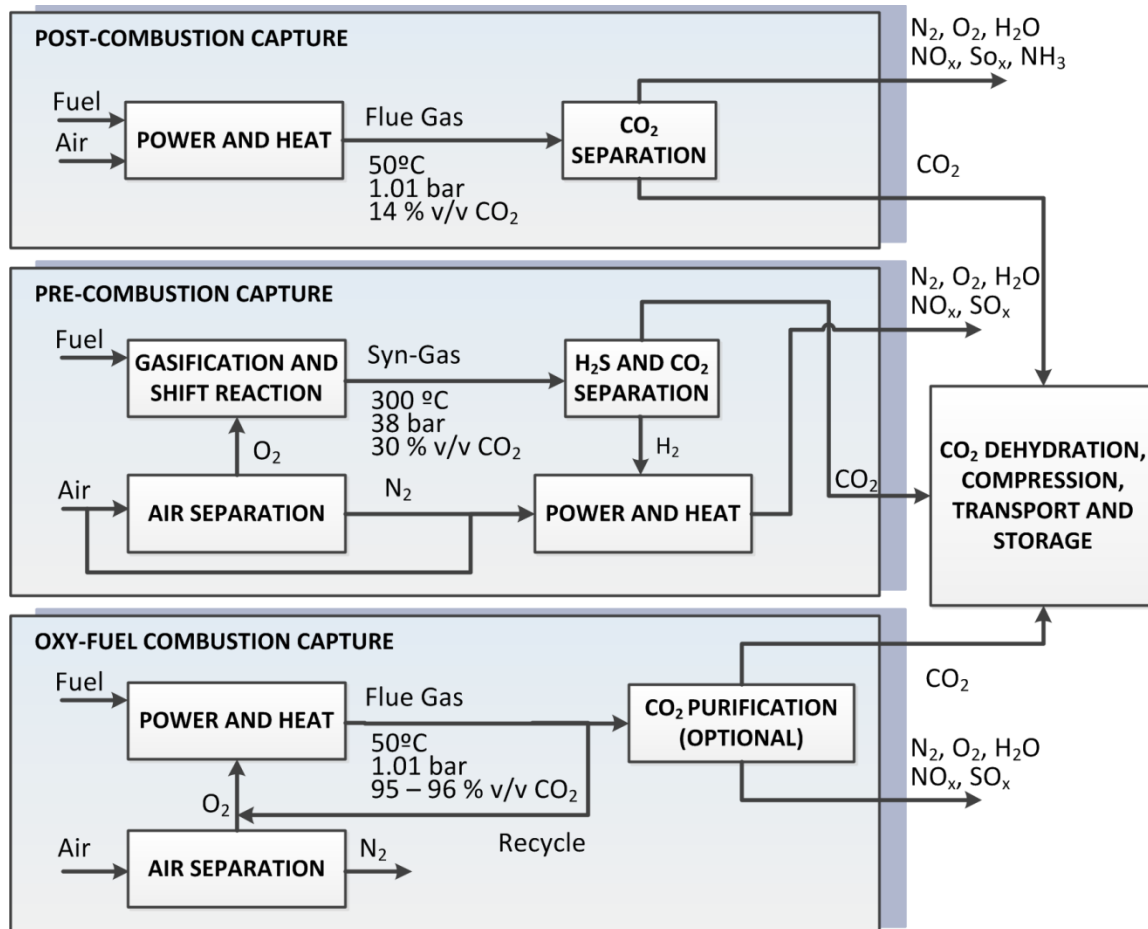


Figure 1.1. Overview of CO<sub>2</sub> capture options for the power sector. Typical operating conditions have been selected from EBTF [21] and IEAGHG [22].

Pre-combustion capture can be applied in coal gasification, which is the necessary step in order to use coal fuel in a combustion turbine. Integrated Gasification Combined Cycle plants (IGCC) are considered the next step in “clean coal” energy conversion. In IGCC technology, coal is first converted into gas using steam and rich oxygen stream. The separation of CO<sub>2</sub> takes place before the gas is combusted in the gas turbine (GT). The capture technologies are similar to those in post-combustion capture. However, the CO<sub>2</sub> concentration in the gasifier exhaust gas is substantially higher than that in conventional boilers; therefore, the separation of CO<sub>2</sub> is more efficient. Technology options such as absorption with physical solvents, membranes [23] and adsorption are more likely to succeed in this application. Other technologies, such as membrane reactors and SEWGS [24, 25], seek the integration of the water shift reactor (reaction that shifts the gasifier exhaust gas composition to more CO<sub>2</sub> and H<sub>2</sub>) and the CO<sub>2</sub> separation step to improve power plant efficiency. Besides a more efficient CO<sub>2</sub> separation, the integration with combined cycle allows benefit from gas turbine technology advances, which could increase the plant efficiency to 60% LHV [7]. These two facts make IGCC plants promising candidates to mitigate CO<sub>2</sub> emissions in coal power generation.

Oxyfuel combustion is another option for CO<sub>2</sub> abatement. The technology uses a pure oxygen stream for coal combustion instead of air, with partial dilution using exhaust flue gas for temperature control. Operation has been demonstrated at relatively small scale, producing a raw

CO<sub>2</sub> product that contains mainly water vapour, oxygen, nitrogen and argon as contaminants. In principle, direct liquefaction of this stream will approach near zero emissions (*i.e.* 100% CO<sub>2</sub> removal). However, it is still uncertain if this possibility will be accepted for transportation and injection in deep reservoirs. There are also acid gases in this stream such as SO<sub>2</sub>, SO<sub>3</sub>, HCl and NO<sub>x</sub> produced as by-products of combustion and there is debate about necessary purification to acceptable CO<sub>2</sub> purities [26]. The main advantages of this technology, as highlighted in the reviews of Burhe [26] and Wall [27] are the power industry familiarity with the technology (implying lower risk than CO<sub>2</sub> capture), the fact that it could be allowed in new plant design for retrofit at a later time (switch between air-fired and oxy-fired combustion) and the lower NO<sub>x</sub> emissions relative to conventional air-combustion.

The challenges and barriers for the implementation of CCS technologies are multi-fold. On one hand there are economic considerations. The application of these technologies requires a substantial investment and has an important impact in the cost and availability of electricity. The major hurdle lies in the high energy required for CO<sub>2</sub> separation and compression step, which decreases the net efficiency of power plants [13]. This justifies the continuous research efforts to improve the efficiency of CCS technologies. Moreover, the screening and selection of more efficient technologies for implementation requires the definition of baselines to assess their technical and economic potential. A great deal of research effort is committed to this [13-15, 21, 22, 28-31], creating a growing need for harmonizing and reviewing the assumptions taken for the technical and economic evaluations of CCS technologies [21] in order to faithfully support the technology selection. On the other hand, the impact of CCS on air pollution is a matter of great concern. The mitigation of CO<sub>2</sub> by a certain carbon capture technology has an effect in the emissions of other air pollutants, which can be positive or negative depending largely on the air pollutant considered [32-34]. Clarifying the environmental impact of CCS requires a prior evaluation of the effect that the different carbon capture technologies may have on air pollution.

Social acceptance of CCS is another barrier for its implementation. Although there is consensus among the research community on the needs and justification of CCS, many of the public are not aware of its benefits. The public's risk perception is frequently based or influenced by social and cultural factors of human behaviour. Once public opinion is strongly formed, it is very difficult to change. Therefore, substantial efforts shall be invested in analysing public's perception, educating and communicating to the public the essence and benefits of CCS [35-38].

This thesis addresses the first issue for the implementation of CCS and is concerned with the development of new carbon capture processes that require less energy for CO<sub>2</sub> separation and are, at the same time, more environmentally friendly. Although the lower energy requirements of IGCC for capturing CO<sub>2</sub> has been established, this technology is not presently competitive on cost and on availability with conventional pulverised coal power plants. On the other hand, oxyfuel combustion requires an oxygen separation plant that reduces efficiency significantly. Therefore, after a brief analysis of the different carbon dioxide capture options, in terms of efficiency and environmental aspects, it was decided to focus this thesis on post-combustion capture, due to the maturity of the technology and the possibility to retrofit existing pulverised coal plants.

Prior to the development of any new process, the current state of the art needs to be analysed and updated in order to set realistic targets for the new technology and benchmark the potential of the new developed processes. This important aspect is also addressed in this thesis.

## 1.2 Post-Combustion Capture: Overview of technologies based on absorption

Chemical absorption processes are applicable to gas streams that have a low CO<sub>2</sub> partial pressure [3kPa-15kPa]. They use reversible chemical reactions, which are affected by temperature. Amines are the most common choice as chemical solvent, however, amino acid salts and alkalis can be used as an alternative to amines. Figure 1.2 shows a list of the most relevant commercial and research programmes with the most important solvents that have been tested at least at pilot plant scale.

There are many amines that have been used industrially for acid gas removal [39]. Depending on the type of amine, there are differences regarding their reversible reaction with CO<sub>2</sub> [40-42]. In the case of primary and secondary amines, carbamate is predominantly formed according to the equilibrium reaction (1.1):

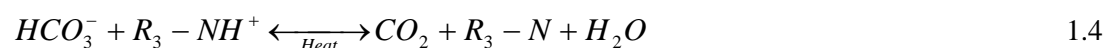
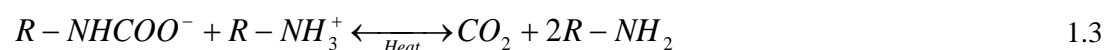


In the case of tertiary amines and hindered amines, bicarbonate is predominantly formed according to the equilibrium reaction (1.2):



Therefore, the maximum capacity based on stoichiometry for primary and secondary amines, like monoethanolamine (MEA) or diethanolamine (DEA), is 0.5 mol CO<sub>2</sub> / mol amine, while tertiary amines, like methyldiethanolamine (MDEA), or hindered amines, like 2-amino-2-methylpropanol (AMP), have a maximum loading capacity that approaches 1.0 mol CO<sub>2</sub> / mol amine. The rates of CO<sub>2</sub> absorption also differ among the amine types, being primary and secondary amines are more reactive than tertiary and hindered amines[40].

The process configurations of all amine technologies are relatively similar. Figure 1.3 illustrates a conventional amine based capture process. This process generally consists of an absorption column, where the CO<sub>2</sub> is chemically bond to the alkanol amine, following reaction (1.1) or (1.2). The CO<sub>2</sub> loaded product is extracted at the bottom of the absorption column. The remaining gas is clean and can be vented to the atmosphere after a final wash in order to avoid solvent evaporation. The loaded solvent is further processed in a stripper, where it can be thermally regenerated for further use, according to one of the following reactions (1.3) or (1.4):



The thermal energy requirements for regeneration are one of the most important process parameters to consider when selecting a specific technology. Stripping CO<sub>2</sub> from primary and secondary amines during regeneration requires a larger amount of energy as compared to tertiary amines [39]. Besides thermal energy for regeneration, other aspects to consider are the availability and matureness of the technology, solvent volatility [43], solvent toxicity, solvent

degradation [44, 45], corrosion [46, 47] and solvent price. The commercial options available are described and compared in reference books [10, 11] and publications [19, 48-52]. Examples of commercial applications are shown in Figure 1.2. The Fluor Econamine process (based on MEA) has been designed to recover CO<sub>2</sub> from flue gas emitted by coal fired power plants. The thermal energy for regeneration of this process is around 3.2 – 3.6 GJ/t CO<sub>2</sub> [15, 53] and it has become a state-of-the-art process commonly used in benchmarking studies. These values can be further reduced with advanced stripper configurations [54-56]. The KS-1 solvent, from Mitsubishi Heavy Industries, has been shown to have less heat requirements than the conventional MEA solvent as well as reduced solvent degradation [57].

Moreover, there are many research programmes committed to the development of better amine based solvents [16]. One line of research is the development of mixed amines where a tertiary amine is blended with a primary or secondary amine. The goal with respect the use of these blends is to retain much of the reactivity of the primary amine but with low regeneration energy, similar to those of tertiary amines [58]. At the International Test Centre for CO<sub>2</sub> capture several pilot plant studies have been performed of the CO<sub>2</sub> capture performance of concentrated MEA and mixtures of MEA and MDEA. These studies show the potential reduction in regeneration energy when MEA is blended with MDEA [58-62]. Within the Luminant carbon management programme, it was found that the requirements for one of the piperazine promoted K<sub>2</sub>CO<sub>3</sub> solvents was much less than the conventional MEA due to increased absorption capacity and rates. Moreover, concentrated piperazine has been reported to consume 2.6 GJ/t CO<sub>2</sub> [63]. In the European projects CASTOR and CESAR, several solvents were selected for pilot plant trials. The identified solvent CASTOR-2, operated in pilot plant scale with lower steam requirement and liquid-to-gas ratio than the conventional MEA solvent [64]. Within the CESAR project, CESAR-1 (AMP and PZ) operated in pilot plant scale with a steam requirement of 3.1 GJ/t CO<sub>2</sub>, based on a conventional process configuration. More advanced process configurations can reduce this figure to 2.8 GJ/t CO<sub>2</sub> [65].

Amino acid salts are also attractive solvents for PCC due to their unique properties over alkanol amines such as: low environmental impact and high biodegradability [66], negligible volatility and high resistance to oxidative degradation [67]. Several amino acid salt based processes have also been developed for PCC of carbon dioxide from flue gas (Figure 1.2). One example of this is the process provided by Siemens, which has energy consumption around 73% of the conventional MEA process [68]. TNO has also investigated processes based on the potassium salt of certain amino acids, showing increased stability and resistance to degradation over conventional MEA [67].

In the recent years, interest has grown in the performance of different amino acid salts for PCC application and the CO<sub>2</sub> absorption characteristics for common amino acids are under extensive investigation. Several researchers have reported the CO<sub>2</sub> absorption on sarcosine, glycine, alanine, taurine and proline solutions [69-73]. Also properties that are necessary for mass transfer evaluation, such as density, viscosity, N<sub>2</sub>O solubility [74, 75] CO<sub>2</sub> diffusivity [76], and solvent kinetics [77-79] have been investigated and reported for the mentioned amino acids under different conditions.

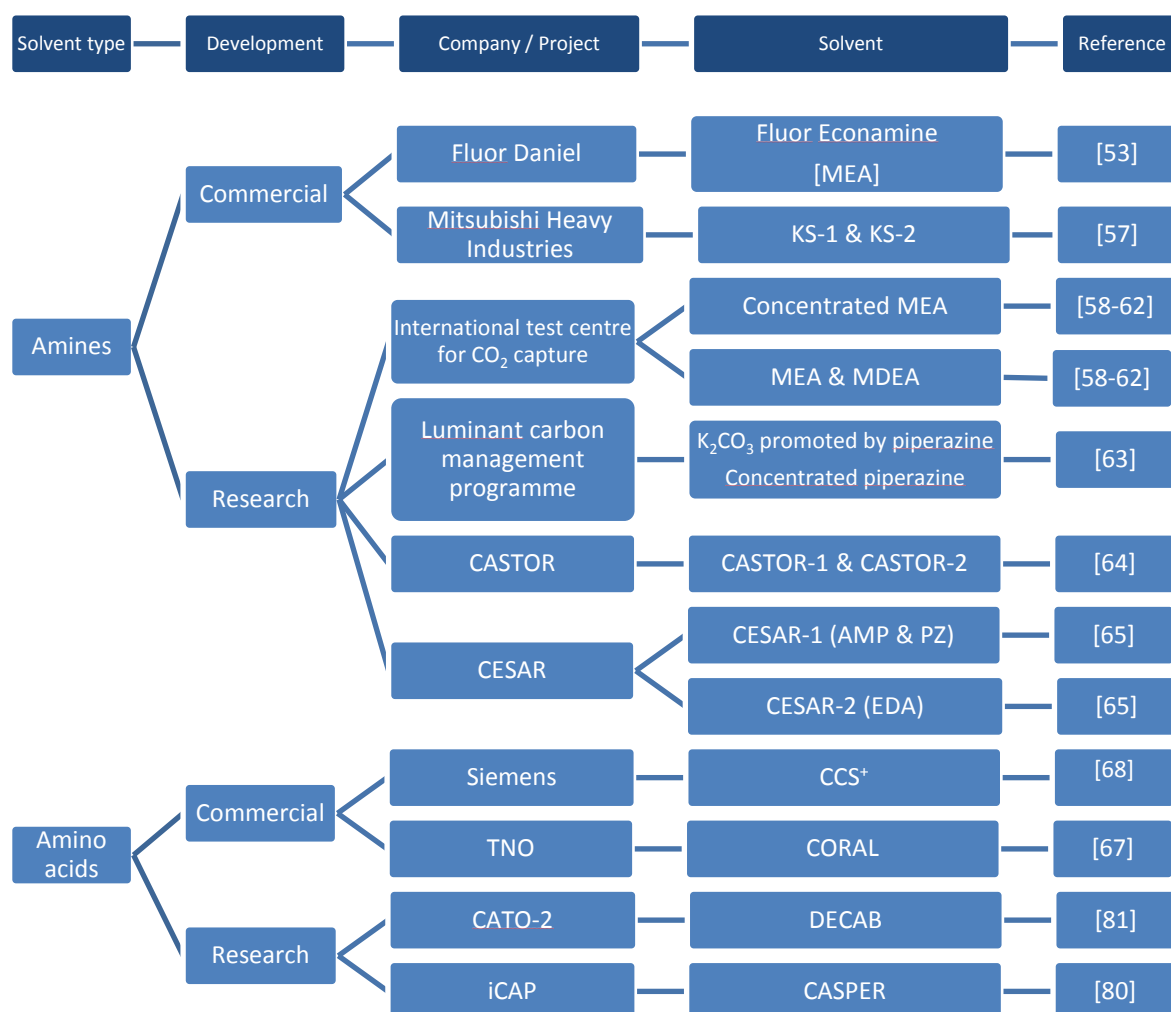


**Figure 1.2. Summary of technology options for CO<sub>2</sub> capture based on amine technology. The figure shows the main commercially available options and the main research options (at least tested at pilot plant scale).**

Within large research consortiums, other possible technologies based on amino acid salts have been identified. These options have not yet been tested at pilot scale but are under development. The CASPER process, developed within the iCAP consortium, aims for the simultaneous separation of CO<sub>2</sub> and SO<sub>2</sub> from flue gas based on the potassium salt of  $\beta$ -alanine [80]. The DECAB process uses precipitating amino acid salts in order to improve the thermal energy requirements of the capture process [81]. The last process has been identified as a promising option to capture CO<sub>2</sub> from flue gas. The concept of precipitating amino acid systems is analysed in more detail in the next section.

### 1.3 Precipitating systems with amino acid salts

Precipitating amino acid salts were suggested in the early 2000's as a promising alternative to amine conventional processes [82]. The identified benefits were related to an enhancement of the specific CO<sub>2</sub> capacity of amino acid salt solutions due to precipitation. Amino acids react with CO<sub>2</sub> like alkanol amines, having the same reaction mechanism. However, unlike amines, amino

acids form electrolytes in aqueous solution that comprise a zwitterion. In order to react with CO<sub>2</sub>, this zwitterion species needs to be neutralised with a strong base. The reactions between CO<sub>2</sub> and amino acids neutralised with potassium hydroxide have been added to the general amine based scrubbing process illustrated in Figure 1.3. Due to the limited zwitterion solubility in water, which is a function of pH, and the strong electrolyte characteristics of the amino acid salt solutions, precipitates may be formed when the pH of the solution decreases, as a consequence of CO<sub>2</sub> absorption. For the conventional amine scrubbing process depicted in Figure 1.3, which is not designed to handle solids, this physical behaviour limits the concentration of active amino acid in the solvent, which is generally kept below saturation conditions [83].

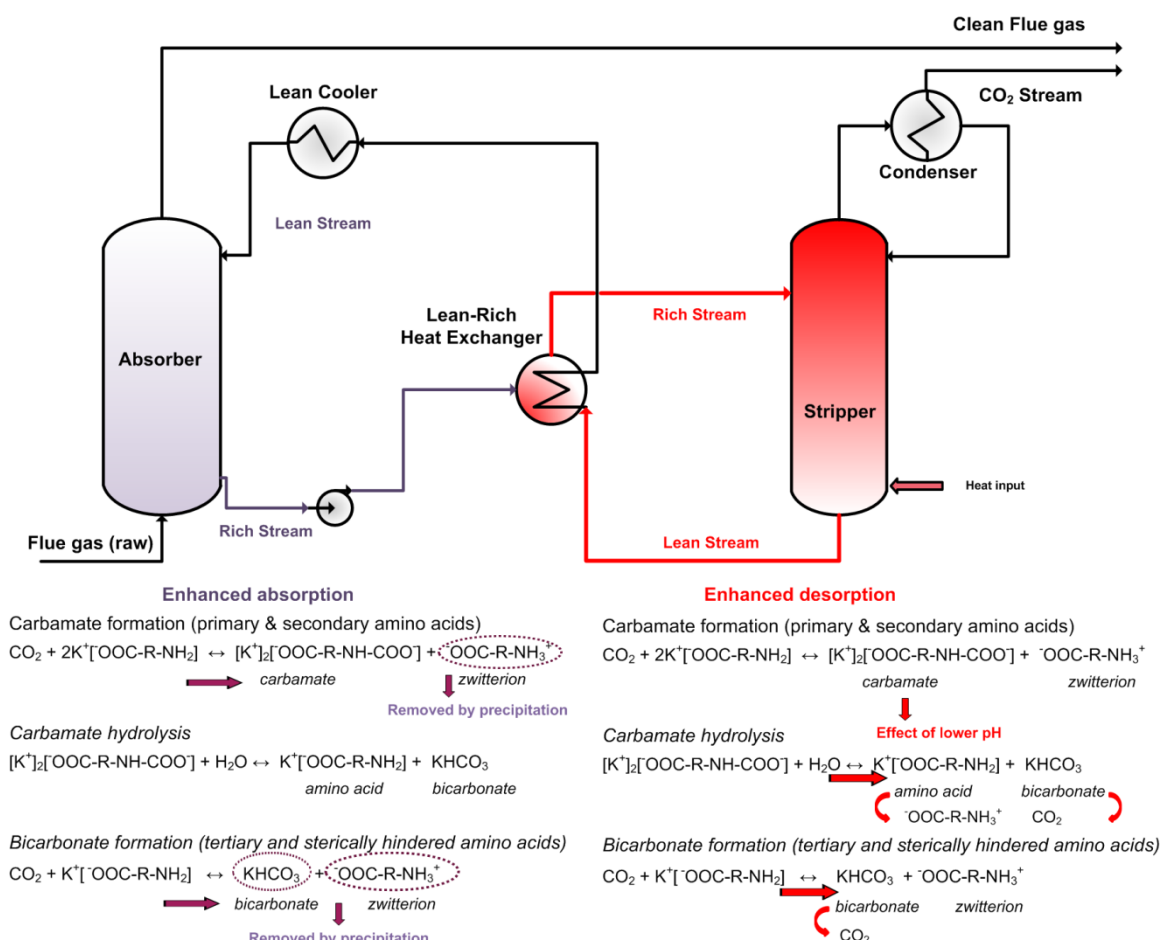


Figure 1.3. Conventional amine based process for CO<sub>2</sub> capture where the reactions specific to amino acid salts have been added at the bottom of the absorber and the stripper. Besides the heat input necessary to regenerate the solvent, in the case of precipitating amino acids two more effects are possible: Enhanced absorption (takes place in the absorber) due to the precipitation of reaction products during absorption and enhanced desorption (takes place in the stripper) due to a lower pH that is brought about by partially separating the liquid from the precipitate to concentrate the amino acid in the rich solution (*i.e.* increasing the amino acid to K<sup>+</sup> ratio in solution).

Nevertheless, the precipitation during CO<sub>2</sub> absorption can contribute to decrease the energy consumption of the capture process influencing the equilibrium reactions (1.1) and (1.2) by other means than heat. Different precipitate types can be encountered depending on the amino acid structure and solubility. Amino acids with a primary amino group, such as taurine, precipitate

only the zwitterion species [84]. In other cases, the precipitate formed is potassium bicarbonate. This is the case of amino acids with a hindered amino group and relatively high zwitterion solubility, such as proline [85]. Independently of the precipitate type, the formation of a solid reaction product during absorption and its removal from the liquid phase by precipitation shifts the reaction equilibrium towards the production of more products (carbamate or bicarbonate). This effect has been indicated in the reactions in Figure 1.3 (enhanced absorption), where the possible precipitating species are shown. Moreover, the formation of the precipitate allows for phase separation (solid from liquid) and formation of a new rich solution, in which acidity can be manipulated. For instance, in the case that the amino acid zwitterion is concentrated in the solid phase, the effect of partial removal of the liquid will result in a higher reduction of  $K^+$  compared to the reduction in amino acid. After re-dissolution of the solid phase, this will induce a lower pH in the rich solution that is treated in the stripper due to a higher ratio of amino acid to  $K^+$ . The lower pH promotes the hydrolysis of the carbamate species, resulting in the formation of amino acid salt and bicarbonate, which revert to the zwitterion species and carbon dioxide at even lower pH. This effect has also been indicated in the reactions in Figure 1.3 (enhanced desorption). As net effect, a lower pH during desorption will enhance the release of  $CO_2$ .

The concepts illustrated in Figure 1.3 have been registered in different patents [86-88] and suggest the possibility to design novel processes for  $CO_2$  separation based on precipitating amino acid solvents that are more energy efficient than the conventional processes. Obviously, the presence of solids in the process requires the selection of different contactor equipment for absorption, such as a spray tower, and the selection of appropriate pumps that can manipulate slurries. This process alternative has been evaluated by conceptual design [89], resulting in process performance similar to conventional MEA and capital investments lower than conventional MEA. Moreover, in order to induce a pH shift during desorption, a solid-liquid separation equipment, such as a hydrocyclone, needs to be included for the separation of the precipitate and part of the supernatant. The latter is recycled to the absorption column with an effect on solvent capacity since the supernatant also contains carbonated species. This process alternative needs to be evaluated to determine technical and economic feasibility.

## **1.4 Scope and organisation of this thesis**

This thesis provides the development and evaluation of novel  $CO_2$  separation processes based on precipitating amino acid solvents. The key objectives established for the development of the new processes are a significant reduction in the regeneration energy of the post-combustion capture process (at least a 30% reduction), compared to a current conventional amine process, and the use of solvents that are more biodegradable and, as a whole, more environmentally friendly, than the conventional process. These objectives and the main tasks in this thesis have been defined and developed within two different CCS projects: the European CESAR [90] and the Dutch CATO-2 project [91].

Chapter 2 in this thesis, analyses the effect of carbon capture technologies on the emissions of three different power plants with and without carbon capture. The selected technologies are: an Ultra Supercritical Pulverized Coal plant, both air and oxyfuel mode (USC PC), and Integrated Gasification Combined Cycle (IGCC) and a Natural Gas Combined Cycle (NGCC). For the given reference cases, plant performance was evaluated based on the mass and energy balances of the

selected cases and compared to the averaged emissions factors reported in the literature for the selected technologies.

To establish the potential of the innovative processes, the definition of baseline performance of post-combustion capture is necessary for the evaluation of potential reductions in the energy required by the novel processes. As discussed in Section 1.1, there is need for harmonizing and updating these baselines in order to faithfully support the technology evaluation. As part of the work of this thesis work, the definition of baselines for a conventional amine capture process and an advanced amine capture process has been performed. Chapter 3 provides the thermodynamic performance of fossil fuel power plants (coal fired and gas fired) with integrated PCC based on the conventional monoethanolamine (MEA) solvent and a more advanced amine solvent, CESAR-1, which is an aqueous solution of 2-amino-2-methyl-propanol and piperazine. Based on the conditions and assumptions taken in this study, it is shown that the CESAR-1 solvent can reduce substantially the energy requirements of the CO<sub>2</sub> capture unit for coal and gas fired power plants. The impact of this reduction in the power plant economics is presented in Chapter 4. The economics of the power plant cases presented in Chapter 3 are investigated in detail for the two different chemical solvents (MEA and CESAR-1). The CESAR-1 solvent reduces the costs of CO<sub>2</sub> avoidance with respect to MEA due to a higher CO<sub>2</sub> capacity and lower energy requirements for regeneration. Moreover, it has also been indicated in Section 1.1 that more advanced process configurations can decrease the regeneration energy of a given amine process. An example of one of these process configurations, the lean vapour compression option, is also investigated in this thesis as part of the benchmarking effort. In Chapter 5, this process configuration is analysed technically and economically. The analysis shows that this option is always advantageous for a CO<sub>2</sub> capture process based on MEA.

The novel process concepts introduced in this thesis have been developed based on the combination of enhanced absorption and desorption, effects described in Section 1.3, considering all phenomena and factors involved. The conceptual design of a novel CO<sub>2</sub> separation process based on precipitating amino acid solvents is presented in Chapter 6. The new concept introduced, named DECAB Plus, requires the precipitation of the pure amino acid species and the partial recycle of the remaining supernatant to the absorption column. This induces a shift in the pH of the rich solution that has substantial benefits during CO<sub>2</sub> desorption. Proof of principle for this process concept has been achieved using a potassium taurate solution. The evaluation of the process required the experimental investigation of the key properties and parameters that govern the absorption and desorption in precipitating amino acid solvents. The experimentally derived properties were used for process modelling and the evaluation of the process proposed. In Chapter 7, different process alternatives to the process analysed in Chapter 6 are discussed and evaluated. The alternative processes analysed are based on the DECAB Plus process concept (described in Chapter 6) and include the following options: lean vapour compression (option described in Chapter 5), split flow and the use of alternative solvents. Chapter 8 provides an overview of the achievements of the precipitating amino acid solvent processes. The final assessment in this thesis shows the differences between the novel processes and conventional MEA and shows alternative routes to further improve their performance.

---

# EMISSIONS OF SUBSTANCES OTHER THAN CO<sub>2</sub> FROM POWER PLANTS WITH CCS TECHNOLOGIES

## ABSTRACT

*This work analyses the effect of Carbon Capture Technologies (CCT) on the emissions of three different power plants with and without CCT. The selected reference cases were: an Ultra Supercritical Pulverized Coal plant, both air and oxyfuel mode (USC PC), an Integrated Gasification Combined Cycle (IGCC) and a Natural Gas Combined Cycle (NGCC). For the given reference cases, plant performance was evaluated based on the mass and energy balances and the emissions of air pollutants (SO<sub>x</sub>, NO<sub>x</sub>, CO, particulates, Hg, other trace metals, chlorine and fluorine) were estimated. The effect of CCTs in the emissions of air pollutants depends on the primary energy consumption of the CCT, which demand a significant amount of energy for CO<sub>2</sub> separation and compression, and the specific interaction of air pollutants with CCT technology. With respect to the impact of CCT on plant efficiency, pre-combustion capture on the IGCC case had the lowest energy penalty (efficiency reduction of 6.5 percentage points), followed by the oxyfuel case (8.6 percentage points) and the post combustion capture cases (9.1-9.2 percentage points). The emissions of SO<sub>2</sub> are significantly reduced together with the reduction in CO<sub>2</sub> emissions for all coal power plant cases. Particulate emissions are also reduced for most coal cases analysed. NO<sub>x</sub> emissions increase for post-combustion capture (both USC PC and NGCC) but decrease for oxyfuel combustion (USC PC oxyfuel) and remain constant for pre-combustion capture (IGCC). The values predicted from the mass and energy balances were compared with emissions factors reported in literature. The literature value is an average of the emission factors derived from an extended database of emissions of air pollutants, corrected for specific parameters, such as fuel type, percentage of CO<sub>2</sub> removal and CO<sub>2</sub> final pressure. Although, CO<sub>2</sub> emissions were comparable with the literature values, most of the other air pollutants were higher than the ones obtained from the mass balances except for the IGCC power plant case.*

*This chapter is based on:*

*E. Sanchez Fernandez, E.L.V. Goetheer, M. Juzvicka, T. van Harmelen, A. van Horssen, M. Oldenburg, "Emissions of Substances other than CO<sub>2</sub> from Power Plants with CCS". IEAGHG report NO. 2012/03. Available at [http://ieaghg.org/docs/General\\_Docs/Reports/](http://ieaghg.org/docs/General_Docs/Reports/)*

## 2.1 Introduction

Carbon Capture and Storage (CCS) is considered as one of the short to medium term options in the portfolio of actions for stabilising acceptable concentrations of atmospheric greenhouse gas, of which CO<sub>2</sub> is the main contributor. The essence of CCS is to capture CO<sub>2</sub> from large point emission sources (power stations, refineries, other industries) and transport and store this permanently in suitable underground geological formations, such as depleted gas fields, deep reservoirs or other suitable formations [1]. In power generation, CO<sub>2</sub> emissions from fossil fuels are directly linked to the efficiency in energy conversion. This efficiency is improving with the development of advanced combustion and gasification technologies [6-8]. Nevertheless, within the European Union, it is foreseen that CCS will be implemented, along with extended use of renewable energy, in order to achieve the long term target of greenhouse gas emissions reduction of 80-95% by 2050 [9].

For the future deployment of this technology in the power sector, the impact of CCS on air pollution is a matter of concern. Clarifying the environmental impact of CCS requires a prior evaluation of the effect that the different Carbon Capture Technologies (CCTs) may have on air pollution. This effect has been quantified in several studies on air pollution from power plants. As shown in Koorneef, [34], Harmelen [32], Horssen [33] and more recently by the EEA [92], the mitigation of CO<sub>2</sub> by a certain Carbon Capture Technology (CCT) has an effect in the emissions of other air pollutants, which can be favourable or unfavourable depending largely on the air pollutant considered. Despite the existing background, the assessment and standardisation of the effect that CCTs have on advanced energy conversion technologies is complicated due to the high variability of coal composition (for coal-fired power plants), and the variability in energy conversion technology, power plant configuration and steam cycles that lead to different energy conversion efficiencies. Current challenges are:

- 1) The environmental data information in relation to CO<sub>2</sub> capture is still scarce. For instance, there is lack of information to quantify the effect of CCTs on the emissions of certain air pollutants such as volatile organic components [92] or trace metals [93].
- 2) Benchmarking and comparing the effect of different CCTs in power plant emissions is still difficult. In addition to the already mentioned variability in fuel type and plant configuration, other aspects such as plant location, the stage of technology development of the CCT applied and the Air Pollution Control Systems (APCS) implemented in power plants to maintain air pollution under acceptable levels, also contribute to a great variability in the reported emissions. For instance, the different gasification technologies applicable to IGCC or the variability in the performance of steam cycles applicable to pulverized coal result in an extensive variation in power plant efficiencies [32]. Also, the APCS implemented in power plants vary broadly, depending on local legislation and cost [32]. This variability provides a wide spread in the average air pollutant emissions derived from multiple literature studies.
- 3) Much of the information published on air pollutant emissions from power plants with CO<sub>2</sub> capture is based on assumptions, which need to be validated. Actual measurements are still limited by the scale (mainly laboratory studies and pilot plant studies) and the analytical techniques (sampling methods and detection limits).

In this chapter, the effect of three CCTs on the emissions of three different power plants is evaluated and reported. The selection of reference cases meets the following criteria: realistic representation of advanced energy conversion technology for each case and the use conventional technologies for air pollutant control. The selected reference power plants; Ultra-Supercritical Pulverized Coal (USC PC), Natural Gas Combined Cycle (NGCC) and Integrated Gasification Combined Cycle (IGCC) have been selected from the state-of-the-art in energy conversion and air pollution control technology [6, 7, 94, 95]. This work contributes to the existing studies of air pollution in conjunction with CCTs by providing a detail analysis of the emissions of these cases, which are specific to the technology and configuration selected. The effects of including CCTs in the selected power plants are analysed by combining the mass and utility balances of the power plants and the estimation of emissions using revised assumptions based on information from literature. The focus of the study is on the power plant integrated with the capture plant, excluding transport and storage. Fugitive emissions and emissions that result from fuel preparation were not included in the scope of this work. Furthermore, emissions directly stemming from the solvents used to capture CO<sub>2</sub>, such as the possible solvent degradation products were left outside scope, with the only exception of ammonia, primary indicator of amine solvent degradation.

The chapter is organised as follows: the different CCTs evaluated in this work are briefly described in Section 2 of this publication together with the review of the recent literature on this topic. For each CCT a power plant reference case was selected for evaluation. The final plant configuration for the reference cases is also briefly described in this section. The methodology followed in this work covers the simulation of the specific power plant performance and the estimation of emissions using revised assumptions. This approach is addressed in Section 3. The results are first summarized per technology, showing the effects of CCTs on emissions of the different reference cases (Section 4). Then, the effects of each CCT are discussed and compared in Section 5 per air pollutant. The discussion analyses the discrepancies found between the results for the reference cases and the averaged values for relatively similar plants found in the literature. The conclusions of the study are presented in Section 6.

## 2.2 Literature review

The technology options for CCS are generally grouped under three different capture strategies: post-combustion capture, pre-combustion capture and oxyfuel combustion.

Post-combustion capture (PCC) refers to the partial removal of CO<sub>2</sub> from flue gases produced by combustion of fossil fuels in boilers (in the case of coal fired stations) or in gas turbines (in the case of gas fired stations) after all the air pollution control systems (APCS). Amine scrubbing is generally the technology choice due to the matureness of the technology [16, 17]. The current state-of-the-art technology for PCC is chemical absorption with an aqueous solution of monoethanolamine (MEA)[10, 96] although other technologies such as adsorption [19, 97] or membrane based separation [18, 20] are applicable.

Pre-combustion capture is commonly applied in coal gasification, which is the necessary step in order to use coal fuel in a combustion turbine. In IGCC technology, coal is first converted into gas using steam and a rich oxygen stream. The exhaust gas from the gasifier, mainly a mixture of

H<sub>2</sub>, CO<sub>2</sub>, CO and water vapour, is quenched and treated in the shift reactor with steam, to further convert CO into H<sub>2</sub> and CO<sub>2</sub>. The separation of CO<sub>2</sub> takes place before the gas is combusted in the gas turbine. Although fuel preparation and treatment is more complicated in gasification, the CO<sub>2</sub> concentration in the gasifier exhaust gas is substantially higher than that in pulverised coal combustion. Therefore, the separation of CO<sub>2</sub> is more efficient in IGCC plants. There are multiple gasification technologies available [98]: mainly entrained flow (Shell, GE-Texaco, Conoco-Philips), fixed bed (BGL, Lurgi), fluidized bed (SoutherCo, KRW). For this reason there is a broad variation in plant configurations for IGCC that results in different plant efficiencies. Also, IGCC can be used to produce other products (*i.e.* co-production of chemicals, gas and power) and can process many different feed stocks (coke, heavy oils, biomass, etc.). The focus in this work is on production of power only and using bituminous coal as feed-stock.

Oxyfuel combustion is another option for CO<sub>2</sub> abatement [26, 27]. The technology uses a pure oxygen stream for coal combustion instead of air, which is partially diluted using exhaust flue gas for temperature control. The combustion product is a raw CO<sub>2</sub> stream product that contains mainly water vapour, oxygen, nitrogen and argon as contaminants. In principle, direct liquefaction of this stream will approach near zero emissions (*i.e.* 100% CO<sub>2</sub> removal). However, there are also acid gases in this stream such as SO<sub>2</sub>, SO<sub>3</sub>, HCl and NO<sub>x</sub> produced as by-products of combustion and there is debate about necessary purification to acceptable CO<sub>2</sub> purities for transportation and storage [26]. There are different treatments suggested in the literature that will result in different emissions of air pollutants [99].

Background information on the impacts of CO<sub>2</sub> capture technologies on air pollution are given by [92], [34], [32] and [33] based on a study of air pollution in the Netherlands. A database was created during the studies of [32] and [33], containing 176 cases from 37 data sources, each of them representing a set of air pollutant emission factors (based on primary energy) of a given power plant with a specific configuration and specific CCT. The average emission factors for the carbon capture technologies (presented in Table 2.1) have been derived from this database after calibration of the following important parameters for all cases:

- Degree of CO<sub>2</sub> removal: corrected fuel penalty when the CO<sub>2</sub> removal deviates from 90% captured except for the oxyfuel power plants because these plants have normally CO<sub>2</sub> removal rates higher than this value
- Sulphur content in coal: corrected when the sulphur content in coal deviates from the bituminous coal from Eastern Australia, 0.95wt% dry.
- Primary energy related to compression: the power loss by compression, expressed in primary energy, is corrected when the pressure ratio of the CO<sub>2</sub> compressor deviates from the reference cases.

Table 2.1 shows a summary of the primary energy use and emission factors based on net electricity output for different air pollution substances. The implementation of all capture technologies will result in an increase in primary energy. In this respect, pre-combustion capture on IGCC has higher potential for lower energy consumption than post-combustion capture and oxyfuel (*i.e.* averaged plant efficiency found is 42%LHV). USC PC plants without CO<sub>2</sub> capture show the highest SO<sub>x</sub> emissions. The emissions are significantly reduced by applying a post combustion process due to the deep sulphur removal required by amine solvents. The oxyfuel process can result in near zero emissions of this component in the case of co-sequestration or

very low emissions depending on the cleaning process of the CO<sub>2</sub> stream. The IGCC process shows a low level of SO<sub>x</sub> emissions because of the efficient cleaning of the syngas prior to combustion. Since the sulphur content of natural gas is very low, SO<sub>x</sub> emissions are expected to be negligible for NGCC. For the post combustion CO<sub>2</sub> capture technology (both USC PC and NGCC) the NO<sub>x</sub> emissions per kWh increase due to the increase in fuel penalty and no removal of this component in the amine capture unit. NO<sub>x</sub> emissions from the oxyfuel concept are expected to be low, but are highly dependent on the treatment and purification within the concept. The PM emission from NGCC are considered negligible in most literature studies. For coal fired oxyfuel power plants PM emissions are estimated to be lower compared to conventional pulverized coal fired power plants. The already low PM emissions for IGCC power plants are not expected to be significantly affected due to the application of pre-combustion capture and thus will result in an increase due to the efficiency penalty.

Trace metals are also emitted during coal combustion or gasification. However, any form of standardisation on the emissions of trace metals is very challenging. The quantity of any given metal emitted depends on many parameters such as: the physical and chemical properties of the metal itself, the concentration of the metal in the coal, the combustion or gasification conditions, the type of particulate control device used, and its collection efficiency as a function of particle size. Various classification schemes, based on metal volatility, have been proposed to describe partitioning behaviour of metals during combustion and gasification [93, 100, 101]. [93] have reviewed trace metals emissions during combustion and gasification and the efficiencies of particulate matter control technologies. Generally, metal volatility is higher in gasification compared to air combustion, as reducing conditions are favourable to the formation of volatile gaseous species of the trace elements, such as hydrides and carbonyls [100]. Although most metals are trapped in the slag during gasification or retained in ash during combustion, some of them can be emitted in the vapour phase or condensed on the particulates (soot particles or fly ash). The emissions of these metals can be controlled after gasification or combustion. In the case of oxy-fuel combustion, gas phase concentration of volatile elements (Hg, Se and probably As) is expected to be higher under oxy-firing conditions than under air-firing conditions [102].

**Table 2.1. Literature averaged emissions factors of selected air pollutants. Calibration has been applied to the CO<sub>2</sub> removal (set to 90% with the exception of the oxyfuel cases), sulphur content in coal (set to 0.95wt% dry) and primary energy use related to compression. Data from [32, 33].**

		Plant efficiency % LHV	Fuel use MJ/kWh	CO <sub>2</sub> kg/MWh	SO <sub>2</sub> kg/MWh	NO <sub>x</sub> kg/MWh	PM10 kg/MWh	Hg kg/MWh	NH <sub>3</sub> kg/MWh
USC PC	No-CC	43.9%	8.21	735	0.30	0.36	0.04	2.7·10 <sup>-6</sup>	3.5·10 <sup>-3</sup>
	PCC	34.1%	10.57	97	0.00	0.50	0.05	5.5·10 <sup>-6</sup>	8.2·10 <sup>-2</sup>
	OXY	35.6%	10.24	93	0.01	0.20	0.01	3.5·10 <sup>-7</sup>	[-]
IGCC	No-CC	42.2%	8.57	761	0.04	0.23	0.01	2.2·10 <sup>-6</sup>	0.0
	PreCC	34.8%	10.42	93	0.01	0.21	0.03	2.7·10 <sup>-6</sup>	0.0
NGC C	No-CC	56.4%	6.39	366	0.00	0.12	0.00	0.0	3.7·10 <sup>-4</sup>
	PCC	48.8%	7.48	43	0.00	0.13	0.00	0.0	[-]

No-CC: No carbon capture.

PCC: Post-combustion capture.

OXY: oxyfuel.

PreCC: Pre-combustion capture.

With respect to emission abatement technologies after gasification or combustion (air-fired or oxygen-fired), the reduction of the emissions of a metal that tends to condense over particulates is directly related to the reduction of total particulate matter emissions, while for a more volatile metal particulate abatement technologies have a very limited impact on its emissions. Because of variability in efficiency of particulate control technologies, metal emissions can vary substantially. In Table 2.1 only the emission factors of mercury are shown.

## 2.3 Reference cases description

This work has selected three power plant configurations for evaluation of emissions in which the capture technologies described in the previous section have been implemented. The main configuration of the power plants, fuel type and APCS are summarized in Table 2.2 and are briefly described in the following sections. The selection of suitable APCS depends on country legislation and economic considerations. Although the technology cost is an important factor to consider, it was not prioritised in this selection. A description of the conventional and emerging technology choices for the mitigation of main air pollutants can be found elsewhere [8, 12, 103-105].

### 2.3.1 USC PC Power Plant

This case is based on the advanced Rankine cycle with steam operating conditions of 290 bar, 600/620°C. Mass and utility balances were taken from [22, 31], revised and modified for better accuracy. The boiler is equipped with low NO<sub>x</sub> burners and is fitted with selective catalytic reduction (SCR) for NO<sub>x</sub> abatement. Limitation of SO<sub>x</sub> emissions is accomplished with the flue gas desulphurisation (FGD) system. In the case with no CCT, the FGD system is designed to reduce the sulphur dioxide level in the flue gas from the boiler to around 70 ppm at 6% O<sub>2</sub> v/v

(dry). However, in the case with CCT, the FGD system is designed to reduce the sulphur dioxide level in the flue gas from the boiler to around 10 ppm at 6% O<sub>2</sub> v/v dry (a level which does not exceed the inlet requirement of the carbon dioxide absorption plant). The CO<sub>2</sub> Amine Absorption unit is based on monoethanolamine (MEA) scrubbing technology [53] and consists of three main units: direct contact cooler, absorber and stripper. The capture unit is designed with split flow and solvent heat integration to reduce the reboiler consumption [106]. The stripper reboiler is heated by condensing the steam extract from the IP/LP cross over in the power island. Condensate at saturation conditions is returned to the power island de-aeration system. Overhead vapour from the stripper is cooled with recycled condensate from the boiler island. The remaining cooling duty is achieved with sea water. Carbon dioxide from the stripper is compressed, dehydrated to remove water to a very low level and is finally delivered at a pipeline pressure of 110 bar.

### 2.3.2 NGCC Power plant

This case is derived from [21]. Mass and utility balances were modelled using Aspen Plus®. The power plant is located inland and consists of one gas turbine (Siemens SGT5-4000F) equipped with dry low NO<sub>x</sub> burners, SCR, heat recovery steam generator (HRSG) steam turbine, generator, and water treatment equipment. Water cooling is done with a draft cooling tower system. Besides the above mentioned units, the case with CCT has a CO<sub>2</sub> capture unit integrated into the power plant. The CO<sub>2</sub> Amine Absorption unit is also based on MEA scrubbing technology. Nevertheless, the capture unit has a simpler design than that of the USC PC case and includes no split flow or MEA heat integration. The reason for choosing a simpler design is that complexity of control and operation is significantly reduced. In return, this design has slightly higher steam requirements in the stripper. The stripper reboiler is heated by condensing the steam extract from the IP/LP cross over in the power island in the same manner as in the USC PC case. However, there is no integration of the boiler island condensate in this design. Therefore, overhead vapour from the stripper is cooled directly with cooling water. Also inter-stage cooling during compression is done with cooling water. The other units in the capture plant are designed in a similar manner to the USC PC case.

### 2.3.3 IGCC (GE) Power plant

The selected reference case (derived from [22]) employs the GE gasification process to convert feedstock coal into syngas. Environmental measures are included in the design, such as facilities for scrubbing particulates from the syngas prior to combustion and facilities for removing the coarse and fine slag from the quench and scrubbing water. Moreover, the syngas from the gasification section is contaminated with acid gases, CO<sub>2</sub> and H<sub>2</sub>S, and other chemicals, mainly COS and HCN. The sulphur contaminants are converted to H<sub>2</sub>S in the hydrolysis reactor. The resulting syngas is treated in the acid gas removal (AGR) unit, where the sulphur components are removed by employing the Selexol process. The sulphur recovery unit (SRU) is an O<sub>2</sub> assisted Claus Unit, with Tail gas catalytic treatment (SCOT type) and recycle of the treated tail gas to AGR. NO<sub>x</sub> are controlled with injection of compressed N<sub>2</sub> from the air separation unit (ASU) to the gas turbines. This has two effects: dilution of syngas for temperature control and turbine power augmentation.

### 2.3.4 USC PC Power plant (oxyfuel)

The selected reference plant is the same USC steam plant described in Section 2.2.1 converted to oxyfuel fired operation. Design characteristics, utility and heat and mass balances have been retrieved from [22]. Coal is pulverized and fed into the boiler. The flue gas exiting the boiler is treated in order to remove particulates in the ESP unit. Two streams of recycled flue gas are required for the oxy-combustion system: the primary recycle passes through the coal mills, after drying, and transports the pulverized coal to the burners. The secondary recycle provides additional gas to the burners to maintain temperatures within the furnace at similar levels to air firing. The remaining CO<sub>2</sub> product stream is further purified to meet the specifications for geological disposal applications. The carbon dioxide purification and compression unit employed in this study is based on a purification process proposed by [107, 108] and commercialized by Air Products and Chemicals Inc. The process uses two successive water-wash columns. SO<sub>x</sub> removal process takes place in the first water-wash column at 15 bar. It separates out all the SO<sub>2</sub> and SO<sub>3</sub> as sulphuric acid, in a process catalysed by NO<sub>2</sub>. After the first column, the flue gas is compressed to 30 bar and introduced into the next water-wash column, where NO is converted to NO<sub>2</sub> and removed as nitric acid. The CO<sub>2</sub> stream is then sent to the sections of inert removal, based on cryogenic phase separation, water removal, based on adsorption on desiccants, and compression. The source of all gaseous emissions in this plant is the vent stream from the inert removal unit, which contains mainly CO<sub>2</sub> and impurities such as NO<sub>x</sub>.

## 2.4 Methodology

The methodology adopted in this work, illustrated in Figure 2.1 for one of the power plant cases, can be divided into two steps:

- Step 1: Process modelling of the selected power plant reference cases
- Step 2: Estimation of air pollutants emissions for the reference cases

In the first step, mass and energy balances are calculated for the power plant reference cases selected. In the case of the coal power plants, the mass and energy balances were retrieved from literature and revised. In the NGCC power plant case, the Aspen Plus® tool was used to estimate the mass and energy balances.

The second step is a systematic accounting of air pollutant emissions which are not included in common simulation software packages. Uncontrolled emission factors and removal efficiencies of the APCTs present in each power plant case (listed in Table 2.2) were used to estimate the emissions of trace components. An in-house Microsoft Excel based spread-sheet was used for the estimation of air pollutant mass balances. The estimation of a single air pollutant follows from a mass balance:

$$F_i = (C - U) \cdot E_i \cdot \prod_1^{N_{APCS}} (1 - R_i) \quad 2.1$$

In the equation above,  $F_i$  is the mass flow of component  $i$  emitted (kg/s),  $C$  is the flow of coal (as fired) / fuel to the boiler / gas turbine (t/s),  $U$  is the unburned coal (when applicable) (t/s),  $E_i$  is the specific uncontrolled emissions factor for component  $i$  (kg/t coal/gas) and  $R_i$  is the removal

efficiency of component  $i$  in a given air pollution control system (APCS) and  $N_{APCS}$  is the number of APCSs in the plant configuration. Mass balances developed in the prior stage were used as a basis for the estimation of  $C$  and  $U$ .

**Table 2.2. Plant configuration and main components of the reference cases of this study.**

Type	USC PC <sup>a</sup>		USC Oxyfuel <sup>b</sup>	IGCC <sup>c</sup>		NGCC <sup>d</sup>	
	no CCT	CCT		no CCT	CCT	no CCT	CCT
Steam Cycle bar(a)/°C/ °C	290/600/ 620	290/600/ 620	290/600/ 620	161/600/ -	161/600/ -	124/561/ 234	124 /561/ 234
Gas Turbine	NA	NA	NA	Advanced F class	Advanced F class	Advanced F class	Advanced F class
Boiler type	Supercritical PC			GE	GE	NA	NA
Oxidant	Air	Air	95% O <sub>2</sub>	95% O <sub>2</sub>	95% O <sub>2</sub>	Air	Air
NO <sub>x</sub> Controls <sup>e</sup>	LNB & OFA & SCR		Air Products. Inc	Dilution with N <sub>2</sub>		LNB & OFA & SCR	
PM Controls <sup>e</sup>	ESP					NA	NA
H <sub>2</sub> S controls	NA	NA	NA	Selexol		NA	NA
SO <sub>x</sub> /Sulphur control <sup>e</sup>	FGD (Wet Scrubber, Limestone)		Air Products. Inc	Claus		NA	NA
CO <sub>2</sub> separation <sup>e</sup>	NA	MEA		NA	Selexol	NA	MEA
Fuel Type	Eastern Australian Bituminous coal					Natural Gas	

<sup>a</sup> Pulverized coal fired plant with Ultra-Super critical steam cycle. Configuration from [22].

<sup>b</sup> Pulverized coal fired plant with Ultra-Super critical steam cycle and oxy-fired mode. Configuration from [22].

<sup>c</sup> Integrated Gasification combined cycle. Configuration from [22].

<sup>d</sup> Natural Gas combined cycle. Configuration from [21].

<sup>e</sup> Air Products-CO<sub>2</sub> stream cleaning process based on [108], FGD-Flue Gas Desulphurisation unit, LNB- Low No<sub>x</sub> Burners, OFA-Over fired air, SCR-Selective catalytic Reduction.

In order to apply equation 2.1, it is necessary to find accurate values for uncontrolled emission factors for the fuel in question and the specific combustion technology. Also, the effects of the APCTs on each air pollutant need to be known. The carbon capture plant is also considered as an APCS and its effect on air pollutants has been investigated in this work by reviewing the available literature. The values assumed for  $E_i$  and  $R_i$  are presented in Appendix 9.2, together with supporting references. The inherent assumption when applying equation (2.1) is that the additional flows ( $F_i$ ) do not modify the mass and energy balances calculated during step 1. The overall mass flows can be corrected when necessary by normalizing stream flows (*i.e.* forcing the sum of mass fractions to be unity). For oxy-fired boilers and gasification, the application of this equation is more difficult due to data scarcity (in the case of oxy-combustion) and the degree of integration between the different plant components (in the case of IGCC), which makes the evaluation of a singular component's effect more difficult. However, for the IGCC case, it is still assumed that additional flows of trace substances such as metals, do not affect gas turbine or steam turbine efficiencies because the changes in syngas composition are minimal.

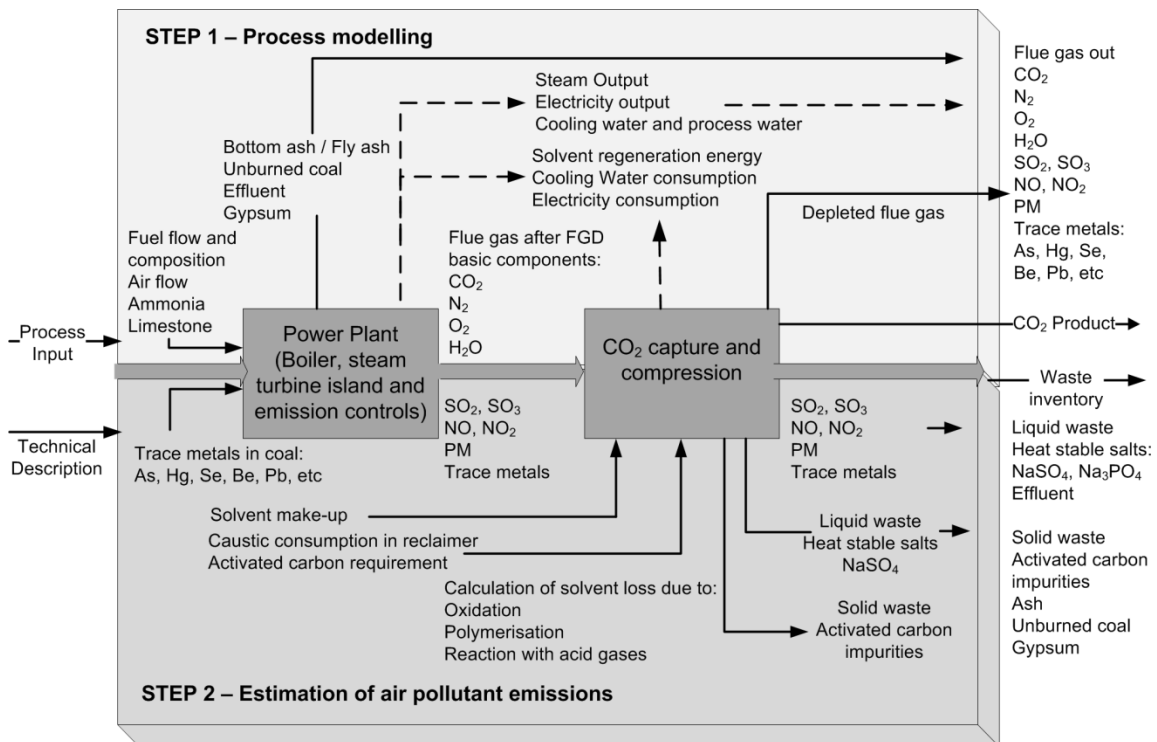


**Figure 2.1. Schematic representation of the estimation of mass and energy balances. The figure illustrates how the overall assessment of mass and energy balances is performed in two steps for a Post-combustion example: During Step 1 the heat rate of the power plant, main requirements of the capture plant and main component mass balances are calculated. During Step 2, the emissions of trace substances is calculated based on equation 2.1.**

## 2.5 Results

This section presents the evaluation of emissions of the power plants described in Section 2.2. As shown in Tables 2.3 to 2.7, the implementation of CCTs in the power plants has different effects on the emissions of pollutants. On one hand, the emissions of some pollutants decrease per unit electricity basis because they are substantially removed in the capture unit. On the other hand, the emissions of more relatively inert components increase per unit electricity basis, due to the energy penalty that the CCTs cause to the host power plant. The relative increase or decrease in the emission factor of a substance is represented by the Carbon Capture Quotient (CCQ), which represents the ratio between the specific emissions a power plant (per unit electricity produced) with and without CCT [34].

### 2.5.1 Energy penalty

The net efficiency and performance of the selected reference cases are shown in Table 2.3. The highest efficiency is achieved by the NGCC power plant (58.3%LHV). Among the coal cases investigated, the most efficient are the USC PC plant (44%LHV) and the IGCC plant (38%LHV). Regarding the efficiency reduction due to CCT implementation, the results show an efficiency reduction of 9.1-9.2 percentage points for post combustion capture, 6.5 percentage points for pre-combustion capture and 8.6 percentage points for oxyfuel.

### 2.5.2 Emissions of USC PC power plant with post combustion capture

Table 2.4 shows the results for the USC PC power plant with and without post combustion capture technology. The SO<sub>2</sub> emissions for the USC PC case are decreased to very low levels because the amine based PCC technologies generally require SO<sub>2</sub> concentration levels below 10 ppmv in flue gas. The process model assumes 95% removal efficiency for the FGD unit using limestone, although, other systems, such as dual alkali systems, give higher removal rates, up to 98% (Appendix 9.2). At 95% removal efficiency, the concentration in the flue gas entering the CO<sub>2</sub> capture unit is 34mg/Nm<sup>3</sup>, concentration just in the limit for the amine operation (10ppmv or 29mg/Nm<sup>3</sup> at 6% O<sub>2</sub>). Moreover, since SO<sub>2</sub> and SO<sub>3</sub> are more acidic than CO<sub>2</sub>, the remaining SO<sub>x</sub> (SO<sub>2</sub> and SO<sub>3</sub>) are also removed by the amine solvent. For this reason, SO<sub>2</sub> emissions are the lowest possible for the USC PC plant with PCC. Other acid gases also interact with the amine systems. For this reason the emissions for HCl and HF are also reduced when carbon capture is implemented.

With regard to particulate emissions (PM-10), the results show a reduction on PM-10 emissions per unit electricity basis. This implies that the removal of particulates and dust in the capture process off-sets the additional emission due to the extra fuel consumption in PCC technology.

The results on Table 2.4 also indicate an increase in NO<sub>x</sub> emissions when PCC is implemented into the USC PC plant. Since NO, the main component in the NO<sub>x</sub> mixture, does not interact with amine solvents, NO<sub>x</sub> emissions increase for post-combustion carbon capture technologies due to the reduction in power efficiency. Moreover, NO<sub>2</sub> interaction with amines, mainly secondary amines, might lead to the formation of potential hazardous components (nitrosamines), solvent degradation and heat stable salts formation [109]. Nevertheless, due to these interactions, some researchers also suggests that suppliers will also require levels of NO<sub>x</sub> in the order of 10ppmv [110, 111]. The mentioned NO<sub>x</sub> controls are capable of reducing the NO<sub>x</sub> level to 13ppmv in this case.

**Table 2.3. Performance of the selected reference cases with carbon capture technology (CCT) and without carbon capture technology (no CCT)**

Parameter	Units	USC PC <sup>a</sup>		USC OXY <sup>b</sup>	IGCC (GE) <sup>c</sup>		NGCC <sup>d</sup>	
		no CCT	CCT		no CCT	CCT	no CCT	CCT
Coal Flow rate (air dry)	t/h	239.8	266.3	209.1	303	323.1	56.1	56.1
Fuel heat value LHV	kJ/kg	25870	25870	25860	25870	25869	46502	46502
Thermal energy based on fuel LHV (A)	MWt	1723.2	1913.7	1502	2177	2322	724.5	724.5
Gross electricity output (D)	MWe	831	827	737	988.7	972.8	430.3	430.3
Power plant auxiliaries (E)	MWe	73.3	78.3	54	162.2	203.5	7.7	7.7
Consumption due to CO <sub>2</sub> capture (F)	MWe	NA	83.1	151.6	NA	39.0	NA	66.0
Net electric output (C=D-E-F)	MWe	757.7	665.6	531.4	826.5	730.3	422.6	356.6
Gross electrical efficiency (D/A*100)	% [LHV]	48.2	43.2	49.1	45.4	41.9	59.4	53.6
Net electrical efficiency (C/A*100)	% [LHV]	44.0	34.8	35.4	38.0	31.5	58.3	49.2
Specific fuel consumption	MWt/MWe	2.074	2.875	2.827	2.634	3.018	1.71	2.03
Specific CO <sub>2</sub> emissions	kg/MWh	743	117	85	818	152	354	41.9
Cooling water consumption <sup>e</sup>	t/MWh	138.6	240.5	176.7	146.9	185.2	45.6	82.7
Specific water consumption <sup>f</sup>	t/MWh	0.104	0.41	0.063	0.126	0.411	1.02 <sup>g</sup>	1.21

<sup>a</sup> Pulverized coal fired plant with Ultra-Super critical steam cycle. Configuration from [22].

<sup>b</sup> Pulverized coal fired plant with Ultra-Super critical steam cycle and oxy-fired mode. Configuration from [22].

<sup>c</sup> Integrated Gasification combined cycle. Configuration from [22].

<sup>d</sup> Natural Gas combined cycle. Configuration from [22].

<sup>e</sup> For the cases with a once through cooling system (Cases 1 to 3) cooling water consumption indicates the sea cooling water supply. For the cases with cooling towers (Case 4), cooling water consumption indicates the cooling water make up.

<sup>f</sup> Specific water consumption indicates the consumption of raw water.

<sup>g</sup> Factor estimated for NGCC plants from [15].

Ammonia emissions increase drastically with the application of post combustion capture due to the degradation of the amine solvent. The amount of MEA degraded depends on the type of degradation inhibitors that suppliers include in the solvent formulation. Different studies suggest that this rate ranges from 0.29 kg/t CO<sub>2</sub> to 0.73 kg/t CO<sub>2</sub> [112-115] and have identified the dependence of the MEA degradation rate on solvent concentration, CO<sub>2</sub> loading, SO<sub>2</sub> and O<sub>2</sub> concentrations in the gas phase [116]. For this study the geometric mean of the given range was taken as nominal MEA loss (0.46 kg/t CO<sub>2</sub>) with a molar yield on ammonia of 1 mol per mol of MEA degraded [117]. Using these assumptions, the impact on ammonia emissions is substantial, increasing baseline emissions by a factor 27.

**Table 2.4. Emission factors for USC PC power plant with carbon capture technology (CCT) and without carbon capture technology (no CCT). Results show the amount emitted per unit electricity, the concentration of each air pollutant in exhaust gas and the CCQs (on a electricity basis).**

Basic components	Units	USC PC <sup>a</sup>		Units <sup>b</sup>	USC PC <sup>a</sup>		CCQ <sup>c</sup>
		no CCT	CCT		no CCT	CCT	
CO <sub>2</sub>	kg/MWh <sub>net</sub>	739	93	mg/Nm <sup>3</sup>	NA	NA	0.13
SO <sub>2</sub>	kg/MWh <sub>net</sub>	0.26	6.50·10 <sup>-4</sup>	mg/Nm <sup>3</sup>	85	0.19	0.00
NO <sub>x</sub>	kg/MWh <sub>net</sub>	0.08	0.10	mg/Nm <sup>3</sup>	28	45	1.30
CO	kg/MWh <sub>net</sub>	0.07	0.09	mg/Nm <sup>3</sup>	24	26	1.29
HCl	kg/MWh <sub>net</sub>	9.00·10 <sup>-3</sup>	5.40·10 <sup>-4</sup>	mg/Nm <sup>3</sup>	3	0	0.06
HF	kg/MWh <sub>net</sub>	1.00·10 <sup>-3</sup>	6.80·10 <sup>-5</sup>	mg/Nm <sup>3</sup>	0.4	0	0.07
PM-10	kg/MWh <sub>net</sub>	0.01	6.00·10 <sup>-3</sup>	mg/Nm <sup>3</sup>	3	2	0.60
Ammonia	kg/MWh <sub>net</sub>	0.004	0.107	mg/Nm <sup>3</sup>	1	31	26.75
Total mercury	kg/MWh <sub>net</sub>	5.70·10 <sup>-6</sup>	5.30·10 <sup>-6</sup>	mg/Nm <sup>3</sup>	1.9·10 <sup>-3</sup>	1.5·10 <sup>-3</sup>	0.93

<sup>a</sup> Pulverized coal fired plant with Ultra-Super critical steam cycle. Configuration from [22].

<sup>b</sup> based on dry conditions at 6% O<sub>2</sub>.

<sup>c</sup> CCQ: Carbon capture Quotient calculated from model results, which represents the ratio between the emission factors of a power plant (on a electricity basis) with and without CCT and indicates the relative increase or decrease in the emission factor of a substance due to the application of a certain capture technology [34].

### 2.5.3 Emissions of NGCC power plant with post-combustion capture

Table 2.5 shows the results for the NGCC Power plant with and without carbon dioxide capture. Air pollution related to the NGCC power plant is substantially lower than coal fired power plants. Emissions of SO<sub>2</sub> and particulates are negligible for the NGCC power plant case. Generally, the emissions of these pollutants are zero, as already indicated by the literature review (Table 2.1). However, for a more sour gas some emissions of SO<sub>2</sub> will be present but in low marginal quantities. In that particular case, emissions would be drastically reduced when PCC is implemented in the power plant. Also in some cases dust could be carried over to the gas turbine, resulting in low emissions of particulates.

Emissions of NO<sub>x</sub> are the primary pollutant from gas turbines. They can be controlled by steam injection in the turbine, the addition of LNB, with a removal efficiency of 33% -55%, the addition of SCR, with a removal efficiency of 75%-85% or the combination of LNB and SCR, giving a removal efficiency of 84% - 93% [8]. Results on Table 2.5 correspond to the latest option, which is generally only employed in countries with very tight environmental legislation. Regardless the option adopted for NO<sub>x</sub> control, deployment of PCC will result in an increase of emissions, as indicated by the calculated CCQ.

Some emissions of CO are expected as a result of partial combustion of the fuel. It is also foreseen that the addition of PCC to the plant will result in an increase of specific CO emissions by a factor 1.11. No verification of this was found in literature due to the lack of information regarding this component.

Ammonia emissions shall be also expected as a result of PCC deployment due to solvent degradation. The emissions have been estimated under the same assumptions as in the USC PC case. Since the initial emissions of ammonia are minor (close to zero) the CCQ tends to infinite. No actual value was found in the literature for this component.

**Table 2.5. Emission factors for NGCC power plant case with carbon capture technology (CCT) and without carbon capture technology (no CCT). Results show the amount emitted per unit electricity, the concentration of each air pollutant in exhaust gas and the CCQs (on a electricity basis).**

Basic components	Units	NGCC <sup>a</sup>		Units <sup>b</sup>	NGCC		CCQ <sup>c</sup>
		no CCT	CCT		no CCT	CCT	
CO <sub>2</sub>	kg/MWh <sub>net</sub>	354	42	mg/Nm <sup>3</sup>			0.12
SO <sub>2</sub> <sup>d</sup>	kg/MWh <sub>net</sub>	0 / 1.0·10 <sup>-2</sup>	0 / 5.9·10 <sup>-5</sup>	mg/Nm <sup>3</sup>	0 / 2.2	0 / 0.0	0 / 0.01
NO <sub>x</sub>	kg/MWh <sub>net</sub>	0.03	0.03	mg/Nm <sup>3</sup>	5.8	6.2	1.17
CO	kg/MWh <sub>net</sub>	0.09	0.1	mg/Nm <sup>3</sup>			1.11
PM-10 <sup>e</sup>	kg/MWh <sub>net</sub>	9.7·10 <sup>-5</sup>	5.70·10 <sup>-5</sup>	mg/Nm <sup>3</sup>	4.2	0,0	0.59
Ammonia	kg/MWh <sub>net</sub>	0	0.04	mg/Nm <sup>3</sup>		8.5	∞

<sup>a</sup> Natural Gas combined cycle. Configuration from [22].

<sup>b</sup> Dry basis at 6% O<sub>2</sub>.

<sup>c</sup> CCQ: Carbon capture Quotien calculated from model results. They represent the ratio between the emission factors of a power plant with and without CCT and indicate the relative increase or decrease in the emission factor of a substance due to the application of a certain capture technology [34].

<sup>d</sup> SO<sub>2</sub> emissions are negligible for natural gas (value 0 kg/MWh<sub>net</sub>). However, some sources of natural gas contain sulphur (H<sub>2</sub>S) and all sulphur in the fuel is assumed to be converted to SO<sub>2</sub>. For the cases where the sulphur content in the fuel might be significant but the actual value is not available, [103] suggests a factor of 3.4 E-03 lb/MMBtu for natural gas. The calculated values in the table for SO<sub>2</sub> (when different to zero), are a result of the application of said emission factor for stationary turbines to the mass balance of the reference cases.

<sup>e</sup> PM can be carried over to the turbine.

#### 2.5.4 Emissions of IGCC power plant with pre-combustion capture

Air pollution from IGCC coal power plants is generally lower than conventional PC power plants. This is reflected in the results presented in Table 2.6. For instance, SO<sub>2</sub> emissions are 0.08 kg/MWh for the IGCC power plant case without CCT. These emissions are approximately 30% lower than the USC PC case without CCT. When CCT is implemented in the power plant, these emissions are reduced by a factor 0.13 (as indicated by the CCQ). Regarding particulates, the IGCC case has similar PM emissions compared to the USC PC case. There is, apparently, no effect of the CCT on the emission of particulates. This result indicates that the increase in primary energy is compensated by a reduction in particulates emissions in the IGCC plant designed with CCT. NO<sub>x</sub> emissions are the main air pollutant for IGCC power stations and they remain relatively constant with and without CO<sub>2</sub> capture. The reference case for IGCC controls NO<sub>x</sub> emissions by diluting the feed to the gas turbine with N<sub>2</sub>. This control measure is sufficient to compensate the efficiency drop due to the auxiliary consumption of the capture unit. Therefore, NO<sub>x</sub> emissions are somewhat equal for the IGCC case with and without CO<sub>2</sub> capture. Carbon monoxide emissions are also not affected by the implementation of CCT in the IGCC case. In the case of HCl and HF emissions, no information was found to provide with an adequate estimate for the case with CCT. It is unclear whether the Selexol solvent has more or less affinity for these components than for CO<sub>2</sub>.

One point of attention in Table 2.6 is CO<sub>2</sub> emissions, which are higher than the USC PC case. This is a direct result of the selected reference case for IGCC, with efficiencies of 38%LHV and 31.5%LHV for the cases without and with CCT. Nevertheless, higher cycle efficiency (42%-45%LHV) will result in emissions of 745 kg/MWh which are more comparable to the averaged value found in the literature.

**Table 2.6. Emission factors for the IGCC power plant case with carbon capture technology (CCT) and without carbon capture technology (no CCT). Results show the amount emitted per unit electricity, the concentration of each air pollutant in exhaust gas and the CCQs (on a electricity basis).**

Basic components	Units	IGCC Power Plant <sup>a</sup>		Units <sup>b</sup>	IGCC Power plant		CCQ <sup>c</sup>
		no CCT	CCT		no CCT	CCT	
CO <sub>2</sub>	kg/MWh <sub>net</sub>	818	152	mg/Nm <sup>3</sup>			0.19
SO <sub>2</sub>	kg/MWh <sub>net</sub>	0.08	0.01	mg/Nm <sup>3</sup>	10	1	0.13
NO <sub>x</sub>	kg/MWh <sub>net</sub>	0.39	0.39	mg/Nm <sup>3</sup>	51	50	1.03
CO	kg/MWh <sub>net</sub>	0.24	0.25	mg/Nm <sup>3</sup>	31	31	1.04
HCl	kg/MWh <sub>net</sub>	$6.80 \cdot 10^{-3}$		mg/Nm <sup>3</sup>			
HF	kg/MWh <sub>net</sub>	$3.60 \cdot 10^{-4}$		mg/Nm <sup>3</sup>			
PM-10	kg/MWh <sub>net</sub>	0.03	0.03	mg/Nm <sup>3</sup>	4	4	1
Total mercury	kg/MWh <sub>net</sub>			mg/Nm <sup>3</sup>			

<sup>a</sup> Integrated Gasification combined cycle. Configuration from [22].

<sup>b</sup> Dry basis at 15% O<sub>2</sub>.

<sup>c</sup> CCQ: Carbon capture Quotien calculated from model results. They represent the ratio between the emission factors of a power plant with and without CCT and indicate the relative increase or decrease in the emission factor of a substance due to the application of a certain capture technology [34].

### 2.5.5 Emissions of USC PC power plant with oxyfuel technology

The USC plant described in Section 2.3 was used as reference case for the estimation of emissions of oxyfuel technology. For the selected reference case, the source of all gaseous emissions is the vent stream from the inert removal unit. Table 2.7 shows the emissions to the atmosphere of this case.

SO<sub>2</sub> emissions under oxyfuel conditions have been found to be lower than that in air combustion [26]. Measurements at the Clean Coal Test Facility (CCTF) of Doosan Babcock in Scotland show that the concentration of SO<sub>2</sub> in oxyfuel raw flue gas is approximately 3 times higher than that of air-firing flue gas [118]. This contradicts prior modelling studies that estimate concentrations of SO<sub>2</sub>, SO<sub>3</sub> and HCl in flue gas up to six times higher than found in air-combustion for coals with 2% dry sulphur content if FGD is not installed before the primary and secondary flue gas recirculation [102]. Also, measured emissions are lower than that expected from mass balances. This fact indicates that SO<sub>2</sub> is being removed from the system. Most likely it is being adsorbed on the fly ash. When emissions are expressed per energy unit the emissions of SO<sub>2</sub> are about 25% lower for oxyfuel than for air-firing. For this reference case, SO<sub>2</sub> emissions are virtually zero since any SO<sub>2</sub> present in the CO<sub>2</sub> rich stream will be removed during the cleaning process.

NO<sub>x</sub> emissions are also significantly lower under oxyfuel firing (factor 2) than for air firing [26]. In any case, results in Table 2.7, indicate that the emissions of SO<sub>2</sub> and NO<sub>x</sub> resulting from the combustion process under oxy-firing conditions can be virtually completely removed from the flue gas in the compression plant leading to no emissions to the environment [118]. Particulate emissions are also negligible, since particulates are not present in the vent stream of the inert removal unit. White *et al.* [107] have investigated experimentally the factors that influence the removal of SO<sub>2</sub> in this configuration. Their findings show that high conversions are possible for SO<sub>2</sub>. The presence of NO<sub>2</sub> catalyses the oxidation reaction of SO<sub>2</sub> to SO<sub>3</sub> which is further removed as H<sub>2</sub>SO<sub>4</sub> in the presence of water. The ratio SO<sub>2</sub>/NO<sub>2</sub> affects the removal of SO<sub>2</sub>. At SO<sub>2</sub>/NO<sub>2</sub> ratios of approx. 2.8, conversion is above 95% and at ratios of around 4 conversion decreases to 85%.

**Table 2.7. Emission factors for the USC PC oxyfuel reference case.**

Basic components	Units	USC PC oxyfuel
CO <sub>2</sub>	kg/MWh <sub>net</sub>	85
SO <sub>2</sub>	kg/MWh <sub>net</sub>	0
NO <sub>x</sub>	kg/MWh <sub>net</sub>	0.03
PM-10	kg/MWh <sub>net</sub>	0
Total mercury	kg/MWh <sub>net</sub>	NA

### 2.5.6 Trace metals in coal fired power plants

Studies on trace metal emissions that include measurements at pilot plant and operating facilities [103, 119] have been used for the estimation of emission factors ( $E_i$ ) and removal efficiencies ( $R_i$ ) necessary for the application of equation (2.1) (Appendix 9.2). One characteristic of many of these studies is the lack of accuracy in achieving a closed mass balance between metal inputs in coal and emerging streams from combustion. This could be due to flaws in sampling methods, and flaws in analytical methods [100]. For these reasons, any form of generalization on the emissions of trace metals is very challenging. An example of trace metals emissions is given in Figure 2.2 based on the application of equation (2.1), for the USC and IGCC power plant cases without CCT. The results in Figure 2.2 show that emissions for most metals are similar for both USC PC and IGCC cases.

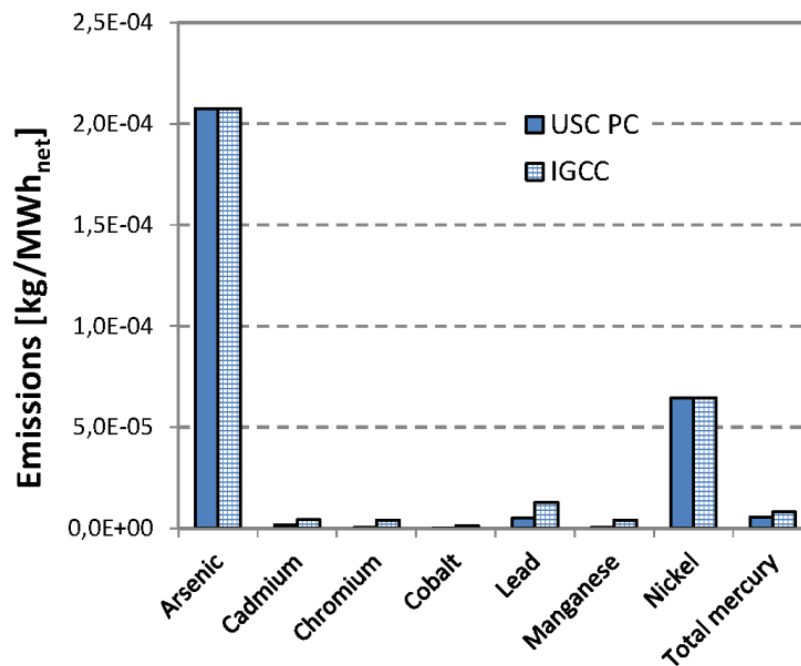


**Figure 2.2. Emissions of selected trace metals (in kg/MWh<sub>net</sub>) for the USC PC power plant case without CCT and the IGCC power plant case without CCT.**

Moreover, accurate data sources on trace metals emissions when CCTs are applied are more limited, especially in the gasification case. For this reason equation (2.1) could not be applied for the estimation of emissions in the cases with CCTs.

Nevertheless, in the USC PC case the reduction of particulates also suggests an equal reduction in the emissions of heavy metals that have the tendency to distribute mainly on particulates and fines. This is not the case of mercury. Mercury is a very volatile metal and is found in different oxidation states after combustion ( $\text{Hg}^{2+}$ ,  $\text{Hg}^0$ ). Only the oxidized mercury is dissolved in alkaline solutions [120]. The elementary mercury can be partially adsorbed on particulates and fines and be washed on the capture unit. The final mercury removal efficiency of the capture unit (in the absence of any other prior treatment, such as activated carbon injection) depends therefore on the mercury distribution, dictated by the combustion conditions. The value of the CCQ for mercury found in Table 2.4 is around 1, indicating no effect of PCC on the emissions of this metal.

With respect to the oxyfuel case, the emissions of metals in the  $\text{CO}_2$  stream cleaning process is still under investigation. White *et al.* [107] have investigated mercury emissions during the first testing campaigns of the Oxycoal – UK project at the sour compression set-up at Imperial College (London), although they have not reported them. However, in the liquid samples all the mercury was present in the condensate from the first flue gas cooler. The mercury content was found to be negligible in all vessels located after the first compression step. Ideally, this will result in no mercury emissions for the USC oxyfuel case.

## 2.6 Discussion

### 2.6.1 Energy penalty

The performance of the different power plants was initially evaluated without any capture technology. Among the cases considered, the NGCC power plant case has the highest efficiency (58% LHV). With regard to power plant performance without CCT, the results are in good agreement with what can be realised today in terms of energy conversion efficiency [5, 7] and are in line with the literature findings summarised in Table 2.1 with the exception of the IGCC power plant (with calculated efficiency 38% LHV). Table 2.1 indicates an averaged efficiency for IGCC around 42% LHV. Current IGCC power plants, operating only on coal, can realise efficiencies ranging from 38.5% LHV to 45% LHV [7] depending on the gasification technology and degree of plant integration. The result obtained from the evaluation, although valid, is on the low end of the range for this technology, probably due to the technology choice. Higher efficiencies are reported for IGCC, where some studies technically predict 46% LHV efficiency [15, 21] but it has not been widely demonstrated in operation.

CCTs demand a significant amount of energy for  $\text{CO}_2$  separation and compression. This increases the primary energy use of all the investigated power plants with integrated CCT, requiring more fuel per MWh generated. Based on the sections above, the lowest increase on primary energy use is for the IGCC power plant case (15% raise in primary energy use), followed by the NGCC case (19% raise in primary energy use) and the UCS PC cases, oxyfuel and PC (36% and 39% respectively). These values are in line with literature findings (Table 2.1).

### 2.6.2 *SO<sub>2</sub> emissions*

As expected, SO<sub>2</sub> emissions are negligible for gas turbines; therefore, the NGCC reference case analysed in this work has no emissions of this pollutant. With regard to the coal cases, the power plant with lowest SO<sub>2</sub> emissions is the IGCC reference case, when no CCT is considered. For all cases analysed, the implementation of CCT will lead to lower SO<sub>2</sub> emissions per unit electricity basis. The extension of the reduction depends on the CCT applied. The USC PC oxyfuel has near zero emissions for SO<sub>2</sub>, because the CO<sub>2</sub>-stream cleaning process of this case leaves virtually no presence of SO<sub>2</sub> in the CO<sub>2</sub>-stream, and, consequently no SO<sub>2</sub> is present in the vent stream from the inert removal unit (source of gaseous emissions). Also, the SO<sub>2</sub> emissions from the USC PC are drastically reduced. Amine scrubbing requires very low levels of SO<sub>2</sub> in the original flue gas, that are further reduced after the capture unit. The SO<sub>2</sub> emissions from the IGCC case are reduced to a less extent. In this case, the gas cleaning takes place prior to combustion, where the sulphur gaseous components are removed as H<sub>2</sub>S. The Selexol® solvent employed to capture CO<sub>2</sub> has also affinity to H<sub>2</sub>S, contributing to the observed reduction in sulphur emissions.

When results are compared to the findings in literature (Table 2.1), the average emission factor found for USC PC power plants (0.30 kg SO<sub>2</sub>/MWh<sub>net</sub>, which corresponds to a concentration of 99 mg/Nm<sup>3</sup> in flue gas) is higher than the one found in this work (0.26 kg SO<sub>2</sub>/MWh<sub>net</sub>, which corresponds to a concentration of 85 mg/Nm<sup>3</sup> in flue gas). Nevertheless, new build power plants have a stricter goal in SO<sub>2</sub> emissions. The EBTF [21] selected 85mg/Nm<sup>3</sup> as emission limit, which is the average of the range given by the Best Available Technologies document from the European commission [121]. [122] report SO<sub>2</sub> emissions as 45 mg/Nm<sup>3</sup> (dry basis at 6% O<sub>2</sub>) for the new build power plant at Maasvlakte (Rotterdam). Moreover, the average emission factor found for IGCC power plants (0.04 kg SO<sub>2</sub>/MWh<sub>net</sub>) is lower than the one found in this work (0.08 kg SO<sub>2</sub>/MWh<sub>net</sub>). This could be directly linked to the lower efficiency of our IGCC case compared to the literature average.

### 2.6.3 *Particulate matter emissions*

PM emissions are also negligible for NGCC. With respect to the coal cases, the USC oxyfuel power plant shows the lowest emissions in particulates (near zero emissions) related to the specific treatment of the CO<sub>2</sub> stream. There are discrepancies between the values found in literature and the results of this study. The baseline for particulate emissions from USC PC power plants given in Table 2.1 is relatively high (0.04 kg/MWh), four times higher than the emission factor calculated in this work. Nevertheless, [122] report emissions of 4 mg/Nm<sup>3</sup> (dry basis at 6% O<sub>2</sub>) for an advanced supercritical plant fuelled with bituminous coal. This is in line with the results of this work for the USC PC case. The variability observed in particulate emissions is partially due to the variation in PC technology but mainly due to the wide variation on the PM-10 emissions control performance. For state-of-the art USC PC technology, it is safe to assume PM-10 emissions in the range 3-5 mg/Nm<sup>3</sup>.

More discrepancies with literature are found when carbon capture technologies are applied to the reference power plants. In the case of post combustion capture in USC PC plants, the average literature values show an increase of the emissions of this pollutant by 25% (Table 2.1). Other authors [92] suggest a modest reduction in PM (around 74% based on primary energy) due to the

necessity of stable operation in the capture unit. In any case, this reduction is not sufficient to offset the energy penalty associated with PCC giving a relative increase in direct emissions of this pollutant per unit electricity. However, the amine process consists of several washing steps which take place in vessels that contain fine structured packing and the absorber column. The efficiency of these washing units is high with respect to PM removal with the exception of aerosols. This effect has been checked experimentally, in the results of [65], and by modelling, in the recent FEED study by Fluor Daniel for the Maasvlakte demonstration plant [122].

Regarding the IGCC case, the baseline for particulate emissions found in Table 2.1 is considerably lower than the results of this work. As in the case of SO<sub>2</sub> emissions, this is due to the lower efficiency of our IGCC case. Also, the same discrepancy has been found with respect to the effect of CCT. The averaged literature values foresee an increase of the emissions of this pollutant by 23% (Table 2.1), while it is possible to maintain the same emission levels in the selected reference case of this study indicating partial removal of particulates in the capture unit.

#### 2.6.4 NO<sub>x</sub> emissions

NO<sub>x</sub> emissions are present in all the power plants analysed. The NGCC power plant is the one with lowest emissions of NO<sub>x</sub>. When compared to Table 2.1, the NO<sub>x</sub> emissions are over predicted by the literature for this case. This reflects the wide variety on NO<sub>x</sub> control performance for NGCC plants. SCR can be incorporated in gas turbines as a post-combustion control of NO<sub>x</sub> emissions. However, the use of SCR depends on the legislation of each country. For most cases water steam injection and the use of low NO<sub>x</sub> burners is sufficient to reduce emissions to acceptable levels [94]. For this reason the NO<sub>x</sub> emissions shown in Table 1 are higher than the ones obtained in this study.

With respect to the coal cases, the power plant with lowest NO<sub>x</sub> emissions is the USC PC oxyfuel. Also the results of this study are lower than the one reported in literature. The CO<sub>2</sub> cleaning process selected for this case has potentially lower emissions than the conventional NO<sub>x</sub> control systems (SCR), which are commonly found in literature. The same trend is found in the USC PC power plant. The NO<sub>x</sub> emissions estimated in this work are lower than the estimates from the literature (0.36kg/MWh<sub>net</sub>; equivalent to 119 mg/Nm<sup>3</sup> in the exhaust gas). The process model assumes 95% NO<sub>x</sub> removal for the combination LNB & OFA & SCR, resulting in 28mg/Nm<sup>3</sup>. Although this combination is commercially available, it has not been widely demonstrated as a combined technology. The removal efficiency might vary in operation from 85% to 95%, which would lead to NO<sub>x</sub> concentrations in the exhaust gas between 28 and 84 mg/Nm<sup>3</sup>, which are still below the emissions reported in the literature.

Moreover, the results of this study show that NO<sub>x</sub> emission factors for the IGCC power plant are higher than for the USC PC power plant. This also contradicts the values retrieved from literature and shown in Table 2.1. One explanation is the lower efficiency of the IGCC power plant of this study compared to the average efficiency presented in Table 2.1. Moreover, the IGCC power plant of this study only includes pre-combustion NO<sub>x</sub> controls, which consist of diluting the feed to the gas turbine with nitrogen. New designs for IGCC plants might incorporate post-combustion SCR technologies to further reduce the NO<sub>x</sub> emissions. If SCR would be applied to the reference plant in this study, the NO<sub>x</sub> emissions for the IGCC case will be reduced from 0.39 kg/MWh (Table 6) to 0.11 kg/MWh, level comparable to the best performance of the USC cases.

Nevertheless, it is important to highlight that the use of SCR in coal IGCC systems is not yet guaranteed. Problems might arise in the form of ammonium sulphate deposits in the HRSG causing corrosion and plugging. For this reason SCR requires high sulphur removal to reduce sulphate formation to low levels. The new build IGCC plants are also designed with deeper sulphur removal to accommodate the SCR. These emission controls result in a substantial reduction in emissions for IGCC [123].

### 2.6.5 $NH_3$ emissions

One major impact of PCC technology is the emission of ammonia [124]. Ammonia is one of the degradation products of amines. The increase in ammonia emissions could be substantial, depending on the resistance of the solvent towards oxidative degradation, which is the main degradation pathway in the case of MEA [125]. Ammonia emissions are correlated to the dissolved metals in solution, specially Fe, therefore maintaining a clean solvent by conventional reclaiming is essential to secure low formation of volatile degradation products such as ammonia.

### 2.6.6 Trace metals

The effect of CCTs in trace metal emissions could not be evaluated in this work due to the absence of important data, such as the interaction of these air pollutants with the different CCTs. A comparison between the IGCC and USC PC cases without carbon capture technology was given in Figure 2.2. The emissions levels are comparable for both cases.

Based on existing knowledge, it can be asserted that the removal rates for particulates have a direct effect in the removal rates of trace metals that are preferentially adsorbed or condensed on particles [93]. Therefore, most of the metals that are enriched in the fly ash during combustion will be captured in the downstream filters (ESP), which are present in all the coal fired power plants analysed.

In the post combustion capture case, part of these metals is also removed in the capture unit. Recent pilot studies [65] show a deep reduction in fine particulates and metals for the  $CO_2$  capture unit. Experiments were performed with a 30% wt MEA solution at 90%  $CO_2$  capture removal present in flue gas from the coal fired station at Esbjerg (Denmark). The reduction has been correlated to the reduction in fines and dust due to the washing and scrubbing effect of the absorber. In principle, the same trend should apply to the case of pre-combustion capture unit with similar absorber design.

Mercury is a volatile metal that is present in the flue gas. Part of the emitted mercury absorbs in the unburned carbon in fly ash and will be removed in the ESP and the capture unit in the same way as the above mentioned metals. The fraction of mercury that does not absorb in the fly ash will be present in flue gas as elemental mercury or as oxidized mercury. The oxidized mercury solubilises in alkaline solutions (such as the ones used in the FGD and post combustion capture units). However, the elemental mercury is not soluble in these solutions and will not be removed. Nevertheless, no pilot studies have been found that have explicitly monitored mercury.

### 2.6.7 Other acid gases

Estimates for hydrogen halides (HCl and HF) have been evaluated for the USC PC case following the modelling methodology. Confirmation on these estimates via the literature database was not possible due to the lack of relevant data at the scale and plant type defined in this case. For this reason, these values are indicative and should be carefully used. Emissions of HCl and HF decrease substantially when CO<sub>2</sub> capture is integrated into the power plant. This is due to the acidic nature of these gases and the alkalinity of the solvent. This impact is also corroborated by recent pilot studies [65]. Nevertheless, more thorough measurements are needed in order to give an accurate estimate on the extension of this reduction.

## 2.7 Conclusions

This study has evaluated the emissions of three power plants with and without CO<sub>2</sub> capture. The methodology assessment was based on the calculation of mass and energy balances of the power plants and the estimation of emissions factors for a selected number of air pollutants. When compared to existing literature data, it was found that the literature derived emissions were higher than the predicted values in this work for most cases with the exception of the IGCC power plant. One possible reason for this observation, is the variability in different air pollution control techniques and its performance. The different trend found for the IGCC power plant was attributed to the lower efficiency of the plant selected for this study, compared to the literature average.

With respect to air pollutant emissions, different effects have been identified depending on the air pollutant:

- SO<sub>2</sub> emissions are significantly reduced together with the reduction in CO<sub>2</sub> emissions for all coal power plant cases. The extent of this reduction depends on the CCT technology applied. The USC PC oxyfuel case has near zero emissions of SO<sub>2</sub>. The USC PC with post-combustion capture shows a drastically decrease in SO<sub>2</sub> emissions. The IGCC also shows SO<sub>2</sub> emissions reduction but to a less extent than in the other cases. No SO<sub>2</sub> is present in NGCC power plants (unless the initial fuel contains traces of sulphur).
- NO<sub>x</sub> emissions are present in all cases investigated (including the NGCC power plant). NO<sub>x</sub> emissions increase due to the deployment of CO<sub>2</sub> capture approximately to the same extent as the increase in fuel use for the post combustion cases (USC PC and NGCC). The other power plant cases show a reduction in NO<sub>x</sub> emissions (USC PC oxyfuel when compared to the USC PC with no capture) or no effect in the case of IGCC.
- Particulates are only emitted in the coal cases and have been a case of contradiction between the literature (which predicts an increase in particulates emissions due to CO<sub>2</sub> capture) and the modelling (which predicts a decrease in particulates and fines when the capture technology is integrated). This is a trend observed for the three coal cases (USC PC with post combustion capture, USC PC oxy fuel and IGCC with pre-combustion capture). For post-combustion capture there are pilot studies that indicate a substantial reduction in particulates and fines and a reduction in trace metals that are typically adsorbed on particulates, such as Fe, Si, and As.

- Ammonia emissions significantly increase when CO<sub>2</sub> capture (based on amine technology) is integrated into power plants due to amine degradation.
- Mercury is a very volatile metal under coal combustion and gasification conditions. Under gasification conditions is mainly present in the form of elemental Hg (g). Under combustion conditions mercury can be in elemental or oxidised form (Hg<sup>2+</sup>). Only oxidized mercury is fully dissolved in alkali solutions and can be partially removed in the FGD and CO<sub>2</sub> absorber. Elemental mercury can be adsorbed in the fly ash (Hg<sub>p</sub>) and char and be removed along with fines. The percentage of mercury that is removed in the air pollution control systems (APCS) depends on the speciation in the flue gas exhausting from the coal combustor and there are many factors that have an effect in the oxidation state of mercury. In the cases analysed, emissions are expected to be slightly reduced in the USC PC power plant with PCC and substantially reduced with oxy-fuel operation due to the CO<sub>2</sub> cleaning process. In the IGCC case the emissions of this pollutant increase due to the application of CCT.

---

# THERMODYNAMIC ASSESSMENT OF NOVEL AMINE BASED CO<sub>2</sub> CAPTURE TECHNOLOGIES IN POWER PLANTS BASED ON EBTF METHODOLOGY

## ABSTRACT

*Post combustion CO<sub>2</sub> capture (PCC) with amine solvents is seen as one of the possible technologies which can be implemented in the near term to significantly reduce CO<sub>2</sub> emissions from fossil fuel power plants. One of the major concerns for its implementation at large scale in power plants is the high capital and operating costs of the technology. This chapter examines the performance of advanced supercritical (ASC) pulverised coal and natural gas combined cycle (NGCC) power plants with two post-combustion CO<sub>2</sub> capture units. The capture units are based on chemical absorption with an advanced amine solvent, CESAR-1, which is an aqueous solution of 2-Amino-2-Methyl-Propanol (AMP) and piperazine (PZ), and the conventional Monoethanolamine (MEA) solvent. The comparison between the mentioned technologies is based on the technical assumptions and method provided by the European Benchmarking Taskforce (EBTF) methodology, which is a first attempt for establishing a common European Standard for comparative studies. The resulting net electric efficiencies for the power plants without capture are 45.25% and 58.3% for the ASC PC and NGCC cases respectively. When CO<sub>2</sub> capture is applied, the net electrical efficiencies of the studied plants decreases. In the ASC power plant, the MEA capture unit decreases the efficiency by 11.7 percentage points, while the CESAR-1 capture unit decreases the efficiency by 9.4 percentage points. For the NGCC power plant, the reductions are 8.4 and 7.6 percentage points for the MEA and CESAR-1 capture units respectively. Therefore, the evaluation of CESAR-1 under the EBTF standards shows a reduction on power production penalty of 25% for the coal fired plant and 12% for the gas fired plant compared to conventional MEA.*

*This chapter is based on:*

*E. Sanchez Fernandez, E.L.V. Goetheer, G. Manzolini, E. Macchi, S. Rezvani, T.J.H. Vlugt. "Thermodynamic assessment of amine based CO<sub>2</sub> capture technologies in power plants based on European Benchmarking Task Force methodology." Submitted to the Chemical Engineering Journal.*

### 3.1 Introduction

Carbon Capture and Storage (CCS) is seen as one of the promising technologies to abate CO<sub>2</sub> emissions from fossil fuelled power plants at a relatively high plant reliability and flexibility level [126, 127]. One of the promising CCS strategies is post-combustion capture (PCC) since it is more easily applicable to existing power plants. However, it must be outlined that oxy-fuel and pre-combustion routes can have other benefits such as reduced efficiency penalties [128, 129].

Among the different technologies that can be applied to PCC, the chemical absorption concept is indicated as one of the best options for short term implementation [16] because it is partially proven at smaller scale and it has been used for different purposes in the process industry [39]. There are various PCC technological options commercialized or under development [10]. A large effort is currently underway to improve the technology readiness of PCC and its integration with the power plants. Large scale demonstration projects are currently under development worldwide: *e.g.* the ROAD project in The Netherlands [130], the NRG project within Clean Coal Power Initiative in the USA [131] and the NewGenCoal Project in Australia [132]. Due to the research efforts, continuous improvements related to the efficiency of PCC technology are made. Therefore, the establishment and definition of baselines to assess the technical and economic potential of new solvents or processes is of importance. In this respect, baseline represents a realistic, reproducible and up-to-date performance of PCC technology that is used as a point of reference for other studies.

The baselines for PCC are constantly under review in order to provide an updated analysis on this technology. For specific technologies, baselines are provided by vendors [133]. There are studies that compare the impact of specific amine scrubbing technologies on the efficiencies of different power plants [13-15, 29] and evaluate the potential improvements (either in solvent formulations or process design) of amine based systems [31]. More recent studies [134] have also provided an updated financial baseline for the implementation of CO<sub>2</sub> abatement technology in power plants.

Most studies focus on defining a baseline for a fixed percentage of CO<sub>2</sub> removal, which varies upon study. Also, alternative capture process schemes based on the Monoethanolamine (MEA) solvent are found in the literature and compared to the same baseline [54-56]. These process schemes focus on decreasing operating costs and, generally, increase the process complexity. This multivariable system characteristic makes the assessment of amine technologies difficult, especially when it is desired to compare between different amine solvents. Other studies, such as Front End Engineering Designs or Conceptual Designs, give the design and overall investment costs of the capture plant as a quote given by the suppliers of the technology [122]. Consequently, these studies cannot be used to assess the influence of process parameters on the overall technical performance. Some authors have overcome this issue by developing models for the analysis of capture processes with the MEA solvent [135-139]. Together with these studies, which provided a very good insight of advantages and drawbacks of PCC technologies, there is also a growing need for harmonizing methodology and assumptions taken for the technical and economic evaluations of capture technologies, in particular when different concepts are being compared. For this reason, the European Commission created a public project to unify the modelling methodologies of the European projects involved in Carbon Capture within the 7<sup>th</sup> framework R&D Programme [90, 140, 141]. This effort has been done within the European

Benchmarking Task Force (EBTF) [21]. Models have been revised (*e.g.* in the CESAR [90] project) and the findings have been used to update the baselines.

This work compares the adoption of an innovative amine based solvent, named CESAR-1 (aqueous solution of 23% w/w AMP (2-amino-2-methyl-propanol) and 12% w/w PZ (piperazine)) [65] to standard MEA solvent. The assessment is based on the EBTF methodology which allows a fast assessment of potential capture solvents. This work also can be used as baseline for assessing other prospective solvent systems in the future. The two solvents and the methodology are applied to two different type of power plants: Advanced Supercritical Coal (ASC) and Natural Gas Combined Cycles (NGCC). The revised technical and economic assumptions are consistent with the benchmarking work performed in other European projects.

## 3.2 Plant description of the selected reference cases (ASC PC and NGCC)

### 3.2.1 ASC PC power plant case

The plant is based on an Advanced Super-Critical (ASC) Boiler and Turbine designed for a gross power output of about 819 MWe without any carbon capture. The general arrangement layout for the reference power plant is based on an inland site with natural draft cooling towers and delivery of the coal by rail. Figure 3.1 shows the power plant scheme. The flue gas that exits the boiler goes through selective catalytic reduction (SCR) to control the polluting nitrogen oxides ( $\text{NO}_x$ ), an electrostatic precipitator (ESP) for particulate removal, and flue gas desulfurization (FGD) to remove the pollutant sulphur dioxide ( $\text{SO}_2$ ) before being released to the atmosphere through the stack. Emission limits for  $\text{NO}_x$  and  $\text{SO}_x$  are assumed equal to  $120 \text{ mg/Nm}^3$  and  $85 \text{ mg/Nm}^3$  (based on dry gas at 6%  $\text{O}_2$ ), respectively [21]. These values represent the average of the emissions levels given by the analysis of best available technologies for coal power plants of the European commission [121]. The mass flow rates and conditions of the streams illustrated in Figure 3.1 are shown in Table 3.1.

### 3.2.2 NGCC power plant case

The selected reference NGCC case for electricity production without carbon capture is based on two large-scale identical gas turbines (GT), “F class”, each equipped with a heat recovery steam generator (HRSG), and a single steam turbine. The plant layout is shown in Figure 3.2. This arrangement is commonly found among utilities, since it adds operational flexibility as required by a competitive electricity market [142]. The HRSG is a three pressure level and reheat type. Before feeding the gas turbine combustor, natural gas is preheated up to  $160^\circ\text{C}$  by means of feed water extracted from the intermediate pressure (IP) drum, increasing the overall plant efficiency. The fuel flow rate to the gas turbine combustor is set to obtain an assumed turbine inlet temperature (TIT) of  $1360^\circ\text{C}$  and air mass flow at compressor inlet is set at  $650 \text{ kg/s}$ . The characteristics of the main streams such as compositions and thermodynamic conditions are reported in Table 3.2.

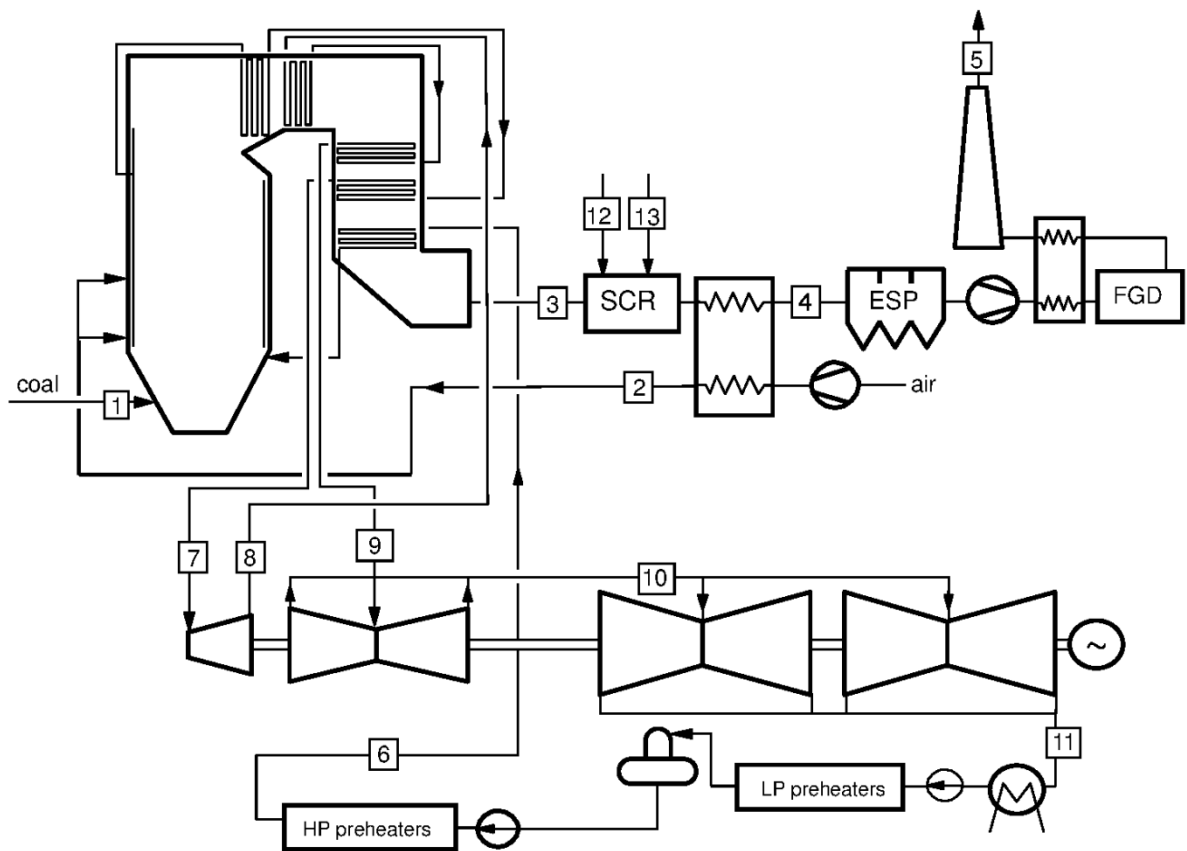


Figure 3.1. Schematic layout of the ASC plant without carbon capture. SCR – Selective catalytic reduction. ESP – Electrostatic precipitator. FGD – Flue gas desulphurization.

### 3.3 Capture plant description of the selected reference cases (MEA and AMP/PZ)

#### 3.3.1 Capture technology selection

Most amine technologies are relatively comparable in terms of flow-sheet configurations. The thermal energy requirement for regeneration is one of the most important process parameters to consider when selecting a specific technology. The thermal energy for regeneration in the Fluor Econamine process (based on MEA and flue gas from coal fired power plants) has decreased from the early values of 4.2 GJ/t CO<sub>2</sub> [133] to 3.2 – 3.6 GJ/t CO<sub>2</sub> [15, 53] thanks to improved solvent formulations, advanced process configurations and the introduction of heat integration. These figures can be further reduced with advanced stripper configurations [54-56]. Besides thermal energy for regeneration, other aspects to consider are the availability and maturity of

the technology, solvent volatility, solvent toxicity, solvent degradation and cost. MEA is used at small scale in three existing power plants in the USA [143]. It has relatively low volatility and is less toxic than other solvents such as piperazine [66]. Moreover, properties of MEA solutions have been widely published in the literature. For these reasons, MEA is historically used as the standard solvent for PCC evaluation and it is a competitive baseline, despite other solvents having a lower thermal regeneration energy (*e.g.* PZ has been reported to consume 2.6 GJ/t CO<sub>2</sub> [63]). With respect to the capture process configuration, a standard flow-sheet of a 30% wt MEA process is used as baseline. The thermal energy consumption of this process is around 3.6 to 3.7 GJ/t CO<sub>2</sub> captured, based on the results of [65]. The energy consumption of the CESAR-1 solvent, for a standard flow-sheet of a 23% wt AMP and 12% wt PZ process is around 3.1 GJ/t CO<sub>2</sub> [65].

**Table 3.1. Mass flow rate, pressure, temperature and composition of the main fluxes of the ASC reference plant (Numbers refer to Figure 3.1).**

Point	Mass flow	T	P	Composition, % mol.					
	[kg/s]	[°C]	[Bar]	Ar	N <sub>2</sub>	O <sub>2</sub>	CO <sub>2</sub>	H <sub>2</sub> O	SO <sub>2</sub>
1	66.6	15.0	-	See coal composition as in Appendix 9.1.3					
2	686.6	15.0	1.0	See Air composition as in Appendix 9.1.1					
3	753.2	377.0	1.0	0.90	74.10	2.90	14.90	7.20	0.00
4	780.5	128.0	1.0	0.90	74.20	3.80	14.10	6.90	0.00
5	782.0	128.0	1.0	0.90	72.00	3.70	13.70	9.70	0.00
6	607.4	306.1	320.0					100.00	
7	607.4	600.0	270.0					100.00	
8	497.1	364.6	64.0					100.00	
9	497.1	620.0	60.0					100.00	
10	440.4	263.6	5.2					100.00	
11	360.1	32.2	4.8 · 10 <sup>-2</sup>					100.00	
12	0.1	9.0	-	Ammonia					
13	2.2	18.0	-	See Air composition as in Appendix 9.1.1					

Notes:

Net Power Output 758.6 MW<sub>e</sub>.

Net Electric Efficiency 45.25% LHV.

### 3.3.2 Capture plant description

The capture plant is designed to capture 90% of the CO<sub>2</sub> contained in the flue gas. Figure 3.3 shows a generic scheme on how the standard capture process is designed for both solvents: MEA and CESAR-1. For the solid fuel case, the flue gas SO<sub>2</sub> content was assumed to be reduced to approximately 30 ppmv for the case without CO<sub>2</sub> capture. Further reduction to 10ppmv is necessary for amine solvents and can be achieved by up-grading the FGD unit or by adding an SO<sub>2</sub> polishing step upstream the CO<sub>2</sub> absorber. For the present study case, FGD system modification was considered. As shown in Figure 3.3, the flue gas is initially pre-treated in the direct contact cooler. At this unit the flue gas temperature is reduced to a suitable level for absorption. In the absorber, the flue gas is brought into contact with the solvent. The CO<sub>2</sub> is chemically bound to the amine solvent and leaves the column at the bottom. The clean flue gas

exits the absorber and it is washed in the washing section to avoid solvent evaporation and balance water in the system. The loaded solvent is sent to the stripper via the lean-rich heat exchanger. In the stripper, the solvent is thermally regenerated. The vapour leaving the stripper is condensed at 40 °C. The condensate is separated from the gas in a flash vessel (40 °C, 1.6 bar) and recycled back to the stripper at the top stage (water reflux). The CO<sub>2</sub> product gas, once separated from the condensate, is compressed, liquefied and pumped to 110 bar as set by storage requirements.

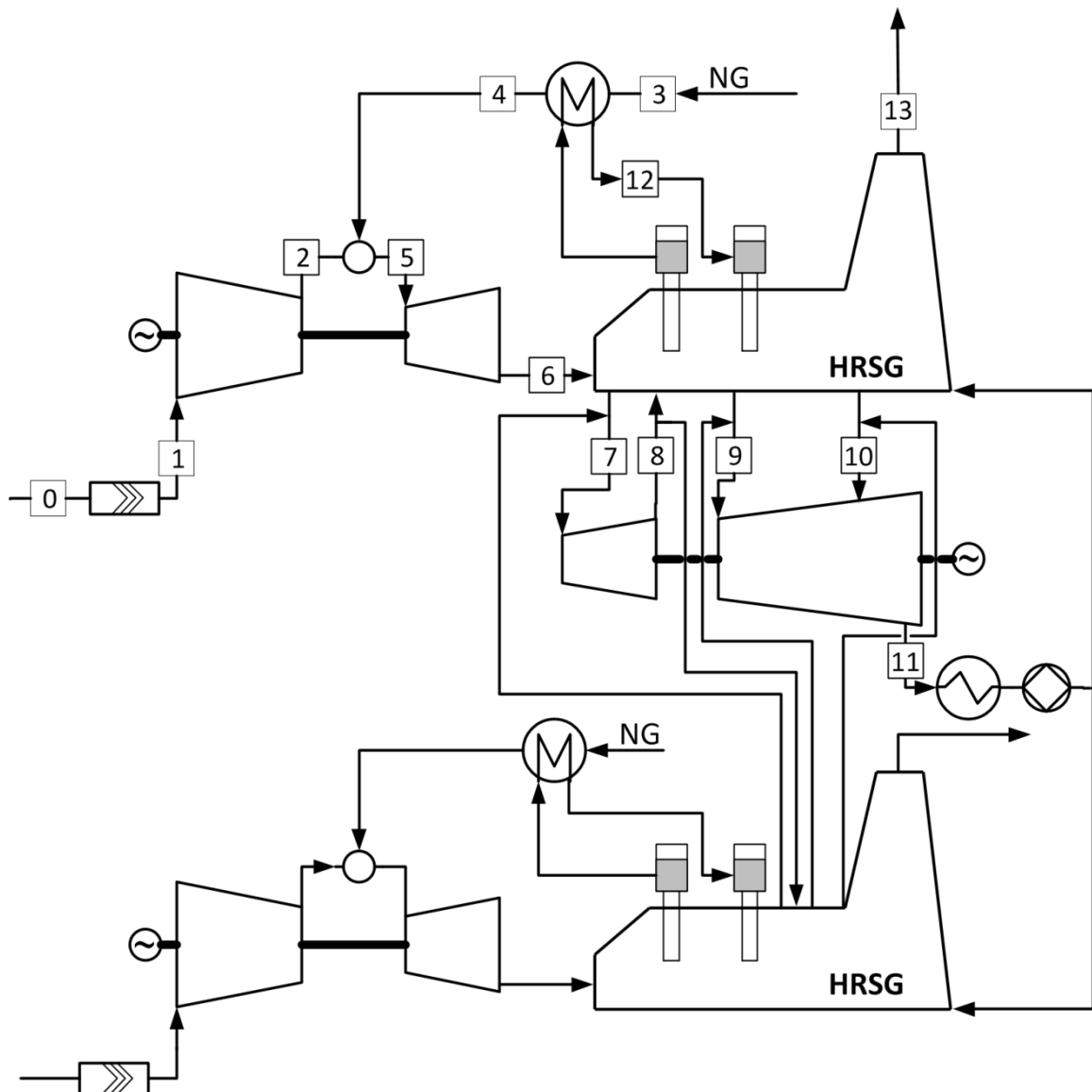


Figure 3.2. Layout of the NGCC plant without carbon capture. NG – Natural Gas. HRSG – Heat recovery steam generator.

**Table 3.2. Mass flow rate, pressure, temperature and composition of the main fluxes of the NGCC reference plant (Numbers refer to Figure 3.2); for point 5 (maximum cycle temperature) the table indicates the three most commonly used definitions in the international literature [142].**

Point	Mass flow	T	P	Composition, % mol.					
	[kg/s]	[°C]	[Bar]	Ar	N <sub>2</sub>	O <sub>2</sub>	CO <sub>2</sub>	H <sub>2</sub> O	NO <sub>x</sub>
0	650.0	15	1.01	Air composition, as in Appendix 9.1.1					
1	650.0	15	1.00						
2	523.4	417.5	18.16						
3	15.3	10	70	NG composition, as in Appendix 9.1.2					
4	15.3	160	70						
5	538.7	COT 1443.3	17.6	0.88	73.71	10.47	4.87	10.07	1.4·10 <sup>-3 a</sup>
		TIT 1360.0							
		TIT <sub>iso</sub> 1265.7							
6	665.3	608	1.04	0.89	74.38	12.39	3.96	8.38	1.4·10 <sup>-3</sup>
7 <sup>b</sup>	153.7	559.5	120.9	-	-	-	-	100	-
8 <sup>b</sup>	153.7	337.7	28	-	-	-	-	100	-
9 <sup>b</sup>	185.0	561	22.96	-	-	-	-	100	-
10 <sup>b</sup>	20.9	299	3.52	-	-	-	-	100	-
11 <sup>b</sup>	205.9	32.2	4.8·10 <sup>-2</sup>	-	-	-	-	100	-
12	6.8	230	28	-	-	-	-	100	-
13	665.3	86.8	1.01	0.89	74.38	12.39	3.96	8.38	1.4·10 <sup>-3</sup>

Net Power Output 829.9 MW<sub>e</sub>.

Net Electric Efficiency 58.3 %LHV.

<sup>a</sup> Value equivalent to 15 ppmv.

<sup>b</sup> Two Gas Turbines.

COT- Combustor outlet temperature.

TIT -Turbine inlet temperature.

The process scheme is essentially the same for both solvents studied in this work. However, there are some differences regarding flue gas cooling and washing sections that depend on the flue gas type and the solvent used. Flue gas cooling depends on the initial conditions of the flue gas and the solvent volatility. For the ASC case, flue gas at FGD outlet is water saturated. Flue gas cooling is achieved by direct contact with water where the excess of water is sent to water treatment system. The final temperature must be controlled in order to limit solvent emissions and close the water balance. Therefore, the temperature depends on the solvent used. The low volatility of MEA allows final temperatures of the exhaust gas of around 50°C without major losses of solvent. These temperatures can be achieved without the gas cooling step. The water balance and exhaust gas temperature are maintained by a small water make-up in one washing section. When the AMP/PZ mixture is considered, the flue gas exit temperature must be reduced to 30°C to avoid substantial evaporation of the solvent. In this case, the flue gas fed to the absorber column needs to be cooled to similar temperatures to avoid water accumulation in the system. After cooling, the flue gas is contacted in the absorber with the solvent mixture. Due to the high volatility of AMP, two washing sections are adopted to decrease the temperature of the flue gas leaving the absorber at 30°C approximately. The final concentration of AMP in the off-gas is below 1ppmv for this case.

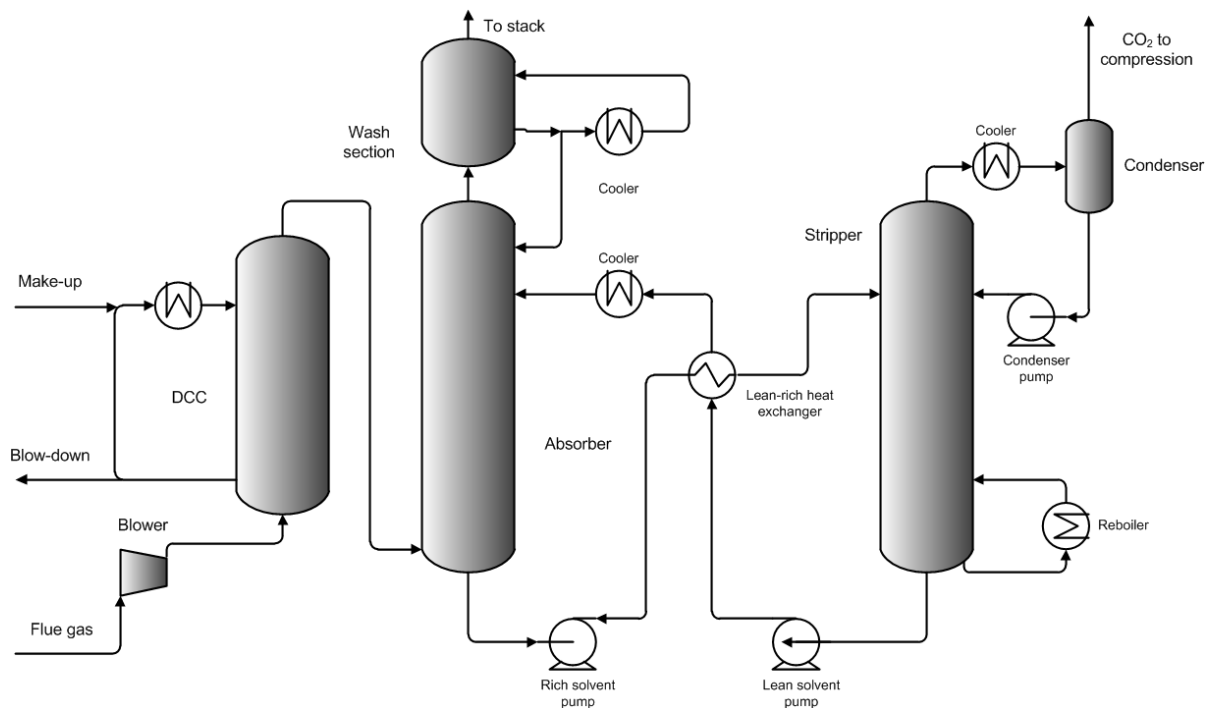


**Figure 3.3. CO<sub>2</sub> capture section. Generic flowsheet for the two solvents investigated: MEA and CESAR-1.**

For the NGCC case, flue gas is not saturated with water. Therefore, flue gas cooling could be achieved by direct contact with water (as in the previous case) or via humidification. Regarding MEA, flue gas temperature is reduced to 40°C with direct contact with water, resembling the coal case. With respect to the AMP/PZ mixture, the flue gas temperature is reduced to 40°C by humidifying the gas. Two washing sections are used to reduce the temperature of the flue gas leaving the absorber to 40°C approximately. The final concentration of AMP in the off-gas is below 3ppmv for this case. Although this case has higher AMP emissions, it requires less cooling water for gas cooling and does not generate a blow down waste water stream. In the case that environmental regulators do not allow this option, the direct cooling system could be also used in this case to reach temperatures of 30°C in the flue gas leaving the absorber and consequently reducing AMP emissions to 1ppmv. The entrainment of solvent droplets or in the form of aerosols has not been included in this analysis. This aspect is also important from environmental and operational aspects. Nevertheless, choosing appropriate demisters reduces entrainment to a level that emissions can be predicted with the present models.

### 3.3.3 Power plant integration

The integration of PCC technology in the power plant will result in plant power output and efficiency reduction, regardless of the solvent system. In this work the capture plant has been integrated in the power plant cycle with the same degree of heat integration for all the solvents evaluated. Therefore, this evaluation shows the effect of the different solvent systems in plant performance.

The reboiler requires a steam pressure of 3 bar. The steam necessary to supply the reboiler is extracted from the steam turbine IP/LP crossover in both NGCC and ASC plants in order to limit steam turbine modification with respect to the reference case. The resulting steam pressure is at 5.2 bar in the ASC case and 4.0 bar for the NGCC case. The steam is then suitably conditioned (through pressure reduction and attemperation) for reboiler use. Steam conditions at the reboiler entrance are 134°C and 3.05 bar. The condensate is returned into the boiler feed water train in the ASC case and to the HRSG feed water train in the NGCC case. No advanced heat integration is included in the design. The investigated cases, assumed a new build power station with carbon capture; it is therefore considered that they would be designed simultaneously and the steam turbines would be optimised for steam extraction at nominal conditions. As the power plant is considered a base load power plant, the effect of the turbine re-design and steam extraction on the efficiency at part load has not been considered.

### 3.4 Methodology

The modelling procedures for the simulation of the power cycles and the capture processes are consistent with EBTF common framework document [21]. A summary of modelling parameters, including fuel and air composition, boiler, turbine and pump efficiencies can be found in Appendix 9.1.

The mass and energy balances of the power cycles were carried out using a proprietary computer code (GS) developed by the GECoS group at the Department of Energy of the Politecnico di Milano to assess the performance of gas/steam cycles [144-147]. The code has been calibrated and is capable of generating accurate estimations of combined cycle's performance. Calibration and accuracy have been described in previous publications [25, 148]. In the coal power plant case, ultrasupercritical live steam parameters (300 bar, 600/620 °C) are selected according to today state-of-the-art large plants. The steam turbine plant consists of HP turbine, IP turbine and LP turbine with extraction points for regenerative heating of feed water and condensate. There are nine feed water heaters that produce boiler feed-water at 315°C. For the gas power plant, the typology of gas turbine considered is large-scale "F class" 50 Hz. There is a triple pressure heat recovery steam generator (HRSG) with single reheat.

The capture process technical data and performance are determined by simulation using Aspen Plus® commercial software. The E-NRTL thermodynamic package was selected to predict CO<sub>2</sub> solubility in the MEA solvent. MEA model parameters were retrieved from MEA data package released in 2008. The absorption process is modelled with three unit operations: direct contact cooler (simulated as a flash unit), absorber and water wash section (simulated with the ASPEN RadFrac® model). The RadFrac® model assumes a sequence of equilibrium stages. Stage efficiencies are considered during sizing of the equipment. The lean-rich heat exchanger is designed on the basis of a fixed overall heat transfer coefficient and a temperature approach of 5°C (cold in-hot out approach). The stripper is also simulated with the ASPEN Radfrac® model. The top two stages serve as a washing section. Moreover, the stripper is designed at a constant molar recovery ratio. This value is used to control the lean loading at which the process operates and its value was selected to adjust the specific heat consumption to the experimental optimum. The experimental values for specific heat consumption from Knudsen [65] were used to fine-tune the models. The CO<sub>2</sub> compressor, consists of four inter-cooled stages with a fixed isentropic

efficiency for each stage equal to 85%. The Peng Robinson equation of state was selected to predict CO<sub>2</sub> properties during compression.

The results of the thermodynamic simulations are expressed in terms of the (net electrical LHV) efficiency, the CO<sub>2</sub> capture ratio (CCR) and the CO<sub>2</sub> avoided, given respectively by:

$$\eta = \frac{\text{Net Power}}{\text{Thermal Power Input (LHV)}} \quad 3.1$$

$$CCR = \frac{\text{CO}_2 \text{ captured}}{\text{CO}_2 \text{ at capture system inlet}} \quad 3.2$$

$$\text{CO}_2 \text{ avoided} = \frac{E_{REF} - E_{CC}}{E_{REF}} \quad 3.3$$

Finally, a measure of the energy consumption related to CO<sub>2</sub> capture is given by the Specific Primary Energy Consumption for CO<sub>2</sub> Avoided (SPECCA, GJ/t CO<sub>2</sub>), which is defined as:

$$SPECCA = \frac{HR - HR_{REF}}{E_{REF} - E} = \frac{3600 \cdot \left( \frac{1}{\eta} - \frac{1}{\eta_{REF}} \right)}{E_{REF} - E} \quad 3.4$$

Where  $HR$  is the heat rate of the plants, (kJ<sub>LHV</sub>/kWh<sub>e</sub>),  $E$  is the CO<sub>2</sub> emission rate, (kg<sub>CO2</sub>/kWh<sub>e</sub>),  $\eta$  is the net electric efficiency of the power plant and the subindexes REF and CC refer to the reference case for electricity production without carbon capture and the case with integrated carbon capture respectively (for the ASC PC and NGCC cases defined in Section 3.2).

## 3.5 Results and discussion

### 3.5.1 ASC PC power plant case

The ASC case was simulated according to the procedures described in Section 3.4. The performance attributes of the power plant with and without carbon dioxide capture using the two solvent systems evaluated in this work are summarised in Table 3.3. Both solvent systems have been modelled to capture 90% of the CO<sub>2</sub> in exhaust gases and have been integrated in the power plant cycle with the same degree of heat integration (Section 3.3).

The power plant has a steam turbine output of 819 MW, with about 60 MW of auxiliaries of which 50% is due to the feed-water pump. The resulting net electric efficiency is 45.25% with specific emissions of 772 kg<sub>CO2</sub>/MWh<sub>e</sub> which are consistent with the state of the art of pulverised coal plants (advanced supercritical and ultra-supercritical plants) [7, 149]. When CO<sub>2</sub> capture is applied, the steam turbine gross power output decreases, because of steam bleeding for solvent regeneration. Boiler and other components are not affected by CO<sub>2</sub> capture.

Regarding the MEA solvent, the steam turbine power output reduces approximately 130 MW (-15%), while auxiliaries consumption remains constant except for heat rejection and extra condensate pump. CO<sub>2</sub> capture consumptions account for 67.4 MW of which 44.8 MW are due to CO<sub>2</sub> compressor work. The solvent recirculation pump requires 9.3 MW because of the high solvent flow rate and absorber height. Resulting efficiency penalty is 11.7% with 86.6% of CO<sub>2</sub>

avoided. The resulting avoidance is lower than the capture rate, because it is calculated as a function of specific emissions, at the same time dependent on the overall plant efficiency, which decreases compared to the reference case.

The innovative solvent named CESAR-1 requires less reboiler heat duty than MEA with benefits for steam turbine gross power output (+35.7 MW than MEA case). Another advantage is the higher capacity, thus reducing solvent flow rates and recirculation pump consumption. The resulting net electric efficiency is 35.9% (+2.4% higher than in the MEA case) with slightly higher CO<sub>2</sub> avoided. Focusing on SPECCA, CESAR-1 has a primary energy consumption of 3.1 GJ/t<sub>CO<sub>2</sub></sub>, which is 25% lower than MEA.

It is of importance to mention that the heat of regeneration obtained for MEA is consistent with the experimental value found by Knudsen [65]. However, the thermal energy for regeneration obtained for CESAR-1 is lower than the experimental value obtained by this author (Section 3.1). One possible explanation for this discrepancy is that the absorption column used by Knudsen [65] is designed for MEA, and, having CESAR-1 slower reaction kinetics than MEA, the approximation to equilibrium obtained in operation does not correspond to the real capacity of this solvent, resulting in higher heat of regeneration. The results presented in Table 5 are obtained by simulation. Regarding the CESAR-1 solvent, the specific heat of regeneration is reduced by 27% compared to MEA.

### 3.5.2 NGCC power plant case

The performances of the NGCC case without capture and the investigated case with CO<sub>2</sub> capture are presented in Table 3.4. The NGCC power plant without capture shows a net electric efficiency of 58.3% which is a value in the range of modern NGCC large power plants [142]. The predicted net electric efficiency penalty for MEA is 8.4 percentage points, predominantly due to lower steam turbine power output (65% of the impact), but also additional auxiliaries. Compared to the ASC case, the efficiency penalty is lower because of the lower specific emissions of natural gas as well as the fact that the steam turbine power share is about 35%, so penalization for steam extraction is lower. Adoption of CESAR-1 as solvent reduces the efficiency penalty for CO<sub>2</sub> capture because of lower reboiler heat duty and reduced recirculating pump consumption.

The calculated SPECCA for MEA is 3.36 MJ/kg<sub>CO<sub>2</sub></sub> which reduces to 2.94 MJ/kg<sub>CO<sub>2</sub></sub> for CESAR-1 (12% reduction). Compared to the ASC case, the advantages of CESAR-1 over MEA are reduced. The main factors affecting this reduction can be found by analysing the different contributions to the overall energy consumption of the CO<sub>2</sub> capture plant:

- Reboiler duty, related to the thermal requirements to regenerate the solvent.
- Auxiliary consumption of pumps and blower. Pump work is related to the solvent capacity. Lower capacities require higher solvent circulation and will lead to higher pump work. Blower work is related to absorber's pressure drop, which has been fixed in the common frame work.
- Compression work. It is equal for both solvent systems per unit CO<sub>2</sub> captured, since the operating pressure of the regenerator is the same.

**Table 3.3. Investigated Advanced supercritical pulverised coal power plant cases with two different solvents for CO<sub>2</sub> capture: Power plant with no capture (ASC PC no capture), power plant with MEA capture process (ASC PC MEA) and power plant with CESAR-1 capture process (ASC PC CESAR-1).**

	ASC PC No capture	ASC PC MEA	ASC PC CESAR-1
<b>Power plant</b>			
Steam turbine [MW]	819.18	686.85	722.56
Feed water pump [MW]	-32.05	-32.05	-32.05
Forced fans [MW]	-3.50	-3.50	-3.50
Induced fans [MW]	-9.60	-9.60	-9.60
Condensate extra pump [MW]	-0.55	-0.28	-0.35
Auxiliaries for heat rejection [MW]	-6.32	-3.06	-3.95
Pulverised coal handling [MW]	-3.33	-3.33	-3.33
Ash handling [MW]	-1.89	-1.89	-1.89
FGD auxiliaries [MW] <sup>a</sup>	-3.32	-3.32	-3.32
<b>CO<sub>2</sub> Capture plant</b>			
CO <sub>2</sub> compression [MW]	-	-44.80	-44.80
Blower [MW]	-	-8.50	-8.50
Pump auxiliaries [MW]	-	-9.30	-4.10
Capture section heat rejection auxiliaries [MW]		-4.80	-5.40
<b>Performance summary</b>			
Net power output [MW]	758.62	562.42	601.77
Thermal power input [MW]	1676.55	1676.55	1676.55
Net electric efficiency [%]	45.25	33.55	35.89
CO <sub>2</sub> emissions [kg CO <sub>2</sub> /MWh <sub>el</sub> ]	771.90	104.30	97.51
CO <sub>2</sub> avoided [%]	-	86.48	87.37
Solvent Regeneration energy [GJ/t CO <sub>2</sub> ]	-	3.70	2.71
SPECCA [GJ/t CO <sub>2</sub> ] <sup>b</sup>	-	4.16	3.07

Notes:

<sup>a</sup> Flue Gas Desulphurization auxiliaries.

<sup>b</sup> Specific primary energy consumption for CO<sub>2</sub> avoided.

Table 3.3 and Table 3.4 show the thermal requirements to regenerate the MEA and the CESAR-1 solvents for the ASC Power plant and NGCC power plant respectively. As shown in these tables, the predicted MEA specific heat of regeneration is higher for the NGCC case than for the ASC case. The reason behind this difference is the lower content of CO<sub>2</sub> present in the NGCC flue gas (ca 4% vol), which requires more energy for separation per unit of CO<sub>2</sub> captured due to the lower driving force.

Regarding the CESAR-1 solvent, the specific heat of regeneration is reduced by 27% for the ASC case and only 15% for the NGCC case. This reduction difference is explained by the different options used in the flue gas cooling unit. The NGCC case with CESAR-1 solvent uses a humidifier that reduces the temperature to only 47°C. This option reduces the cooling costs but the absorber operates at a slightly higher temperature at the bottom of the absorption column than that of the MEA case. At higher temperature, the capacity of the CESAR-1 solvent is lower, resulting in a lower reduction of the regeneration energy compared to the ASC case, where both solvents use the same flue gas cooling option.

**Table 3.4. Investigated Natural Gas combined cycle power plant cases with two different solvents for CO<sub>2</sub> capture: Power plant with no capture (NGCC no capture), power plant with MEA capture process (NGCC MEA) and power plant with CESAR-1 capture process (NGCC CESAR-1).**

	NGCC no capture	NGCC MEA	NGCC CESAR-1
Power plant			
Gas Turbine [MW]	2x272.12	2x272.12	2x272.12
Heat Recovery Steam Cycle [MW]	292.78	215.67	226.5
HRSC auxiliaries [MW]	3.42	3.41	3.41
CO <sub>2</sub> Capture plant			
CO <sub>2</sub> compression [MW]	-	22.60	22.60
Blower [MW]	-	14.96	14.96
Pump auxiliaries [MW]	-	4.65	2.89
Heat rejection auxiliaries [MW]	3.74	4.37	4.27
Performance summary			
Net power output [MW]	829.86	709.92	722.61
Thermal power input [MW]	1422.57	1422.57	1423.57
Net electric efficiency [%]	58.34	49.90	50.76
CO <sub>2</sub> emissions [kg CO <sub>2</sub> /MWh <sub>el</sub> ]	351.67	41.10	40.40
CO <sub>2</sub> avoided [%]	-	88.31	88.52
Solvent Regeneration energy [GJ/tCO <sub>2</sub> ]	-	3.95	3.39
SPECCA [GJ/tCO <sub>2</sub> ] <sup>a</sup>	-	3.36	2.94

<sup>a</sup> Specific primary energy consumption for CO<sub>2</sub> avoided.

### 3.5.3 Comparison with other studies

This section compares the results of the MEA solvent to the data available in the literature. The review is not exhaustive (since that is not the focus of this chapter). Instead, the most recent studies on this topic have been selected for comparison. Table 3.5 compares the main results of this study for the ASC and NGCC cases to other evaluations. Based on the comparison shown in this table, the estimated total power loss per unit of CO<sub>2</sub> captured is comparable to the results of Le Moullec [55] in the ASC case. The small differences in steam turbine power loss (*i.e.* the turbine power loss due to the steam bleed necessary for the reboiler) arise from integration aspects, such as, pressure of the steam stream, conditioning of this steam stream and return of steam condensate in the boiler feed water line. Nevertheless, the estimated reboiler duty is similar. There are also differences in blower and pump consumption. These differences are mainly related to the assumed absorber pressure drop. The EBTF assumption is conservative (100 mbar). The small difference in compression work might be related to different operating pressure in the stripper.

Table 3.5 also compares the main results of this study for the NGCC case to the evaluation of Amrollahi *et al.* [54, 150]. In this case, the steam turbine power loss estimated in this work is about 15% higher than that found in the mention study. Different integration with the power plant could be one reason for this difference. However, differences in the estimated reboiler duties might also play a role. Although the reboiler duty is not explicitly mention in Amrollahi *et al.*, this work has used Aspen Plus for simulation while Amrollahi and co-workers have used Unisim (Honeywell). Differences in the prediction of MEA properties might lead to different reboiler duties, which will explain the different results.

**Table 3.5. Comparison of the ASC and NGCC results to other studies. Solvent is MEA 30%wt.**

	Units	This work	Le Moullec [55]	This work	Amrollahi <i>et al.</i> [150]
Reference Power plant		ASC		NGCC	
Gross power output	MW	819.18	1200	837.02	391.3
Net power output	MW	758.62	not disclosed	829.86	384.3
Gross efficiency	LHV%	48.86	not disclosed	58.84	57.4
Net efficiency	LHV%	45.25	not disclosed	58.34	56.4
Base case capture					
Reboiler duty <sup>a</sup>	GJ/t CO <sub>2</sub>	3.7	3.6	3.95	not disclosed
Abs pressure drop	mbar	100	not disclosed	100	50
Steam turbine power loss <sup>b</sup>	GJ <sub>e</sub> /t CO <sub>2</sub>	0.9	0.95	1.06	0.9
CO <sub>2</sub> compression	GJ <sub>e</sub> /t CO <sub>2</sub>	0.31	0.36	0.31	0.33
Pumps & Blower	GJ <sub>e</sub> /t CO <sub>2</sub>	0.15	0.1	0.27	0.15
Total	GJ <sub>e</sub> /t CO <sub>2</sub>	1.36	1.41	1.64	1.39
Reference power plant + Capture plant					
Gross power output	MW	819.18	1200	759.91	357.8
Net power output	MW	562.42	not disclosed	709.92	335
Gross efficiency	LHV%	40.97	not disclosed	53.42	52.5
Net efficiency	LHV%	33.55	not disclosed	49.9	49.2
Efficiency loss	% points	11.7	11.94	8.44	7.2

Notes: All values are expressed per tonne of CO<sub>2</sub> captured.

<sup>a</sup>[137] reports 3.54-3.6 GJ/t CO<sub>2</sub> for reboiler duty.

<sup>b</sup>[56] reports 0.94 GJ<sub>e</sub>/t CO<sub>2</sub> and [137] reports 0.93 GJ<sub>e</sub>/t CO<sub>2</sub> for Steam turbine power loss.

### 3.5.4 Sensitivity analysis

As shown in the previous section, the selection of different design parameters of the equipment involved in the process, software type and thermodynamic package might influence the results. For this reason, a parametric sensitivity analysis was conducted with the models developed for this study. This sensitivity shows how plant efficiency varies to variations on reboiler duty, pump and blower efficiency and compressor efficiency.

The sensitivity analysis was done by varying one single parameter at a time. The following variations were taken:

- Reboiler duty: -10% to +10% of the nominal result
- Pump efficiency: 75% to 85%
- Blower and Compressor efficiency: 80% to 90%

Results are summarized in Tables 3.6 and 3.7 for the ASC and the NGCC case respectively. As it is appreciable from the Tables, the parameter that mostly affects the results is the reboiler duty. For the MEA solvent, variations of 10% in the reboiler duty will change the net plant efficiency of the ASC and NGCC cases by 2.4 and 1.10% respectively. For the CESAR-1 solvent, the influence is lower, 1.7% and 1.20% respectively. This is important since different software types or amine property data packages might lead to different specific reboiler duty, as also discussed in [151].

**Table 3.6. Sensitivity analysis for the ASC case with MEA solvent and CESAR-1 solvent. Parameters varied are reboiler duty, pump efficiency, blower and compressor efficiencies.**

ASC case with MEA										
	No capture	BASE case	Reboiler duty		Pump efficiency		Blower efficiency		CO <sub>2</sub> compressor efficiency	
Reboiler duty [GJ/t CO <sub>2</sub> ]	-	3.7	3.3	4.1	3.7	3.7	3.7	3.7	3.7	3.7
Pump efficiency [%] <sup>a</sup>	-	80	80	80	75	85	80	80	80	80
CO <sub>2</sub> compressor efficiency [%] <sup>b</sup>	-	85	85	85	85	85	85	85	80	90
Blower Efficiency [%] <sup>b</sup>	-	85	85	85	85	85	80	90	85	85
Net efficiency [%LHV]	45.2	33.5	34.4	32.7	33.5	33.6	33.5	33.6	33.4	33.7
ASC case with CESAR-1										
Reboiler duty [GJ/t CO <sub>2</sub> ]	-	2.7	2.4	3.0	2.7	2.7	2.7	2.7	2.7	2.7
Pump efficiency [%]	-	80	80	80	75	85	80	80	80	80
CO <sub>2</sub> compressor efficiency [%]	-	85	85	85	85	85	85	85	80	90
Blower Efficiency [%]	-	85	85	85	85	85	80	90	85	85
Net efficiency [%LHV]	45.2	35.9	36.5	35.3	35.9	35.9	35.9	35.9	35.7	36.0

<sup>a</sup> Refers to hydraulic efficiency.<sup>b</sup> Refers to isentropic efficiency.**Table 3.7. Sensitivity analysis for the NGCC case with MEA solvent and CESAR-1 solvent. Parameters varied are reboiler duty, pump efficiency, blower and compressor efficiencies.**

NGCC case with MEA										
	No capture	Base case	Reboiler duty		Pump efficiency		Blower efficiency		CO <sub>2</sub> compressor efficiency	
Reboiler duty [GJ/t CO <sub>2</sub> ]	-	4.0	3.6	4.4	4.0	4.0	4.0	4.0	4.0	4.0
Pump efficiency [%] <sup>a</sup>	-	80	80	80	75	85	80	80	80	80
CO <sub>2</sub> compressor efficiency [%] <sup>b</sup>	-	85	85	85	85	85	85	85	80	90
Blower Efficiency [%] <sup>b</sup>	-	85	85	85	85	85	80	90	85	85
Net efficiency [%LHV]	58.3	49.9	50.4	49.3	49.9	49.9	49.8	50.0	49.8	50.0
NGCC case with CESAR-1										
Reboiler duty [GJ/t CO <sub>2</sub> ]	-	3.4	3.0	3.8	3.4	3.4	3.4	3.4	3.4	3.4
Pump efficiency [%]	-	80	80	80	75	85	80	80	80	80
CO <sub>2</sub> compressor efficiency [%]	-	85	85	85	85	85	85	85	80	90
Blower Efficiency [%]	-	85	85	85	85	85	80	90	85	85
Net efficiency [%LHV]	58.3	50.8	51.3	50.2	50.8	50.8	50.6	50.9	50.7	50.9

<sup>a</sup> Refers to hydraulic efficiency.<sup>b</sup> Refers to isentropic efficiency.

### 3.6 Conclusions

This work has provided an updated reference for Post-Combustion Capture (PCC) from fossil fuel power plants based on standard MEA solvent. The underlying assumptions and methods were taken from the benchmarking effort of the European Benchmark Task Force (EBTF), which is a first attempt for establishing a common European Standard for benchmarking and comparison studies. Regarding the benchmark, the chapter has evaluated the performance of two

different types of power plants (Advanced Supercritical Pulverized Coal and Natural Gas Combined Cycle) with and without carbon dioxide capture unit. The results of energy balances are similar to the results obtained in other studies available in the literature. However, larger deviations have been encountered for the NGCC power plant.

This work also shows the application of this method to a more advanced amine solvent, CESAR-1, (mixture of AMP 23%wt and PZ 12% wt). Evaluation of this solvent under the EBTF standards shows a reduction on energy penalty of 25% for the ASC reference plant and 12% for the NGCC reference plant compared to the MEA baseline. On the basis of these results, the better performance of CESAR-1 solvent has been established. Nevertheless, the net efficiency of power plants with capture can be improved by better heat integration between capture and power plant. This later aspect has not been addressed in this evaluation.

There are a number of important issues to consider when benchmarking new scrubbing technologies for post-combustion capture. The two main focus areas are the degree of heat integration and the characteristics of the solvent. With regard to the former, it is important to highlight that higher degrees of heat integration will further reduce the values for power penalty presented here. However, when one is concerned with comparing solvent scrubbing performance special care needs to be taken so all solvents are benchmarked under equal conditions. The standard adopted by EBTF considers a low degree of heat integration. Based on the performance here reported, a separate optimization could be undertaken to investigate the effects of heat integration for every solvent.

The characteristics of the solvent are the other focus area. The design of the capture unit depends on the solvent characteristics such as solvent volatility and toxicity and on flue gas conditions and composition. These aspects need to be carefully considered per case so a plausible design is implemented. In this study, several modifications to the baseline process were included in the capture model for the CESAR-1 solvent due to its higher volatility. These modifications are intended to avoid substantial evaporative losses of this solvent. Finally, process economics are also important for the selection of the preferred technology. A separate study will be dedicated to estimate the economic viability of the described cases (Chapter 4).

---

# ECONOMIC ASSESSMENT OF NOVEL AMINE BASED CO<sub>2</sub> CAPTURE TECHNOLOGIES IN POWER PLANTS BASED ON EBTF METHODOLOGY

## ABSTRACT

*The objective of this chapter is to study the economics of advanced supercritical pulverised (ASC) coal and natural gas combined cycle (NGCC) power plants with post-combustion CO<sub>2</sub> capture units using novel and state-of-the-art solvents. The methodology includes process model developments using commercial simulation programs, which determine the thermodynamic properties of the selected power plants and the performance of the CO<sub>2</sub> capture units. The CO<sub>2</sub> capture units are designed to operate using two different chemical solvents namely mono-ethanolamine (MEA) and CESAR-1 solvent, which is an aqueous solution of 2-amino-2-methyl-propanol (AMP) and piperazine (PZ). The results show that the techno-economic benefit of CESAR-1 vs. MEA is more significant for ASC than that for NGCC due to a higher concentration of CO<sub>2</sub> in the flue gas. This follows from the fact that the switch from MEA to CESAR-1 solvents reduces the electricity cost by 4.16 €/MWh in the case of the ASC plant compared to 0.67 €/MWh in connection with the proposed NGCC plant. Based on the above figures, we can conclude that CESAR-1 reduces the cost of CO<sub>2</sub> avoided compared to MEA by 6 €/t CO<sub>2</sub> and 2 €/t CO<sub>2</sub> for the selected ASC and NGCC plants respectively. In view of that, the techno-economics can be improved if the CO<sub>2</sub> capture plant is designed to operate using the CESAR-1 absorption technology due to a reduction in the regeneration energy and the solvent recirculation rate (considering its higher CO<sub>2</sub> net capacity).*

*This chapter is based on:*

*G. Manzolini, E. Sanchez Fernandez, S.Rezvani, E. Macchi, E. L.V. Goetheer, T. J.H. Vlugt. "Economic assessment of novel amine based CO<sub>2</sub> capture technologies integrated in power plants based on European Benchmarking Task Force methodology" Submitted to the Applied Energy Journal.*

## 4.1 Introduction

Within the power generation sector, post-combustion capture (PCC) is one of the options in the portfolio of CO<sub>2</sub> abatement technologies [10, 12] that will reduce CO<sub>2</sub> emissions from fossil fuels in order to bridge the gap presented by switching from our current fossil-fuel dependency to a low-carbon energy generation. The broad number of innovations in the field, over five hundred patents have been published in the last thirty years [152], confirms the growing interest in technologies related to CO<sub>2</sub> capture. Among the patented CO<sub>2</sub> capture technologies, the majority relate to solvent development, in particular amines. The current state-of-the-art in PCC is amine based absorption systems because the technology is commercially available and it has been proven at smaller scale [16]. The major challenge facing implementation on a large scale is the high capital cost and operating cost of the technology together with an uncertain CO<sub>2</sub> emissions regulation. Information about the cost of CO<sub>2</sub> capture and storage is subjected to extensive research. There are works published in the literature assessing the economics of fossil fuel based plants performed by agencies and independent authors [15, 30, 31, 139, 153-155]. A recent work by Finkenrath [156] summarized and aligned the economic evaluation of fossil fuel based power plants with carbon capture and storage (CCS). The original values from Finkenrath [156] have been calibrated to match the assumptions of this work (values in € 2008). The calculated average of the specific investment cost for ASC plants without capture is about 1398 €/kW (based on bituminous coal) with an increase of 60% when CO<sub>2</sub> capture is applied. The increase is due to both higher capital investment costs and lower net power outputs. The resulting cost of electricity increases from 48 €/MWh for no capture case to 71 €/MWh with capture resulting in a cost of CO<sub>2</sub> avoided of 36 €/t CO<sub>2</sub>. The specific costs of NGCC are significantly lower and equal to 674 €/kW without capture which increases to 1204 €/kW for a capture case. The determined cost of electricity is 48 €/MWh and 59 €/MWh for no capture and with capture respectively. This corresponds to a CO<sub>2</sub> avoidance cost of 44 €/t CO<sub>2</sub>. The cost of electricity increase in the first industrial scale CO<sub>2</sub> capture plant installed in China confirmed the values shown above. In this particular case, the cost of electricity increase was quoted equal to 29% [157]. As a basis for comparison, the cost of CO<sub>2</sub> avoided for renewable energies is in the range of 80-250 €/t CO<sub>2</sub> [158], making CCS a competitive technology from an economic perspective, when carbon abatement is required.

All the costs described correspond to the state-of-the art chemical absorption process based on monoethanolamine (MEA). One important research area to improve PCC performance is the development of novel solvents that require less energy for regeneration and, therefore, lead to lower operating costs than that of the state-of-the-art technology [49, 60, 159]. This chapter examines the economic characteristics of two post combustion capture (PCC) technologies based on chemical absorption integrated within two different fossil fuel based power plants. The first technology is based on the innovative solvent named CESAR-1, which is an aqueous solution of 2-amino-2-methyl-propanol (AMP) and piperazine (PZ) [65]. The second technology is based on monoethanolamine (MEA) and it has been used as a reference baseline for comparison. For both case studies, Advanced Supercritical (ASC) pulverized coal and natural gas combined cycle (NGCC) technologies have been selected for the economic analysis of post-combustion capture based on the mentioned technologies. The economic assessment will determine the impact of CO<sub>2</sub> capture on the cost of electricity and resulting cost to avoid the emission of a unit of CO<sub>2</sub> in

the atmosphere. This work seamlessly ties up with the thermodynamic assessment presented in our previous work [160], which established the potential of the innovative CESAR-1 solvent. Compared to the MEA baseline, CESAR-1 reduces the efficiency penalty points related to CO<sub>2</sub> capture by 2% in the NGCC case and by 6% in the ASC case.

There are however, several issues regarding the reporting of CCS costs. As highlighted in the recent work by Rubin [161], there are differences in methodology, measures for cost estimates and underlying assumptions that are not always explicit in the published cost estimates. When assessing the potential of a new technology, as compared to an already published evaluation of a state-of-the-art technology, these issues are likely to influence the final evaluation of the new technology leading to a certain degree of confusion. With the aim of comparing novel capture technologies to a well-defined baseline, the European Benchmarking Task Force (EBTF) was created by the European commission to unify the modelling methodologies and to align both technical and economic assumptions taken in benchmarking studies of this type, within European projects involved in CCS [90, 140, 141].

The aim of this work is the comparison from economic point of view of the CESAR-1 solvent with the reference solvent, MEA. In line with the best practice guidelines of the European Benchmarking Taskforce (EBTF) [21], the adopted methodology provides a consistent and systematic framework for assessing the techno-economic performance features of power plants with CO<sub>2</sub> capture. For the total plant cost assessment, two different methodologies have been adopted to determine the influence of the method on the results: top-down (TD) and bottom-up approach (BU). In the TD approach, the power plant specific costs were defined and agreed upon in joint effort by the European power plant companies supporting the study (as in the method of [135]). In the BU approach, the cost was estimated by economic models (as in the method of [25]). Further to the estimation of capital investment requirements and electricity costs, a series of sensitivity assessments are carried out to disclose the effect of dominant parameters such as capital investment, fuel price and capacity factor variations as well as discounted cash flow, and operating expenses on the electricity costs. Finally, the CO<sub>2</sub> avoidance costs of the proposed technologies are calculated.

## **4.2 The economic assessment methodology**

The cost assessment in this work is carried out using both top-down (TD) and bottom-up (BU) approach. The BU option relies on a detailed process flow, mass and energy balance, which comprises all the stream and equipment data. The generated information is used to obtain individual equipment cost data either through appropriate economic models published in the literature [162-165] or through specific vendor quotes for each equipment piece. Many chemical process development software packages such as ASPEN, Thermoflow and ECLIPSE [166-168] already include economic evaluation toolboxes for such a cost analysis. This type of cost estimates corresponds to the class II level as defined by Rubin [161]. With regard to the TD approach, historical data from past projects or similar works are gathered in relation to the performance data of the key components, such as the power block, flue gas cleaning train or CO<sub>2</sub> capture plant. Key components generally comprise several integrated equipment pieces and make up a significant share of the overall plant cost. Since it is not always possible to find identical or appropriate analogues, this approach has to be combined with adaptation methods using

mathematical models or cost indices, scaling and complexity factors. This type of cost assessment is similar to the class I cost estimate defined by Rubin [161]. On the grounds of the lack of experience and real-world scenarios, the cost estimation of the CO<sub>2</sub> capture plant is implemented using only a BU approach. The cost for the power plant itself is assessed according to both TD and BU methods. The latter predicated a consistent baseline scenario. The TD approach, on the other hand, offers a kind of validation due to the availability in the literature [156] of a good number of real world analogues.

The BU cost estimation presupposes a deep insight into major cost contributors – detailed equipment lists – and a good knowledge about the relationships among different cost elements. Since only the bare equipment costs are reflected in estimations, further cost factors (installation costs:  $I_i$ ) such as civil, structural and erection costs as well as instrumentation, piping, valves, insulation, electrical and painting needs to be factored in as a percentage of the bare equipment cost. The values will vary from case to case and depend on the equipment types. The possibility of forgetting important elements is one of the major pitfalls. In general, the main cost contributors will account for the high percentage of incurring costs. The set of equations given below show simplified presentations of different cost types. The calculations factor in additional variables such as indirect costs, contingencies and owner's costs as a portion of the total plant cost. Each individual equipment cost is derived from specific equipment costs ( $\sigma_k$ ), as a function of the equipment performance rate ( $r_k$ ), which is made up of dominant variables. The equipment performance rate is made of a factor, which includes extra costs to the base design due to additional functionality and/or improved performance attributes such as material upgrades, additional facilities, or capacities. Moreover, depending on the project complexity, further factors can be added to the equation accounting for higher equipment integrations, soft costs, fixed and variable engineering costs etc.

$$TEC = \sum \sigma_k(r_k) \quad 4.1$$

$$TDPC = TEC \cdot (1 + I_k) \quad 4.2$$

$$EPC = TDPC + TIPC = TDPC \cdot (1 + IC) \quad 4.3$$

$$TPC = EPC \cdot (1 + \beta) \quad 4.4$$

*TEC*: Total Equipment Cost,  $\alpha_i$ : specific equipment cost,  $r_i$ : equipment performance rate, *TDPC*: Total Direct Plant Costs,  $I_i$ : installation cost [%], *EPC*: Engineering Procurement and Construction cost, *IC*: indirect cost percentage relative to the TDPC [%], *TPC*: Total Plant Costs,  $\beta$ : contingency + Owner's Costs [%]

An indirect cost (*IC*) of 14% is applied to the total direct plant costs (*TDPC*) studied in this work making up the Engineering, Procurement and Construction (*EPC*) cost. The total indirect plant cost (*TIPC*) entails outlays such as service facilities, buildings, yard improvements etc. The *EPC* is further inflated to a total plant cost (*TPC*) including a contingency and an owner's cost of 15% ( $\beta$ ).

Regarding the operational costs, the fixed and variable operating costs are induced based on material flow, labour and maintenance requirements. The raw materials and utility requirements were determined by detailed simulations of the power plants with and without CO<sub>2</sub> capture [160]. The maintenance and labour cost have been determined using typical factors and constants from

unit operators and technology suppliers, which are validated over the years, and additional expenditures for overhead costs and insurance. These values were taken from the economic model in [139].

The economic assessment is based on the net present value calculation to achieve a breakeven electricity-selling price (*COE*). The *COE* represents the price that a generator must charge for the electricity supply to the grid system in order to achieve a net present value of zero. The calculation is carried out by subtracting the present value of the net incomes during the plant lifetime from the net present value of the total capital investment. The net income includes the revenue sources through the sale of electricity minus all the expenditures such as fuel, operating and maintenance costs, insurance premiums and taxes. The calculation also includes the interest rates incurred during the plant construction time. Table 4.1 summarises the main assumptions used in the calculation. The sale of potential by-products such as gypsum from the Flue Gas Desulphurisation (FGD) plant is not considered in this chapter. The values in the bracket show the range of values studied in the sensitivity analysis. Further parameters included in the sensitivity analysis comprise specific investments along with operating and maintenance costs.

Finally, the CO<sub>2</sub> avoidance costs are computed covering a plant capital investment requirement of ±30% and a discounted cash flow of between 4% and 12%. This cost excludes the transport and storage charges as these strongly vary from case to case considering factors such as location, topography, geological formations and socio-economic aspects. Apart from improved *COE* and CO<sub>2</sub> capture rates of the plants with CO<sub>2</sub> capture, the calculation also accounts for CO<sub>2</sub> capture energy requirements. Reductions in energy penalties will lower the CO<sub>2</sub> avoidance costs. The CO<sub>2</sub> avoidance cost can be calculated from:

$$\text{Cost of CO}_2 \text{ avoided} = \frac{(COE)_{CC} - (COE)_{REF}}{E_{REF} - E_{CC}} \quad 4.5$$

Where *COE* is the cost of electricity of the plants, (€/kWh), *E* is the CO<sub>2</sub> emission rate, (kg<sub>CO2</sub>/kWh) and the subindexes REF and CC refer to the reference case for electricity production without carbon capture and the case with integrated carbon capture respectively for the ASC PC and NGCC cases.

**Table 4.1. The main economic assumptions used for the economic assessment of the ASC and NGCC power plants based on the EBTF recommendations [21].**

Parameter	ASC	NGCC
Discounted cash flow rate [%]	8 (4-12)	8 (4-12)
Interest during the construction [%]	8	8
Plant life time [Years]	40	25
Plant location	Europe	Europe
Plant capacity factor [%]	85 (40-90)	85 (40-90)
Fuel cost [€/MWh]	3 (1.5-4.5)	6.5 (3.25-9.75)
MEA cost [€/kg]	1.042	1.042
AMP cost [€/kg]	8.0	8.0
PZ cost [€/kg]	6.0	6.0
Activated carbon [€/kg]	2.7	2.7
Process water [€/m <sup>3</sup> ]	6	6
Labour cost [€/h]	45	45
Construction period [years]	4	3
Budget allocation first year [%]	20	40
Budget allocation second year [%]	30	30
Budget allocation third year [%]	30	30
Budget allocation fourth year [%]	20	0
Depreciation & tax	0	0

### 4.3 Total cost assessment of ASC PC and NGCC power plants with CO<sub>2</sub> capture based on MEA and AMP/PZ

In this section, the total costs (investment and operational) of the proposed power plants with integrated carbon capture units are estimated. Following the methods described in the previous section, the capital investment requirements of the power plants are determined based on the TD and BU approaches. The cost for CO<sub>2</sub> capture plants – MEA and CESAR-1 – are calculated using only a bottom-up approach (BU) due to the lack of sufficient historical data. The technical process characteristics of MEA and CESAR-1 absorption processes are described in our previous work [160]. The operational costs are estimated based on the utility requirements estimated in this technical assessment [160] and additional factors as described in the previous section. The costing model and capture process adopted for CESAR-1 is the same as the one developed for MEA. Nevertheless, there are some differences regarding the solvent loss abatement system and solvent degradation with respect to MEA that are addressed in this section.

The capture process is briefly summarised here once again. In the initial phase after the gas cleaning stage, the flue gas is cooled in a direct contact cooler (DCC) to 40 °C before it is fed to the absorber, which facilitates the optimum contact between the flue gas and the solvent. The CO<sub>2</sub> in the flue gas chemically attaches itself to the solvent. The CO<sub>2</sub> loaded product is extracted at the bottom of the absorption column. The remaining gas is clean and can be vented to the atmosphere after a final wash in order to avoid solvent evaporation. The loaded solvent is further processed in a stripper, where it can be thermally regenerated for further use. This process requires a lean-rich heat exchanger to pre-heat the solvent, reducing the stripper heat duty. The stripper is similar to a distillation column where the bottom product is the lean solvent. The overhead gas contains mainly CO<sub>2</sub> and some amount of solvent vapours, which needs to be

condensed using a dedicated heat exchanger and a condenser drum. The condensate is pumped back to the stripper. The CO<sub>2</sub> stream leaves the top of the condenser ready for compression. The circulation of the CO<sub>2</sub> lean and rich solvents are maintained using dedicated pumps. This process is used for MEA and CESAR-1 solvents with the only difference of the solvent loss (higher for CESAR-1) abatement system. In order to limit the evaporation losses of CESAR-1 solvent below 1-3 ppmv, two washing sections (instead of one for the MEA case) have been added on top of the absorber packing.

Solvent degradation is relatively well understood for MEA [44, 45, 113, 116, 125, 169-171]. Several authors have studied the AMP and Piperazine solvent degradation in contrast to MEA. Lepaumier reports an overall degradation rate of AMP that is half of the degradation rate of MEA [172]. On the other hand, Piperazine is known to be more stable than MEA [173]. Based on the extrapolation of the values found from the mentioned references, the following assumptions are taken as the nominal loss for solvents, due to oxidative and thermal degradation, as well as the reaction with other acid gases:

- AMP: 0.5 kg/t CO<sub>2</sub>
- Piperazine: 0.05 kg/t CO<sub>2</sub>
- MEA: 1.5kg/t CO<sub>2</sub> [139]

With regard to solvent costs, it seems difficult to predict accurate and standard market prices for AMP and Piperazine because these solvents are not traded as commodities. At relatively large quantities, Piperazine is sold at around 6 €/kg (Table 4.1). AMP is a more expensive solvent with a price estimated at around 8 €/kg (Table 4.1).

#### 4.3.1 Total cost assessment of the ASC PC power plant case

The EPC cost of the reference ASC case without CO<sub>2</sub> capture is approximated at around 1266 M€ using a TD approach; cost breakdowns are shown in Table 4.2. As indicated, the boiler, which includes gas clean-up, fuel and ash handling as well as heat recovery, represents the element with the highest cost followed by the Balance of Plant and Civil works. The table also juxtaposes the cost estimations according to the BU approach. Similarly, the boiler, which includes fuel and ash handling, ESP (particulates control system), DeNO<sub>x</sub> (NO<sub>x</sub> control system) and FGD (Flue Gas Desulphurisation) constitutes the largest cost component followed by the balance of the plant. In both TD and BU approaches, the flue gas SO<sub>2</sub> content was assumed to be reduced to approximately 30ppmv for the case without CO<sub>2</sub> capture. Further reduction (necessary for amine solvents) can be achieved by upgrading the FGD unit or by adding an SO<sub>2</sub> polishing step upstream the CO<sub>2</sub> absorber. These options may require extra investment and auxiliaries' consumption. The selection of any of these options depends on a close evaluation of solvent degradation and price. For the present study case, FGD system modification costs are considered relatively minor as compared to the other new equipment required in the capture plant [174]. Therefore, they have not been accounted for. The oxidative and thermal degradation of the MEA solvent and the solvent loss due to the irreversible reactions with SO<sub>2</sub> and other acid gases was taken into account during the estimation of operational costs.

**Table 4.2. Cost breakdown of EPC estimation for the reference ASC plant without CO<sub>2</sub> capture. The table shows the percentage contribution to the EPC of the key plant components and the calculated cost for both estimation approaches (TD and BU).**

	TD estimation % of EPC [175]	TD estimation (M€)	BU estimation % of EPC	BU estimation (M€)
Boiler	40	506.3	47	511.6
Turbine Train	7	88.6	9	100.1
Balance of Plant	21	265.8	14	155.7
Generator	3	38.0	4	42.9
Civil Works	13	164.5	8	84.8
Electrical + Instrumentation	6	75.9	9	102.6
Erection/Project Management	10	126.6	9	102.3
Total EPC	100	1265.7	100	1100.0

In connection with the CO<sub>2</sub> capture plant, the cost estimation is only performed according to a BU approach. Table 4.3 shows the main equipment types, cost and the total equipment investment requirements for both MEA and CESAR-1 absorption processes. The main advantage of the CESAR-1 solvent over MEA is its higher net capacity, 94 kg CO<sub>2</sub>/m<sup>3</sup>, versus the MEA baseline, 44 kg CO<sub>2</sub>/m<sup>3</sup> (for ASC power plant flue gas). However, due to environmental constraints the limit of amine emissions of the used solvent (MEA, AMP, PZ) was set to around 1 ppm by volume or less in line with other studies [176, 177]. The previous modelling work [160] predicted that 30 wt% MEA solvent solutions had extremely low emissions using a single wash stage (once through direct contact with process water). However, in connection with the CESAR-1 solvent (AMP, PZ), the AMP emissions were found to be unacceptably high, using a single wash stage, due to its higher volatility compared to MEA. The solution to reduce emissions of AMP consisted of introducing a secondary wash stage, which has a height of 2.5m and the same diameter as the absorber. This height has been proven sufficient for an adequate mixing in the washing section [178]. The packing material selected for the washing section, Mellapak 250Y, is the same as the one used in the entire absorber. Moreover, each washing section consists of a pumped solvent loop. The pumps serving this recycle flow were also added to the equipment list (Table 4.3) and the pump consumption was taken into account in the total auxiliary power consumption of the capture plant. In the case of MEA, an alternative washing equipment was chosen (gas impingement scrubber), which has not been used in the CESAR-1 case due to its lower washing efficiency. Once all the extra equipment is considered, Table 4.3 shows that the overall equipment cost for the CESAR-1 capture plant is lower than that of MEA. The cost differences reflect the physical requirements. The main contributors to the equipment cost (absorber, LRHX and stripper) are considerably smaller (cheaper) due to the higher solvent net capacity of CESAR-1. Table 4.4 shows the total capital requirements covering installation and indirect expenditures for establishing the capture plants. The result for conventional amine process (MEA) is calculated at around 173 M€, which is higher than CESAR-1.

**Table 4.3. Detailed equipment cost (in million €) of the CO<sub>2</sub> capture plant for the ASC case, designed for the MEA and CESAR-1 solvents.**

EQUIPMENT	MEA M€	CESAR-1 M€
Flue gas (FG) blower	2.36	2.17
Lean solvent pump	1.04	0.47
Absorber column	5.96	4.09
Absorber Packing <sup>a</sup>	11.74	8.06
Lean-rich exchanger <sup>b</sup>	10.6	3.54
Lean Liquid cooler	1.50	1.12
Reboiler	3.47	2.7
Stripper	1.75	1.29
Stripper packing	1.57	1.16
Rich solvent pump	0.87	0.47
Condenser	3.12	1.8
Condenser fluid pump	0.05	0.03
Cooling water pump	1.34	1.17
Storage vessel	0.63	0.32
CO <sub>2</sub> compressor	25.9	25.9
Scrubber	0.55	NA
FG direct contact cooler (DCC) <sup>c</sup>	NA	4.33
FG cooling water cooler	NA	1.62
Absorber cooler	NA	3.75
Absorber. washing pumps	NA	0.24
Total equipment cost (TEC)	72.45	64.23

<sup>a</sup> Structure packing Mellapak 250Y [179].

<sup>b</sup> Plate and frame heat exchanger of the Packinox type [180].

<sup>c</sup> Includes column, packing and pumps.

Regarding operational costs, the operation and maintenance costs for the ASC power plant without CO<sub>2</sub> capture is estimated at around 36 M€per annum, according to the information provided by unit operators and technology suppliers [175]. This includes all variable and fixed costs. The variable operating costs reflect all the expenses for consumables such as catalysts, cooling and process water. By-products such as gypsum credit can serve as an additional income. However, this chapter does not include this revenue factor in the economic analysis.

The estimation of the capture plant's operating costs includes the variable costs for chemical solvents, which is based on the overall consumptions, and the fixed costs for maintenance and labour. Table 4.5 summarises the breakdown of the capture plant operating costs. Solvent degradation rates and costs have a significant impact on the capture plant's operating costs.

**Table 4.4. Overall cost of the installed CO<sub>2</sub> capture plant for the ASC case based on the MEA and CESAR-1 solvents. All assumptions are consistent with the EBTF common framework document [21].**

	MEA M€	CESAR-1 M€
Direct costs		
TEC	72.45	64.23
Erection	35.50	31.47
Instrumentation and Controls	6.50	5.78
Piping	14.13	12.85
Electrical Equipment and Materials	8.70	7.71
Civil works	7.96	7.06
Solvent Inventory	6.50	6
<i>TDPC</i>	151.74	135.1
Indirect costs		
Yard Improvements	2.28	2.03
Service Facilities	3.03	2.7
Engineering and Supervision	9.86	8.78
Buildings	6.07	5.4
<i>TIPC</i>	21.24	18.91
<i>EPC (TDPC+TIPC)</i>	172.98	154.01

**Table 4.5 Operating and maintenance cost (O&M) of the CO<sub>2</sub> capture plant for the ASC case. All assumptions are consistent with the EBTF common framework document [21].**

	MEA [M€]	CESAR-1 [M€]
Fixed O&M Costs		
Maintenance and Repairs (M) <sup>a</sup>	5.08	4.5
Operating Labour (OL) and Laboratory Charges <sup>b</sup>	1.24	1.24
Operating Supplies	0.8	0.68
Insurance <sup>c</sup>	3.05	2.72
Plant Overhead Costs <sup>d</sup>	3.73	3.41
Total Fixed O&M costs	13.9	12.55
Variable costs		
Raw Materials <sup>e</sup>	6.2	17.21
Utilities <sup>f</sup>	9.1	5.29
Total variable O&M costs	15.3	22.5
Total O&M Costs	29.2	35.05

<sup>a</sup> 2.5% of TPC [21].

<sup>b</sup> Total operating labour (OL) includes: Labour (2job/shift ) and Supervision (30% of OL) [21, 139].  
Laboratory charges (10% of OL) [21, 164].

<sup>c</sup> 1.5% of TPC [21].

<sup>d</sup> 60% of M+OL [21, 164].

<sup>e</sup> Includes: Solvent Make-up (1.5 kg/t CO<sub>2</sub> for MEA [139], 0.5 kg/t CO<sub>2</sub> for AMP [this work], 0.05kg/t CO<sub>2</sub> for PZ [this work]) and activated carbon (0.075kg/t CO<sub>2</sub> for MEA solvent [139] and 0.0375 for CESAR-1 solvent [this work])

<sup>f</sup> Includes cooling water and process water [21].

The higher resistance to degradation reported for the amines in the CESAR-1 solution [172, 173], implies a positive effect on the solvent replenishment costs. However, the costs of the amines in the CESAR-1 solution have a substantial impact in the variable costs of the CESAR-1 capture plant. As indicated in Table 4.5, the CESAR-1 plant requires higher operating costs compared to the MEA plant, due to the higher price of AMP and PZ. To reduce the operating and maintenance costs of the CESAR-1 plant, an optimised management of solvent is required in order to reduce losses and degradation. It is important to understand the implications of degradation and solvent management on the overall economics of CO<sub>2</sub> capture. In the sensitivity analysis, the costs associated to the solvent losses and degradation are demonstrated in operating and maintenance costs.

Considering the integration of the ASC plant with CO<sub>2</sub> capture, some outlays such as the cost for power and utilities are already included as energy penalty in the overall economics. Furthermore, some plant components in ASC with CO<sub>2</sub> capture are downsized requiring lower operating costs. For this reason, the overall operating and maintenance costs of the power plant with integrated CO<sub>2</sub> capture are not automatically given as a sum of the annual expenses for the reference power plant and the CO<sub>2</sub> capture unit requiring a more detailed analysis.

The detailed results for capital investment requirements, operating costs and cost of CO<sub>2</sub> avoidance are summarised in Table 4.6. The total plant cost is derived as a sum of power plant and CO<sub>2</sub> capture unit EPC with the addition of contingencies (10%) and owner's costs (5%). As previously mentioned, the capital investment requirements of the ASC power plant without CO<sub>2</sub> capture are determined based on the TD and BU approaches. The TD approach, which is based on the information provided by a utility company, seems to provide a slightly higher capital cost. This could be due to a missing cost component outside the mass and energy balances (basis for the BU approach), which probably influences the final capital estimate. Other possible explanation is an over estimation in the budget quote provided (basis of the TD approach), due the timing and characteristics of the cost structure, where it was not completely clear which additional costs were included in each cost category. Therefore, higher contingency figures are recommended for plants with limited empirical knowledge base. For novel plants, contingencies can be higher than 35% [181]. The contingency and owner's costs are fixed to 15%, since the cost estimation refers to an established technology without developing costs and unexpected issues. It is left to the readers to consider and apply appropriate correction factors.

Comparing to the specific investments previously published in the literature for MEA, the results shown in Table 4.6 fall within the expected range. The adjusted capital investment (€2008) for ASC PC with MEA based CO<sub>2</sub> capture unit is reported to be in the range of €1100/kW and €3550/kW for plants with nominal outputs between 500 MW and 800 MW [156, 182-184]. The higher values correspond to smaller plants.

Due to lower energy requirements for solvent regeneration and higher net capacity, the use of CESAR-1 solvent improves the plant efficiency and the plant cost leading to lower specific plant cost. The variable operating cost for CESAR-1 solvent is, however, higher due to the higher price of the solvent's components.

**Table 4.6. The summary of the economic details of the ASC power plant without capture (Conv.) and the ASC power plant with MEA based capture (MEA) and CESAR-1 based capture (CESAR-1).**

Parameter	Unit	Top-down			Bottom-up		
		Conv.	MEA	CESAR1	Conv.	MEA	CESAR1
<b>Power balances and emissions</b>							
Gross power output	MW	819.18	686.85	722.56	819.18	686.85	722.56
Net power output	MW	758.62	562.42	601.77	758.62	562.42	601.77
Thermal input	MW	1676.55	1676.55	1676.55	1676.55	1676.55	1676.55
Net electric efficiency	%	45.25	33.55	35.89	45.25	33.55	35.89
CO <sub>2</sub> emissions	[kg <sub>CO2</sub> /MWh]	771.9	104.3	97.51	771.9	104.3	97.51
SPECCA	[MJ/kg <sub>CO2</sub> ]	-	4.16	3.07	-	4.16	3.07
<b>Economic assessment</b>							
Power plant EPC	M€	1266	1239	1247	1100	1077	1083
Capture plant EPC	M€	0	173	154	0	173	154
Total plant cost	M€	1456	1624	1611	1265	1411	1423
SI (gross)	€kW	1777	2365	2229	1544	2055	1969
SI (net)	€kW <sub>net</sub>	1919	2888	2677	1668	2510	2364
Fuel	M€yr	133	133	133	133	133	133
Fixed O&M costs	M€yr	27	41	42	27	41	42
Var. O&M costs	M€yr	9	24	31.5	9	24	31.5
Total O&M	M€yr	169	198	206.5	169	198	206.5
Fixed O&M costs	€kW <sub>net</sub>	36	73	70	36	73	70
Var. O&M costs	€MWh <sub>net</sub>	1.58	5.69	6.98	1.58	5.69	6.98
COE	[€MWh]	56.29	86.91	82.75	52.87	82.40	78.49
Cost of CO <sub>2</sub> avoided	[€tCO <sub>2</sub> ]	-	45.9	39.2		44.2	38.0

#### 4.3.2 Total cost assessment of the NGCC power plant case

The EPC cost of the reference NGCC case without CO<sub>2</sub> capture is shown in Table 4.7. Based on the TD approach the EPC is approximated at around 514 M€. The original estimate provided by suppliers had to be up-scaled to account for the different power output between the present reference case and that of the estimate provided. Cost breakdowns are also shown in Table 4.7. Since the TD estimate was provided without cost breakdown, this was taken from a recent work of Gas Turbine World [185] which discusses NGCC cost assessment. Regarding the BU approach, the basic equipment cost of the gas turbines and heat recovery steam cycle were taken from [15] and cross-checked with [186]. With this approach, the most expensive component is the gas turbine, and equipment installation accounts for 36% of total plant costs.

The individual equipment costs of the capture units are summarized in Table 4.8. Technical utility data are used to perform this cost estimation. The capture plant design is similar to that used in ASC (refer to Section 4.3 for a short description). The only difference, which had to be taken into account, is the gas composition – the flue gas in NGCC contains less CO<sub>2</sub>. Compared to ASC, the capture section in NGCC application is cheaper since the higher cost for the absorber are more than balanced by lower reboiler and CO<sub>2</sub> compressor costs. In general, the absorption section is more expensive because the CO<sub>2</sub> is more diluted, while regeneration and compression are cheaper for the lower amount of CO<sub>2</sub> captured. Additional expenses such as piping, structural, and civil works, electrical, instrumentation and insulation costs are taken into account using appropriate multipliers and constants. Table 4.9 summarises the overall cost of the capture plant.

Using CESAR-1 the total plant cost is around 146 M€ The total plant cost using the MEA solvent is calculated at around 163 M€ The higher cost of the MEA capture plant is attributed to the elevated energy requirements for solvent regeneration and lower solvent net capacity.

**Table 4.7. Cost breakdown of EPC estimation for the reference NGCC plant without CO<sub>2</sub> capture unit. The table shows the percentage contribution to the EPC of the key plant components and the calculated cost for both estimation approaches (TD and BU).**

	TD estimation % of EPC <sup>a</sup>	TD estimation (M€) <sup>b</sup>	BU estimation % of EPC	BU estimation (M€)
Gas Turbine [M€]	27	138	22	99
Heat Recovery Steam Generator [M€]	12	62	10	46
Steam Turbine [M€]	11	54	9	43
Heat Rejection & miscellaneous [M€]	18	92	11	50
Installation costs [M€]	25	130	36	162
Indirect costs [M€]	8	39	12	56
EPC	100	514 <sup>b</sup>	100	455

<sup>a</sup> Since the supplier of the TD estimate did not provide a cost breakdown [187], the EPC cost breakdown has been taken from [185], based on a NGCC power plant with only 1 gas turbine, total power output of 555.1MW and specific total plant costs of 617.1€/kW.

<sup>b</sup> The TD estimate has been up-scaled from the original value based on total power output.

**Table 4.8. Detailed equipment cost (in million €) of the CO<sub>2</sub> capture plant for the NGCC case, designed for the MEA and CESAR-1 solvents.**

EQUIPMENT	MEA M€	CESAR-1 M€
Flue gas (FG) blower	4.55	4.46
Lean solvent pump	0.58	0.55
Absorber column	10.53	6.70
Absorber Packing <sup>a</sup>	16.90	10.75
Lean-rich exchanger <sup>b</sup>	1.55	0.94
Lean Liquid cooler	1.16	1.01
Reboiler	2.90	2.51
Stripper	1.97	1.47
Stripper packing	0.94	0.70
Rich solvent pump	0.57	0.55
Condenser	2.92	2.28
Condenser fluid pump	0.04	0.04
Cooling water pump	0.89	0.84
Storage vessel	0.50	0.34
CO <sub>2</sub> compressor	17.80	17.80
Scrubber	1.05	0.00
FG direct contact cooler (DCC) <sup>c</sup>	2.45	5.92
FG cooling water cooler	0.68	NA
Absorber cooler	NA	3.64
Absorber washing pumps	NA	0.26
Total equipment cost (TEC)	67.99	60.84

<sup>a</sup> Structure packing Mellapak 250Y [179].

<sup>b</sup> Plate and frame heat exchanger of the Packinox type [180].

<sup>c</sup> Includes column, packing and pumps.

With respect to the operational costs, the information about the operating and maintenance costs for the reference case without CO<sub>2</sub> capture are provided by unit operators and technology suppliers resulting in a total annual value of around €28 million. These costs are consistent with similar publications [31]. The operating costs of the capture plant are given in Table 4.10. The estimation includes the expenses for consumables and chemical solvent make-ups as well as costs for maintenance and labour. With regard to the NGCC plant with CO<sub>2</sub> capture, the operating costs are not given as the sum of the capture and the reference plant since some components have to be downsized. The operating and maintenance costs for the power plant with a CO<sub>2</sub> capture using MEA and CESAR-1 solvents is estimated at around €43 million and €48 million per annum respectively.

**Table 4.9. Overall cost of the installed CO<sub>2</sub> capture plant for the NGCC case based on the MEA and CESAR-1 solvents. All assumptions are consistent with the EBTF common framework document [21].**

	MEA M€	CESAR-1 M€
Direct costs		
TEC	68.00	60.84
Erection costs	34.00	30.42
Instrumentation and Controls	6.12	5.48
Piping	13.60	12.17
Electrical Equipment and Materials	8.16	7.30
Civil works	7.48	6.69
Solvent Inventory	5.78	5.17
TDPC	143.14	128.07
Indirect Costs		
Yard Improvements	2.15	1.92
Service Facilities	2.86	2.56
Engineering and Supervision	9.31	8.33
Buildings	5.72	5.12
TIPC	20.04	17.93
EPC (TDPC+TIPC)	163.18	146.00

Table 4.11 summarises the cost results for the proposed plants. As in the case of the ASC power plant, the specific investment of the NGCC power plant without CO<sub>2</sub> capture differs upon the estimated approach used. The TD approach provides also a higher capital cost than the BU approach. Whether this could be due to a missing cost factor within the BU approach or an overestimation of the TD approach is not certain. This reflects the need to consider carefully the cost method when dealing with economic data and consider the addition or manipulation of contingencies for cases that lack sufficient background knowledge. However, the results shown in Table 4.11 can be validated for the power plants without CO<sub>2</sub> capture (Conv.) with already published data for both approaches. The adjusted cost provided in the literature (following a TD cost estimation approach) suggests values around €720/kW [188]. The chemical plant simulation software ECLIPSE (following a BU cost estimation approach) gives a value at around €665/kW [189].

**Table 4.10. Operating and maintenance cost (O&M) of the CO<sub>2</sub> capture plant for the NGCC case. All assumptions are consistent with the EBTF common framework document [21].**

	MEA [M€]	CESAR-1 [M€]
Fixed O&M Costs		
Maintenance and Repairs (M) <sup>a</sup>	4.68	4.31
Operating Labour (OL) and Laboratory Charges <sup>b</sup>	1.21	1.21
Operating Supplies	0.70	0.65
Insurance <sup>c</sup>	2.81	2.55
Plant Overhead Costs <sup>d</sup>	3.10	3.22
Total Fixed O&M costs	12.50	11.94
Variable costs		
Raw Materials <sup>e</sup>	3.17	10.54
Utilities <sup>f</sup>	6.35	2.95
Total variable O&M costs	9.52	13.49
Total O&M Costs	22.02	25.43

<sup>a</sup> 2.5% of TPC [21].

<sup>b</sup> Total operating labour (OL) includes: Labour (2job/shift ) and Supervision (30% of OL) [21, 139].Laboratory charges (10% of OL) [21, 164].

<sup>c</sup> 1.5% of TPC [21].

<sup>d</sup> 60% of M+OL [21, 164].

<sup>e</sup> Includes: Solvent Make-up (1.5 kg/t CO<sub>2</sub> for MEA [139], 0.5 kg/t CO<sub>2</sub> for AMP [this work], 0.05kg/t CO<sub>2</sub> for PZ [this work]) and activated carbon (0.075kg/t CO<sub>2</sub> for MEA solvent [139] and 0.0375 for CESAR-1 solvent [this work]).

<sup>f</sup> Includes cooling water and process water [21].

Moreover, the capital requirements for the two CO<sub>2</sub> capture plants are estimated using a BU approach. Regarding NGCC with a CO<sub>2</sub> capture, the cost estimations in the literature indicate slightly higher costs between €1200/kW and €1300/kW [139]. This is due to a higher cost of the CO<sub>2</sub> capture unit. However, the BU approach carried out in this work provides the confidence that the post-combustion plant can be established at lower costs.

## 4.4 Economic assessment and sensitivity analysis of the selected case studies

### 4.4.1 Economic assessment of the ASC power plant case

The economics of the ASC fuel power plant are described in this section. The proposed reference power plant without a CO<sub>2</sub> capture requires 4 years to build and it is expected to have a lifetime of 40 years. The default capacity factor is set to 85%. The assumed operating hours per annum are typical of early 2000, where large-scale fossil fuel power plant worked predominantly at base load, with hydro-power and small scale plants as peak-load. Recently, because of increased renewable energy penetrations in many locations, this value has significantly decreased. However, it is difficult to predict the future and the extent, how power plants with CO<sub>2</sub> capture will be adapted to green-energy sources. The COE is calculated at around €6.29/MWh. A reduced lifetime to 25 years increases the cost by around €3.05/MWh. The calculated COE is close to similar work on power plants discussed in Section 4.1.

**Table 4.11. The summary of the economic details of the NGCC power plant without capture (Conv.) and the NGCC power plant with MEA based capture (MEA) and CESAR1 based capture (CESAR-1).**

Parameter	Unit	Top-down			Bottom-up		
		Conv.	MEA	CESAR1	Conv.	MEA	CESAR 1
<b>Power balances and emissions</b>							
Gross power output	MW	833.6	756.5	767.33	833.6	756.5	767.33
Net power output	MW	829.9	709.9	722.6	829.9	709.9	722.6
Thermal input	MW	1422.6	1422.6	1422.6	1422.6	1422.6	1422.6
Net electric efficiency	%	58.34	49.90	50.76	58.34	49.90	50.76
CO <sub>2</sub> emissions	[kg <sub>CO2</sub> /MWh]	351.67	36.15	35.52	351.67	36.15	35.52
SPECCA	[GJ/tCO <sub>2</sub> ]	-	3.30	2.91	-	3.30	2.91
<b>Economic assessment</b>							
Power plant EPC	M€	514	485	493	455	431	438
Capture plant EPC	M€	0	163	146	0	163	146
Total plant cost	M€	591	745	735	523	683	672
SI (gross)	€kW	709	985	958	628	903	876
SI (net)	€kW <sub>e,net</sub>	712	1050	1017	630	962	930
Fuel	M€yr	244	244	244	244	244	244
Fixed O&M costs	M€yr	24	35	37	24	35	37
Var. O&M costs	M€yr	3.9	7.6	10.7	3.9	7.6	10.7
Total O&M	M€yr	271.9	286.6	291.7	272.0	286.6	291.7
Fixed O&M costs	€kW <sub>net</sub>	29	49	52	29	49	52
Var. O&M costs	€MWh <sub>net</sub>	0.63	1.43	2.01	0.63	1.43	2.01
COE	[€MWh]	55.09	70.55	69.88	53.89	69.26	68.59
Cost of CO <sub>2</sub> avoided	[€t <sub>CO2</sub> ]	-	49.0	46.8	-	48.7	46.5

Figure 4.1 shows a summary of the sensitivity assessment of the power plant without capture in connection with 30% variation in capital investment and 50% variations in fuel prices, discounted cash flow rates and operating and maintenance costs. The latter seems to have a relatively minor effect on the electricity costs. The capacity factor – not shown in Figure 4.1- has the highest impact on the economics resulting in a *COE* of around €2/MWh at a DCF of 8% if the assumed capacity factor used in this assessment is reduced by 50%. Considering the power plant cycling rates including shorter start-ups and shutdowns intervals, the above cost will further increase due to part load operations at lower efficiencies as well as higher operating and maintenance costs due to thermal stresses. This analysis does not include the costs of cycling. The capital investment and fuel prices have a moderate influence on the overall economics. However, the effect of capital investment on the electricity cost becomes more significant with increasing discounted cash flow rates (DCF) (not shown in Figure 4.1). That is why it is vital to secure favourable discounted cash flow rates, for example through government supports.

The *COE* for the ASC plant with a CO<sub>2</sub> capture using the MEA solvent is estimated at around €6.91/MWh. The use of CESAR-1 solvent improves the economics by €4.16/MWh resulting in an expected *COE* of €2.75/MWh. The *COE* is greatly influenced by plant efficiency. The lower energy requirements of the CESAR-1 solvent (compare to that of MEA) contribute to a reduction in the *COE* and CO<sub>2</sub> avoidance costs. The overall sensitivity analysis is summarised in Figure 4.2 showing specific investment and fuel cost variations as main parameters. The default *COE* value culminates to €1.5/MWh for MEA and €7.0/MWh for CESAR-1 if the plant lifetime is reduced

to 25 years (not shown in the figure). There are many other parameters affecting the economics. Capacity factor and DCF are among the most significant ones. Fixing all the other parameters to the default value, a low DCF value down to 4% will be conducive to achieving significantly lower electricity costs (€75/MWh for MEA and €72/MWh for CESAR-1). Plant operations below the base load will considerably affect the economics. A 50% lower capacity factor (3500 hours per annum) will lead to a much higher *COE* at around €142/MWh for MEA solvent and €135/MWh for CESAR-1. These values do not include the cost incurred due to the plant cycling.

The  $\text{CO}_2$  avoidance cost for the ASC plant with  $\text{CO}_2$  capture using MEA solvent is around €45.87/t  $\text{CO}_2$ , which is higher than average values found in literature (39 €t $\text{CO}_2$  assuming a currency exchange change €\$ of 1.3). The use of CESAR-1 solvent improves the avoidance cost to €39.25/t  $\text{CO}_2$ . Figure 4.3 shows the  $\text{CO}_2$  avoidance cost sensitivity in relation to the discounted cash flow variation and different specific investments. The default value corresponds to the one given in Table 4.6 for TD approach.

#### 4.4.2 Economic assessment of the NGCC power plant case

This section describes the economics of the proposed NGCC power plants. The assessment results in a typical *COE* of around €55.09/MWh for the power plant without capture considering a construction time of 3 years and a plant lifetime of 25 years. The determined *COE* is about 5 €/MWh higher than the average cost determined in similar works even with similar investment costs. This is because, differently from ASC, more than 50% of *COE* in NGCC depends on fuel price (which is more expensive in EU than in America) [163]. Hence, the assumption on fuel price has significant impact on the overall result.

Figure 4.4 illustrates the sensitivity assessment of the plant in connection with some dominant parameters. In contrast to ASC, a higher fuel price and lower capital investment is required for this technology. This characteristic makes the plant economics to be more sensitive to fuel price fluctuations than to other factors such as the capital investment, DCF or operating and maintenance costs. The effect of capacity factor is slightly below that of the fuel price. The NGCC plant with  $\text{CO}_2$  capture using MEA solvents requires a *COE* of €70.55/MWh. This is considerably lower than that of ASC due to lower capital requirements and higher efficiencies. Only a negligible cost improvement can be achieved by using CESAR-1 solvent in the NGCC plant with  $\text{CO}_2$  capture. This can be attributed to the fact that the gas composition unlike ASC contains lower amount of  $\text{CO}_2$  resulting in lower partial pressures. This property necessitates higher solvent recirculation rates and higher regeneration energy. Furthermore, the operating costs are increased due to a higher price of solvent's amine components. The electricity price of NGCC with  $\text{CO}_2$  capture using CESAR-1 solvent is given at around €69.88/MWh.

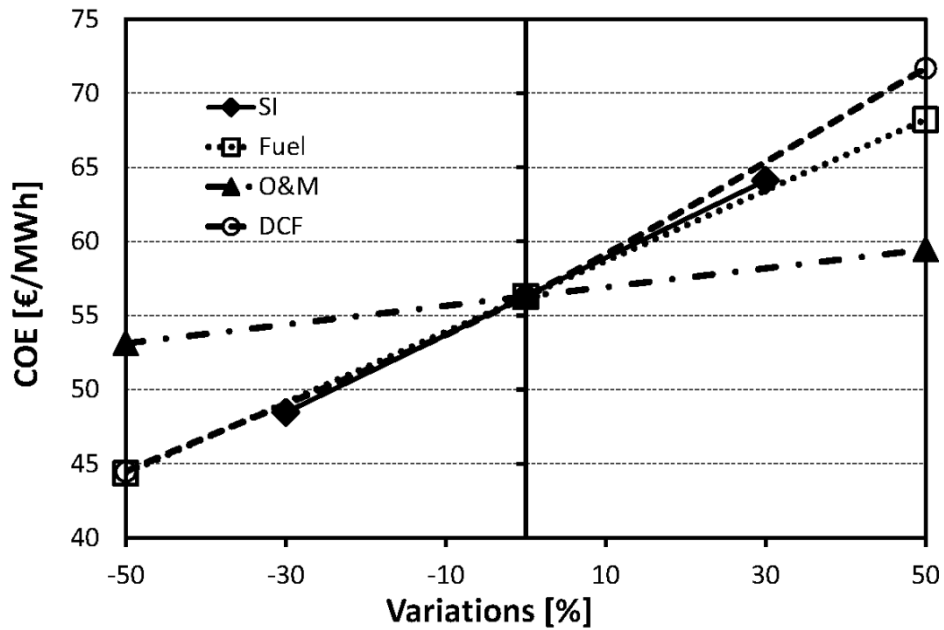


Figure 4.1. The economics of the ASC power plant without capture. The figure illustrates the influence of single variations in specific investment (SI), fuel price (Fuel), operational and maintenance cost (O&M) and discount cash flow rate (DCF) on the cost of electricity (COE) at a constant capacity factor (85%).

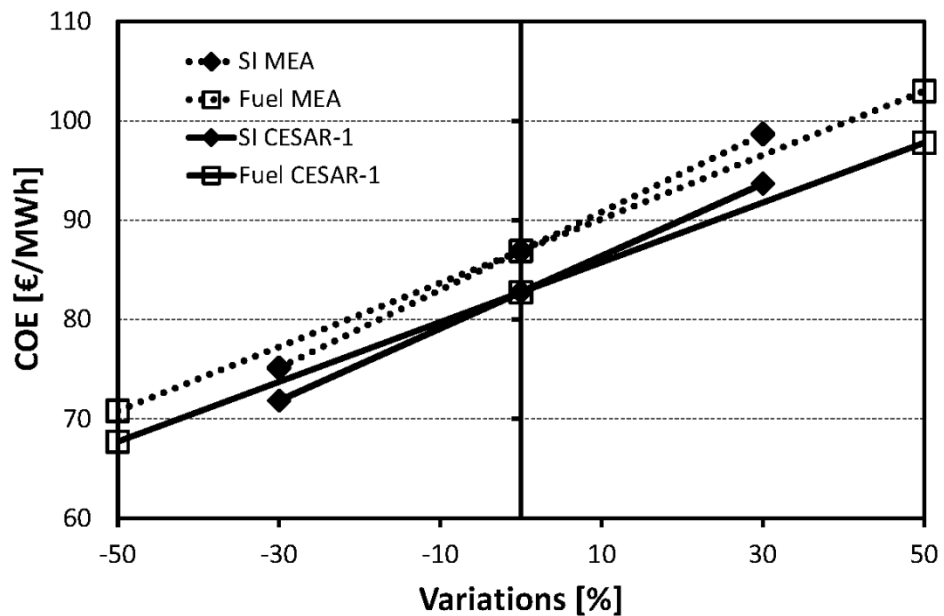


Figure 4.2. The economics of the ASC reference case using MEA and CESAR-1 solvents for CO<sub>2</sub> capture. The figure illustrates the influence of single variations in specific investment (SI) and fuel price (Fuel) for both solvent systems (MEA represented by dotted lines and CESAR-1 represented by continuous lines) on the cost of electricity (COE) at a constant capacity factor (85%) and constant DCF (8%).

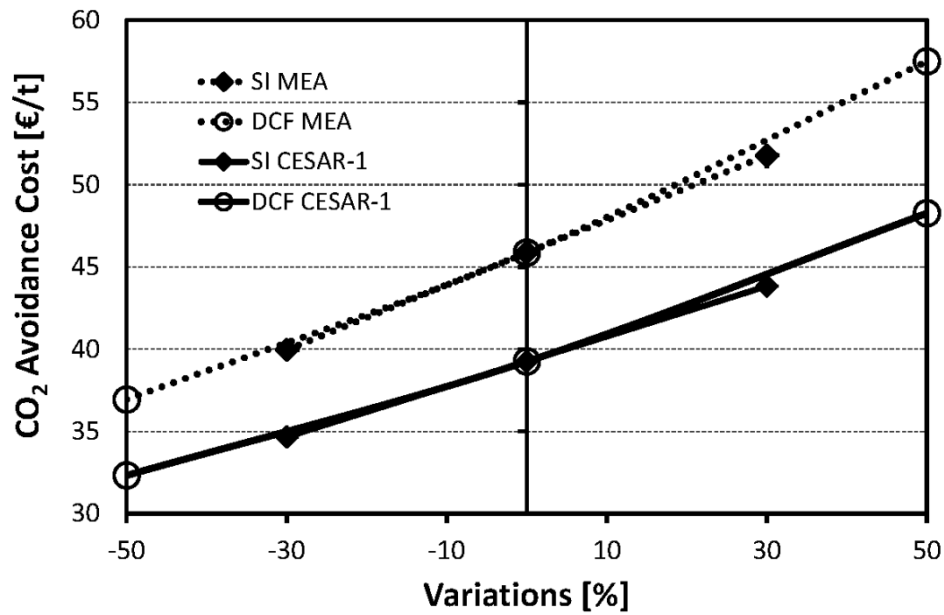


Figure 4.3. CO<sub>2</sub> avoidance costs of the ASC reference case with MEA and CESAR-1 solvents. The figure illustrates the influence of single variations in specific investment (SI) and discount cash flow (DCF) rate for both solvent systems (MEA represented by dotted lines and CESAR-1 represented by continuous lines) on the CO<sub>2</sub> avoidance cost at a constant capacity factor (85%).

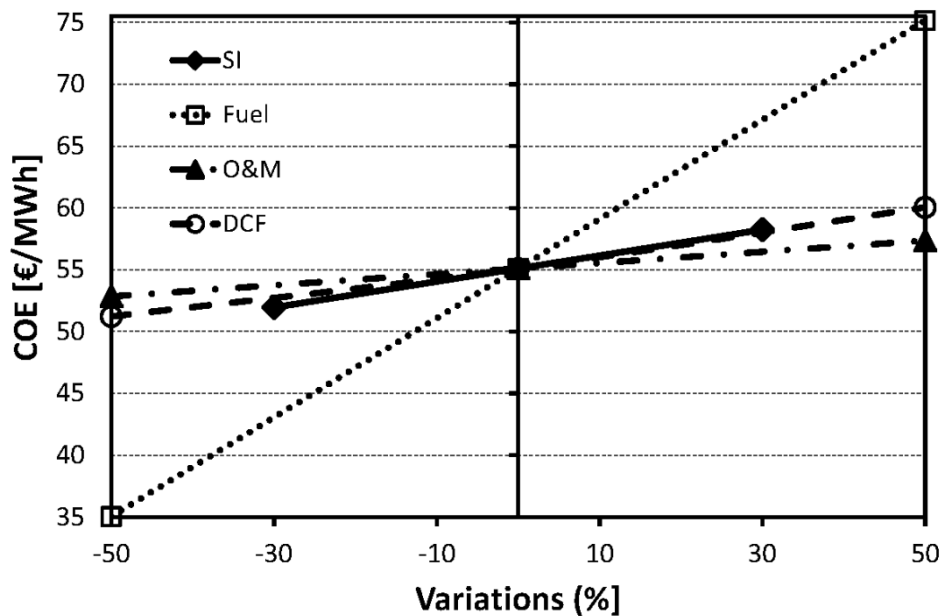


Figure 4.4. The economics of the NGCC reference case without CO<sub>2</sub> capture. The figure illustrates the influence of single variations in specific investment (SI), fuel price (Fuel), operational and maintenance cost (O&M) and discount cash flow rate (DCF) on the cost of electricity (COE) at a constant capacity factor (85%).

Figure 4.5 shows the economic sensitivity of the plant using both solvent types. The *COE* sensitivity behaviour in connection with DCF is similar to Figure 4.4. The effect of operating and maintenance costs is however, amplified due to a higher costs of operating the CO<sub>2</sub> capture plant resulting in a cost variation between €7/MWh and €15/MWh. With regard to the capacity factor, *COE* increases above €6/MWh at a capacity factor of 40%. As mentioned before, this value does not include the costs associated to plant cycling. The CO<sub>2</sub> avoidance cost for the NGCC plants with CO<sub>2</sub> capture using MEA solvent is estimated at around €48.98/t CO<sub>2</sub> compared to that of CESAR-1 solvent, which requires €46.77/t CO<sub>2</sub>. The cost of CO<sub>2</sub> avoided for MEA is close to data available in literature. The CO<sub>2</sub> cost sensitivities are summarised in Figure 4.6.

### 4.5 Conclusions

The economics of advanced supercritical pulverised fuel (ASC) and natural gas combine cycle (NGCC) power plants with CO<sub>2</sub> capture were evaluated using the novel solvent CESAR-1, which is an aqueous solution of AMP and PZ, and compared to the MEA solvent. The capital cost evaluation of the reference power plants without CO<sub>2</sub> capture has been performed using both the bottom-up (BU) and the top-down (TD) approach. The former method uses the mass and energy balance to obtain individual equipment cost data through appropriate economic models. The TD approach, on the other hand, requires a good knowledgebase from past projects.

With regard to the ASC reference case, the specific investment found by the TD approach is €1919/kWe<sub>net</sub> for the power plant without carbon capture. This value is incremented by 50% when MEA based CO<sub>2</sub> capture is implemented and by 39% when the CESAR-1 based CO<sub>2</sub> capture is implemented in the power plant. The values for specific investment found by the BU approach are around 13% lower for all cases. With regard to the NGCC reference case, the specific investment found by the TD approach is €712/kWe<sub>net</sub> for the power plant without carbon capture. The specific investment increases by 47% when MEA based CO<sub>2</sub> capture is implemented and by 43% when the CESAR-1 based CO<sub>2</sub> capture is implemented in the power plant. When the BU approach was applied, the specific investments found to be 8%-12% lower, depending on the case. It is not clear why TD shows higher specific investments costs compared to the BU approach. This could be due to missing cost factors within the BU approach or an overestimation of the TD approach due to uncertainties or inaccuracies in past project quotes.

The CO<sub>2</sub> avoidance cost for the ASC plant with CO<sub>2</sub> capture using MEA solvent is around €45.9/t CO<sub>2</sub>, which is reduced to €39.2/t CO<sub>2</sub> with the use of CESAR-1 solvent. In the case of the NGCC plants with CO<sub>2</sub> capture using the MEA solvent, the CO<sub>2</sub> avoidance cost is estimated at around €49.0/t CO<sub>2</sub> compared to that of CESAR-1 solvent, which requires €46.8/t CO<sub>2</sub>. The above values do not include the cost of transport and storage. The better performance of the CESAR-1 solvent over MEA is related to the higher net capacity of the solvent and the lower energy requirements for regeneration.

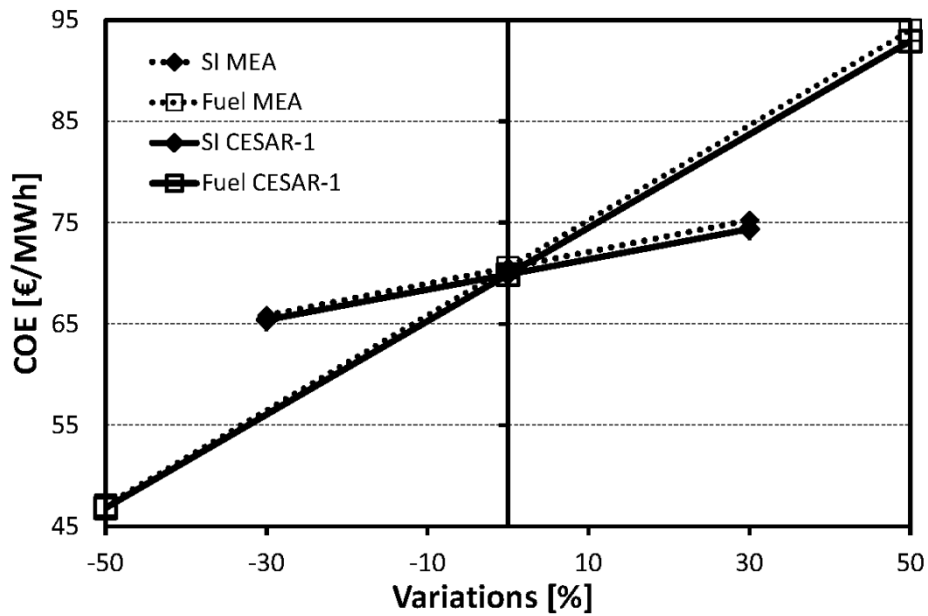


Figure 4.5. The economics of the NGCC reference case using MEA and CESAR-1 solvents for CO<sub>2</sub> capture. The figure illustrates the influence of single variations in specific investment (SI) and fuel price (Fuel) for both solvent systems (MEA represented by dotted lines and CESAR-1 represented by continuous lines) on the cost of electricity (COE) at a constant capacity factor (85%).

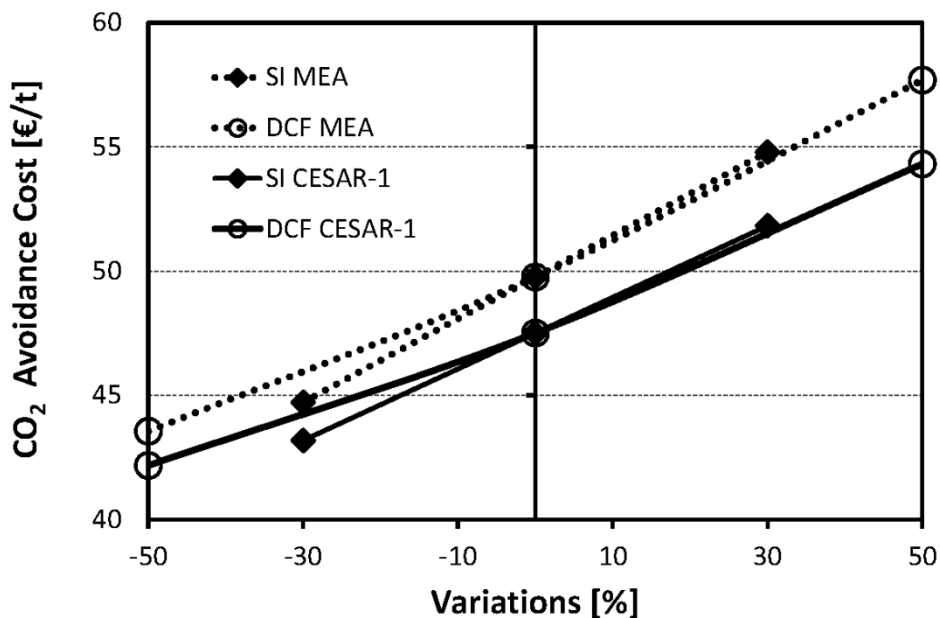


Figure 4.6. CO<sub>2</sub> avoidance costs of the NGCC reference case with MEA and CESAR-1 solvents. The figure illustrates the influence of single variations in specific investment (SI) and discount cash flow (DCF) rate for both solvent systems (MEA represented by dotted lines and CESAR-1 represented by continuous lines) on the CO<sub>2</sub> avoidance cost at a constant capacity factor (85%).

The study has finally implemented a series of sensitivity analysis to show the impact of dominant parameters on the *COE* and CO<sub>2</sub> avoidance cost. Reduced CO<sub>2</sub> avoidance costs necessitate measures such as government supported discounted cash flow rates and/or adequate CO<sub>2</sub> market costs as part of the emission trading to ensure viability. In connection with the CESAR-1 solvent introduced in this study, it can be concluded that the techno-economics can be improved if the CO<sub>2</sub> capture plant is designed to operate using this absorption technology due to a reduction in the solvent recirculation rate (connected to its higher CO<sub>2</sub> net capacity) and in the regeneration energy within the system. The benefits become more significant when the flue gas contains higher concentrations of CO<sub>2</sub> (such as the ASC case).

---

# OPTIMISATION OF LEAN VAPOUR COMPRESSION BASED ON NET PRESENT VALUE MAXIMISATION

## ABSTRACT

*Many process schemes have been proposed in literature to decrease the energy demand of amine based carbon dioxide processes. These process schemes are generally analysed in terms of energy demand savings and compared to a common baseline based on the solvent monoethanolamine (MEA). In this work, the application of one of these process schemes (Lean Vapour Compression or LVC) has been evaluated and optimised based on maximising the net present value (NPV) of the process scheme savings (including capital investment), rather than minimising energy demand in the form of equivalent work. Two scenarios have been analysed. In the first scenario, the capture plant was fully adapted to the effect of LVC. In the second scenario, LVC is retrofitted to a basic capture plant design. For both scenarios the net present value (expressed in M€) of the process scheme over the whole plant life was calculated as a function of the LVC operating conditions. It was found that the NPV of the LVC process scheme is always positive and attractive from a financial point of view. The first scenario has been identified as the most attractive scenario for LVC application. Although the extent of the savings depends on design conditions and financial assumptions, this approach shows that the optimisation based on minimising equivalent work does not necessarily match the optimisation based on maximising net present value.*

*This chapter is based on:*

*E. Sanchez Fernandez, E. J. Bergsma, F. de Miguel Mercader, E. L.V. Goetheer, T. J.H. Vlugt. "Optimisation of lean vapour compression (LVC) as an option for post-combustion CO<sub>2</sub> capture: Net present value maximisation." International Journal of Greenhouse Gas Control 11S (2012) S114–S121.*

## 5.1 Introduction

Amine CO<sub>2</sub> absorption systems are considered as the most suitable technologies to capture carbon dioxide from flue gases in the power sector. The reasons behind this technological choice are, among others, the availability and reliability of the technology (already proven at smaller scale) and the possibility of retrofitting existing power plants [16, 190]. One major hurdle in the implementation of these technologies at large scale is the cost of carbon dioxide capture, which prevents utility companies from making the necessary investments. This cost varies per capture process and per power production process [14, 135, 156, 191]. In the case of bituminous coal fired power plants the cost of electricity can increase in the range 46% - 77% [156]. The reduction of this huge impact in electricity cost will be a condition for the application of CO<sub>2</sub> capture as a carbon abatement technology. In order to reduce costs, one of the main focuses of CO<sub>2</sub> capture research is the reduction of its energy demand. There are two main research lines to reduce energy demand: improvements in solvent formulation or improvement in the capture process for an existing solvent formulation. This research is concerned with the latter option.

There are different process schemes proposed in the literature to decrease the operating costs of the CO<sub>2</sub> capture process. Normally, new process schemes are evaluated and compared to a conventional amine scrubbing process based on monoethanolamine (MEA), which has become a common baseline for capture processes [21]. These schemes can be classified in three groups, depending on the type of modification introduced with respect to the baseline [106]:

- 1) Operating modifications without addition of new unit operations to the process.
- 2) Minor process modifications with limited number of new unit operations added to the process.
- 3) Major process modifications. In this category fall the more complex changes to the capture process, such as, intermediate stripper heating (which requires full modification of the stripper), integration of stripper and compressor, etc.

This work is focused on the second group and, more specifically on the LVC scheme. This scheme includes flashing the lean hot stream that leaves the stripper in a conventional amine scrubbing process, re-compressing the vapour formed and re-injecting it at the stripper's base (definitions and description of a conventional MEA process are further explained in the following sections in this chapter). This simple arrangement allows for partially recovering the sensible heat of the hot lean stream in the form of latent heat and, it is anticipated, that has potential to reduce energy demand without increasing greatly process complexity.

There are various studies in the literature that have addressed this process scheme and investigated its effect in capture performance in various ways. Van Wagener and Rochelle [192] included lean vapour compression in their study on stripper configurations. Their work is based on the minimisation of equivalent work in the stripper and indicates the benefits of stripping at higher pressures (above 6 bar). However, their evaluation is only concerned with the stripper optimisation and the absorber is left out of scope. Le Moullec and Kaniche [55, 106] have also investigated lean vapour compression in a technical evaluation of process options. This study includes integration aspects with the host power plant and shows a reduction in plant efficiency penalty from 11.95% (penalty points) to 11.2% (penalty points) for LVC, which is the highest

reduction given in their work when only minor modifications to the process are considered. Nevertheless, extra investments required for the application of LVC to the conventional MEA process are not taken into account in this study. The evaluation method is only based on the minimisation of the plant efficiency penalty. Karimi et al [137] have also included this option in a techno-economic review of process capture options. In this work, LVC is also addressed and the authors conclude that it will reduce equivalent work by 9.37% with respect to a standard MEA plant at the expense of increasing capital investment by 2.78%. In this case, the optimal operating conditions of the LVC are initially found by minimizing energy demand and capital investments are considered in a second stage for an energy optimized design.

In this study, the effect of the application of LVC on a conventional MEA capture process has also been investigated. The focus in this chapter is on the design modifications, associated capital investments and optimisation of operating conditions. As opposed to the studies above mentioned, the method applied here consists in optimising process conditions based on financial analysis rather than energy analysis. The study is restricted to a conventional design of a MEA plant that could be easily implemented in relatively short term. Therefore, high pressure desorption has been left outside of this chapter's scope. Two different scenarios are analysed: Optimised design of a standard MEA plant with LVC and retrofit of LVC to an existing standard MEA plant. For each scenario, operating conditions are evaluated and optimised based on maximising the Net Present Value (NPV) of the process modification.

This chapter is organised as follows. In Section 5.2, the methodology is described. The reference capture process, LVC design boundary conditions and modelling technique are addressed in this section. The findings, which include among others the financial benefit of implementing LVC regardless the scenario considered, are summarized in Section 5.3. For the two scenarios considered, the energy demand of the process and the net present value of the process, are discussed and compared to other literature sources in Section 5.4. Finally, the conclusions are summarised in Section 5.5.

## 5.2 Methodology

### 5.2.1 Reference case plant description

The scenarios analysed in this work are compared to a reference case, in which a 30% w/w MEA solution is used to capture 90% of the CO<sub>2</sub> present in a given flue gas stream. The reference case, here referred to as a standard MEA plant, is schematically depicted in Figure 5.1. The plant processes 254 kg/s of flue gas containing 13.75 mol% CO<sub>2</sub>. This stream is a split stream of the flue gas generated by a 1070MW Advanced Supercritical coal fired power plant and is 250 MWe equivalent [122]. The flue-gas is fed to the absorber (C-01), where it is brought in contact with the solvent, which flows downwards over a packed bed. In order to minimise MEA losses, the CO<sub>2</sub> lean flue-gas is washed and cooled in two washing beds at the top of the absorber. The resulting scrubbing liquid is cooled with cooling water in a separate cooler (E-05). The CO<sub>2</sub> rich solvent is pumped to the stripper (C-02) via a counter current lean-rich heat exchanger (LRHX) (E-03). In the stripper, the chemically bound CO<sub>2</sub> is removed from the solvent in a packed bed at the expense of reboiler heat. The reboiler (E-01) receives all solvent leaving the bed and partially

vaporizes the stream before feeding it to the stripper sump. Most of the water in the CO<sub>2</sub> stream leaving the stripper is condensed (E-02) and fed to a washing section at the top of the stripper. The lean liquid is pumped through the lean-rich exchanger and cooled to 40°C in a cooler (E-04) before being sent back to the absorber.

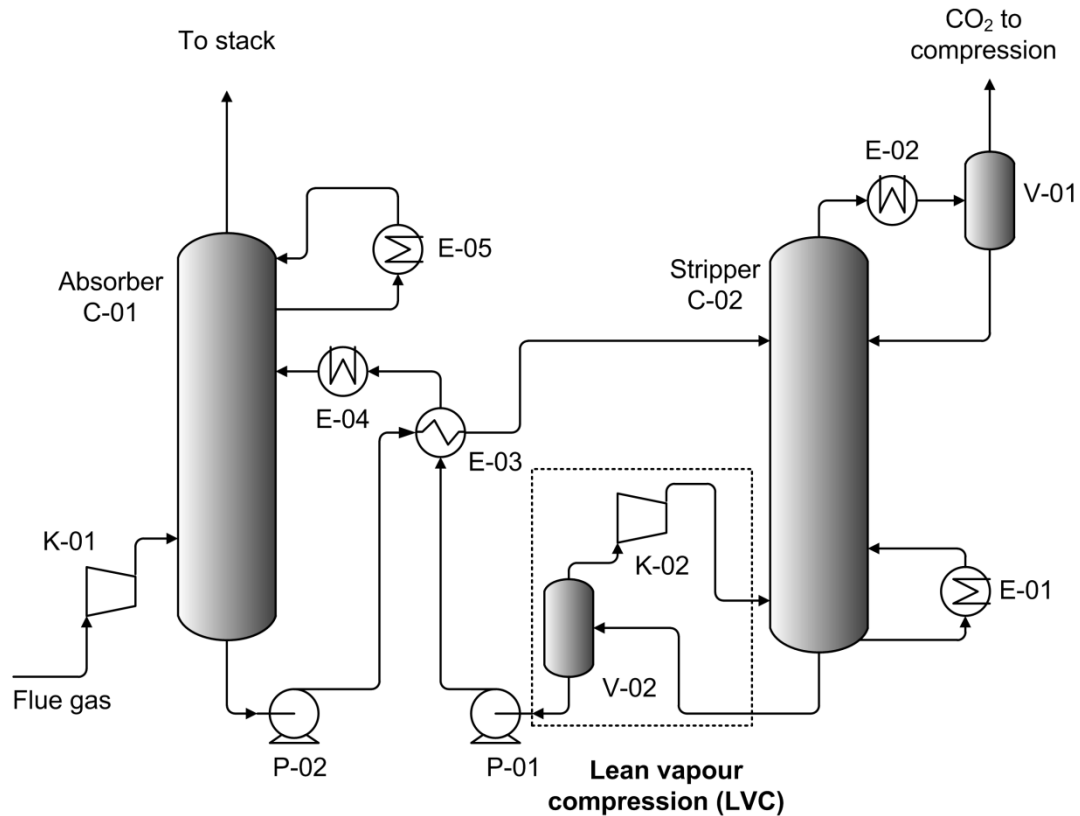


Figure 5.1. Standard MEA plant with LVC. Main unit operations in LVC, which are flash vessel (V-02) and compressor (K-02), are included in the dotted box. The rest of the equipment is included in a standard MEA process: Flue gas blower (K-01), absorber (C-01), rich pump (P-02), Lean pump (P-01) stripper (C-02), reboiler (E-01), condenser (E-02), lean-rich heat exchanger (E-03), cooler (E-04), washing section cooler (E-05), condenser drum (V-01).

### 5.2.2 Lean vapour compression (LVC): Design boundaries and scenarios

Application of LVC to the process described in the previous section requires additional equipment. The new LVC lines are highlighted in Figure 5.1. In this case, the hot lean solvent is flashed in an additional vessel (V-02). The resulting vapour is compressed (K-02) to a pressure slightly higher than the stripper bottom pressure and fed to the stripper base. An additional pump is added (P-01) to recover the pressure loss in the lean stream.

The addition of the LVC has the following general implications to the process operation:

- The reboiler duty decreases due to the extra stripping vapour coming from the LVC flash vessel.
- Additional electricity is needed to drive the LVC compressor.
- Condenser and LRHX duties decrease due to the loss of heat from the lean stream.

- The stripper needs to accommodate a slightly higher vapour flow compared to that of the standard MEA case.
- Additional equipment is needed, such as a flash vessel, and compressor and a pump.

Two different scenarios can be encountered if LVC is applied to the standard MEA plant: LVC is included in capture plant design or LVC is retrofitted to an existing capture plant. In the first scenario, it is assumed that the decision of adding an LVC process modification is taken prior to investment. Therefore, the design of the capture plant is affected by the process modification. Design modifications are taken into account to calculate new investment and process operating costs:

- The stripper diameter might be increased to accommodate more vapour flow without losing separation efficiency.
- The heat transfer area might be decreased for both LRHX and condenser when they are designed at a constant temperature approach (pinch).
- The LVC compressor is a turbo-compressor. It has a specific working range. Outside of this range the required duty will be high. The LVC should be operated so that the efficiency of the compressor remains high.

In the second scenario, it is assumed that the LVC is retrofitted to an existing plant or to an existing designed plant without any modifications in the affected equipment. The LVC compressor can still be designed to operate at its optimal range. However, the heat transfer equipment shall not be modified and remains identical to the standard MEA plant. This will result in relatively higher investment costs for LRHX and condenser, compared with the first scenario.

Both scenarios are investigated in this study. The final pressure in the flash vessel determines the savings in energy and, at the same time, the capital investment. For both scenarios, the reboiler duty and the LVC compressor and pump work have been calculated as a function of flash vessel pressure. Moreover, the extra investment in additional equipment has been estimated as a function of flash vessel pressure. For the first scenario, design modifications to the heat transfer equipment have been also analysed for different flashing pressures in the flash vessel. Nevertheless, the effect on stripper diameter was not considered since the vapour stream generated in the flash vessel is small at the stripper and flashing pressures considered in this study.

### 5.2.3 Modelling

Simulations were performed with Aspen Plus® version 7.1. The absorber is modelled with three equilibrium stages and the stripper is modelled with 8 equilibrium stages. This simulation method is an approximation to the phenomena that take place in absorption with chemical reaction. It is based on the minimum number of equilibrium stages, as derived from a pressure – liquid loading plot. The accuracy and applicability of this simulation scheme and its comparison to the rate-based simulation procedure has been already discussed in other papers [136]. When the reboiler duty is the main parameter of interest, it was found that the simulation results of this approach are in good agreement with the results of the rate-based approach. The model parameters for both scenarios are listed in Table 5.1. The CO<sub>2</sub> capture percentage is maintained at 90% capture by

manipulation of the solvent flow. The lean and rich solvent CO<sub>2</sub> loadings are a result from the calculations. The CO<sub>2</sub> recovery in the stripper is a design constraint added to the stripper to control the loading of the lean stream leaving this unit operation. It is defined as the ratio (mol basis) of the product streams to the feed streams for a specific component (CO<sub>2</sub> in this case). The product stream in the present modelling case is only the lean stream leaving the stripper. Feed streams are the rich stream and the re-compressed vapour entering the stripper.

**Table 5.1. List of parameters that are fixed for all simulations of the capture plant.**

Parameter	Value
CO <sub>2</sub> capture percentage	90%
Solvent	30wt% MEA
<b>Absorber</b>	
Feed Temperature /Pressure (flue gas and solvent)	40°C/1.1 bar
Equilibrium stages absorption	3
Equilibrium stages washer	2 loops of 3 stages
Pressure drop	90 mbar
<b>LVC compressor</b>	
Output pressure	1.9 bar
Total efficiency compressor	77%
Flue gas composition	
CO <sub>2</sub> mol%	13.7
H <sub>2</sub> O mol%	12
N <sub>2</sub> + Ar mol%	71
O <sub>2</sub> mol%	3.3
<b>Stripper</b>	
Rich solvent feed stage	3
Equilibrium stages stripping	6
Equilibrium stages wash	2
Pressure of stripper feed	4 bar
Pressure drop	100 mbar
Reboiler pressure	1.8 bar
CO <sub>2</sub> recovery in stripper	0.57
Condenser temperature	40°C

The energy analysis is performed in equivalent work. The total equivalent work for each simulation is calculated as follows:

$$W_{eq} = \lambda \cdot Q_R + W_{PUMP} + W_{LVC} \quad 5.1$$

In the equation above,  $Q_R$  is the specific reboiler duty,  $W_{PUMP}$  is the estimated work for pumps and  $W_{LVC}$  is the estimated work for the LVC compressor. The term  $\lambda$  accounts for the loss of turbine power due to steam extraction for the reboiler. This factor depends on the necessary steam quality. Since steam quality remains unchanged in this analysis, a constant value for  $\lambda$  of 0.23 has been assumed. This value was derived from power plant and capture plant integration studies by [193] for the case where the steam temperature for heating the stripper is in the range 120-150°C. For the calculation of pump work pump efficiencies of 85% have been assumed (including mechanical and drivers efficiency). This is in line with similar studies [21]. For compressor and blower, efficiencies of 77% have been assumed [194].

### 5.2.4 Economic frame work and analysis

The costs and estimating methodology are directed toward the “study-level” estimate with a nominal accuracy of  $\pm 30\%$ . The purpose of the study-level estimate is to compare the different scenarios to the reference case. The estimating procedure relies in the calculation of the mass and energy balances of the different cases (as described in the previous section). The generated information is used in the calculation of main equipment design. Once mass and energy flows and main equipment data are available, equipment cost is estimated.

There are different methods for cost estimation. The most accurate procedure is to request budget quotes from different vendors, specific to the location and conditions of each case. This method is unpractical when the number of cases is high. Instead, historical data from previous projects and/or vendor quotes can be used to estimate equipment cost specific to a given case. This latter option requires the manipulation of cost data to account for differences in scale, construction material, design pressure or time [164]. Finally, if no historic data points are available, cost data can be also obtained from various models published in the literature [135, 195] or from commercial software packages.

The approach followed in this work consists in the construction of an in-house model based on a combination of the above mentioned options. At a first stage in model development, several vendors were approached to give quotes for the scale, construction materials and design parameters estimated for the reference case and the optimal case found for each scenario. These quotes were included in a historical database to create significant ground information. At a second stage of model development, different correlations published in the literature and/or suggested by vendors were used to fit the data. As a result of this fitting procedure, a set of price correlations was developed that allows for equipment price estimation under a broad range of operating conditions. All data in the historical database were manipulated in the following order: material correction, calibration to year 2010 by using the Chemical Engineering Plant Cost Index and currency exchange to Euro. Quotes were received during years 2009 and 2010. The ones from 2009 were calibrated also to the year 2010. All quotes were received in Euro.

The economic analysis is based on calculating the energy savings with respect to the standard MEA plant and calculating the extra investment costs or savings for each particular case. Results are given in net present value (NPV) of the cash flows associated with each case over the entire project life time. The cash flow represents the savings obtained as a function of the flash operating pressure. They are estimated by calculating the difference in utility cost and investment compared to the reference case, according to the formulas:

$$NPV = \sum_{j=0}^n \frac{CF_j}{(1+IR)^j} \quad 5.2$$

$$CF_j = \Delta Energy_j - \Delta Depreciation_j \quad 5.3$$

$$\Delta Depreciation_j = \frac{\Delta TC_{HEX}}{20} + \frac{\Delta TC_{LVC}}{10} + \frac{\Delta TC_{VESSEL}}{25} \quad 5.4$$

In the equations above, NPV is the net present value for a given case,  $CF_j$  is the cash flow in year  $j$ ,  $n$  is the number of years in the project,  $IR$  is the interest rate,  $\Delta Energy_j$  is the difference in utility costs (only steam and electricity) between a given case and the reference case for year  $j$ ,  $\Delta Depreciation_j$  is the difference of the depreciated total equipment costs between a given case

and the reference case for year  $j$  and  $\Delta TC_{\text{HEX}}$ ,  $\Delta TC_{\text{LVC}}$ ,  $\Delta TC_{\text{VESSEL}}$ , are the difference in total cost of heat exchangers (E-01, E-02, E-03), compressor (K-02) and vessel (V-01) between a given case and the reference case respectively.

The parameters used in the calculation of NPV are listed in Table 5.2. Linear depreciation over the whole equipment life time has been used. Selecting the right value for equipment life time that corresponds to the estimated price is crucial in this analysis. For the LVC compressor the most convenient equipment choice is the turbo-blower with a pressure ratio up to 2. Most vendors consulted agreed that the life time of the turbo-blower is substantially lower than the other pieces of equipment in this process [196]. Equipment life time might be extended by purchasing a more expensive compressor for which materials are selected to extend the operating life of the equipment. This point is often overlooked in conceptual designs of this type. In this work, the life time of the relevant equipment was adjusted to the type of equipment selected as shown in equation 5.4 and Table 5.2.

**Table 5.2. Parameters for the economic evaluation of the different cases.**

Parameter	Value	Reference
Installation factor	4	[164]
Interest percentage	8%	[21]
Turbine power loss to reboiler energy [MWe/MWth]	0.23	[193]
Electricity [€/MWh]	50	[194]
Project life time (years)	25	[194]
Compressor life time	10 years	[196]
Flash vessel life time	25 years	[164]
Heat exchangers Life time	20 years	[164]

## 5.3 Results

### 5.3.1 Case 1: Capture plant design adapted to LVC operation

In this scenario, the LRHX was modelled at a constant temperature approach (*i.e.* constant LMTD). Several simulations were conducted with varying LVC flash pressure. Table 5.3 shows a summary of the equipment duties affected by the LVC. Due to the loss of latent heat in the lean stream leaving the stripper column, the temperature of the feed stream to this column also decreases. This phenomenon results in a reduction of condenser duty as the flash pressure decreases. The reduction can be as high as 44%. The reboiler duty also decreases with decreasing flash pressures. Energy savings up to 18% can be achieved in the reboiler. However, when the extra pump and compressor work are considered, the energy savings (expressed in total equivalent work) are limited to 7.3%. Moreover, the duty required in the LRHX decreases significantly with decreasing flash pressure. Based on the minimisation of equivalent work, the optimal pressure in the flash vessel is 1.1 bar. However, the changes in equipment duty also have an effect in the cost of equipment.

**Table 5.3. Overview of equipment duties and equivalent work as a function of LVC flash pressure. Case 1: Design adapted to LVC. The total duty of equipment affected by the LVC operation is shown. Equipment names are followed by the corresponding tag in Figure 5.1.**

Flash pressure bar	Reboiler (E01) MWth	Pump (P01) MWe	Compressor (K02) MWe	LRHX (E03) MWth	Condenser (E02) MWth	Equivalent work MJ/t CO <sub>2</sub>
1.8	172	0.000	0.0	197	60	819.4
1.6	164	0.182	0.2	166	48	789.2
1.4	158	0.197	0.8	153	42	773.3
1.2	150	0.214	2.0	149	40	760.4
1.1	146	0.222	2.8	142	37	758.1
1.0	141	0.227	4.0	132	34	759.2

**Table 5.4. Affected purchased equipment cost as a function of LVC flash pressure. Case 1: Design adapted to LVC. Equipment names are followed by the corresponding tag in Figure 5.1.**

Flash pressure bar	Reboiler (E01) M€	Flash vessel (V02) M€	Compressor (K02) M€	LRHX (E03) M€	Condenser (E02 & V01) M€	$\Delta(TC_i)^a$ M€
1.8	1.30	0.00	0.0	1.11	0.31	0.00
1.6	1.25	0.11	0.1	0.79	0.25	-0.25
1.4	1.20	0.20	0.3	0.65	0.22	-0.20
1.2	1.14	0.32	0.6	0.61	0.21	0.20
1.1	1.11	0.39	1.0	0.54	0.2	0.47
1.0	1.07	0.47	1.4	0.44	0.18	0.86

<sup>a</sup> Total change in equipment cost: difference in total equipment cost between the reference case (at 1.8 bar), which is 2.72 M€ and any other given case. Only significant changes in equipment cost are considered. Values in this table do not include installation cost. Installation costs are included when calculating depreciation.

**Table 5.5. Calculation of NPV as a function of flash pressure. Case 1: Design adapted to LVC. Yearly energy cost, energy savings, equipment depreciation difference and NPV for each operating flash pressure.**

Flash pressure bar	Energy cost M€/y	Energy savings <sup>a</sup> M€/y	Depreciation difference <sup>b</sup> M€/y	NPV energy savings <sup>c</sup> M€	NPV total savings <sup>d</sup> M€
1.8	16.77	0.00	0.00	0.0	0.0
1.6	16.23	0.55	-0.04	5.9	6.3
1.4	15.84	0.93	0.00	9.9	9.9
1.2	15.58	1.19	0.15	12.7	11.1
1.1	15.54	1.24	0.27	13.2	10.3
1.0	15.54	1.24	0.44	13.2	8.5

<sup>a</sup> Difference in energy cost between the reference case (at 1.8 bar) and any other given case.

<sup>b</sup> Equipment depreciation difference calculated with equation (5.4).

<sup>c</sup> NPV calculated with equation (5.2) without taking into account the depreciation difference.

<sup>d</sup> NPV calculated with equation (5.2) taking into account energy savings and depreciation difference.

At each pressure, the investment costs have been estimated using the economic model described in Section 5.2.4. Table 5.4 lists the estimated purchased equipment cost of the items considered in this analysis. Compared to the reference case, costs of the reboiler, LRHX and condenser decrease with decreasing flash pressure. This reduction is explained by the lower duties of

reboiler and condenser and the loss of latent heat of the lean hot stream as shown in Table 5.3. Therefore, the heat transfer area of the mentioned heat exchange equipment can be reduced resulting in lower costs. Obviously, the cost for the LVC compressor, LVC pump and flash vessel increase when the flash pressure decreases due to higher pressure ratio for compression and pumping and higher vapour flow in the flash vessel. However, the cost of LVC equipment is compensated by the lower costs of reboiler, condenser and LRHX at pressures below 1.2 bar. Above that pressure, the cost of LVC equipment becomes dominant.

The net present values (NPV) of the yearly savings due to the application of LVC have been calculated according to the procedure described in Section 5.2.4. The results are tabulated in Table 5.5. The variation of NPV with flash pressure is represented in Figure 5.2. The dash line represents the hypothetical case, where the investment in the extra equipment is not included in the calculation of annual savings. The solid line represents the actual case, where both investment and energy are included in the calculation of total savings. From the latter case, it can be concluded that the benefit of applying LVC is maximal at a flash pressure of 1.2 bar. Below that pressure the increase in energy savings is small compared to the increase in equipment cost (mainly the compressor).

### 5.3.2 Case 2: LVC retrofitted to an existing plant

In this scenario, the LRHX, condenser and cooler were modelled with constant heat transfer area and heat transfer coefficient and equal to the values used in the simulation of the standard MEA plant. Again, several simulations were conducted with varying LVC flash pressures. Table 5.6 shows a summary of the equipment duties, which are similar to the first scenario (Table 5.3). The difference in maintaining the heat exchange equipment design unaltered (Table 5.6) or altered (Table 5.3) is not really appreciable in the equipment duties. Nevertheless, this study predicts 0.5% lower equivalent work for this scenario around the optimal pressure (1.1 bar).

Regarding the investment costs (Table 5.7), condenser, reboiler and LRHX remain unchanged and equal to the standard MEA case. However, extra investment cost needs to be added for the LVC compressor and flash vessel, which is also similar to the cost calculated in the previous scenario. Table 5.8 shows the NPV value for each flash vessel pressure. The NPV results are also plotted in Figure 5.3. Energy costs are comparable between both scenarios (Case 1 and Case 2). The investment costs are higher in this scenario, resulting in a lower final NPV than in the previous one. Also in this case, the flash pressure that minimizes the equivalent work is slightly lower than the one that maximises the NPV.

**Table 5.6. Overview of equipment duties and equivalent work as a function of LVC flash pressure. Case 2: retrofit scenario. The total duty of equipment affected by the LVC operation is shown. Equipment names are followed by the corresponding tag in Figure 5.1.**

Flash pressure bar	Reboiler (E01) MWth	Pump (P01) MWe	Compressor (K02) MWe	LRHX (E03) MWth	Condenser (E02) MWth	Equivalent work MJ/t CO <sub>2</sub>
1.8	172	0.000	0.0	197	60	817.5
1.6	164	0.183	0.2	182	53	789.6
1.4	157	0.195	0.8	168	47	770.6
1.2	149	0.214	1.9	151	41	755.5
1.1	145	0.223	2.8	144	38	754.0
1.0	141	0.228	3.9	144	34	757.6

**Table 5.7. Purchased equipment cost as a function of LVC flash pressure. Case 2: retrofit scenario. Equipment names are followed by the corresponding tag in Figure 5.1. Only significant changes in equipment cost are considered.<sup>a</sup>**

Flash pressure bar	Reboiler (E01) M€	Flash vessel (V02) M€	Compressor (K02) M€	LRHX (E03) M€	Condenser (E02 & V01) M€	$\Delta(TC_i)^b$ M€
1.8	1.30	0.00	0.00	1.11	0.31	0.00
1.6	1.30	0.12	0.08	1.11	0.31	0.19
1.4	1.30	0.21	0.25	1.11	0.31	0.45
1.2	1.30	0.32	0.63	1.11	0.31	0.95
1.1	1.30	0.39	0.97	1.11	0.31	1.35
1.0	1.30	0.46	1.41	1.11	0.31	1.87

<sup>a</sup> Note that the numbers given in this table do not include installation cost. Installation costs are included when calculating depreciation.

<sup>b</sup> Total change in equipment cost: difference in total equipment cost between the reference case (at 1.8 bar), which is 2.72 M€ and any other given case.

**Table 5.8. Calculation of NPV as a function of flash pressure. Case 2: Retrofit scenario. Yearly energy cost, energy savings, equipment depreciation difference and NPV for each operating flash pressure.**

Flash pressure bar	Energy cost M€/y	Energy savings <sup>a</sup> M€/y	Depreciation difference <sup>b</sup> M€/y	NPV of energy savings <sup>c</sup> M€	NPV of total savings <sup>d</sup> M€
1.8	16.77	0.00	0.00	0.0	0.0
1.6	16.20	0.57	0.05	6.1	5.6
1.4	15.81	0.96	0.13	10.3	8.9
1.2	15.50	1.27	0.30	13.6	10.3
1.1	15.47	1.30	0.45	13.9	9.1
1.0	15.54	1.23	0.64	13.1	6.3

<sup>a</sup> Difference in energy cost between the reference case (at 1.8 bar) and any other given case.

<sup>b</sup> Equipment depreciation difference calculated with equation 5.4.

<sup>c</sup> NPV calculated with equation 5.2 without taking into account the depreciation difference.

<sup>d</sup> NPV calculated with equation 5.2 taking into account energy savings and depreciation difference.

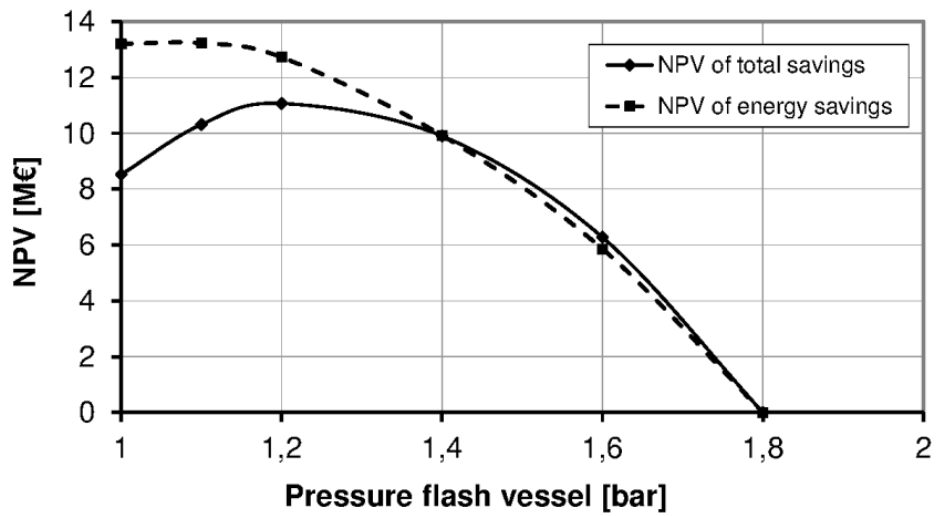


Figure 5.2. NPV of total savings, and energy savings against LVC pressure. Case 1: Design adapted to LVC operation.

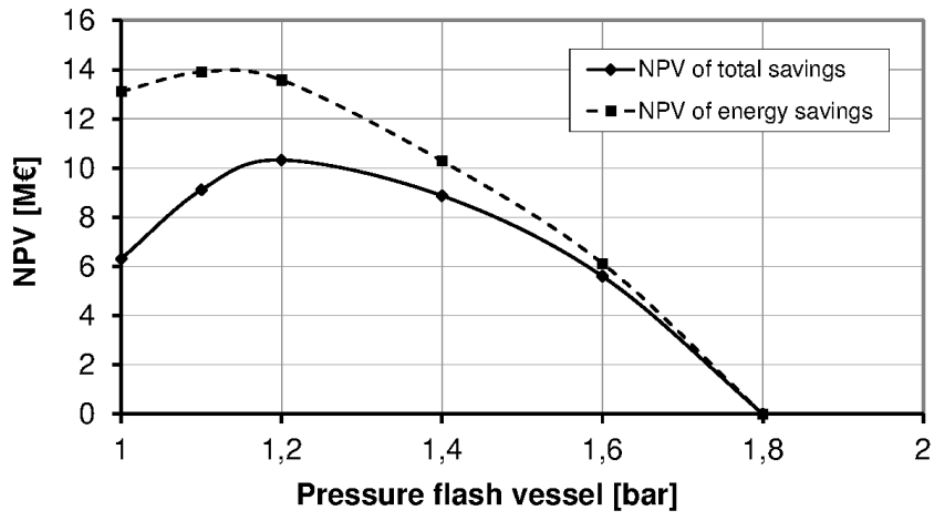


Figure 5.3. NPV of total savings, and energy savings against LVC pressure. Case 2: Retrofit of LVC to capture plant.

## 5.4 Discussion

The results of this study show that the application of LVC in both scenarios will reduce the equivalent work necessary for capturing CO<sub>2</sub>. The reduction is slightly higher in the case that the LVC is retrofitted to the standard MEA process (7.8% compared to the standard MEA plant) than in the case that the design of the plant is adapted (7.3% compared to the standard MEA plant). Table 5.9 shows the comparison of these results to similar studies. The energy savings are expressed in difference in equivalent work between the reference case (generally similar to the standard MEA plant described in this work) and the LVC configuration. The results of this study are in line with the finding of others. The difference in numbers is related to the different conditions adopted for the stripper.

**Table 5.9. Energy savings of LVC as reported in other studies.**

Reference	Energy savings <sup>a</sup>	$\Delta P$ <sup>b</sup>	Stripper Pressure
	%	bar	bar
Karimi <i>et al.</i> [197]	8.39-9.36	0.85-0.9	2
Le Moullec and Kanniche [55]	7.78	1.25	2.5
This work	7.3-7.8	0.6	1.8

<sup>a</sup> Reduction in equivalent work taking a standard MEA plant as basis.

<sup>b</sup> Difference between Stripper pressure and LVC flash pressure.

The operating flash pressure that minimizes equivalent work is 1.1 bar for both scenarios. If the reduction in energy was the only considered criterion for optimisation, the best scenario would be the retrofit of LVC to the standard MEA plant, because the reduction in energy is more significant in this scenario. However, when the trade-off between energy savings and additional capital investment is taken into account, it is found that the optimal flash pressure is 1.2 bar, which implies a pressure difference with the stripper of 0.6 bar. Moreover, when the NPVs of total savings for both analysed scenarios are compared, the best result is achieved when the plant design is adapted to the LVC addition. This example shows the efficacy of this approach.

The differences between the two scenarios are small because the stripper pressure was fixed to 1.8 bar. Therefore, there is small range of pressures to be considered in the optimisation. Nevertheless, higher differences can be expected when the difference between the operating pressure in the stripper and the flash vessel is increased. In that particular case, the approach followed in this work will lead to a better optimisation of operating conditions rather than the approach of minimising equivalent work.

Moreover, the turbine power loss ratio is a very important factor in this type of analysis. For a very well integrated power plant the turbine power loss ratio could be as low as 0.20 (MWe/MWth). This means that the energy savings will be contributing less to the NPV calculated, while the cost of the compressor will remain identical. This fact contributes to the disparity of the pressure that minimises equivalent work and the one that maximises the NPV. In the case of a poorly integrated power plant, this factor could be as high as 0.24 (MWe/MWth). The energy becomes a more dominant factor contributing greatly to the NPV. For this situation, the pressure that minimises the equivalent work will approach the pressure that minimises the NPV.

Besides the equivalent work and NPV minimisation, other aspects should be also addressed to better understand the LVC benefits. One of these aspects is operability and possible LVC trip (due to failure or maintenance). When the LVC is turned off, the operation of reboiler, lean-rich heat exchanger and condenser is affected. The resulting plant performance depends on whether the plant design was adapted to LVC operation (case described in Section 5.3.1) or the LVC was just retrofitted to an existing plant (case described in Section 5.3.2). In the case that plant design was adapted for LVC, the mean temperature difference in the LRHX will rise upon LVC shut down due to the higher energy in the lean stream. The reboiler duty also increases. There will be more flow to the condenser, which will increase its pressure drop, having an effect in the compression train. When not counteracted by adjustment of the reboiler and condenser, shut-down of the LVC will lower the capture percentage of the plant. In the case that the LVC was just retrofitted to the plant, operation returns to nominal values when the LVC is shut off. The plant can be operated normally by increasing the steam supply to the reboiler and the cooling duty of the condenser and lean liquid cooler. This makes a capture plant with retrofitted LVC more flexible than the option where the plant is adapted to the lower duties and gives an additional advantage to this option.

### 5.5 Conclusions

In this work, the application of Lean Vapour Compression to a standard MEA carbon capture plant was investigated. The work focussed on the financial analysis of this process modification and it can be used to make an informed decision on whether this process modification should be added or not to a current situation.

Two scenarios were analysed. In the first scenario, the design of the capture plant was modified to accommodate the changes in duties resulting from LVC application. In the second scenario, the design was unchanged and the affected equipment was not modified.

Under the conditions investigated, it was found that LVC will result in savings for both scenarios chosen for implementation. The operating conditions were optimised based on the NPV of the process design. It can also be concluded that the right choice of operating pressure in the LVC maximises the NPV. Under the investigated conditions, the optimal operating pressure is 1.2 bar for both scenarios. It was also found, that the optimisation of operating conditions based only on energy analysis could lead to a different result.

Finally, the most attractive scenario from an economic point of view is the one where the capture plant is fully adapted. However, the retrofit scenario has other advantages, not quantified in this financial analysis, such as the flexible shut down of the LVC (for maintenance or reparation). This can make this scenario more attractive from a reliability point of view.

---

# NOVEL CO<sub>2</sub> CAPTURE PROCESS BASED ON PRECIPITATING AMINO ACID SOLVENTS

## ABSTRACT

*Amino acid salt based solvents can be used for CO<sub>2</sub> removal from flue gas in a conventional absorption-thermal desorption process. Recently, new process concepts have been developed based on the precipitation of the amino acid zwitterion species during the absorption of CO<sub>2</sub>. In this work, a new concept is introduced which requires the precipitation of the pure amino acid species and the partial recycle of the remaining supernatant to the absorption column. This induces a shift in the pH of the rich solution treated in the stripper column that has substantial energy benefits during CO<sub>2</sub> desorption. To describe and evaluate this concept, this work provides the conceptual design of a new process (DECAB Plus) based on a 4 M aqueous solution of potassium taurate. The design is supported by experimental data such as amino acid speciation, vapour-liquid equilibria of CO<sub>2</sub> on potassium taurate solutions, and solid-liquid partition. The same conceptual design method has been used to evaluate a baseline case based on 5 M MEA. After thorough evaluation of the significant variables, the new DECAB Plus process can lower the specific reboiler energy for solvent regeneration by 35% compared to the MEA baseline. The specific reboiler energy is reduced from 3.7 GJ/tCO<sub>2</sub>, which corresponds to the MEA baseline, to 2.4 GJ/tCO<sub>2</sub>, which corresponds to the DECAB Plus process described in this work, excluding the low-grade energy required to redissolve the precipitates formed during absorption. Although this low-grade energy will eventually reduce the overall energy savings, the evaluation of DECAB Plus has indicated the potential of this concept for post-combustion CO<sub>2</sub> capture.*

*This chapter is based on:*

*E. Sanchez Fernandez, K. Heffernan, L. V. van der Ham, M. J.G. Linders, E. Eggink, F. N.H. Schrama, D.W.F. Brilman, E. L.V. Goetheer, T. J.H. Vlught. "Conceptual design of a novel CO<sub>2</sub> capture process based on precipitating amino acid solvents". *Industrial & Engineering Chemistry Research* 2013, 52, 12223-12235.*

## 6.1 Introduction

In the field of post-combustion CO<sub>2</sub> capture from fossil fuel power plant exhaust gases, the conventional amine processes have well-known drawbacks. The major issues are the high energy required for solvent regeneration, the increased process complexity due to solvent volatility, and the possible air pollution directly attributable to the solvent, such as solvent emissions or emissions of degradation products [14, 198]. These issues justify the research effort to develop more effective and environmentally friendly processes for the separation of CO<sub>2</sub> from flue gas. Amino acid salts have been identified as attractive solvents for this application due to their unique properties; lower toxicity, higher biodegradability than conventional amines [66], negligible volatility and, for certain amino acids, a high resistance to oxidative degradation [67].

Amino acid salts have been used in the past for acid gas removal in refinery applications. One example is the Alkacid process developed in the early 30s for the removal of H<sub>2</sub>S or CO<sub>2</sub> [39]. In post-combustion CO<sub>2</sub> capture application there are also alternatives to conventional amines. The PostCap process, recently developed by Siemens, has an energy consumption for regeneration around 73% of the conventional monoethanolamine (MEA) process [68]. TNO has also investigated processes based on the potassium salt of amino acids, showing increased stability and resistance to degradation over conventional MEA [67]. In the recent years, interest has grown in the performance of different amino acid salts for post-combustion capture and the CO<sub>2</sub> absorption characteristics for common amino acids and their properties are under extensive investigation [69-72, 74-77, 79, 199, 200]. During CO<sub>2</sub> absorption, amino acid precipitates may be formed at high CO<sub>2</sub> loadings because the pH of the solution decreases favouring the formation of the zwitterion species, which has limited solubility. Since the conventional absorption – desorption scrubbing process is not designed to handle solids, the vast majority of the studies with amino acid salts deals with homogenous solutions only, avoiding precipitation by reducing amino acid concentration below the saturation point when the solution is loaded with CO<sub>2</sub>.

Nevertheless, precipitating amino acid solvents were suggested in the early 2000's as a promising alternative to conventional amine processes [82]. The identified benefits were related to an enhancement of the specific CO<sub>2</sub> capacity of amino acid salt solutions due to precipitation. As it follows from Le Chatelier's principle, equilibrium can be shifted by removing one of the constituents in the reaction. In this case, one of the products of the reaction between CO<sub>2</sub> and the amino acid is removed from the aqueous phase by precipitation. Consequently, the equilibrium shifts to favour the absorption of CO<sub>2</sub> [88]. This effect can be seen in the experimental data of Kumar [71, 84]. In order to exploit this effect, Fernandez and Goetheer [81] have investigated a process configuration (named the DECAB process) that can accommodate solids. The DECAB process makes use of a spray tower to handle solids during absorption and a packed column to increase the CO<sub>2</sub> removal efficiency. Both columns work in series. The authors provide a techno-economic analysis of precipitating potassium taurate solutions as a tool to assess the overall capture performance concluding that, in terms of CO<sub>2</sub> capture costs, the DECAB process configuration is comparable to that of the conventional MEA process.

The present study investigates a novel process configuration (DECAB Plus) that provides a further improvement in precipitating amino acid based processes by separating and recycling a fraction of the liquid supernatant from the slurry formed during CO<sub>2</sub> absorption and processing

only the latter in the stripper column. This modification allows for a change in pH in the CO<sub>2</sub> loaded solution that improves the CO<sub>2</sub> desorption in the stripper column. The DECAB Plus process is designed, analysed and compared to a conventional MEA process. The conceptual design methodology has been followed, which required the experimental determination of the key properties that govern the absorption and desorption in precipitating amino acids. These properties were investigated on a 4 M aqueous solution of potassium taurate. The experimentally derived properties were used for process modelling and the evaluation of the process proposed. The models and procedures developed in this work have also been used to evaluate a standard MEA based process, which is used as baseline for process performance. The final assessment of this work shows the differences between the novel process and the conventional MEA process.

## 6.2 Conceptual process design

### 6.2.1 Process description

The DECAB Plus process concept is based on the exploitation of the extra driving force for desorption that occurs when the pH of the solvent is reduced. The fundamental principle that allows this pH shift is the formation of a precipitate during the absorption of CO<sub>2</sub> in amino acid salt solutions. Once a solid phase is formed, the liquid – solid ratio can be manipulated in order to obtain a CO<sub>2</sub> rich solution of lower pH than the one formed during absorption. Different precipitate types can be encountered depending on the amino acid structure and solubility. Amino acids with a primary amino group, such as taurine, precipitate only the zwitterion species [84, 85]. In other cases, the precipitate formed is potassium bicarbonate. This is the case of amino acids with a hindered amino group and relatively high zwitterion solubility, such as proline [85]. Independently of the precipitate type, the formation of a solid reaction product allows for phase separation (liquid from solid) and formation of a new rich solution with lower pH that promotes the release of CO<sub>2</sub> during desorption.

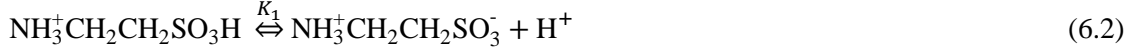
To describe and demonstrate the potential of this process, the selected solvent for the conceptual design is potassium taurate. The selection is based on taurine's proven stability and relatively high specific capacity for CO<sub>2</sub> [81]. The selection of solvent's concentration generally implies a trade-off between capacity and kinetics. However, due to the extension of this work the later has been left outside scope and the discussion focusses on capacity. The concentration has been fixed to 4 M, concentration at which taurine has comparable capacity to MEA on a specific molar basis.

Potassium hydroxide is assumed to dissociate completely in an aqueous solution. After complete reaction of equal molar amounts of taurine and KOH, the final solution will contain equal molar amounts of K<sup>+</sup> and taurate. When CO<sub>2</sub> is added to the system, amino acids in general, and taurine in particular, react forming the same species as amines. Precipitates of taurine zwitterion are formed when the solution reaches the saturation point [71, 84]. The following set of reaction equations is relevant for a CO<sub>2</sub> – potassium taurate – water system (the precipitating species is emboldened):

Dissolution of Taurine in water:



First dissociation constant of Taurine:



Second dissociation constant of Taurine:



Water dissociation constant:



Dissociation of potassium hydroxide:



Carbamate formation:



Bicarbonate formation:



Carbonate formation:



Dissolution of CO<sub>2</sub> in aqueous solution of potassium taurate:



After precipitation, taurine is concentrated in the solid phase. Therefore, the effect of partial removal of the liquid will result in a larger reduction of K<sup>+</sup> compared to the reduction in taurine. Dissolution of the solid rich solution will induce a lower pH in the stream that is treated in the stripper due to a higher ratio of taurine to K<sup>+</sup>.

This enhanced desorption concept can be achieved by the process schematically presented in Figure 6.1. In this case, the flue gas is treated with a solution of potassium taurate containing 1:1 molar amounts of taurine and K<sup>+</sup> in a spray tower contactor (or a spray tower and packed column in series). The result is a rich stream in the form of a slurry that contains taurine solids and a supernatant with the carbonated and potassium species. This slurry is treated in a solid-liquid separator (hydrocyclone or decanter) to partially separate the supernatant from the solids. The fraction of the liquid supernatant that is recycled is referred to as the recycle split fraction (RSF). The resulting slurry, enriched in taurine, is further processed in the stripper for desorption. The supernatant excess, enriched in potassium ions, is recycled to the absorber without passing through the stripper. The pH of the new rich stream is decreased before thermal desorption,

enhancing the release of the chemically bonded  $\text{CO}_2$ . However, in order to induce this pH shift, the solvent capacity might be decreased since part of the remaining supernatant (containing carbonated species) is recycled to the absorption process.

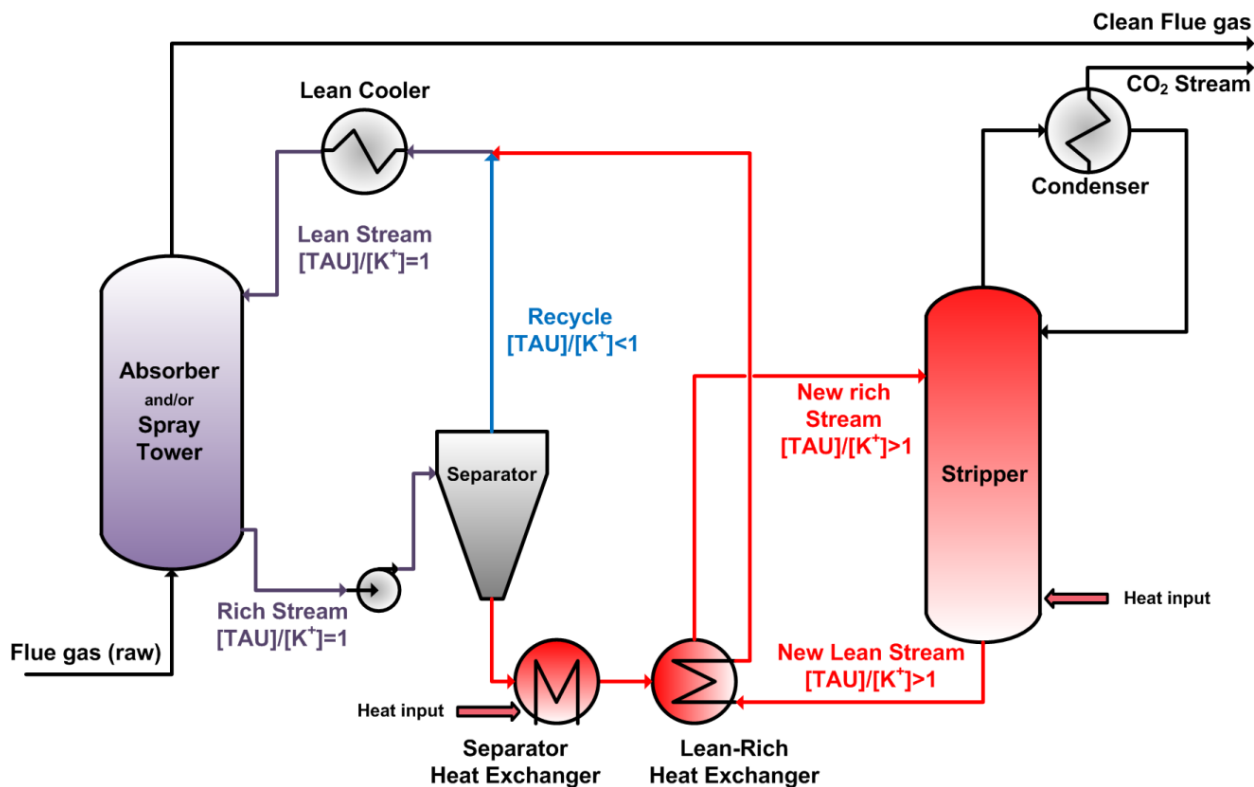


**Figure 6.1.** Schematic representation of the DECAB Plus process concept for  $\text{CO}_2$  capture based on potassium taurate. Enhanced absorption due to the precipitation of reaction products takes place in the absorber and enhanced desorption due to the induced lower pH for regeneration takes place in the stripper, after partial separation of the rich liquid stream and dissolution of the precipitates. The ratio of the total taurine concentration to the total potassium concentration in solution is indicated below the name of each stream. This ratio can be 1 (equimolar solution), higher than 1 (solution with more taurine than the equimolar solution and, therefore, lower pH) or less than 1 (solution with less taurine than the equimolar solution and, therefore, higher pH).

### 6.2.2 Conceptual process design methodology

The design and evaluation of the process illustrated in Figure 6.1 rely on the development of a conceptual model based on equilibrium that predicts absorption, solid-liquid separation and desorption performance. Prior to model development, substantial background information is required on the absorption capacity of the potassium taurate solvent, solid-liquid partition after absorption, the possible taurine to  $\text{K}^+$  ratios ( $[\text{TAU}/\text{K}]$ ) that can be obtained in the new rich stream, the relation between these ratios and the pH of the solution and its influence in the Vapour-Liquid Equilibrium (VLE) of potassium taurate at stripper conditions. The design method, schematically represented in Figure 6.2, can be divided into four steps. The first two steps (Literature review and Solvent properties experimental determination) are concerned with the generation of the necessary information to develop the conceptual model. Based on this information, empirical correlations are derived, which describe the vapour-liquid-solid equilibrium of  $\text{CO}_2$  in potassium taurate solutions. These correlations are used to model absorber,

solid-liquid separator and stripper performance in the next step of the design method (Model development). In the last step (Process analysis), the model is used to predict process performance, estimating the mass and energy balances at different conditions. When necessary, a sensitivity analysis on certain process variables is carried out to optimise process performance. Besides potassium taurate, the same method is used to predict the performance of a conventional MEA capture process, with the purpose of validating the method and providing a basis for comparison.

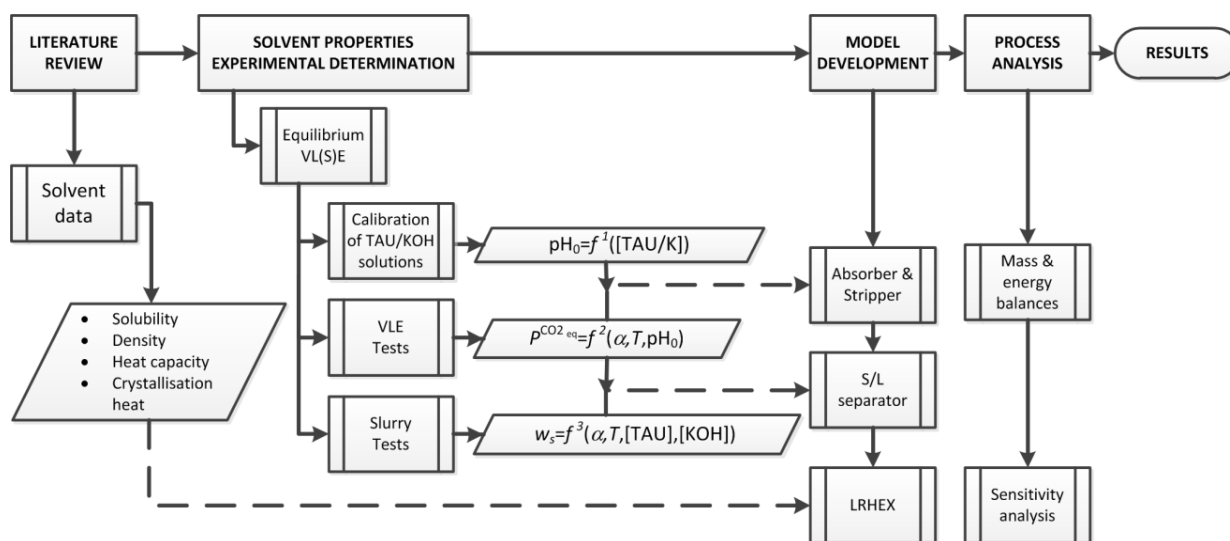


Figure 6.2. Workflow sequence for the conceptual process design of the DECAB Plus process.

### 6.2.2.1 Literature review

Besides the information already mentioned, other solvent data that are necessary for the design and have been retrieved from the available literature (Table 6.1). In the case of MEA (solvent used to give a baseline for comparison), the necessary information for modelling has already been published in literature. Table 6.1 shows the main properties of the molecules used in this study.

### 6.2.2.2 Solvent properties experimental determination

Vapour-Liquid-Solid Equilibrium (VL(S)E) data for potassium taurate are necessary to estimate solid-liquid partition and Vapour-Liquid Equilibrium (VLE) at different conditions. Generally, this requires the estimation, based on experimental data, of the different equilibrium constants that govern the liquid equilibria described in Section 6.2.1. However, for the purpose of conceptual design, this work has derived empirical expressions from experimental data, which represent the VL(S)E. This option provides relatively accurate information on solvent's behaviour avoiding the extensive mathematical procedure of developing a thermodynamic model. As shown in Figure 6.2, the full description of the VL(S)E required three different experimental tests and the development of empirical functions for each type of test:

- 1) Calibration of taurine – KOH solutions: Although the dissociation constants of taurine have been reported in the literature at infinite dilution conditions [199, 201], the effect of electrolytes in solution needs to be accounted for in the estimation of pH. This requires the development of an activity model to take into account the non-ideal behaviour of strong electrolyte solutions. Alternatively, this conceptual design has used an empirical relationship between pH and the [TAU/K] molar ratio in solution. For this purpose, a hypothetical variable,  $\text{pH}_0$ , was introduced (as shown in Figure 6.2), which represents the initial pH of a taurine – KOH solution. This pH was determined experimentally for solutions with known concentrations of taurine and KOH. After calibration of the results, a function denoted by  $f^1$  is derived to predict  $\text{pH}_0$  at high concentrations, different temperatures and different [TAU/K] molar ratios.
- 2) VLE tests: After the first calibration step, the VLE of solutions with different [TAU/K] molar ratios was measured at different temperatures, ranging from 40 to 130°C. Results were fitted to an empirical function denoted by  $f^2$  that relates the partial pressure of  $\text{CO}_2$  to the liquid loading ( $\alpha$ ), temperature and  $\text{pH}_0$ .
- 3) Slurry tests: Slurry characterisation measurements were performed to derive the amount of solids formed as a function of liquid loading ( $\alpha$ ), temperature and taurine and KOH concentrations. The results were correlated in order to obtain a relationship denoted by  $f^3$  between the solids fraction ( $w_s$ ) and the liquid loading ( $\alpha$ ), temperature and taurine and KOH concentrations.

The combination of  $f^1$ ,  $f^2$ , and  $f^3$ , leads to a relationship between the solids fraction and the equilibrium  $\text{CO}_2$  pressure, enabling the full prediction of the VL(S)E.

**Table 6.1. Properties of Taurine, MEA (baseline) and water retrieved from literature and used in the conceptual design. The table indicates the range of validity of the property and the value used in the design.**

Property	Component	Range	Value used	Reference
Molecular weight	Taurine	[-]	125.15 g/mol	[-]
Solubility	Taurine	0-100°C	Function of temperature	[202]
Density	Taurine	0-4 M, 40-120°C	1270 kg/m <sup>3</sup> (4 M solution at 80°C)	[75]
Heat capacity	Taurine	6 M, 40 - 120°C	2.7 kJ/kgK (6 M solution at 80°C)	[81]
Crystallisation energy	Taurine	[-]	24.2 kJ/mol	[203]
Molecular weight	MEA	[-]	61 g/mol	[-]
Density	MEA	5 M, 40 - 120°C	980.26 kg/m <sup>3</sup> (5M solution at 80°C)	[204]
Heat capacity	MEA	5 M, 40-120°C	3.86 kJ/kgK (5 M solution at 80°C)	[204]
Vapour-Liquid equilibrium	MEA	5 M, 40-120°C	Function of $\text{CO}_2$ loading and temperature	[205]
Heat capacity	Water	> -72°C	Function of temperature	[206]
Latent heat	Steam	100 – 120 °C	40.66 kJ/mol	[206]

### 6.3 Solvent properties

#### 6.3.1 Calibration of Taurine / KOH solutions

To correlate the [TAU/K] molar ratio to the initial pH of the solution ( $\text{pH}_0$ ), the pH of solutions containing different ratios of taurine and KOH was investigated at 4 M taurine concentration and different temperatures (21°C and 40°C). No attempt was made to model ionic activity. The results, presented in Figure 6.3, show that the pH decreases with increasing [TAU/K] ratio in solution. The experimental solutions of 4 M concentration, contained taurine solids for [TAU/K] molar ratios above 1.2. For [TAU/K] molar ratios below 1.2 all the taurine solids were dissolved. However, no effect was observed in the measured pH. This suggests that taurine precipitation (or dissolution) cannot be appreciated by merely following the pH line during a given experiment.

All data points in Figure 6.3 were used to estimate the dependence of taurine's second dissociation constant in equation (6.3) with temperature, according to the generic formula:

$$\ln(K_j) = A + \frac{B}{T} + C \cdot \ln T + D \cdot T \quad (6.10)$$

Where  $A$ ,  $B$ ,  $C$  and  $D$  are empirical parameters. The results are shown in Table 6.2, together with the values for the water dissociation constant in equation (6.4) taken from Posey and Rochelle [207] and the estimated coefficients for the solubility product in equation (6.1), which result from correlating the data from Dalton [20] to equation (6.10). Based on these equilibrium constants, the  $\text{pH}_0$  and speciation of solutions containing taurine and KOH can be predicted, combining (6.1-6.5), and the electroneutrality equation (9.15). Figure 6.3 shows also the predicted  $\text{pH}_0$  with the equilibrium equations, which correlates acceptably with the experimental data.

#### 6.3.2 VLE tests

Absorption of CO<sub>2</sub> in potassium taurate solutions was measured in a well stirred jacketed autoclave at different temperatures (40 - 130°C) and different [TAU/K] ratios. The detailed conditions of the experiments and the results can be found in Appendix 9.3.2. The partial pressure of CO<sub>2</sub> in equilibrium has been fitted to the following empirical relationship of loading ( $\alpha$ ), temperature ( $T$ ), and initial pH ( $\text{pH}_0$ ):

$$\ln(P^{CO_2^{eq}}) = A + \frac{B}{T} + C \cdot \alpha + D \cdot \frac{\alpha}{T} + E \cdot \frac{\alpha^2}{T} + F \cdot \frac{\ln(\alpha)}{T} + G \cdot \text{pH}_0 + H \cdot \frac{\text{pH}_0}{T} \quad (6.11)$$

In the equation above,  $P^{CO_2^{eq}}$  is the partial pressure of CO<sub>2</sub> [kPa] in equilibrium with a given loading  $\alpha$  [mol CO<sub>2</sub>/mol TAU],  $T$  is the absolute temperature [K],  $\text{pH}_0$  is the initial pH of the solution and  $A$  to  $H$  are empirical parameters.

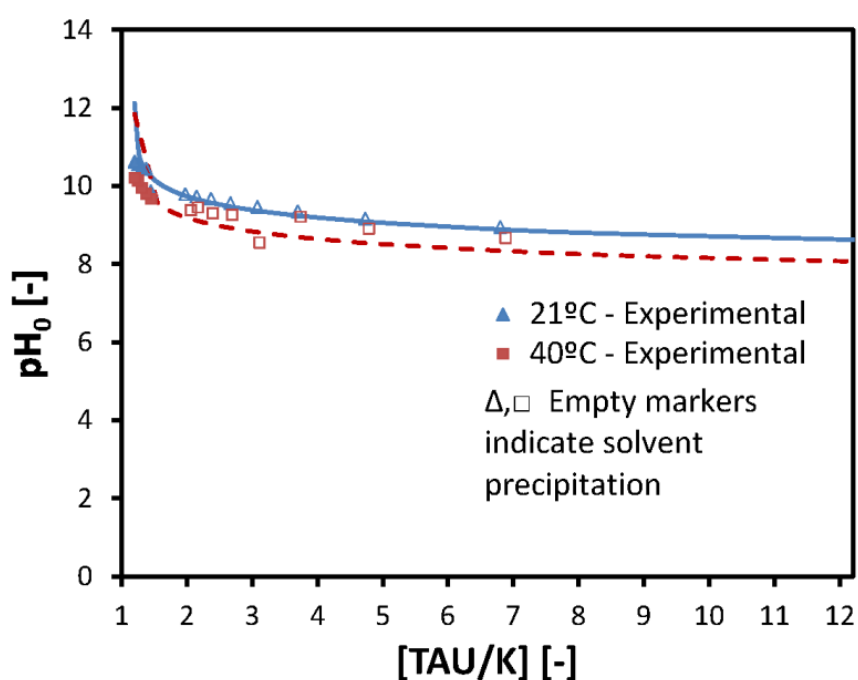


**Figure 6.3.** Neutralization of taurine solutions with KOH. The figure shows the  $\text{pH}_0$  as a function of different  $[\text{TAU}/\text{K}]$  concentration ratios for two different temperatures. Solid and dashed lines represent the empirical model results. The empty markers indicate the presence of taurine solids in solution.

**Table 6.2.** Estimates for the taurine dissociation constant, the water dissociation constant and the solubility product

Parameter	Solubility Product $K_S$ in equation (6.1)	Taurine dissociation $K_2$ in equation (6.3)	Water dissociation $K_3$ in equation (6.4)
Parameters in equation (6.10)			
A	181.46	-4.61	132.9
B	-10521.11	-5000	-13446
C	-25.69	0	22.48
D	0	0	0
Regression results			
Number of observations	11	30	NA
SSE <sup>a</sup>	0.017	6.9	NA
ARD% <sup>b</sup>	1.88%	3.41%	NA

<sup>a</sup>SSE: sum of squared errors between the experimental and model values. Objective function used for the estimation of empirical parameters A to D

<sup>b</sup>ARD%: averaged relative deviation between the experimental and model values.

The generic expression in equation (6.11) is used to describe the experimental VLE data for potassium taurate (4 M) and the literature VLE data for MEA (5 M). However, not all the terms in equation (6.11) are necessary to describe both solvents. The last two terms, with coefficients  $G$  and  $H$ , are concerned with the influence of pH on the absorption equilibrium. When the initial pH of the potassium taurate solution is changed (for instance, by partial neutralization of taurine with KOH), the partial pressure of CO<sub>2</sub> also changes due to the influence of pH on the distribution of species described in equations (6.1) to (6.9). This change in pH and consequent change in  $P^{CO_2^{eq}}$  is well explained by the additional terms  $pH_0$  and  $pH_0/T$ . The specific heat of absorption is derived by differentiating this expression with respect to  $1/T$ :

$$\frac{\partial \ln(P^{CO_2^{eq}})}{\partial \left(\frac{1}{T}\right)} = \frac{\Delta H^{CO_2}}{-R} = B + D \cdot \alpha + E \cdot \alpha^2 + F \cdot \ln(\alpha) + H \cdot pH_0 \quad (6.12)$$

With  $\Delta H^{CO_2}$  representing the specific heat of absorption [kJ/mol],  $R$  representing the gas constant [kJ/mol K] and the same empirical constants as in equation (6.11). Although equations (6.11) and (6.12) are not an accurate representation of the specific solvents considered, they provide solvent capacity and heat of absorption at different process conditions. As shown by Oyeneke and Rochelle [208], these expressions are also consistent with the thermal phenomena that occur during desorption: higher heats of absorption will require more reboiler duty for releasing the bonded CO<sub>2</sub> but, at the same time, will require less energy for stripping steam since the partial pressure of CO<sub>2</sub> increases. This trade-off is addressed in this approach, although the specific heat of absorption might not be consistent with calorimetry data [209].

Figure 6.4 shows the results for the CO<sub>2</sub> absorption in 4 M taurine and 4 M potassium hydroxide solution at different temperatures. Solvent precipitation, indicated by empty markers, only occurs at 40°C for CO<sub>2</sub> loadings above 0.35 mol CO<sub>2</sub>/mol TAU (partial pressure of CO<sub>2</sub> of around 1 kPa) and at 60°C for CO<sub>2</sub> loadings above 0.5 mol CO<sub>2</sub>/mol TAU (partial pressure of CO<sub>2</sub> of around 80 kPa).

The effect of  $pH_0$  was investigated by CO<sub>2</sub> absorption measurements in asymmetric solutions of taurine and KOH (i.e solutions containing different molar amounts of amino acid and base). Results in Figure 6.5 show the absorption isotherms for different asymmetric solutions of potassium taurate and different temperatures. At constant partial pressure of CO<sub>2</sub>, the loading decreases with decreasing KOH concentration (i.e. lower  $pH_0$ ) for any given temperature. In other words, changes in the molar ratio [TAU/K] can have a substantial influence in the partial pressure of CO<sub>2</sub> in equilibrium with the solution. For a given loading, higher partial pressures of CO<sub>2</sub> will be obtained during regeneration when the molar ratio [TAU/K] increases. This will result in less energy needs to strip out the CO<sub>2</sub> from the solution. This important result constitutes proof of the concept described in Section 6.2.1.

The results in Figure 6.4 and Figure 6.5 were fitted to equation (6.11) by multiple linear regression. The estimates for  $A$  to  $H$  coefficients are shown in Table 6.3, together with the results obtained by fitting MEA VLE data from the literature. The correlation between the experimental and calculated values is indicated by the correlation coefficient (multiple R) and the deviation is indicated in the averaged relative deviation (ARD%). This aggregate deviation (25%) is considered acceptable for the conceptual design, as the majority of experimental error is observed to occur at low pressure values only.

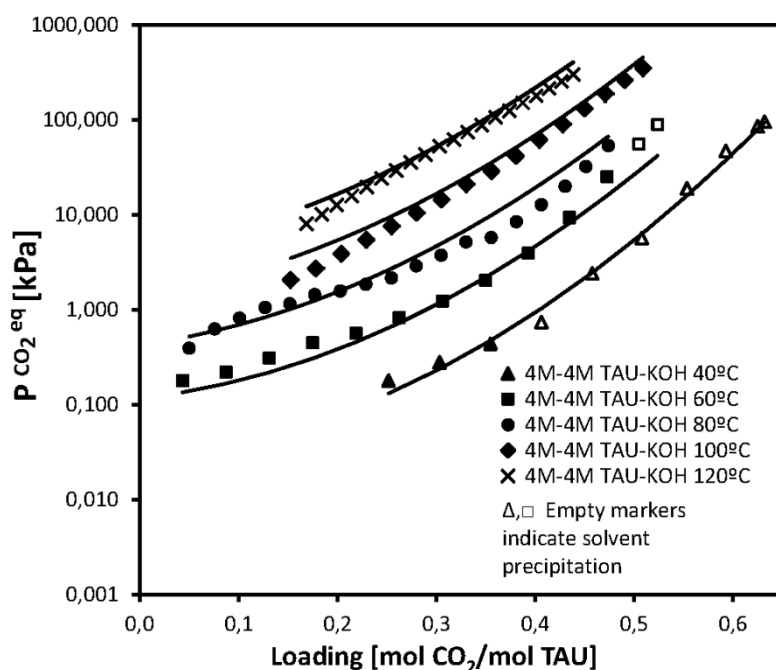


Figure 6.4. Absorption equilibrium of  $\text{CO}_2$  (VLE) in potassium taurate solutions at different temperatures measured in this work. The legend indicates the total concentrations of taurine (TAU) and potassium hydroxide (KOH) in solution. The empty markers indicate the presence of solids in the liquid phase at equilibrium. The continuous lines in the figure indicate the estimated partial pressure of  $\text{CO}_2$  based on equation (6.11) and the coefficients in Table 6.3.

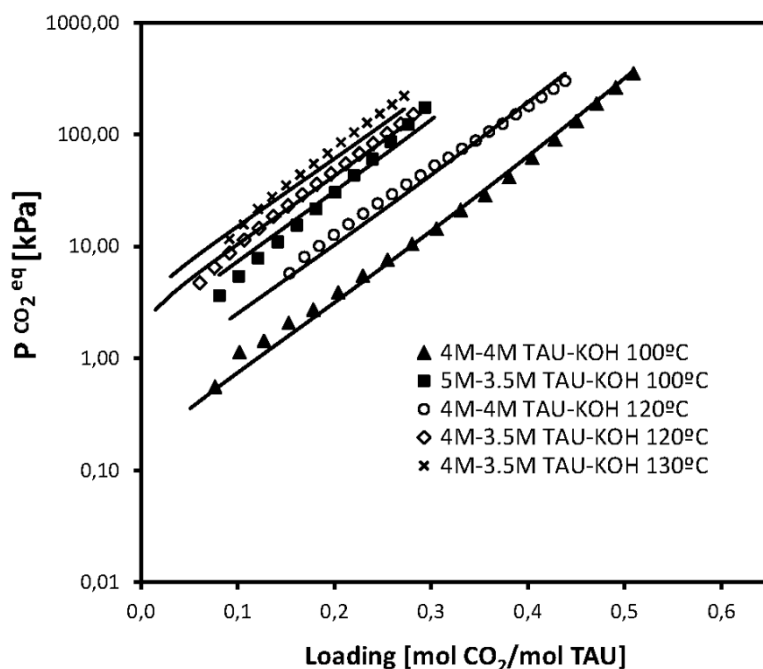


Figure 6.5. Influence of  $\text{pH}_0$  on the absorption equilibrium of  $\text{CO}_2$  (VLE) in potassium taurate solutions at different temperatures. The legend indicates the concentrations of taurine (TAU) and potassium hydroxide (KOH) in solution. The continuous lines in the figure indicate the estimated partial pressure of  $\text{CO}_2$  based on equation (6.11) and the coefficients in Table 6.3.

Together with the absorption of CO<sub>2</sub>, the water vapour pressure of aqueous solutions of potassium taurate can be measured using the same experimental installation. The water vapour pressure of amino acid salt solutions can be substantially lower than that of pure water due to their strong electrolyte nature. This effect was investigated by measuring the water vapour pressure of solutions with different concentrations of potassium taurate. The results, presented in Figure 6.6, show that the depression observed in vapour pressure is more relevant at high concentrations than at low concentrations. The following empirical expression was derived from the experimental data in order to explain this effect:

$$P^{H_2O} = \left( 1 - \left( A + \frac{B \cdot x_s}{T} + C \cdot x_s \right) \cdot x_s \right) \cdot P^{H_2O^0} \quad (6.13)$$

In this equation,  $P^{H_2O}$  represents the vapour pressure of the solution [bar],  $x_s$  is the sum of amino acid and base mol fractions in solution,  $T$  is absolute temperature [K],  $P^{H_2O^0}$  is the vapour pressure of pure water and  $A$  to  $C$  are empirical parameters. Equation (6.13) is thermodynamically consistent and it tends to the value of pure water vapour pressure when the mol fraction of amino acid and base tend to zero. The estimated values for the empirical coefficients in (6.13) are also listed in Table 6.3.

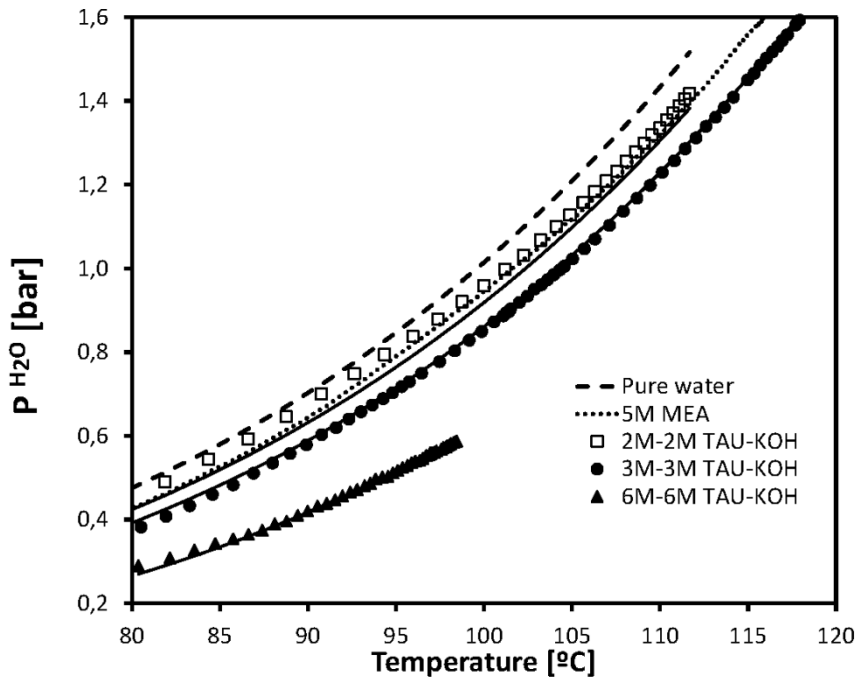


Figure 6.6. Water vapour pressure for different solvents, measured in this work: potassium taurate (TAU-KOH), MEA and pure water. The legend indicates the concentration of the solvents used. The continuous lines represent the estimated water vapour pressure with equation (6.13) and the coefficients in Table 6.3.

**Table 6.3. Estimation of coefficients in equation (6.11) and equation (6.13) by multiple linear regression for potassium taurate (TAU) and MEA.**

Solvent	TAU <sup>a</sup>	MEA <sup>b</sup>	TAU <sup>c</sup>
Parameters	Equation (6.11)		Equation (6.13)
<i>A</i>	-15.44	42.49	0.47
<i>B</i>	9419.69	-17691.20	67.86
<i>C</i>	7.87	-30.10	-0.45
<i>D</i>	1534.81	22210.31	NA
<i>E</i>	1536.86	-5531.43	NA
<i>F</i>	64.52	0.00	NA
<i>G</i>	3.26	0.00	NA
<i>H</i>	-1561.50	0.00	NA
Regression results			
Multiple R	0.984	0.989	0.989
Standard Error	0.322	0.476	0.038
Number of observations	118	112	179
SSE <sup>d</sup>	2.49·10 <sup>4</sup>	7.94·10 <sup>7</sup>	0.059
ARD% <sup>e</sup>	24.82%	41%	3.01%

<sup>a</sup>Derived for potassium taurate solutions and temperatures below 120°C.

<sup>b</sup>Derived for 5 M MEA solution and temperatures below 120°C. Based on data from Lee [205] and Shen and Li [210].

<sup>c</sup>Derived for potassium taurate solutions with concentrations ranging from 2M to 6M.

<sup>d</sup>SSE: sum of squared errors between the experimental and model values.

<sup>e</sup>ARD%: averaged relative deviation between the experimental and model values.

### 6.3.3 Slurry tests

Slurry measurements were performed in order to determine the solid to liquid ratio in the potassium taurate – CO<sub>2</sub> – water system, the dissolving temperature of the slurry formed and liquid pH at different conditions. Table 6.4 shows the results of the slurry tests. The conditions tested were lean and rich conditions and high taurine to KOH ratios at different loadings. The rich solution loading (0.482 mol CO<sub>2</sub>/mol TAU) was determined by the VLE expression in equation (6.11) and the coefficients in Table 6.3 considering conditions of 40°C and 12kPa partial pressure of CO<sub>2</sub> (typical coal-fired power plant flue gas conditions). At these conditions the rich solution contains 15% wt solids, which will completely dissolve at temperatures higher than 76°C. On the other hand, when the [TAU/K] molar ratio increases after the liquid solid separator, the dissolution temperature also increases. As shown in Table 6.4, for [TAU/K] ratios of 1.4, temperatures above 90°C will be necessary if the loading is higher than 0.2 mol CO<sub>2</sub> / mol TAU. This effect imposes a restriction in the attainable [TAU/K] ratio, since no solids can be fed to the stripper column. For this reason the [TAU/K] ratio was limited to 1.2 in the conceptual design. At this ratio no solids were observed above 110°C for any loading.

**Table 6.4. Slurry tests results for loaded solutions of potassium taurate.**

Molarity TAU/KOH (M)	4M/4M	4M/4M	5M/3.5M	5M/3.5M	5M/3.5M
[TAU]/[KOH] ratio (-)	1.0	1.0	1.4	1.4	1.4
Loading (mol/mol)	0.102	0.482	0.085	0.1	0.2
Dissolution temperature (°C)	25	76	71	80	90
pH at dissolution temperature (-)	10.8	8.2	9	8.9	8.5
Solid-Liquid partition ( $w_s$ ) at 40°C (kg/kg)	0.000	0.149	0.122	0.149	0.167

## 6.4 Model development

A VLE Multi-Stage model (VLEMS) has been developed for aqueous solutions of 4 M potassium taurate and 5 M MEA and is used to evaluate the new process concept and compare it to a conventional MEA baseline. The model, implemented in Visual Basic, is divided into the different unit operations described in Section 6.2.1 (Figure 6.1). The absorber and the stripper are modelled as a counter current cascade of equilibrium stages, calculating the vapour-liquid partition and composition at every stage. The other unit operations (heat exchangers and separator) are model as mixing units, calculating the mass and energy balance at every unit but excluding flash calculations. The model assumptions and required parameters are discussed in the following sections.

### 6.4.1 Model assumptions

- 1) The only components that are considered in the VLE calculations are CO<sub>2</sub> and water. Amino acids are non-volatile and in the case of amines, the vaporisation is neglected.
- 2) Each stage is assumed to be well mixed and process conditions and gas and liquid composition are uniform in each stage.
- 3) Temperature, pressure and material equilibrium is reached in each stage.
- 4) The reboiler is considered as an equilibrium stage.
- 5) Heat losses are not considered.

### 6.4.2 Model parameters and inputs

The CO<sub>2</sub> partial pressure under different conditions is represented by the empirical expression in equation (6.11) and the coefficients in Table 6.3. A constant value for the Murphree efficiency is applied at every stage for CO<sub>2</sub>. In the same manner, the water vapour pressure of the different solutions is represented by the empirical expression in equation (6.13) and the coefficients in Table 6.3. No Murphree efficiency is applied to water.

The pressure drop is taken into account by introducing a pressure drop per stage. Values for the pressure drop are taken from Kister [211] for structure packing in the form of pressure drop per HETP. The value of the pressure drop is assigned to each equilibrium stage (*i.e.* Theoretical plate) in the stripper. Since the absorber is considered to be a packing-free column, the pressure drop has been neglected.

The heat of absorption/desorption of CO<sub>2</sub> is calculated with equation (6.12) and the coefficients in Table 6.3. The heat of vaporization of water and the heat capacity of steam are calculated with the equations from the Steam Tables of the IAPWS-IF97 industrial standard [206]. The molar gas heat capacity for CO<sub>2</sub> is calculated with equations from the NIST database [212]. In the case of liquid enthalpy calculation, the overall heat capacity of the entire solution is used. A representative constant value has been used (Table 6.1). This method neglects the addition of CO<sub>2</sub> to the liquid. Solvent density is considered equal for all trays and given a representative constant value (Table 6.1).

A detailed description of the inputs used in the model can be found in Appendix 9.4. The equations per stage or mixing unit are the MESH equations: mass balance, equilibrium (only considered in absorber and stripper columns), summation of mol fractions in each phase and enthalpy balance. These equations are solved simultaneously, giving initial guesses for the temperatures, loading, pH<sub>0</sub> and total molar flows per stage. The model calculates mass and energy balances, temperature and composition profiles and reboiler energy. An example of calculations for a single stage is given in Appendix 9.4.

## 6.5 Results and Discussion

The mass and energy balances for the DECAB Plus process (4 M potassium taurate) were calculated using the VLEMS model and compared to the baseline (5 M MEA). All cases were simulated considering a 90% removal of CO<sub>2</sub> and using a closed flow-sheet to keep the overall CO<sub>2</sub> and water balances to zero. The error in the overall enthalpy balance varied from 0.2% to 1%, depending on the conditions and solvent used. This error arises from the approximations used to estimate enthalpies and it was considered acceptable for the purpose of conceptual design.

### 6.5.1 Baseline case (5 M MEA)

The MEA baseline case was simulated with reboiler conditions of 120°C and 1.9 bar, which were found to be optimal in the experimental results of Knudsen [65]. These experimental results were obtained in a pilot plant with capacity to capture 1 t/h of CO<sub>2</sub> from the flue gas generated at the coal fired power plant operated by Dong in Esbjerg (Denmark). The baseline case is based on a similar flue gas composition to the one treated in the Esbjerg pilot plant but at a larger scale (equivalent to a 250MW power plant). The results of the baseline simulation are presented in Table 6.5 together with the experimental data from Knudsen. The energy requirement of the MEA system is 3.7 GJ/t CO<sub>2</sub>, which is in line with the experimental result. A larger deviation from the experimental data is found in the cooling duty, due to the fact that the model developed for this work does not include a washing section at the absorber's top, which contributes to the cooling duty.

**Table 6.5. Baseline case (5 M MEA) results from the VLEMS model compared to the experimental data of Knudsen [65].**

Parameter	Unit	Value (this work)	Value (literature)
CO <sub>2</sub> recovery	%	90%	88%
Amine lean solvent loading	mol CO <sub>2</sub> /mol MEA	0.21	0.22
Amine rich solvent loading	mol CO <sub>2</sub> /mol MEA	0.48	0.48
Thermal heat required	GJ/t CO <sub>2</sub>	3.66	3.60
Solvent flow rate required	m <sup>3</sup> /t CO <sub>2</sub>	16.64	16.51
Cooling duty	GJ/t CO <sub>2</sub>	2.4	3.7
CO <sub>2</sub> production	kg/h	177000	1090

Notes: Reboiler conditions are 120 °C and 1.9 bar (1.87 bar at Stripper's top).

### 6.5.2 DECAB Plus case (4 M potassium taurate)

The simulations of this case were done under the same assumptions used for the baseline due to the lack of pilot data on the performance of this process. The reboiler pressure was varied from 1.65 to 1.95 bar in order to find an optimum lean loading and solvent flow rate combination that minimises the specific reboiler energy. The optimisation of the lean loading is shown in Figure 6.7. The lean loading that minimises the specific reboiler energy is found at 0.27 mol CO<sub>2</sub>/mol TAU, which corresponds to a reboiler pressure of 1.8 bar. At lower lean loadings, corresponding to pressures around 1.7 bar, the generation of stripping steam is substantially higher than at other pressures, resulting in a high water to CO<sub>2</sub> molar ratio at the top of the stripper column. This requires relatively high reboiler energy per unit of CO<sub>2</sub> desorbed. For pressures higher than 1.7 bar, the lean loading increases. This reduces the specific energy required in the reboiler by decreasing the water to CO<sub>2</sub> molar ratio. However, solvent capacity is also reduced. Therefore the lean solvent flow increases in order to maintain the CO<sub>2</sub> removal rate at 90%. At higher lean loadings (pressures around 1.9 bar), solvent capacity is reduced to the point that the specific reboiler energy increases again due to the high solvent flow rate necessary to maintain the CO<sub>2</sub> removal rate. The specific reboiler duty at the optimum lean loading and 0% recycle split fraction is 3.3 GJ/t CO<sub>2</sub>. This value is 10% lower than the one of the optimised MEA baseline.

After fixing the reboiler pressure at 1.8 bar, several simulations were conducted varying the recycle split fraction in the separator. This variable represents the fraction of the liquid supernatant that is recycled to the absorber column. The optimisation of this variable is shown in Figure 6.8. As already anticipated for the DECAB Plus concept, increasing the recycle split fraction reduces the specific reboiler duty. The optimum value is found at 30%. At this value, the specific reboiler duty is 2.4 GJ/t CO<sub>2</sub> corresponding to a 35% reduction of the reboiler duty in the MEA baseline.

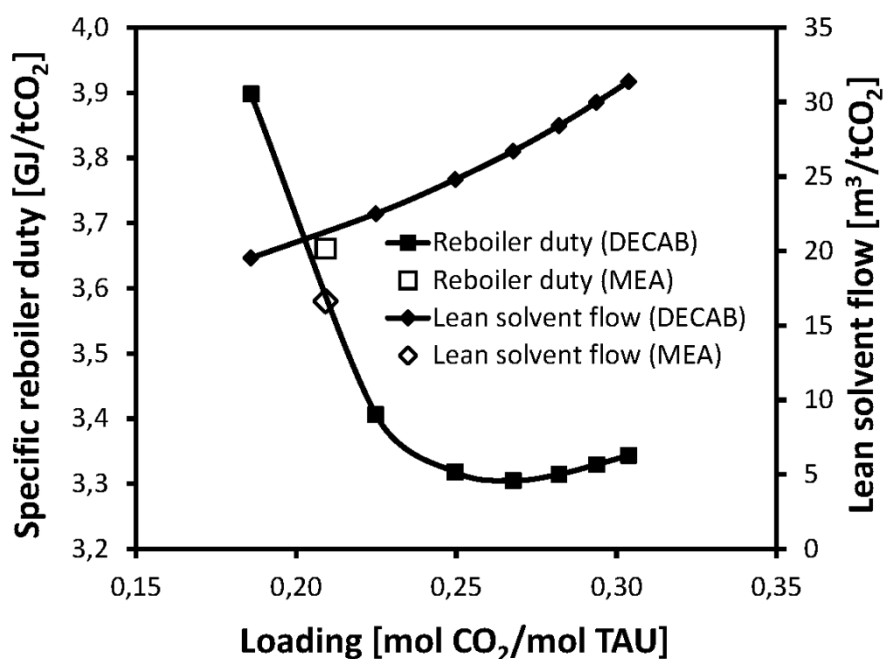


Figure 6.7. Optimisation of lean loading for the DECAB Plus case. The specific reboiler duty and the lean solvent flow are calculated and plotted as a function of lean loading for a constant CO<sub>2</sub> removal rate of 90% and constant stripper temperature of 120°C. The values for the MEA baseline are also shown for the optimum lean loading and 90% CO<sub>2</sub> removal rate and stripper temperature of 120°C.

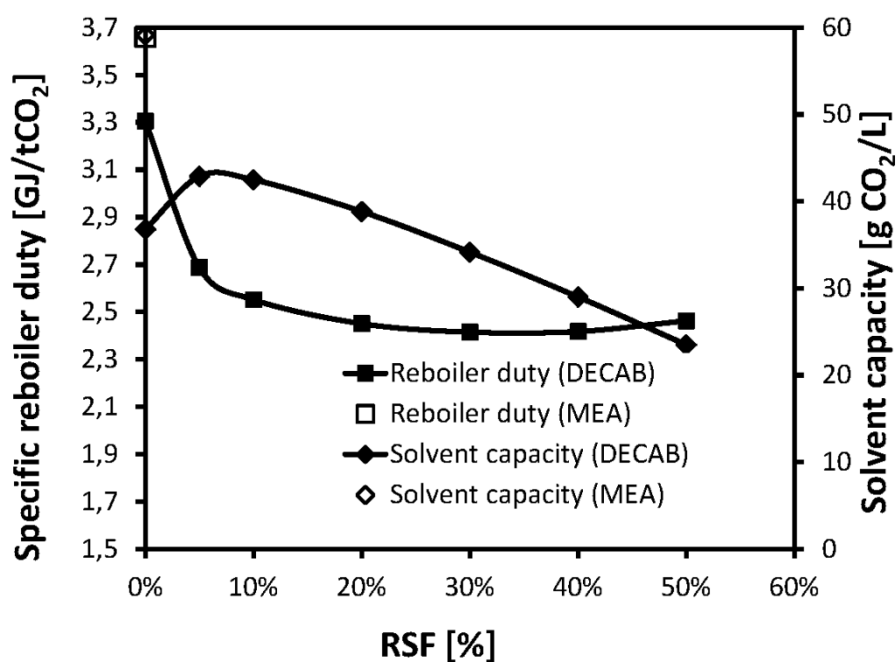


Figure 6.8. Optimisation of the recycle split fraction (RSF) for the DECAB Plus case. The specific reboiler duty and the solvent capacity are calculated and plotted as a function of the recycle split fraction (RSF) for a constant CO<sub>2</sub> removal rate of 90% and constant stripper temperature of 120°C. The values for the MEA baseline are also shown for the optimum lean loading, 90% CO<sub>2</sub> removal rate and stripper temperature of 120°C.

#### 6.5.2.1 Effect of recycle split fraction on solvent capacity

As shown in Figure 6.8, the recycle split fraction has also an effect on solvent capacity. It has been discussed in Section 6.2.1 that the recycled stream to the absorber contains carbonated species. Therefore, a lower process solvent capacity is to be expected. Nevertheless, for small values of the recycle split fraction the solvent capacity is increased. For instance, recycling 10% of the rich supernatant stream to the absorber increases solvent capacity by 16%. This counter-intuitive effect is explained by the fact that the pH-shift effect in the stripper results in a super-lean stream that combined with the recycled supernatant leads to a lower lean loading than in the case with no recycle. Therefore, the pH-shift effect off-sets the capacity loss at values of the recycle split fraction lower than 10%. At higher recycle split fractions the improvement in solvent capacity starts to decline until solvent capacity becomes lower than the initial at 0% recycle split fraction.

#### 6.5.2.2 Effect of the recycle split fraction on the absorption enthalpy

Although all the data points presented in Figure 6.8 have a lower solvent capacity than the MEA baseline (59 g CO<sub>2</sub>/L), the specific energy consumption for the DECAB Plus concept is always lower than for the MEA baseline. The positive aspects of the DECAB Plus concept that explain these results are partially a lower water to CO<sub>2</sub> ratio and mainly a substantial reduction in the absorption enthalpy. In order to analyse the last effect, the absorption enthalpy was calculated using equation (6.12) and the parameters in Table 6.3 at different CO<sub>2</sub> loadings and initial solution's pH (pH<sub>0</sub>). The results, presented in Figure 6.9, show a substantial reduction in absorption enthalpy as the initial pH of the solution decreases. One explanation for this phenomenon is the different ionic distribution in solution when the pH decreases. The solution's lower pH is obtained by increasing the ratio [TAU/K] in solution. This implies that there are relatively fewer K<sup>+</sup> ions in solution than in the original equimolar solution. In order to balance charge, the equilibria need to evolve to a situation where less negatively charged species are present in solution. This could be achieved by reverting the carbamate to taurate (equation 6.5), and the carbonate to bicarbonate (equation 6.7) yielding a solution that is richer in CO<sub>2</sub> and bicarbonate. The carbonate-bicarbonate solvent system is associated with lower heats of absorption [209] which explains the reduction in absorption enthalpy shown in Figure 6.9.

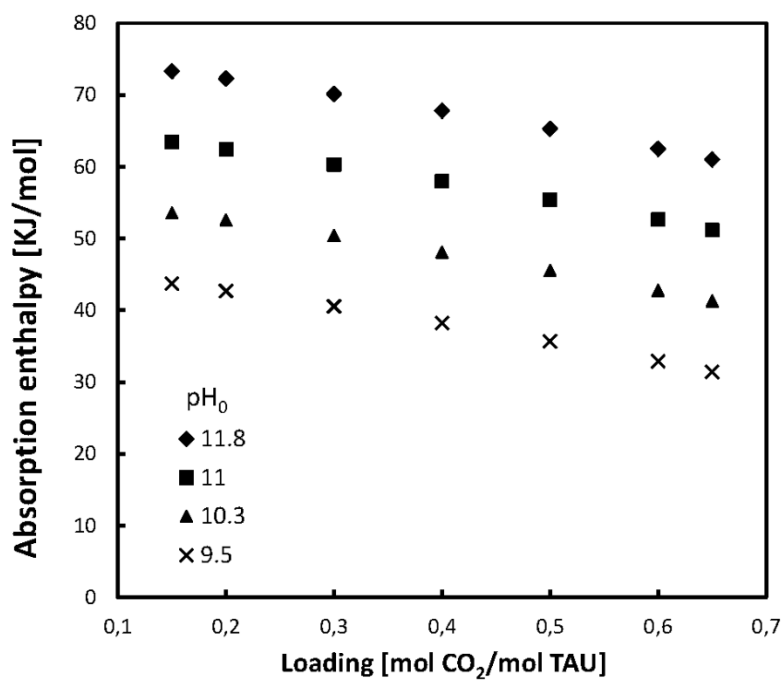


Figure 6.9. Calculated absorption enthalpy at different pH<sub>0</sub> and loadings.

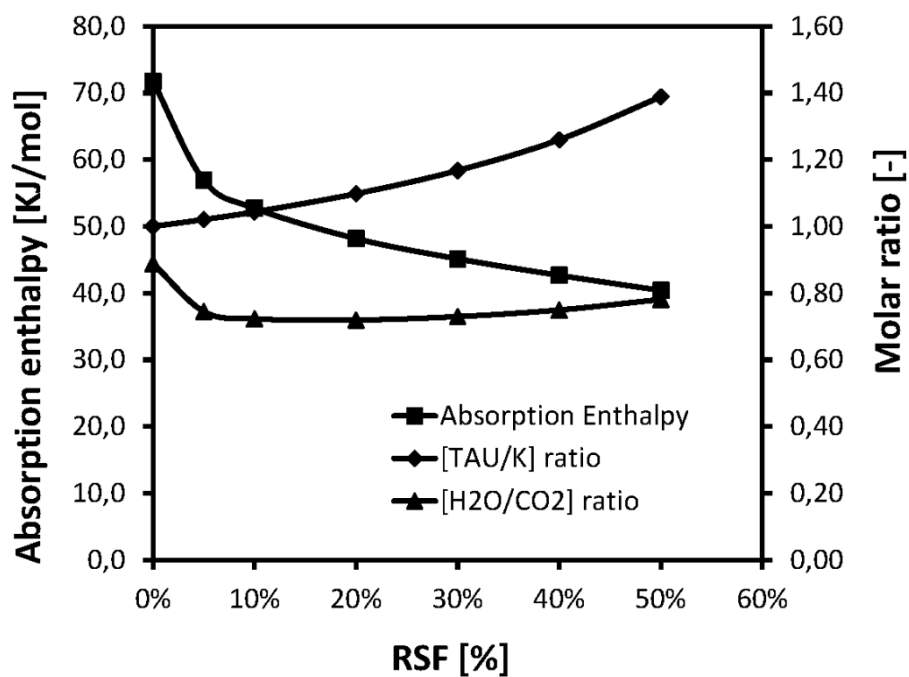


Figure 6.10. Influence of the recycle split fraction on the absorption enthalpy, water to CO<sub>2</sub> ratio ([H<sub>2</sub>O/CO<sub>2</sub>]) and the taurine to potassium ratio ([TAU/K]).

Figure 6.10 illustrates the influence of the recycle split fraction on the absorption enthalpy and other factors such as the water to CO<sub>2</sub> molar ratio calculated at stripper's top stage conditions and the taurine to potassium ratio that results from the recycle of the liquid supernatant. Since the absorption enthalpy depends on the lean loading (Figure 6.9), the values presented in Figure 6.10 are an average for loadings ranging from 0.05 to 0.6 mol CO<sub>2</sub>/mol TAU for each value of the recycle split fraction. Increasing values of the recycle split fraction lead to higher [TAU/K] ratios. This implies lower values of pH<sub>0</sub> and, therefore, a reduction of the absorption enthalpy. As shown in Figure 6.10, the absorption enthalpy is reduced from 72 kJ/mol at 0% recycle split fraction to 45 kJ/mol at the optimum value of the recycle split fraction (30%). On the other hand, the water to CO<sub>2</sub> molar ratio at stripper's top stage conditions decreases initially due to a higher partial pressure of CO<sub>2</sub> that results from the reduction of pH<sub>0</sub>. This effect gradually decreases for values of the recycle split fraction above 20%.

### 6.5.2.3 Energy requirements to re-dissolve the slurry

It must be noted that the slurry feed to the stripper requires the input of low-grade energy to dissolve the taurine crystals. The DECAB Plus process, depicted in Figure 6.1, uses the energy from the hot lean stream to heat the rich stream that is fed to the stripper. The additional energy input required for the phase change is approximated by the dissolution energy, which is supplied in the separator heat exchanger. This energy is not included in the analysis since its quality is completely different to the steam quality required in the reboiler. In principle hot water of around 80°C could be used for this purpose. However, the energy requirements for the DECAB Plus process will need to be sourced efficiently to ensure minimal impact to the power plant.

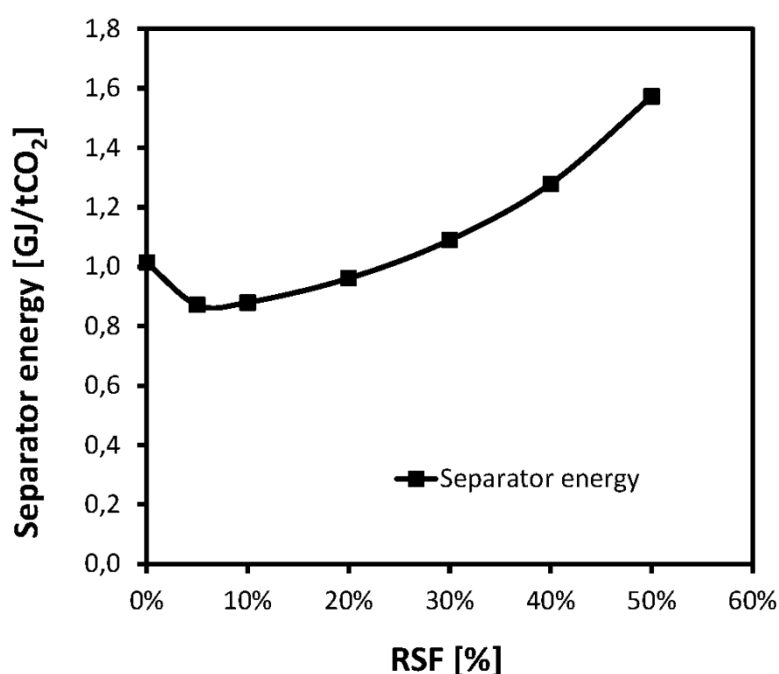


Figure 6.11. Influence of the recycle split fraction (RSF) on the specific separator energy. This energy is necessary to dissolve taurine crystals.

Figure 6.11 shows the specific energy requirements of the separator as a function of the recycle split fraction. The separator energy is linked to the required solvent flow rate which depends on solvent's capacity. Therefore, the energy required in the separator decreases initially due to the improvement in solvent capacity and increases gradually for recycle split fractions above 15%.

## 6.6 Conclusions

In this work a new process for CO<sub>2</sub> capture has been developed based on precipitating amino acid solvents. The novelty of the process consists of enhancing solvent regeneration by inducing a pH-shift, which is achieved by partially separating the liquid and the solid fraction formed during CO<sub>2</sub> absorption. A conceptual design based on 4 M potassium taurate has been presented together with the necessary experimental evidence to proof the concept. Also, the same conceptual design method has been used to evaluate a baseline case based on 5 M MEA. The DECAB Plus concept can lower the specific reboiler energy for solvent regeneration by 35% compared to the MEA baseline. The specific reboiler energy is reduced from 3.7 GJ/ t CO<sub>2</sub>, which corresponds to the MEA baseline, to 2.4 GJ/ t CO<sub>2</sub>, which corresponds to the DECAB Plus process.

There are different effects related to the pH-shift during desorption that contribute to lower the reboiler energy:

- 1) Solvent capacity increases by recycling small fractions of the liquid supernatant in the rich stream back to the absorption column. With respect to the case with no recycle, a 10% recycle of the liquid supernatant leads to a 16% extra solvent capacity. This effect is gradually lost with increasing recycle fractions.
- 2) The absorption enthalpy decreases by recycling fractions of the liquid supernatant in the rich stream back to the absorption column. The estimated absorption enthalpy for the case with no recycle is 72 kJ/mol, while for the optimum recycle split fraction, 30%, this absorption enthalpy is reduced to 45 kJ/mol. This is the effect that contributes the most to the reduction in the reboiler energy.

The DECAB Plus process also requires 0.96 GJ/ t CO<sub>2</sub> to re-dissolve the precipitates formed during absorption. Although this requirement is substantial, due to the high dissolution heat of taurine, the quality of this energy is relatively low, which reduces considerably the impact on the power plant efficiency. After full consideration of all the aspects involved in the conceptual design, the proposed process has lower energy requirements than the MEA baseline and it has potential to significantly reduce the energy required by the capture process by exploring different amino acid solvents.



---

# ANALYSIS OF PROCESS CONFIGURATIONS FOR CARBON DIOXIDE CAPTURE BY PRECIPITATING AMINO ACID SOLVENTS

## ABSTRACT

*Precipitating amino acid solvents are an alternative to conventional amine scrubbing for CO<sub>2</sub> capture from flue gas. Process operation with these solvents leads to the formation of precipitates during absorption that need to be re-dissolved prior to desorption of CO<sub>2</sub>. The process configuration is crucial for the successful application of these solvents. Different process configurations are analysed in this chapter, including the addition of lean vapour compression, multiple absorber feeds and the use of different amino acids to the baseline based on potassium taurate. The analysis is carried out with an equilibrium model of the process that approximates the thermodynamics of the solvents considered. The results show that the precipitating amino acid solvents can reduce the reboiler duty needed to regenerate the solvent with respect to a conventional MEA process. However, this reduction is accompanied by an expenditure in lower grade energy needed to dissolve the precipitates. To successfully implement these processes into power plants, an internal recycle of the rich stream is necessary. This configuration, known as DECAB Plus, can lower the overall energy use of the capture process, which includes the energy needed to regenerate the solvent, the energy needed to dissolve the precipitates, and the energy needed to compress the CO<sub>2</sub> to 110 bar. With respect to the energy efficiency, the DECAB Plus with lean vapour compression configuration is the best configuration based on potassium taurate, which reduces the reboiler duty for regeneration by 45% with respect to conventional MEA. Retrofitting this process into a coal fired power plant will result in overall energy savings of 15% with respect to the conventional MEA process, including compression of the CO<sub>2</sub> stream to 110 bar. Potassium alanate was found to reduce the energy use with respect to potassium taurate under similar process configurations. Therefore, the investigation of potassium alanate in a DECAB Plus configuration is highly recommended, since it can reduce the energy requirements of the best process configuration based on potassium taurate.*

*This chapter is based on:*

*E. Sanchez Fernandez, K. Heffernan, L. van der Ham, M.J.G. Linders, D.W.F. Brilman, E. L.V. Goetheer, T. J.H. Vlugt. "Analysis of process configurations for CO<sub>2</sub> capture by precipitating amino acid solvents". Submitted to the Ind.Eng.Chem.Res journal.*

## 7.1 Introduction

CO<sub>2</sub> capture based on absorption and thermal desorption on a large scale is considered a suitable technology for carbon abatement in the current energy sector (highly dependent on fossil fuels) [2, 92, 127]. Major drawbacks of this technology are the efficiency penalties and high operating cost, related to solvent regeneration and CO<sub>2</sub> compression, which prevent commercial application at large scale [13, 155, 213]. The integration of CO<sub>2</sub> capture into power plants results in a reduction of the net power plant efficiency which depends on the capture technology, power plant type and degree of heat integration [13, 156, 191, 214, 215]. Amine solvents are the most common industrial choice for low pressure absorption [39, 49, 216]. In the case of coal fired power plants reductions of plant efficiencies of 9 to 12 percentage points are expected for the conventional industrial standard monoethanolamine (MEA) [15, 31, 217]. MEA is also degraded in the presence of SO<sub>2</sub>, O<sub>2</sub> and metal ions in solution with the formation of irreversible by-products or degradation products [45], reducing the absorption capacity of the amine and increasing the emissions of undesirable products to the atmosphere [124].

Improvements to the costs of the conventional industrial standard (30% wt MEA solution) can be obtained by screening for solvents that have higher absorption capacity and rates (*e.g.* promoted tertiary amines and hindered amines such as promoted MDEA) [59, 60, 159, 218].

Improvements, both economically and environmentally, can also be made by developing solvents with a higher resistance to degradation and lower toxicity and volatility. Alternative solvents to amines are amino acid salts [68] and promoted potassium carbonate [195, 219, 220]. Besides the solvents suited for the conventional absorption-desorption process, other solvents that are under development are the phase change systems such as the carbonate precipitating processes [221], the de-mixing solvent technology [222], and precipitating amino acid salts [81]. Alternative process configurations have also been proposed to reduce capital and operating costs of the CO<sub>2</sub> capture process [223]. Numerous publications propose flow-sheet modifications to the conventional MEA industrial process in order to upgrade the process or its energetic integration with the steam cycle of the power plant [106, 137, 177, 224]. Frequent configurations to be evaluated are the modification of process operating conditions (*e.g.* stripper process conditions, lean-rich heat exchanger pinch) [55], the use of multiple absorber feeds or staged feed to the stripper (*e.g.* the split flow scheme) [225], and the use of the sensible heat contained in the exit streams of the stripper column (*e.g.* the lean vapour compression configuration) [226].

Precipitating amino acid solvents are a promising alternative to amines. In specific cases, a lower energy required to regenerate the solvent has been reported [227]. Other benefits when compared to MEA, are higher stability and lower corrosion in the case of taurine [228], higher absorption rates in the case of sarcosine [77] and proline [229]. Due to the non-volatile nature of these solvents, lower emissions are foreseen for processes based on precipitating amino acids. The simplest process configuration based on these solvents (DECAB) requires the use of a spray tower to handle solids during absorption. The precipitates are re-dissolved before desorption, which takes place in a conventional stripper [81]. The introduction of an internal recycle in this process configuration (DECAB Plus) can enhance the release of CO<sub>2</sub> without modifications in the stripper [227].

In this work, an evaluation and optimisation of different process configurations based on the precipitating amino acid solvents is presented. The evaluation has focused on two research directions; improvements in process configuration, and screening for alternative solvents with improved performance. The evaluation relies on an equilibrium based model, which includes all the necessary unit operations of the processes to capture CO<sub>2</sub> from coal fired power plants' flue gas. The model uses an approximate thermodynamic representation of the solvents investigated based on empirical correlations that have been derived from experimental data. Initially, an investigation of DECAB and DECAB Plus process conditions is presented based on potassium taurate. The key parameters of the processes are modified with the objective of decreasing the required energy for regeneration. After optimising the process conditions, two process additions are integrated and investigated. These include the lean vapour compression option and multiple feeds to the absorber. The performance of other amino acid solvents is also investigated for the DECAB process configuration.

## 7.2 Baseline configuration (DECAB and DECAB Plus)

CO<sub>2</sub> absorption in aqueous amino acid salt solutions generally leads to the formation of precipitates, depending on the particular amino acid and the concentration in solution [84, 85]. The composition of the precipitates varies with the structure of the amino acid used to prepare the amino acid salt solution. It can contain mainly the pure amino acid, for primary amino acids, KHCO<sub>3</sub>, for highly hindered amino acids, or a combination of amino acid and KHCO<sub>3</sub>, for other amino acids [85]. This phase change can influence the equilibrium reactions in CO<sub>2</sub> absorption and desorption contributing to reduce the energy use of the conventional absorption-desorption capture process. The chemistry of the reaction of CO<sub>2</sub> with amino acid salts in the precipitation regime has been described by Kumar [82]. The identified effects related to precipitation are: (1) the enhancement of the specific CO<sub>2</sub> capacity of amino acid salt solutions [71], (2) the acidification of the rich solution, which is not a direct effect of precipitation but is brought about by introducing a phase separation after precipitation that partially removes the supernatant and results in the concentration of the amino acid in the rich solution once the precipitates have been redissolved [86, 230]. The first effect, enhancement of CO<sub>2</sub> absorption, occurs when precipitates are formed during absorption as a result of the chemical reaction of CO<sub>2</sub> with the amino acid salt. The products of this reaction that have a limited solubility (the pure amino acid and / or the KHCO<sub>3</sub>) precipitate when the saturation point is reached. The removal of the solid reaction product from the liquid phase shifts the reaction equilibrium towards the production of more products. The result is a rich stream in the form of slurry that contains mainly the pure amino acid in the solid phase (for primary amino acids) or a mixture of pure amino acid and bicarbonate (for more hindered amino acids) and carbamate, bicarbonate, amino acid salt counter-ion (*e.g.* potassium, sodium) and remaining amino acid species in the liquid phase. The second effect, acidification of the rich stream, requires the processing of the slurry in a solid-liquid separator to partially separate the supernatant from the solids. This forms a concentrated slurry, which is heated to dissolve the amino acid precipitates. The resulting rich solution, enriched in amino acid, is further processed in the stripper for desorption. The supernatant excess, enriched in amino acid salt counter-ions, is recycled to the absorber without passing through the stripper. After dissolving the amino acid crystals, the pH of the rich stream is decreased before thermal desorption, enhancing the release of the chemically bonded CO<sub>2</sub>.

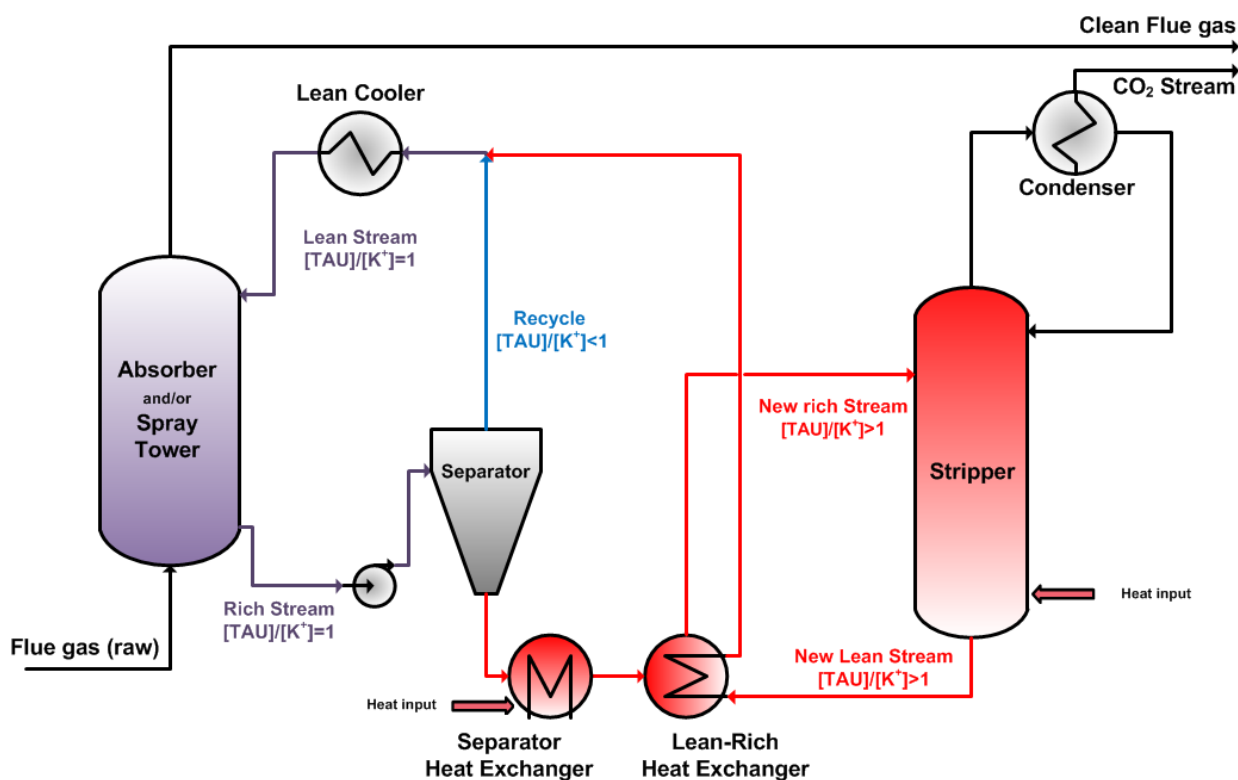


Figure 7.1. DECAB and DECAB Plus process concepts based on precipitating potassium taurate. The separator and recycle stream are only pertinent for the DECAB Plus concept. DECAB can be seen as a simplification of this flowsheet where the recycle stream is set to zero. The ratio of the total taurine concentration to the total potassium concentration in solution is indicated below the name of each stream. This ratio can be 1 (equimolar solution), higher than 1 (solution with less potassium than the equimolar and, therefore, lower  $\text{pH}_0$ ) or less than 1 (solution with more potassium than the equimolar solution and, therefore, higher  $\text{pH}_0$ ).

Figure 7.1 illustrates a generic precipitating amino acid process scheme based on the potassium salt of taurine that exploits both effects. The flue gas, containing circa 13 % v/v CO<sub>2</sub> at 40°C, is treated with a solution of potassium taurate with 1:1 molar amounts of taurine and KOH in a suitable contactor that can handle solids. This can be a spray tower contactor or a sequence of spray tower contactor and packed column [81]. The slurry that results from the absorption of CO<sub>2</sub> can be directly regenerated in the stripper, via the lean-rich heat exchanger, in a process concept known as DECAB [81]. In this case, the separator in Figure 7.1 is not needed. Alternatively, the slurry can be treated in the solid-liquid separator yielding two streams; new rich stream and recycle. The new rich stream is a slurry enriched in taurine, that has a taurine-to-potassium molar ratio ( $[\text{TAU}/\text{K}]$ ) higher than 1. This stream is further processed in the stripper, where the CO<sub>2</sub> is released, yielding the new lean stream. By re-dissolving the amino acid crystals, the pH of the new rich solution is decreased before thermal desorption, which results in higher partial pressures of CO<sub>2</sub> at stripper conditions that facilitate desorption. The recycle stream is the supernatant excess enriched in potassium ions, that has a taurine-to-potassium molar ratio lower than 1. This stream is mixed with the new lean stream and is fed back to the absorber without passing through the stripper. Mixing the recycle and the new lean stream results in the initial lean stream that has a taurine-to-potassium molar ratio of 1. This process alternative is known as DECAB Plus.

The technical analysis of these process concepts with potassium taurate (Chapter 6) shows that the DECAB process concept can decrease the reboiler duty needed for solvent regeneration [230]. Compared to a conventional MEA process, the reboiler duty of the DECAB process concept is 10% lower. This duty can be further reduced with the DECAB Plus concept. Due to the internal recycle in this process concept, the rich stream that is regenerated in the stripper has a substantially higher CO<sub>2</sub> equilibrium pressure due to the pH change that is induced by concentrating the amino acid. For this reason, a “super lean” stream is obtained in the stripper with less energy penalty. At the same time, the recycled stream that is fed back to the absorber contains a high concentration of CO<sub>2</sub>, which decreases the process capacity. With an optimum recycle, the first effect is dominant resulting in a 35% lower reboiler duty compared to a conventional MEA process [230]. Other effects of the internal recycle, which are linked to the change of amino acid speciation due to a lower pH, are the reduction in the heat of desorption and the reduction of the amino acid solubility in the new rich stream. The first effect contributes substantially to the reduction in regeneration energy, but the second effect limits the extension of the internal recycle (and its benefits) to avoid solids in the new rich stream that is fed to the stripper. Another point of attention is that DECAB and DECAB Plus processes require the input of low-grade energy to redissolve the solids formed during absorption. The energy needed for this phase change is approximated by the dissolution energy and is supplied to the new rich stream in the separator heat exchanger (Figure 7.1). This energy is of a relatively low quality compared to the steam quality required by the reboiler, and it could be supplied by low pressure steam (ca. 1 bar), hot water of about 80°C or stripper reboiler condensate. However, in the case of potassium taurate, it is substantial in terms of volume, due to the high heat of dissolution of this amino acid salt [230]. For future development of these processes, the main points for improvement are the net capacity of the solvent, which becomes a dominant factor when high portions of the rich stream are recycled, the solubility of the amino acid, and the heat of dissolution of the amino acid.

### **7.3 Alternative process configurations for DECAB and DECAB Plus**

The use of alternative process configurations or solvents could further reduce the energy requirements of DECAB and DECAB plus processes. The main focus for process improvement is the selection of process conditions that maximize process capacity, which in turn, will minimize the energy required by the reboiler for solvent regeneration. Moreover, the energy required by the separator heat exchanger to re-dissolve the crystals is linked to the required solvent flow rate, which depends on the solvent net capacity. Therefore, increasing the bulk solvent capacity will also reduce the energy requirements of the separator heat exchanger. The process modifications that have been analysed in this work are intended to improve the process capacity of the DECAB and DECAB Plus process concepts. The selected process modifications are; (1) optimisation of the operating conditions of the baselines, (2) the introduction of the lean vapour compression (LVC) configuration, (3) the use of multiple feeds to the absorber and (4) the use of an alternative amino acid solvent to potassium taurate. These options are discussed in the following sections.

### 7.3.1 Optimisation of the operating conditions of DECAB and DECAB Plus

The modifications to the process operating conditions of the baselines have the objective of optimising the combined thermal and pH-shift effects during desorption. The thermal effect depends on the operating temperature of the reboiler and the pH-shift effect depends on the amount of precipitate that is formed during absorption, the temperature at which the solid-liquid separation takes place, and the fraction of the liquid supernatant that is recycled. For the purpose of optimisation, the reboiler temperature, the separator temperature and the flow of the recycle stream have been modified to analyse the combined effect of temperature and different  $[\text{TAU}/\text{K}]$  ratios on the reboiler duty.

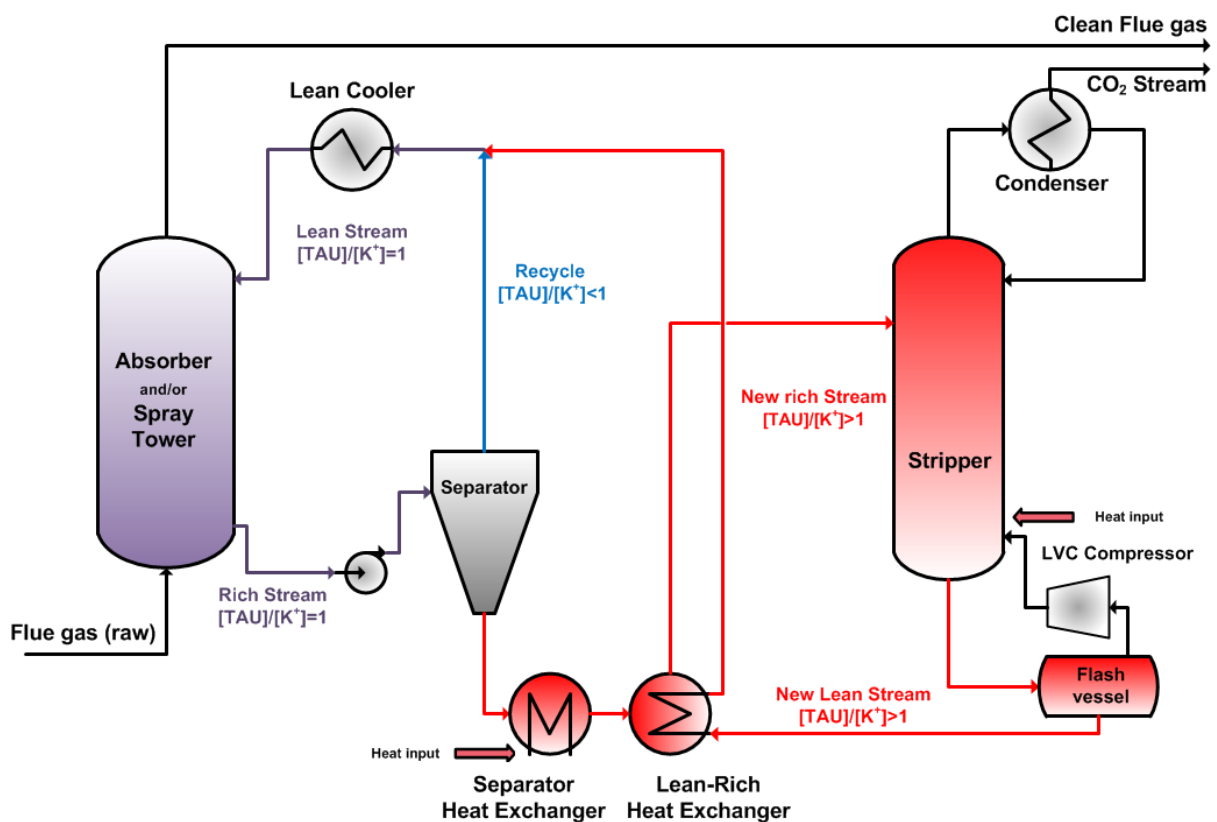


Figure 7.2. DECAB Plus process based on precipitating potassium taurate with LVC. The ratio of the total taurine concentration to the total potassium concentration in solution is indicated below the name of each stream. This ratio can be 1 (equimolar solution), higher than 1 (solution with less potassium than the equimolar and, therefore, lower  $\text{pH}_0$ ) or less than 1 (solution with more potassium than the equimolar solution and, therefore, higher  $\text{pH}_0$ ).

### 7.3.2 Lean vapour compression (LVC)

The LVC option has been described and investigated for other solvent systems, such as MEA [54, 55, 137, 177, 226]. In this process concept, illustrated in Figure 7.2, the lean stream that leaves the stripper column is flashed adiabatically in a separate vessel. As a consequence of the pressure reduction, the solvent is partially evaporated. The vapour generated is re-compressed and re-injected at the base of the stripper column. The benefits of this process concept are that

part of the  $\text{CO}_2$  remaining in the lean stream is flashed, reducing the lean loading and that more steam is generated, reducing the necessary heat input to the reboiler.

### 7.3.3 Multiple feeds to the absorber

The DECAB Plus process concept with multiple feeds to the absorber is illustrated in Figure 7.3. In this configuration, the new lean stream that leaves the stripper column is divided into two streams. One of the streams is mixed with a fraction of the recycle stream and fed to the top of the absorber column. The other stream is mixed with the remaining fraction of the recycle stream and is fed at an intermediate stage within the absorber column. This alternative configuration results in two new streams (one lean and the other semi-lean) with different  $\text{CO}_2$  loadings and different  $[\text{TAU}/\text{K}^*]$  ratios. The lean stream has a lower  $\text{CO}_2$  loading than the corresponding lean stream in the DECAB Plus baseline configuration. This stream is fed at the top of the absorber column with the aim of increasing the absorption capacity at the top stages of the absorber. The semi-lean stream has an intermediate  $\text{CO}_2$  loading between the lean and the rich streams and is fed to an intermediate stage in the absorber column. This configuration also creates a pH gradient within the absorber due to the different  $[\text{TAU}/\text{K}^*]$  ratios. The top stages have a lower pH than the bottom stages.

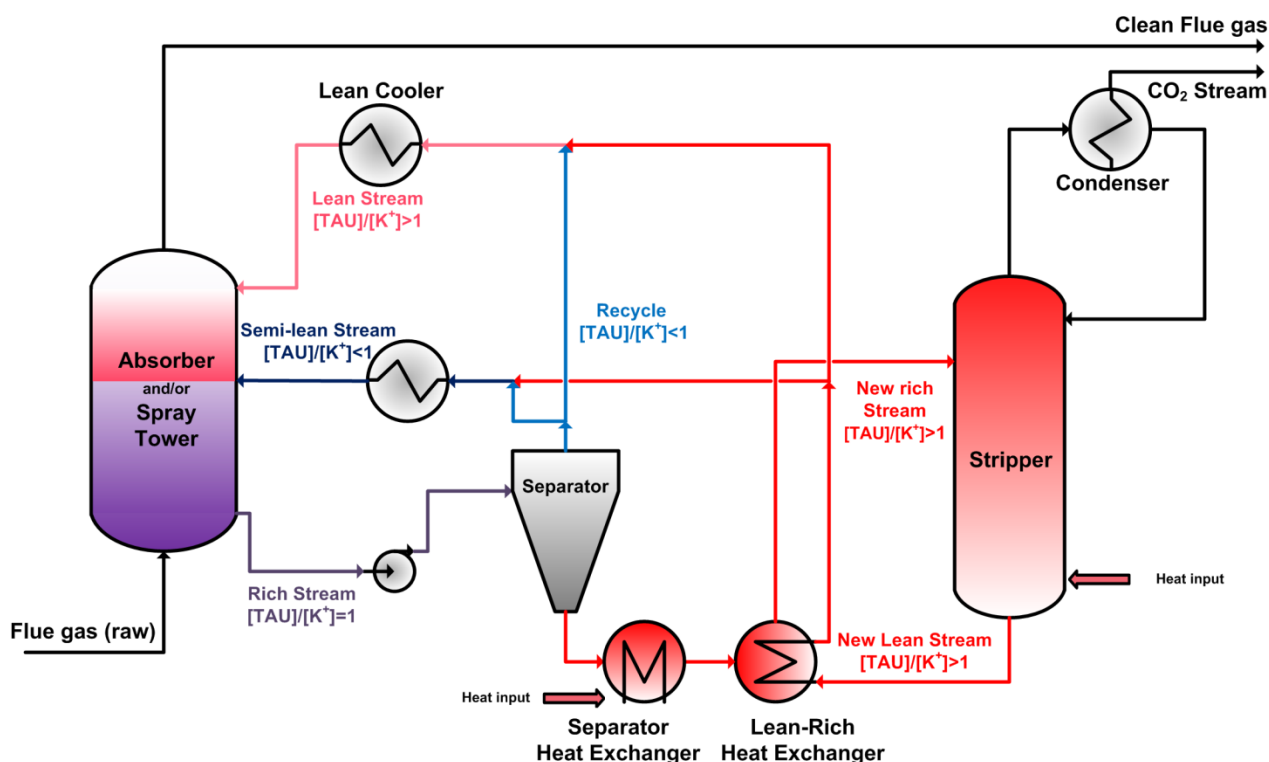


**Figure 7.3.** DECAB Plus process based on precipitating potassium taurate with multiple absorber feeds. The process areas with lower pH are located downstream the separator and at the top of the absorber. The ratio of the total taurine concentration to the total potassium concentration in solution is indicated below the name of each stream. This ratio can be 1 (equimolar solution), higher than 1 (solution with less potassium than the equimolar and, therefore lower  $\text{pH}_0$ ) or less than 1 (solution with more potassium than the equimolar solution and, therefore, higher  $\text{pH}_0$ ).

### 7.3.4 Alternative solvents

Solvent regeneration in the DECAB and DECAB Plus processes relies on the thermal energy provided by the reboiler and the pH-shift effect described in Section 7.2, which helps to the reduction of this energy. Both thermal and pH-shift effects in these processes are influenced by specific amino acid properties. For the purpose of selecting a solvent that requires less regeneration energy, there are key solvent characteristics that are of importance, such as the net CO<sub>2</sub> capacity of the solvent, the absorption rates, the heat of absorption, and the heat capacity of the solvent [70]. The extension of the precipitation reaction during absorption is important to the reduction of the regeneration energy, since the formation of more amino acid precipitates helps to decrease the pH of the new rich stream formed when a fraction of the supernatant is recycled. The precipitates need to be dissolved for the pH-shift effect to be effective. Therefore, the amino acid solubility, which is relevant to the precipitation, and heat of dissolution, which is relevant to the dissolution of the precipitates, are also important properties for the selection of an alternative solvent for these processes.

With the aim of finding alternative solvents to potassium taurate, the properties of natural amino acids were screened in this work in order to improve process performance. The solvent screening strategy was based on the improvement of the process performance with no-recycle (*i.e.* no pH-shift effect). The desired amino acid properties for a successful implementation in a DECAB-like process are high capacity for CO<sub>2</sub>, high stability, relatively higher solubility and lower heat of dissolution than taurine. In order to improve the CO<sub>2</sub> capacity, amino acids with hindered amino groups were targeted, since they generally show higher absorption capacity than primary amino groups [218]. Other relevant characteristic is the precipitate type that is formed during the absorption of CO<sub>2</sub>. The more hindered amino acid species tend to form different precipitates than taurine. In some cases a mixture of amino acid and KHCO<sub>3</sub> is formed [231], or in other cases, only KHCO<sub>3</sub> is formed [85]. Although these precipitates are different to the baseline solvent they are seen as beneficial because they help to increase the net loading (recycling less CO<sub>2</sub> to the absorption column), they will also induce a pH change (the combination of amino acid and HCO<sub>3</sub><sup>-</sup> is more acidic than the pure bicarbonate solution) and they offer the possibility of concentrating the rich solution in CO<sub>2</sub>.

Table 7.1 shows a summary of the amino acids considered most relevant for this application based on these properties. The starting candidates selected were  $\alpha$ -alanine or its derivative, 2-methylalanine (2-aminoisobutyric acid), and the 6-aminohexanoic acid. The CO<sub>2</sub> absorption equilibrium isotherms of solutions of the amino acids listed in Table 7.1 were measured in a well stirred jacketed autoclave at two temperatures (40 and 120°C or 130°C) and concentrations within the precipitation regime of the amino acids. The details of the experimental procedure and results can be found in Appendix 9.3.2. Absorption mass transfer rates are also important, however, they have not been included at this stage because the models developed for DECAB and DECAB Plus are based on equilibrium. Nevertheless, the relative absorption rates of the solvents with respect to a 30% wt MEA solution were inspected during the absorption experiments by comparing the time to reach equilibrium of the different solvents and MEA. This procedure was used to rule out solvents with substantially lower absorption rates than MEA. The precipitates formed during absorption were analysed by the phosphoric acid method in order to determine the presence of carbonates in the precipitates. The experimental procedure is described in Appendix 9.3.3.

**Table 7.1. List of amino acids relevant for implementation in a DECAB process configuration.**

Amino Acid	Formula	Abbreviation	M <sub>w</sub> [g/mol]	Melting point [°C] [232]	Solubility (25°C) [232] [g/100mL]
Taurine	C <sub>2</sub> H <sub>7</sub> NO <sub>3</sub> S	TAU	125	328.0	9.49
α-alanine	C <sub>3</sub> H <sub>7</sub> NO <sub>2</sub>	ALA	89	316.5	16.58
2-aminoisobutyric acid (2-methylalanine)	C <sub>4</sub> H <sub>9</sub> NO <sub>2</sub>	AIB	103	335.0	12.06-18.40
6-aminohexanoic acid (ε-aminocaproic acid)	C <sub>6</sub> H <sub>13</sub> NO <sub>2</sub>	6-AHA	131	205.0	50.50

## 7.4 Model development

An equilibrium process model (VLEMS) has been developed for aqueous solutions of amino acids and MEA and has been used for the evaluation of the different process configurations proposed in this work. The absorption and desorption performances are estimated by a series of equilibrium stages where the mass balances, enthalpy balance and equilibrium relations are simultaneously solved providing the temperature and composition profiles and the reboiler energy. The model is based on the following assumptions:

- 1) The only components that are considered in the VLE calculations are CO<sub>2</sub> and water. Amino acids are non-volatile and in the case of amines, the vaporisation is neglected.
- 2) Each stage is assumed to be well mixed and process conditions and gas and liquid composition are uniform in each stage.
- 3) Temperature, pressure and material equilibrium is reached in each stage.
- 4) The reboiler is considered as an equilibrium stage
- 5) Heat losses are not considered.

The Vapour-Liquid-Solid Equilibrium (VL(S)E) data for the amino acid salts under investigation are necessary to estimate solid-liquid partition and Vapour-Liquid Equilibrium (VLE) at different conditions. In previous work [230], a conceptual design methodology was introduced, which required three different experimental tests: the pH determination of solutions containing different concentrations of amino acid and potassium hydroxide, the measurement of the VLE on those solutions at different temperatures and the determination of the weight of solids and solid type formed during CO<sub>2</sub> absorption of those solutions. The results of each experiments were fitted to empirical expressions that provided the estimation of the VL(S)E at different conditions [230].

Table 7.2 shows the empirical expressions used to estimate the VL(S)E of CO<sub>2</sub> in 4 M potassium taurate [230], 4 M potassium alanate (measured in this work) and MEA (from literature data [205, 210]) solutions and the correlations to estimate the water vapour pressure of these solutions under different conditions. In the equilibrium model, a constant value of 0.8 Murphree efficiency is applied at every stage for CO<sub>2</sub>. This value was selected to fit the experimental results of Knudsen [65] for MEA, which were conducted at the pilot plant of Dong at Esbjerg power plant station. For the other solvents (potassium taurate and alanate), the same value of the Murphree efficiency was used due to the lack of pilot plant experimental results with these solvents. This

assumption is equivalent to assuming similar absorption rates to MEA for these two solvents and could lead to loadings that deviate from those attainable at real operating conditions. Although this could be a limiting factor for future process implementation, it was considered acceptable for the conceptual design because the objective is to screen multiple solvents and process configurations. The model assumptions could be checked in future studies for an optimal solvent and process configuration. The heat of absorption/desorption of CO<sub>2</sub> is calculated by differentiating Eq. 7.5 in Table 7.2 with respect to 1/T. The heat of vaporisation of water and the heat capacity of steam are calculated with the equations from the Steam Tables of the IAPWS-IF97 industrial standard [206]. The molar gas heat capacity for CO<sub>2</sub> is calculated with equations from the NIST database [212]. In the case of liquid enthalpy calculation, the overall heat capacity of the entire solution is used. A representative constant value has been used for taurine [75] and alanine [233]. This method neglects the addition of CO<sub>2</sub> to the liquid. Solvent density is considered equal for all trays and given a representative constant value which has been derived from literature [233].

A number of process variables are important to the evaluation of the DECAB and DECAB Plus process concepts:

- Taurine-to-potassium molar ratio ([TAU/K]) represents the ratio of the total concentration of taurine to the total concentration of potassium, which is equal to the concentration of KOH used to prepare the amino acid salt solution.
- Initial pH of taurine – KOH solutions (pH<sub>0</sub>): represents the pH of an aqueous solution of taurine and KOH measured at 40°C. It is related to the [TAU/K] as shown in our previous work [230]:

$$\text{pH}_0 = f\left(\frac{[\text{TAU}]}{[\text{K}^+]}\right) \quad 7.1$$

- Recycle split fraction (RSF): represents the fraction of the liquid supernatant (excluding the solid phase) that is recycled to the absorber column.

$$\text{RSF} = \frac{L_R}{L-S} \quad 7.2$$

Here,  $L_R$  represents the flow (kmol/s) of the recycle stream,  $L$  represents the flow (kmol/s) of the total rich stream leaving the absorber and  $S$  represents the flow (kmol/s) of the solid phase.

- Specific regeneration energy: The energy necessary for regeneration, calculated by the process model considering the reboiler duty and the energy required to power the compressor, in the cases where the LVC is applied. An isentropic efficiency of 88% and a driver efficiency of 85% are assumed in the calculations of compressor power. The results are presented as steam equivalent (GJ/tCO<sub>2</sub>) energy that will result in the same turbine power loss than deducting the compressor power from the gross turbine power output, according to the formula:

$$Q_t = Q_R + \frac{W_{\text{Comp.}}}{\lambda} \quad 7.3$$

In the equation above,  $Q_t$  is the total specific regeneration energy,  $Q_R$  is the estimated reboiler duty for solvent regeneration and  $W_{\text{Comp.}}$  is the estimated work for LVC

compressor. The term  $\lambda$  accounts for the loss of turbine power due to steam extraction for the reboiler. This factor depends on the necessary steam quality and is derived for each case from the power plant and capture plant integration correlations developed by Le Moullec [55]. Eq. 3 is only used to compare cases where the steam quality is similar.

- Total power plant parasitic load: The integration of DECAB and DECAB Plus into coal fired power plants requires the use of two different energy sources. On one hand, the reboiler needs saturated steam at pressures between 3 and 4 bar, depending of the reboiler conditions. On the other hand the separator requires low grade energy for the dissolution of crystals. In this case, steam of very low pressure (circa 1 bar) has been used in order to provide the necessary energy required by the separator heat exchanger. The model developed by Le Moullec [55] was used to calculate the parasitic load to a hypothetical power plant with implemented capture based on DECAB and DECAB Plus.

$$W_t = W_R + W_{LVC} + W_{SEP} + W_{COMP} \quad 7.4$$

Here,  $W_t$  (kWh/tCO<sub>2</sub>) is the total power plant parasitic load,  $W_R$  (kWh/tCO<sub>2</sub>) is the equivalent work needed for the reboiler,  $W_{LVC}$  (kWh/tCO<sub>2</sub>) is the energy required by the LVC compressor,  $W_{sep}$  (kWh/tCO<sub>2</sub>) is the equivalent work required by the separator and  $W_{COMP}$  (kWh/tCO<sub>2</sub>) is the energy required to compressed the CO<sub>2</sub> from the pressure at the top of the stripper to 110 bar.

**Table 7.2. Empirical representation of the VL(S)E for the different solvents under investigation (potassium taurate [KTAU] and potassium alanate [KALA]) and the corresponding solvent vapour pressures. The coefficients in equations 7.5 and 7.6 are obtained by multiple linear regression, which requires the linearisation of the equations.**

	KTAU VL(S)E <sup>a</sup>	KALA VL(S)E <sup>b</sup>	MEA VL(S)E <sup>c</sup>	KTAU Vapour Pressure <sup>d</sup>	KALA Vapour Pressure <sup>e</sup>	MEA Vapour Pressure <sup>f</sup>
Parameter	Eq. 7.5	Eq. 7.5	Eq. 7.5	Eq. 7.6	Eq. 7.6	Eq. 7.7
A	-15.44	16.02	42.49	0.47	-1.80	-5.939·10 <sup>-2</sup>
B	9419.69	-6229.32	-17691.20	67.86	99.08	7.621·10 <sup>-3</sup>
C	7.87	10.24	-30.10	-0.45	9.00	-1.90·10 <sup>-4</sup>
D	1534.81	0	22210.31	0.00	0.00	2.137·10 <sup>-6</sup>
E	1536.86	0	-5531.43	0.00	0.00	0.00
F	64.52	0	0.00	0.00	0.00	0.00
G	3.26	0	0.00	0.00	0.00	0.00
H	-1561.5	0	0.00	0.00	0.00	0.00
Regression results						
Multiple R	0.984	0.986	0.989	0.989	0.985	0.986
Standard Error	0.322	0.378	0.476	0.04	0.06	0.05
Number of observations	118	28	112	179	227	300
SSE <sup>g</sup>	24900	2633	7.94·10 <sup>7</sup>	0.06	0.08	0.07
ARD% <sup>h</sup>	24.8%	27%	41%	3%	5%	3%

<sup>a</sup> Derived for potassium taurate solutions with [TAU/K] from 1 to 1.3 and temperatures from 40°C to 130°C [230].

<sup>b</sup> Derived for potassium alanate solutions, equimolar and temperatures of 40 and 120°C (this work).

<sup>c</sup> Derived for MEA30% wt based on the data from Lee [205] and Shen and Li[210].

<sup>d</sup> Derived for potassium taurate solutions with concentrations from 2M to 6M [230].

<sup>e</sup> Derived for potassium alanate solutions with concentrations from 2M to 6M (this work).

<sup>f</sup> Derived for MEA solutions of 30%wt [230].

<sup>g</sup>SSE: sum of squared errors between the experimental and model values.

<sup>h</sup>ARD%: averaged relative deviation between the experimental and model values.

$$\text{Eq. 7.5 } \ln(P^{CO_2^{eq}}) = A + \frac{B}{T} + C \cdot \alpha + D \cdot \frac{\alpha}{T} + E \cdot \frac{\alpha^2}{T} + F \cdot \frac{\ln(\alpha)}{T} + G \cdot \text{pH}_0 + H \cdot \frac{\text{pH}_0}{T}$$

$$\text{Eq. 7.6 } P^{H_2O} = \left(1 - \left(A + \frac{B \cdot x_s}{T} + C \cdot x_s\right) \cdot x_s\right) \cdot P^{H_2O^0}$$

$$\text{Eq. 7.7 } P^{H_2O} = A + B \cdot T + C \cdot T^2 + D \cdot T^3$$

$P^{CO_2^{eq}}$  is the equilibrium CO<sub>2</sub> partial pressure [kPa],  $P^{H_2O}$  is the vapour pressure of the solutions [bar],  $P^{H_2O^0}$  is the pure water vapour pressure [bar],  $\alpha$  is CO<sub>2</sub> loading [mol CO<sub>2</sub> / mol AmA],  $T$  is temperature [°C],  $\text{pH}_0$  is the initial pH of the solution,  $x_s$  is the total mole fraction of amino acids and potassium in solution.

## 7.5 Results and Discussion

### 7.5.1 Baseline case optimisation

The optimisation of the lean loading without any recycle (DECAB configuration) at different reboiler temperatures is shown in Figure 7.4. The minimum specific reboiler duty occurs at a CO<sub>2</sub> loading of 0.26-0.27 mol CO<sub>2</sub>/mol TAU for every temperature. The effect of the reboiler operating temperature is not very substantial but is appreciable from the results in Figure 7.4. Higher reboiler temperatures lead to lower specific reboiler duties due to a more favourable water to CO<sub>2</sub> ratio at stripper's top stage conditions. For every temperature analysed in Figure 7.5, the reboiler pressure was fixed at the value that provides the optimum lean loading. Subsequently, the recycle split fraction (RSF) was varied from 0% to 50% in order to induce the pH-shift effect of the DECAB Plus process configuration. This broad range was selected in order to study the influence of the pH-shift effect in a broad operating range. The results of the slurry tests in previous work [230] indicate that the [TAU/K] ratio should be restricted to a range from 1 to 1.2 to avoid the presence of any solids in the new rich stream fed to the stripper. The values of the RSF above 40% fall outside this range, however, they have been included in the simulations in order to develop a full understanding of the pH-shift effect. Figure 7.5 shows the optimisation of the RSF at different reboiler temperatures. The DECAB Plus process configuration reduces the specific reboiler energy by 27-29% depending on the operating reboiler temperature. For all temperatures, the value of the RSF that minimizes the specific reboiler duty is around 30%. For higher values of the RSF, the net capacity of the solvent is considerably reduced due to the recycle of the absorbed CO<sub>2</sub> back to the absorber column. For these cases, the solvent flow needs to be increased substantially, to maintain the CO<sub>2</sub> removal percentage at 90%, leading to an increase in the required reboiler duty. For the DECAB Plus configuration, lower reboiler temperatures lead to lower specific reboiler duties, despite the fact, that for the DECAB configuration (*i.e.* 0% RSF) the opposite behaviour was found. This change can be explained by the variation of the pH-shift effect with temperature. Figure 7.6 shows the influence of pH<sub>0</sub> in the equilibrium partial pressure of CO<sub>2</sub> at optimum lean loading conditions. When the pH<sub>0</sub> is decreased, the equilibrium partial pressure of CO<sub>2</sub> increases significantly. However, for higher values of temperatures the effect becomes less prominent, as indicated by the reduction in the slope of the  $P^{CO_2}$  vs. pH<sub>0</sub> lines represented in Figure 7.6. Therefore, the RSF has a more markedly effect on the reboiler duty at lower temperatures than at higher temperatures.

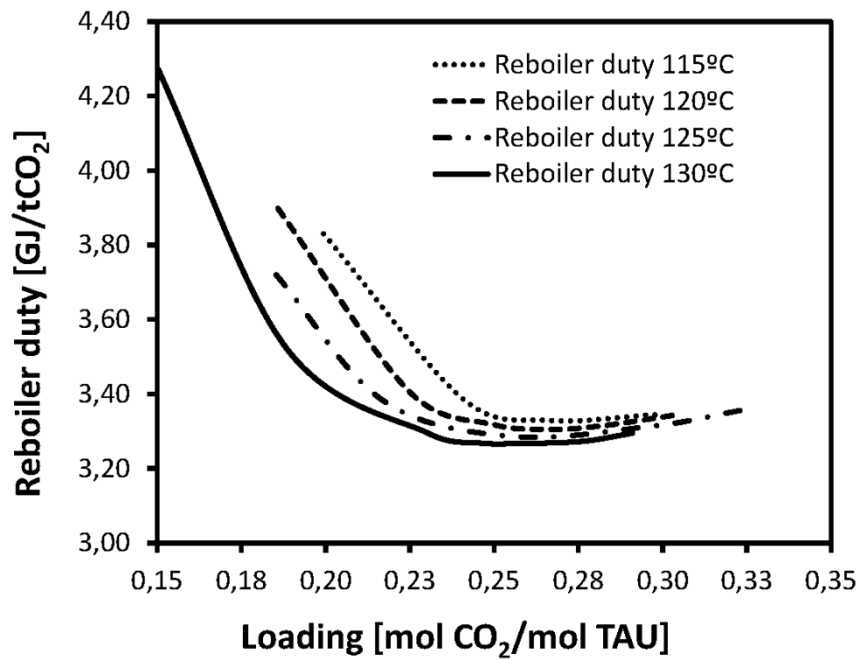


Figure 7.4. Optimisation of specific reboiler duty with respect to reboiler temperature for potassium taurate and DECAB process configuration illustrated in Figure 7.1. Simulations were performed at a constant recycle split fraction (RSF) of 0% and constant CO<sub>2</sub> removal of 90%.

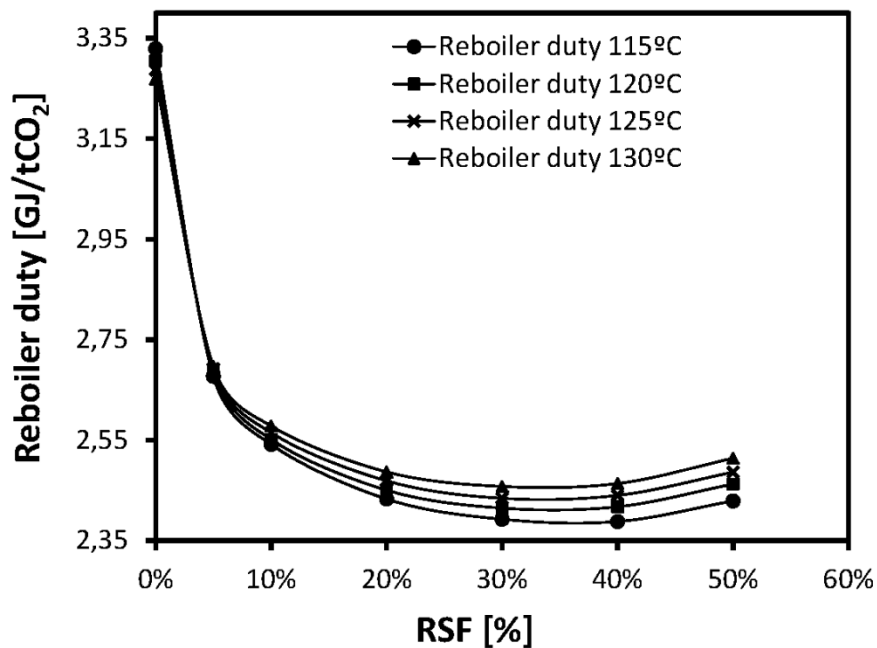


Figure 7.5. Optimisation of the reboiler duty with respect the recycle split fraction (RSF) at different temperatures for the DECAB Plus process configuration illustrated in Figure 7.1. Simulations were performed at the optimum lean loading for every temperature and a constant CO<sub>2</sub> removal of 90%.

For further optimisation of the DECAB Plus process, the reboiler temperature and the RSF were fixed and the separator temperature was decreased from 40°C to 25°C. The implications for the process are the precipitation of more solids, the need of extra cooling duty in the separator and the increase in the specific energy required to re-dissolve the precipitates. This modification results in higher [TAU/K] in the new rich stream for equal values of the RSF. Figure 7.7 shows the results for a reboiler temperature of 120°C and 20% RSF. Although the optimal value found for this variable is 30% (Figure 7.5), the reduction in the reboiler duty when the RSF increases from 20% to 30% is not significant and it will imply the processing of a more dense slurry and a larger recycle stream (with implications to the sizing of the absorption process). Decreasing the separator operating temperature results in lower reboiler duties due to the extra pH-shift effect induced by a higher [TAU/K] ratio in the new rich stream. However, as indicated in Figure 7.7, this also increases the specific separator energy.

### 7.5.2 *Lean vapour compression (LVC)*

For the evaluation of the LVC addition to the DECAB and DECAB Plus concepts, several simulations were performed at different reboiler temperatures. The reboiler pressure was kept constant at the value that minimized the specific reboiler duty for every temperature. The pressure in the flash vessel was decreased gradually, starting from a value equal to the reboiler pressure, to atmospheric conditions. The results of these simulations are shown in Figure 7.8 for reboiler temperatures of 120°C and 130°C. Figure 7.8 shows the specific energy requirements of the reboiler, which include the energy required to power the compressor in the form of steam that would result in a power loss to the turbine equivalent to the LVC compressor power. When the rich stream is flashed, the reboiler duty necessary to regenerate the solvent is reduced due to the extra steam generated. The extra steam is then compressed to the reboiler pressure and fed back to the stripper. As shown in Figure 7.8, the total energy required for regeneration decreases with decreasing flash pressures. However, for flash pressures near atmospheric conditions, the energy required by the compressor becomes a dominant contributor to the total energy requirements and, therefore, the specific energy requirements raise. At 120°C, a pressure difference between the reboiler and the flash vessel of 0.69 bar provides a minimum in the total energy required. At 130°C the minimum is reached at a pressure difference of 1.10 bar. The reduction in the specific energy requirements are 7.9% and 7.7% for 120°C and 130°C respectively. However, operating the reboiler at 130°C requires condensing steam of higher pressure than at 120°C. The implications of changing the steam quality are further discussed in Section 7.5.5.

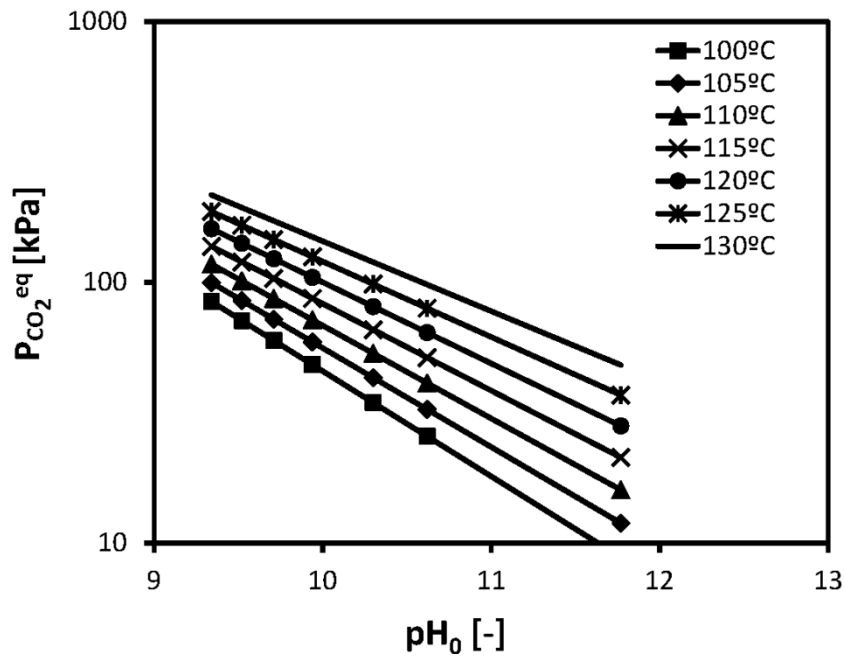


Figure 7.6. Influence of pH<sub>0</sub> in the equilibrium partial pressure of CO<sub>2</sub>. Simulations were performed at a constant loading of 0.26 mol CO<sub>2</sub>/mol TAU and different temperatures.

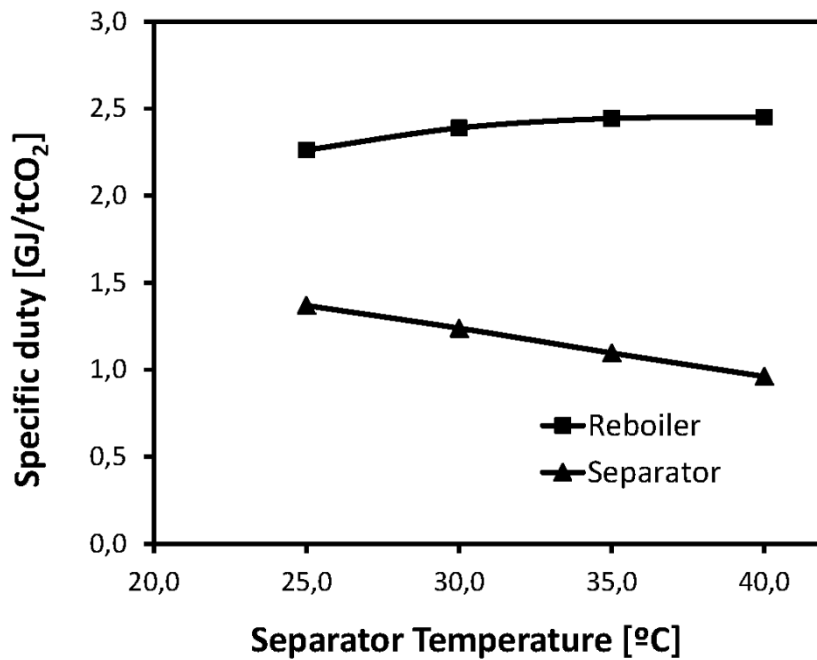


Figure 7.7. Variation of the reboiler and separator duties with the separator operating temperature for the DECAB Plus process concept illustrated in Figure 7.1. Simulations are done at fixed reboiler temperature (120°C), 20% recycle split fraction (RSF) and a constant CO<sub>2</sub> removal of 90%.

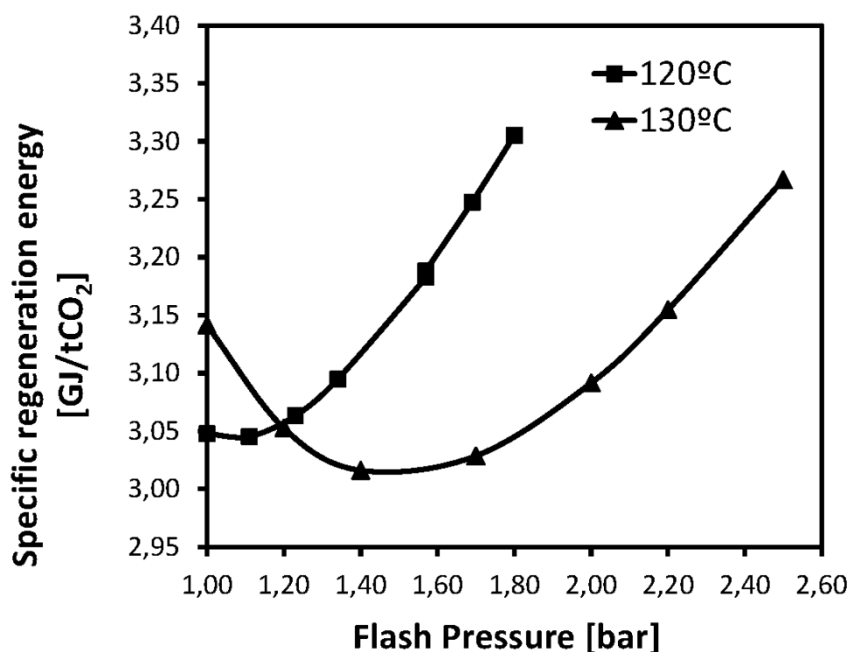


Figure 7.8. Optimisation of LVC flash pressure for the DECAB process concept with LVC illustrated in Figure 7.2. Simulations were performed at constant reboiler pressure corresponding to the optimal value for every temperature, no recycle split fraction (0% RSF) and a constant CO<sub>2</sub> removal of 90%.

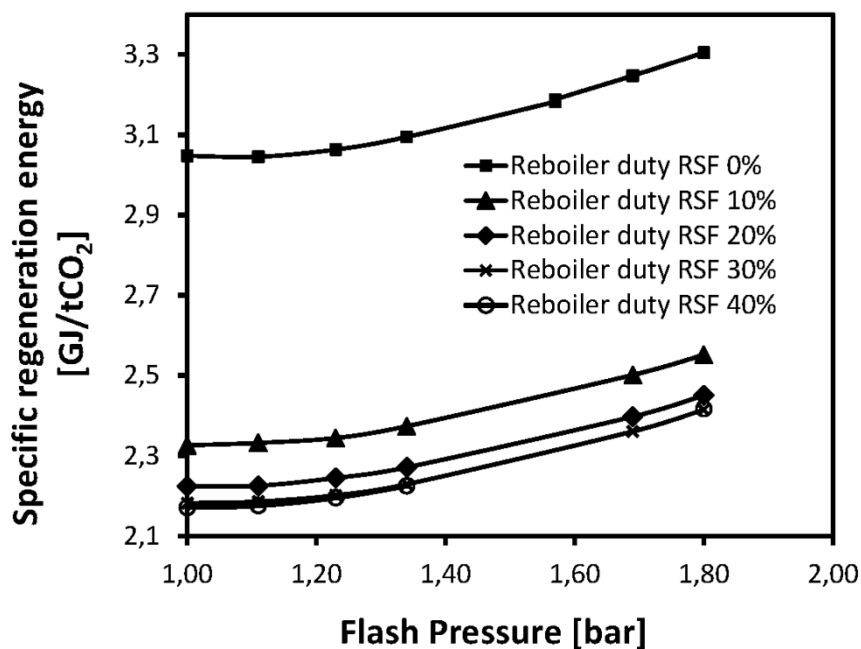


Figure 7.9. Effect of LVC flash pressure on the specific regeneration energy for the DECAB Plus process concept with LVC illustrated in Figure 7.2. Simulations were performed at constant reboiler temperature (120°C) and a constant CO<sub>2</sub> removal of 90%.

The influence of LVC on the DECAB Plus process configuration was also investigated at constant reboiler temperatures and pressures. Figure 7.9 shows the influence of the LVC flash pressure on the specific regeneration energy at 120°C and different values of the RSF. The effect of flashing the lean stream on the total energy required to regenerate the solvent is similar for every value of the RSF. In relative terms, the value of the initial specific energy is reduced from 7.9% to 10.0% when RSF increases from 0% to 40%.

### 7.5.3 Multiple absorber feeds

This process configuration is most appropriate for the cases with a high RSF (above 30%) where the recycle of the absorbed CO<sub>2</sub> back to the absorber column reduces considerably the net capacity of the solvent (Section 7.5.1). The configuration aims, a priori, to increase solvent capacity by using a stream at the top of the absorber of a lower CO<sub>2</sub> loading. For this purpose, the recycle and the new lean stream leaving the stripper are split in two. One fraction of the recycle stream is mixed with the major fraction of the new lean stream from the stripper and sent to the top of the absorber (Figure 7.3). The remaining fraction of the recycle stream is fed at an intermediate stage of the absorber together with the remaining fraction of the new lean stream (if there is one). The effect of this configuration on the required reboiler duty is shown in Figure 7.10. For this case, the RSF was fixed at 30%, which is a relatively high value at which the net capacity of the solvent starts to decline. The new lean stream was entirely sent to the top of the absorber and the fraction of the recycle stream that is mixed with it was gradually decreased from 100% (all the recycle stream is mixed with the new lean stream resulting in a [TAU/K] of 1) to 80% (only 80% of the recycle stream is mixed with the new lean stream resulting in a [TAU/K] higher than 1). By splitting the recycle stream, the pH<sub>0</sub> in the lean stream decreases from 11.77 (value that corresponds to the equimolar solution, [TAU/K]=1.00) to 10.54 (value that corresponds to a [TAU/K] = 1.02). The loading of the lean stream also decreases from 0.29 mol CO<sub>2</sub> / mol TAU to 0.26 mol CO<sub>2</sub> / mol TAU. However, this modification does not have a positive effect on the reboiler duty, which increases gradually. This is due to the effect that pH has on the equilibrium absorption of CO<sub>2</sub>. The equilibrium partial pressure of CO<sub>2</sub> at the top of the absorber increases with lower pH<sub>0</sub> and decreases with lower CO<sub>2</sub> loadings. The reduction in the pH<sub>0</sub> of the lean stream has a substantial impact on the reboiler duty due to the reduction in solvent capacity, which is not compensated by the reduction in lean loading obtained in this process configuration. Therefore, the multiple absorber feeds configuration leads to a higher reboiler duty than in the other process configurations. For this reason this alternative was discarded for further evaluation.

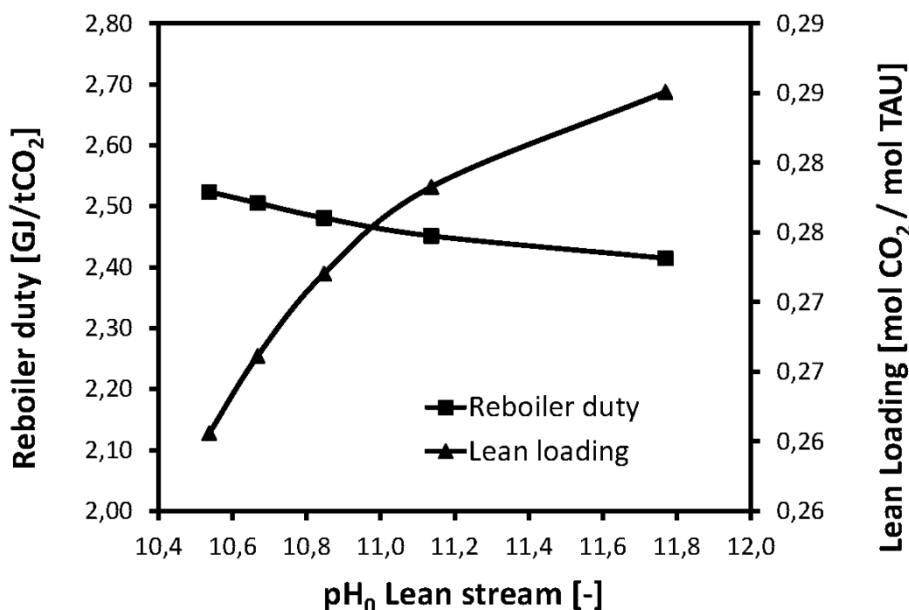


Figure 7.10. Effect of multiple absorber feeds on the reboiler duty for the DECAB Plus process concept illustrated in Figure 7.3. Lean stream loading and reboiler duty vs.  $pH_0$  in the lean stream.

#### 7.5.4 Alternative solvents

The absorption capacity of a selected number of amino acids was investigated at 40°C and 120°C or 130°C and compared to potassium taurate. Figure 7.11 and Figure 7.12 show the isotherms for the absorption of CO<sub>2</sub> in these solvents. The majority of the solutions tested showed higher absorption capacity (on a mol-to-mol basis) than potassium taurate at partial pressures of CO<sub>2</sub> relevant for flue gas application (circa 10 kPa). With respect to regeneration, the 6-aminohexanoic acid solution (6-AHA) showed lower partial pressures of CO<sub>2</sub> than taurine at 120°C, which implies that more stripping steam will be required to regenerate this solvent with the consequent impact on the thermal regeneration energy. The 4 M 2-aminoisobutyric acid (AIB) solution required a temperature of 130°C in order to obtain a similar isotherm to the other amino acids at 120°C. The low CO<sub>2</sub> partial pressures obtained initially at 120°C indicated that this temperature was not suitable for an effective regeneration of this solution. Raising the temperature to 130°C was not required when the AIB concentration was reduced to 2 M, but this reduces the bulk capacity of the solution.

The critical points for solvent precipitation were determined by visual inspection of the samples during CO<sub>2</sub> absorption. These points are shown in Figure 7.11 by empty markers. In the 6-AHA sample, precipitates were formed at relatively high liquid loadings of 0.6 mol CO<sub>2</sub> / mol AmA. This is to be expected since this amino acid is more soluble than the other amino acids tested. However, in the case of  $\alpha$ -alanine and 4 M AIB, precipitation occurred at lower loadings than taurine, 0.26 and 0.15 mol CO<sub>2</sub> / mol AmA respectively, despite these two amino acids are more soluble. Decreasing the concentration of AIB from 4 M to 2 M shifted the precipitation point to 0.64 mol CO<sub>2</sub> / mol AmA. These results have an effect on the application of these solutions to the DECAB and DECAB Plus processes. In the 6-AHA solution, precipitates are formed at a high

CO<sub>2</sub> partial pressure, which decreases the enhancement effect during absorption. On the other hand, in the 4 M AIB solution precipitates are formed at very low CO<sub>2</sub> partial pressures, which will require a deep regeneration to keep the lean loading below the critical point for precipitation. This issue can be solved by reducing the AIB concentration, but this will also reduce the bulk CO<sub>2</sub> capacity of the solution.

Considering the absorption and precipitation characteristics, the most promising amino acid tested is  $\alpha$ -alanine. The potassium alanate solution tested had higher specific capacity than taurine and similar regeneration isotherm. Other attractive properties of  $\alpha$ -alanine for its application in DECAB and DECAB Plus processes are higher solubility than taurine and much lower dissolution energy [234, 235]. Therefore, this amino acid was included in the process model in order to evaluate its performance in a DECAB configuration.

The DECAB process based on 4 M potassium alanate is essentially the same as the one for potassium taurate, which has been described in Section 7.2. For process evaluation, the absorption data of CO<sub>2</sub> on potassium alanate and the vapour pressure data of the potassium alanate solution were fitted to Eq. 7.5 and Eq. 7.6 in Table 7.2 respectively. The empirical correlations presented in this table were used to describe the VLE of this solvent.

The precipitation characteristics of potassium alanate were further investigated by analysing the precipitates formed using titration to determine the amino acid concentration and the phosphoric acid analysis to determine the presence of bicarbonates in the precipitate. The potassium salt of  $\alpha$ -alanine solution formed a slurry containing 21% wt (dry) solids of which 13% wt (dry) were bicarbonate species. The analysis procedure and experimental data are provided in Appendix 9.3.4. The other necessary physical properties were retrieved from literature as explained in Section 7.4.

For a DECAB configuration basis, the optimisation of the lean loading for potassium alanate at different reboiler temperatures is shown in Figure 7.13. The minimum specific reboiler duty occurs at a CO<sub>2</sub> loading of 0.32-0.33 mol CO<sub>2</sub>/mol ALA. At this loading the specific reboiler duty for potassium alanate is lower than for potassium taurate (also included in the figure). Nevertheless, for loadings above 0.26 mol CO<sub>2</sub> / mol ALA, precipitates will form at temperatures around 40°C. Therefore, the loading needs to be restricted at that value to avoid precipitation of the lean stream when it is fed to the absorber. The minimum reboiler duty is then 3.25 GJ/t CO<sub>2</sub>, with a reboiler temperature of 130°C. With the addition of LVC to the process, the specific regeneration energy can be reduced to 2.81 GJ/t CO<sub>2</sub>.

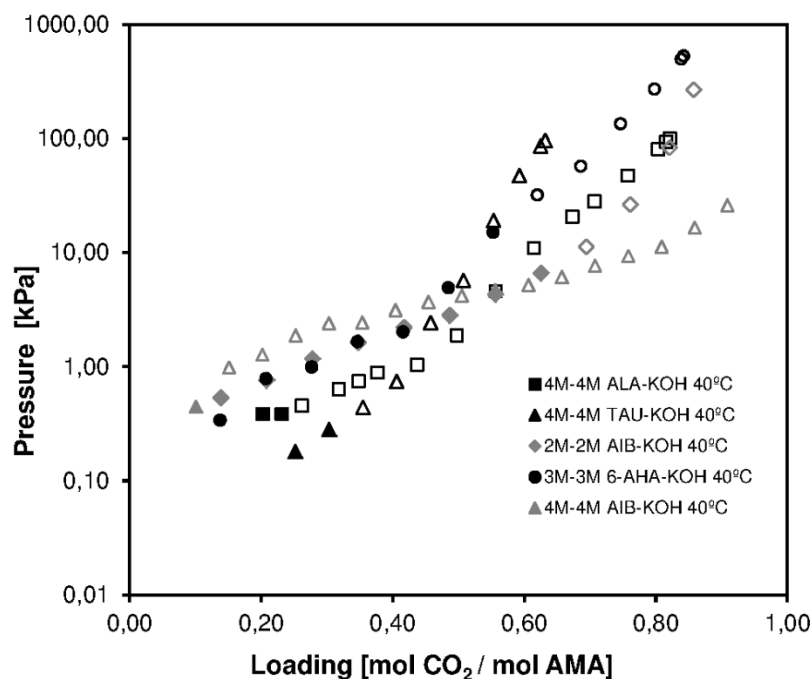


Figure 7.11. Absorption equilibrium of  $\text{CO}_2$  (VLE) in aqueous amino acid solutions at  $40^\circ\text{C}$  measured in this work. The legend indicates the total concentrations of amino acid (ALA – alanine, TAU – taurine, AIB – 2-aminoisobutyric acid, 6-AHA – 6-aminohexanoic acid) and potassium hydroxide (KOH) in solution. The empty markers indicate the presence of solids in the liquid phase at equilibrium.

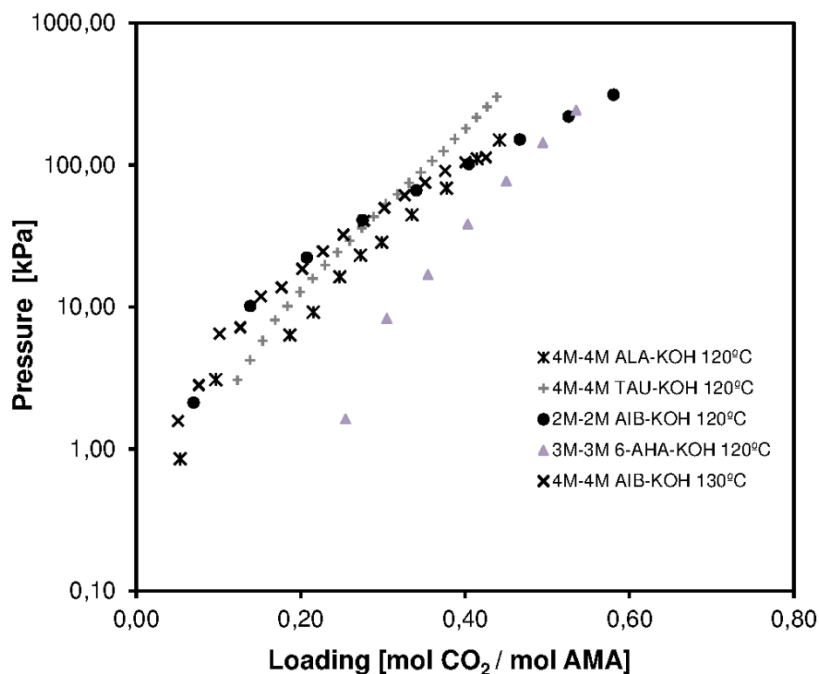


Figure 7.12. Absorption equilibrium of  $\text{CO}_2$  (VLE) in aqueous amino acid solutions at  $120^\circ\text{C}$  and  $130^\circ\text{C}$  measured in this work. The legend indicates the total concentrations of amino acid (ALA – alanine, TAU – taurine, AIB – 2-aminoisobutyric acid, 6-AHA – 6-aminohexanoic acid) and potassium hydroxide (KOH) in solution.

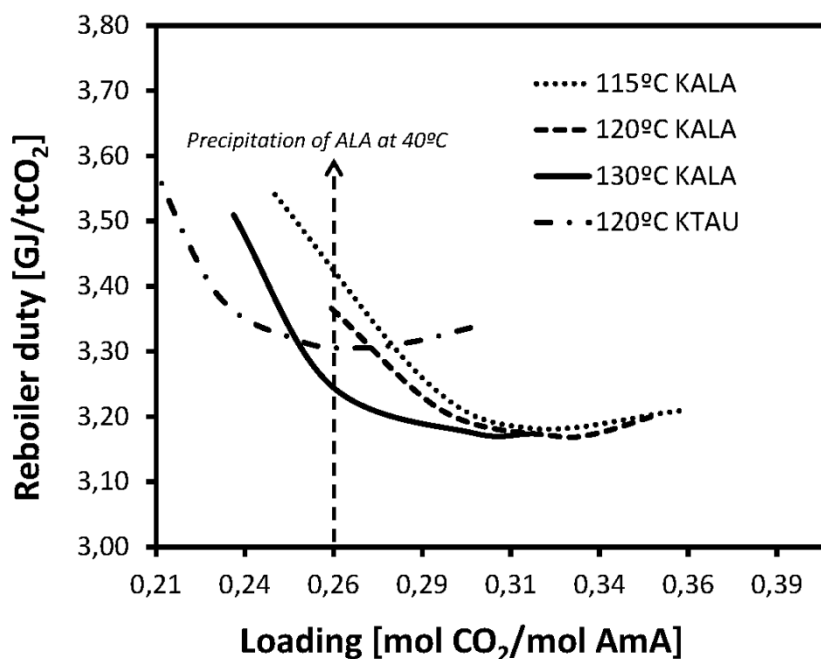


Figure 7.13. Optimisation of specific reboiler duty with respect to reboiler temperature for potassium alanate and DECAB process configuration illustrated in Figure 7.1. Simulations were performed at a constant recycle split fraction (RSF) of 0% and constant CO<sub>2</sub> removal of 90%.

### 7.5.5 Evaluation of process alternatives

This section provides an overview of the process concepts analysed in this chapter. Table 7.3 shows the performance of the process configurations investigated and the most optimal process conditions of each configuration. The evaluation of a conventional 30% wt MEA capture process, based on the same model and assumptions as in the other process configurations, has been added to the table for comparison. The evaluation is based on the equivalent work of each configuration, which has been calculated with the model developed by Le Moullec [55] and includes the energy use of each process configuration, the work of the LVC compressor (when present) and the work to compress the CO<sub>2</sub> to 110 bar. This model focuses on retrofitting a coal fired supercritical power plant of 1200MWe gross with re-superheating of the intermediate pressure steam. The steam for the boiler is drawn off between the IP and LP turbines at 5.9 bar, passes through an auxiliary turbine to reduce the pressure to the optimum working pressure in the reboiler and then cooled by pre-heating the power plant boiler working water before being fed to the capture plant reboiler boiler. The reboiler condensate energy (at around 135°C) is also used in the pre-heating train of working water. A similar scheme could be used for the separator, assuming that the IP/LP turbine line has enough flow to supply the reboiler and separator and to operate the low pressure turbine. A throttle valve is used in the model to apply a pressure drop proportional to the flow rate of the drawn off to the working steam before it enters the low pressure turbine. In this way, the different qualities of steam required by the separator and the reboiler and the electricity supply for the pumps and compressors are considered. The consumption of the CO<sub>2</sub> compressor (used to deliver the CO<sub>2</sub> at a pressure of 110 bar) is also

calculated with this model, considering the differences in the delivery pressure of the CO<sub>2</sub> stream from the stripper.

**Table 7.3. Predicted performance of various solvents and process configurations for 90% CO<sub>2</sub> capture of coal fired power plant flue gas.**

Process configuration	Solvent	Reboiler		S-L separator <sup>b</sup>		LVC	Energy		Work				
		<i>T</i>	<i>P<sub>s</sub></i>	<i>T</i>	<i>RSF</i>	<i>P</i>	<i>Q<sub>R</sub></i>	<i>Q<sub>Sep</sub></i>	<i>W<sub>R</sub></i>	<i>W<sub>LVC</sub></i>	<i>W<sub>Sep</sub></i>	<i>W<sub>Comp.</sub></i>	<i>W<sub>T</sub></i>
		°C	bar	°C	%	bar	GJ/t	GJ/t	kWh/t	kWh/t	kWh/t	kWh/t	kWh/t
Conventional	MEA <sup>a</sup>	120	3.13	NA	NA	1.9	3.66	0.00	309.8	0.0	0.0	93.6	403.4
Conventional + LVC	MEA	120	3.13	NA	NA	1.2	3.18	0.00	272.7	9.2	0.0	93.6	375.5
DECAB	TAU	120	3.13	40	0%	1.8	3.31	1.01	282.7	0.0	63.4	95.2	441.3
DECAB	ALA	120	3.13	40	0%	1.8	3.37	0.56	287.4	0.0	35.4	95.2	418.0
DECAB	ALA	130	4.16	0	0%	2.5	3.20	0.55	301.4	0.0	34.7	85.4	421.5
DECAB + LVC	TAU	120	3.13	40	0%	1.1	2.86	0.93	247.5	12.1	58.3	95.2	413.1
DECAB + LVC	ALA	130	4.16	40	0%	1.4	2.52	0.54	242.1	18.2	34.5	84.2	379.1
DECAB Plus	TAU	120	3.13	40	20%	1.8	2.45	0.96	214.8	0.0	60.2	95.2	370.2
DECAB Plus	TAU	115	2.70	40	40%	1.8	2.39	1.24	199.7	0.0	77.0	100.7	377.4
DECAB Plus	TAU	120	3.13	25	20%	1.8	2.26	1.37	199.3	0.0	84.8	95.2	379.3
DECAB Plus + LVC	TAU	120	3.13	40	20%	1.1	2.07	0.88	183.5	9.9	55.1	95.2	343.6
DECAB Plus + LVC	TAU	120	3.13	25	20%	1.1	1.90	1.24	169.1	9.7	77.4	95.2	351.4

<sup>a</sup> Developed in our previous work [230].

<sup>b</sup> Steam conditions for the solid-liquid separator are the same for all cases (1 bar saturated steam).

The lean loading of the MEA and TAU process configurations was optimised to minimize the reboiler duty. In the case of alanine (ALA) the maximum lean loading was fixed at 0.26 mol CO<sub>2</sub> / mol ALA, because precipitates will form in the lean stream at 40°C and higher loadings. This loading is far from the optimum. Therefore, the reduction in the overall energy required by the DECAB process when the solvent is changed from taurine to alanine is not substantial. The major savings with respect to taurine rely on the lower heat of dissolution of alanine, resulting in lower energy required by the separator to dissolve the precipitates. The optimisation of operating conditions was based on the reduction of reboiler energy. Based on potassium taurate, the DECAB process configuration reduces the reboiler duty but at the expense of increasing the separator energy. Under the integration conditions suggested by Le Moullec [55], which might not be optimal for the integration of the separator energy into the steam cycle, there is no real gain in the overall energy use of the DECAB configuration as compared to conventional MEA.

The addition of the LVC to the process reduces the overall energy requirements of the DECAB process configuration. In the case of potassium alanate, the required energy is lower than the MEA baseline with savings of 6%, which is similar to the savings obtained by adding the LVC to the MEA conventional process configuration. Nevertheless, the DECAB Plus configuration has a net beneficial impact on the energy use of the capture process. However, the reduction of the reboiler duty by RSF values over 20% or by reducing the separator temperature to room

temperature does not result in a reduction of the overall energy required by the capture process. The best configuration is the DECAB Plus with LVC, which provides 15% energy savings with respect to MEA, and 8.5% with respect to MEA with LVC.

## 7.6 Conclusions

DECAB and DECAB Plus are two novel process concepts based on precipitating amino acids that can reduce the regeneration energy required by the CO<sub>2</sub> capture process. An analysis of process conditions and different configurations of these two process concepts has been conducted based on the necessary energy to regenerate the solvent. The configurations analysed contribute to decrease this energy with the only exception of the multiple feeds to the absorber. This configuration was aimed to increase the solvent capacity by using a lean stream at the top of the absorber column with lower loading than the DECAB Plus baseline configuration. However, the lower pH of this stream did not decrease the regeneration energy as expected.

The developed process configurations also require low-grade energy to dissolve the precipitates formed during absorption. The energy requirements of the reboiler and the separator heat exchanger were added to calculate the overall energy requirements of the process. The DECAB process configuration based on taurine reduces the reboiler energy by 10% with respect to conventional MEA and by 12% when LVC is added. However, this reduction is accompanied by an increase in the energy required by the separator heat exchanger to dissolve the precipitates. Under the assumptions considered for the retrofit of these processes into power plants, which are based on a pre-existing model and are not optimal for the integration of the separator energy into the steam cycle, the final energy use of these process alternatives is higher than the conventional MEA process. Nevertheless, all the DECAB Plus configurations analysed reduce the overall energy use of the capture process with respect to the MEA baseline. The best process configuration in this study is the DECAB Plus process configuration based on potassium taurate with a reboiler temperature of 120°C and solid-liquid separation at 40°C. This alternative reduces the overall energy of the capture process by 15% compared to the MEA baseline with compression of the CO<sub>2</sub> to 110 bar.

Other amino acid solvents were investigated in this work in order to explore potential reductions in the energy required by the DECAB process configuration. Among the solvents investigated, the potassium salt of  $\alpha$ -alanine was identified as a potential candidate for the application in the DECAB configuration. The performance of the DECAB configuration based on potassium alanate is better than potassium taurate due to the lower heat of dissolution of  $\alpha$ -alanine. With the addition of LVC it reduces the energy penalty of the baseline by 6%. Considering the benefits that the DECAB configuration with potassium alanate has over potassium taurate, a DECAB Plus configuration based on this solvent has the potential to further reduce the energy requirements of the capture process. Moreover, a better integration within the steam cycle should reduce the energy figures presented in this work.

---

# THE POTENTIAL OF PRECIPITATING AMINO ACIDS FOR CO<sub>2</sub> CAPTURE

## *ABSTRACT*

*Amino acids can be used to capture CO<sub>2</sub> with different configurations, providing several process improvements with respect to the MEA based capture process. In Chapters 6 and 7, alternative capture processes (DECAB and DECAB Plus) based on amino acid salts have been introduced for application to the post-combustion capture of CO<sub>2</sub> from flue gas. Based on the data and models provided in Chapter 6, a comparison of different process configurations (conventional, DECAB and DECAB Plus) and solvents (taurine and alanine) is presented in this chapter. DECAB Plus has more potential to improve the performance of the capture process than the conventional and DECAB process configuration. Therefore, future research in amino acid salts should focus on developments in DECAB Plus.*

## 8.1 Introduction

CO<sub>2</sub> capture based on chemical absorption can be retrofitted to existing power plants or integrated in new build power plants to remove the CO<sub>2</sub> contained in flue gas. The readiness and know-how of this technology are relatively mature for implementation. However, specific research indicates that the impact on the net power plant efficiency will be substantial [155]. The current state-of-the-art in post combustion capture is a chemical absorption process that uses an aqueous solution of MEA. The integration of this process into a newly build ASC PC power plant reduces the net plant efficiency from 45% LHV to 34% LHV (Chapter 3). This reduction implies that more fuel is used to maintain the energy output of the power plant, which has two direct consequences. One is the increase in the cost of electricity, which increases from 56 €/MWh to 87 €/MWh (Chapter 4). The second direct consequence is the change of the emissions profile of the power plant. The emissions of NO<sub>x</sub> increase 30% per unit electricity basis (Chapter 2). However, this is accompanied by a drastic reduction in SO<sub>x</sub> emissions, virtually 100%, and a 94% reduction in the emissions of other acid gases, such as HF and HCl (Chapter 2). Another impact derived from the use of amines is the increase in amine and ammonia emissions, which is a degradation product. In the case of post-combustion capture using MEA, the latter is very substantial (Chapter 2). This thesis is focused on the mitigation of these impacts by investigating novel process designs for CO<sub>2</sub> capture more efficient and environmentally friendly than the state-of-the-art.

One research line to improve the performance of CO<sub>2</sub> capture is the development of solvents with lower energy use than the state-of-the-art. Hindered amines are an alternative option to MEA. An example of a solvent based on hindered amines is CESAR-1, which is an aqueous solution of AMP and piperazine. The integration of CESAR-1 into newly build ASC PC power plants will reduce the net plant efficiency from 45% LHV to 36% LHV, reducing the efficiency penalty of the capture process by 2% percentage points. However, the higher volatility of AMP requires more abatement measures than MEA in order to restrict the solvent emissions to the atmosphere (Chapter 3). An alternative research line to reduce the impact on the power plant efficiency is the development of process improvements that reduce the energy required for solvent regeneration. Different process configurations have been proposed for this [223]. One example is the lean vapour compression configuration, which requires flashing the hot lean stream leaving the stripper column, re-compressing the steam generated and recycling it back to the stripper column. The application of this configuration to the state-of-the-art MEA process will reduce the required energy for regeneration by 7-9% (Chapter 5).

This thesis has introduced alternative capture processes based on amino acid salts. Amino acids are more biodegradable and less toxic than amines and have negligible vapour pressure [66, 236]. Therefore, it is anticipated that a capture process based on amino acid salts will have, a lower environmental impact than amines. The designed processes are based on the use of amino acid salts in the precipitation regime. Chapter 6 and 7 in this thesis provide new data and modelling to evaluate two process concepts, DECAB and DECAB Plus, in which the products of the reaction between CO<sub>2</sub> and the amino acid salt partially precipitate. The results show a 35% reduction in the solvent regeneration energy that can be further increased to a 44% reduction by process optimisation. This substantial reduction in energy encourages further investment in the research of these process alternatives.

In this chapter, the potential of amino acid salts as solvents for CO<sub>2</sub> capture is reviewed and discussed. The following sections describe different process configurations applicable to amino acid salts, which are quantitatively compared based on the impact on the net power plant efficiency. The evaluation provided is based on a number of assumptions and methodology described in detail in Chapters 6 and 7 in this thesis. These assumptions are based on the best available knowledge and the experimental evidence provided in Chapters 6 and 7. However, there are still uncertainties around the precipitation of amino acids can influence the performance presented for the various process configurations. Moreover, the formation of a solid phase in the process has associated costs and risks to handle the solids in a controlled manner. This may be a limiting factor in the implementation of the process configurations developed in this thesis.

The following sections also discuss the potential of each process configuration based on amino acid salts to decrease the energy penalty of the capture process by future developments. The risks associated to the new processes and the evaluation provided in this thesis are described and guidelines for future process development are provided.

## **8.2 Potential of amino acid salts as solvents for CO<sub>2</sub> capture**

Amino acids can be used to capture CO<sub>2</sub> under different configurations, providing several process improvements with respect to the state-of-the-art process as discussed in Chapters 6 and 7. Different process configurations applicable to amino acid salts are shown in Figure 8.1. New developments in any of these process configurations can bring improvements to the capture process.

The conventional absorption and thermal desorption process configuration uses homogeneous solutions of amino acids in a similar way to amines. Interest in this process configuration is growing among the research community, which is reflected by the growing body of publications related to the topic of carbon capture with amino acid salts (Chapter 1). In this configuration, the concentration of the amino acid is restricted to the soluble regime. Amino acids can be applied as the main solvent component [229, 237, 238] or as promoters of other solvents, such as potassium carbonate [219]. Some amino acids have similar absorption capacity as conventional MEA and, depending on operating conditions, a higher absorption rate. Another advantageous aspect is the lower vapour pressure of aqueous solutions of amino acids, which can provide a more favourable water to CO<sub>2</sub> ratio during regeneration with energy savings.

Other possible process configurations are more advantageous than the conventional ones in terms of the energy required for regeneration. These process configurations include the DECAB process configuration, which requires solvent precipitation, and the DECAB Plus process configuration, which requires an internal recycle of the solvent after precipitation to manipulate the solvent composition for a more favourable desorption. These processes have been investigated in this thesis and have shown improvements in the reboiler duty required by the process to regenerate the solvent. As discussed in Chapters 6 and 7 of this thesis, the DECAB Plus process configuration improves the energy required for regeneration over conventional MEA.

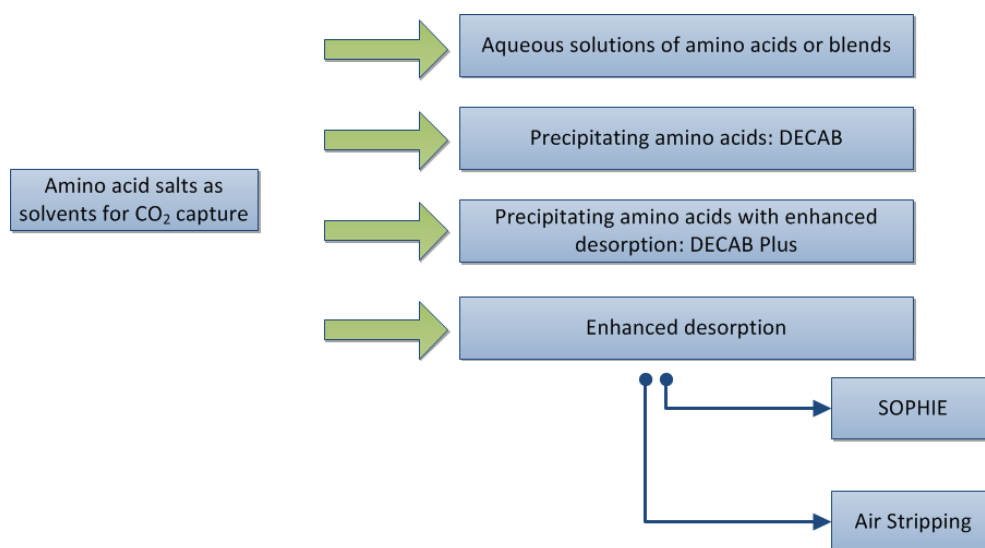


**Figure 8.1.** Development lines for CO<sub>2</sub> capture processes based on amino acid salts.

Besides DECAB and DECAB Plus, amino acids can also be used in other process configurations. In Figure 8.1, two new ideas for application of amino acids (SOPHIE and Air Stripping) have been grouped under the term “Enhanced desorption”, although they have not been investigated in this thesis. These processes include an improved desorption concept but do not require the precipitation of the amino acid during absorption. The SOPHIE process concept (Swing of pH), introduced for the first time in this thesis, creates more favourable desorption conditions by recirculating an amino acid around the stripper. The amino acid is partially recovered prior to absorption via crystallization. The remaining amino acid that is fed to the absorption column serves as promoter for other amino acid or alkali solutions such as potassium carbonate. An alternative to enhance desorption is the use of air to remove the CO<sub>2</sub> from the rich solvent [239]. Due to the negligible volatility of amino acids, this step will partially remove the CO<sub>2</sub> from the solvent without amino acid evaporation. The stripping air, containing higher concentrations of CO<sub>2</sub> and water can be then recycled to the boiler for coal combustion, in a similar way as in the oxy-fuel technology (Chapter 2).

Based on the data and models provided in Chapter 6, a comparison of different carbon capture process configurations (conventional, DECAB and DECAB Plus) and solvents (MEA, AMP/PZ, potassium taurate and potassium alanate) is presented in Table 8.1 The ASC power plant described in Chapter 3 of this thesis, has been used as reference power plant for the implementation of the selected processes. The net power plant efficiency for each case with capture has been estimated by subtracting the total parasitic load of each capture process configuration from the net plant efficiency without carbon dioxide capture provided in Chapter 3. The total parasitic load for the capture process configurations is estimated based on already existing correlations [55] that relate the total plant parasitic load for an ASC power plant to the flow and pressure of the steam necessary for regeneration, the compression work and auxiliary consumption of the capture process. The results in Table 8.1 show performance examples of the different development lines discussed above with the exception of “Enhanced desorption”, which is beyond the scope of this thesis.

The use of potassium taurate in a conventional configuration has been evaluated based on the VLEMS model (Chapter 6) and CO<sub>2</sub> equilibrium absorption data for a 2.8 M potassium taurate solution. In this case the concentration of potassium taurate is restricted to 2.8 M. The experimental data are provided in Appendix 9.3.2 and have been obtained following the procedure described in that section. The integration of this process into an ASC PC Power plant results in a net efficiency reduction similar to that of conventional MEA. Process performance could be improved with the use of other amino acids with more capacity than taurine. Solvent screening studies have investigated the absorption capacity of amino acids. Results can vary widely due to the different screening methods, concentration and definition of capacity. Generally, the more promising amino acids with respect to absorption characteristics, sarcosine [69, 77] and proline [72, 229], have relative low stability. For stable molecules, like taurine or alanine, the absorption rates are generally lower than MEA [78, 240, 241]. In this process configuration, solvent CO<sub>2</sub> capacity cannot be increased by increasing amino acid concentration in solution due to precipitation. Potential developments in this line could be the use of amino acid blends or derivatives of stable amino acids that have improved specific capacity or reaction rate. However, the lower solubility of amino acids will make it difficult to compete with the developments in amines in terms of the energy required to regenerate the solvent. Although, other aspects of amino acids, such as the lower toxicity and high biodegradability, may influence the decision of power plant companies, in order to implement a more environmentally friendly process.

The DECAB process configuration has been investigated for both taurine and alanine, showing a modest reduction in the regeneration energy (Table 8.1). However, when the process is integrated into the power plant, the lower regeneration energy does not result in a reduction of the efficiency penalty of the capture process because of the energy required to dissolve the precipitated amino acids. Nevertheless, the DECAB Plus configuration (investigated only for taurine) reduces the required energy in DECAB by almost 0.9 GJ/t CO<sub>2</sub>. The addition of the LVC process configuration reduces the required energy by 1.3 GJ/t CO<sub>2</sub>, providing a reduction of the efficiency penalty similar to the CESAR-1 solvent investigated in Chapter 3 of this thesis.

Alanine has some characteristics that are more advantageous over taurine; 1) The dissolution energy is substantially lower than taurine [234], 2) absorption rates are more favourable than in the case of taurine [78], 3) solvent capacity is higher than taurine (Chapter 7). Therefore, The DECAB Plus configuration for alanine (not investigated in this thesis) might decrease the energy for regeneration to values below that of taurine. Regarding the process configuration, DECAB Plus has more potential to improve the performance of the capture process than the conventional and DECAB process configuration. Future research in amino acid salts should focus on developments in DECAB Plus.

**Table 8.1. Evaluation of different process concepts based on the VLEMS model for the capture process (Chapter 6) and its integration into the ASC PC power plant described in Chapter 3.**

Process configuration	Solvent	Regeneration Energy	ASC Net efficiency
		GJ/t	% LHV
No capture	NA	NA	45.2
Conventional	MEA	3.66	32.6
Conventional	AMP/PZ	2.81	34.6
Conventional	TAU	3.69	33.5
DECAB	TAU	3.31	31.4
DECAB	ALA	3.20	32.0
DECAB Plus	TAU	2.45	33.6
Conventional + LVC	MEA	3.20	33.4
DECAB + LVC	TAU	2.86	32.3
DECAB + LVC	ALA	3.20	33.3
DECAB Plus+ LVC	TAU	2.07	34.3

However, the results in Table 8.1 are subjected to a certain degree of inaccuracy in the assumptions taken for this evaluation. Solvent performance in Table 8.1 has been estimated based on equilibrium models. In Chapter 3, it was already mentioned that for the AMP/PZ solvent the estimated regeneration duty was lower than the experimental regeneration duty obtained in pilot experiments. A possible explanation for the discrepancy is the lower absorption rates of AMP/PZ as compared to MEA. The CESAR-1 solvent will require, therefore, an absorption column higher than that of MEA to provide the necessary contact time and area in order to approach equilibrium conditions. In this case, the experimental pilot plant was designed for MEA, and, therefore a substantial approach to equilibrium cannot be reached, resulting in a regeneration energy of 3.1 GJ/t CO<sub>2</sub> instead of 2.8 GJ/t CO<sub>2</sub>. The risk associated to the use of equilibrium models is also applicable to taurine and alanine, since both amino acids have absorption rates lower than MEA under precipitation conditions [231].

Other assumptions during the evaluation, such as the performance of the solid-liquid separator and the heat transfer equipment in DECAB Plus, have also an associated risk, since the operation of with solids is new to the process and there is no previous experience for capture processes of this type. The following section analyses the potential risks of precipitating amino acid solvents.

### 8.3 Risks associated with precipitating amino acid solvent processes

The potential gains of the DECAB Plus process presented in the previous section, have been evaluated with an equilibrium model based on empirical data on the absorption of CO<sub>2</sub> in precipitating amino acids solutions. To achieve the full potential of the analysed concepts, the absorption unit will have to provide the necessary contact area and time to obtain the predicted loadings. Moreover, the presence of solids in the process requires a substantial modification of the equipment used by the conventional absorption process. These modifications have an associated risk and may have an impact on the process performance presented in this work. The scheme in Figure 8.2 shows an analysis of the main risks associated with each unit operation in the DECAB Plus process. The following sections present a discussion on these risks and the necessary research to understand their impact on the process.

Scaling up a suitable contactor for the absorption unit is an important risk in the development of the DECAB Plus process. The evaluation presented in Chapter 6 is based on an equilibrium model. The model uses Murphree efficiencies to take into account the lack of approach to equilibrium for solvents with similar absorption rates as MEA (see Chapter 6). For other solvents, the value used for Murphree efficiency should be validated by pilot plant absorption experiments in the same way as it has been done with MEA. The risks associated with scaling-up the absorption unit are having short contact times and slow solvent kinetics. These two facts will result in lower rich loadings than those predicted in this work with the subsequent impact in the reboiler duty (which will be higher) or in CO<sub>2</sub> removal percentage (which will be lower than 90%). Possible mitigation options are the use of a dual column system [81] or an increase of the absorption temperature in order to increase the absorption rate. However, the last option will also result in a loss of absorption capacity.

Other risks associated to the presence of solids are related to the design of an efficient solid-liquid separation. The main risks associated to this operation are blockage and erosion of the equipment, which will impair process operation. Moreover, having an inefficient separation, where some of the solids are carried over in the recycled liquid stream, will have an impact on the pH-shift effect predicted in this work (Chapter 6) resulting in higher reboiler duties than expected. The analysis of these risks requires a detailed evaluation of solid-liquid separation technology applied to this process.

The design of heat exchange equipment is also important in order to obtain the performance provided in this work. Fouling and inefficient heat exchange are the most important risks associated with this unit operation. The impact on the process will also increase the reboiler duty.

The mentioned risks have been quantitatively compared by analysing the sensitivity of the process performance to the assumptions taken in the evaluation of these unit operations. The VLEMS model described in Chapter 6 has been used for this purpose. The parameters that have been modified are the Murphree efficiency applicable to CO<sub>2</sub> in each absorption stage in the absorber, the solid-liquid separation efficiency and the lean-rich heat exchanger efficiency. The separator efficiency has been defined as the fraction of input solids that remains in the rich stream (*i.e.* 100% efficiency is equal to zero carry over in the liquid). The heat exchanger efficiency is defined as the relative deviation from the temperature approach assumed in the process model (10°C).

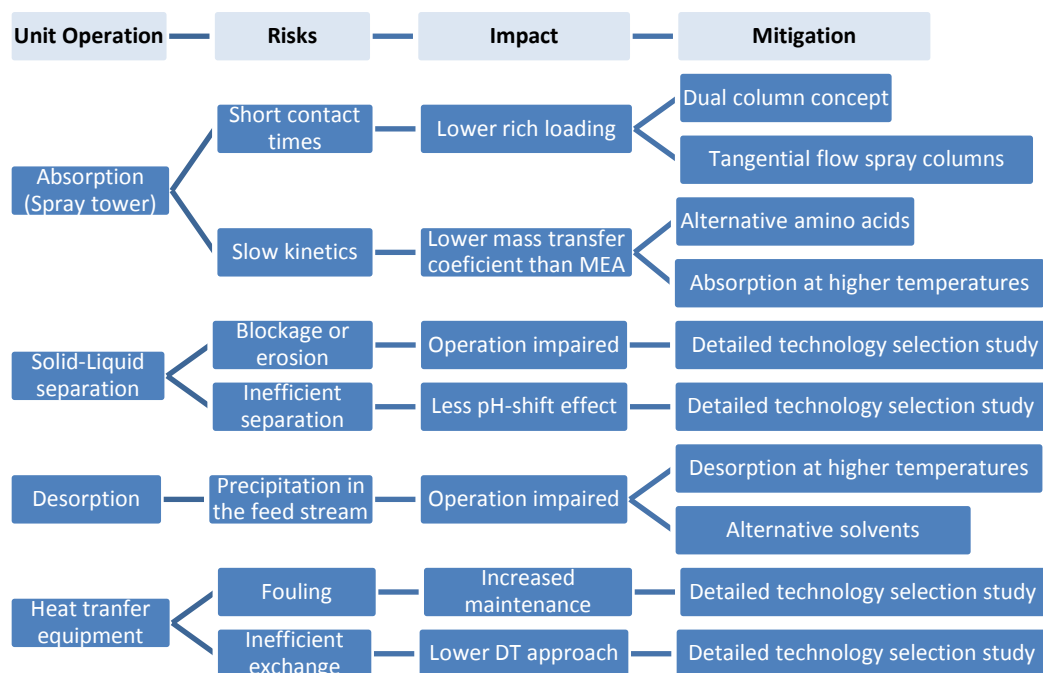
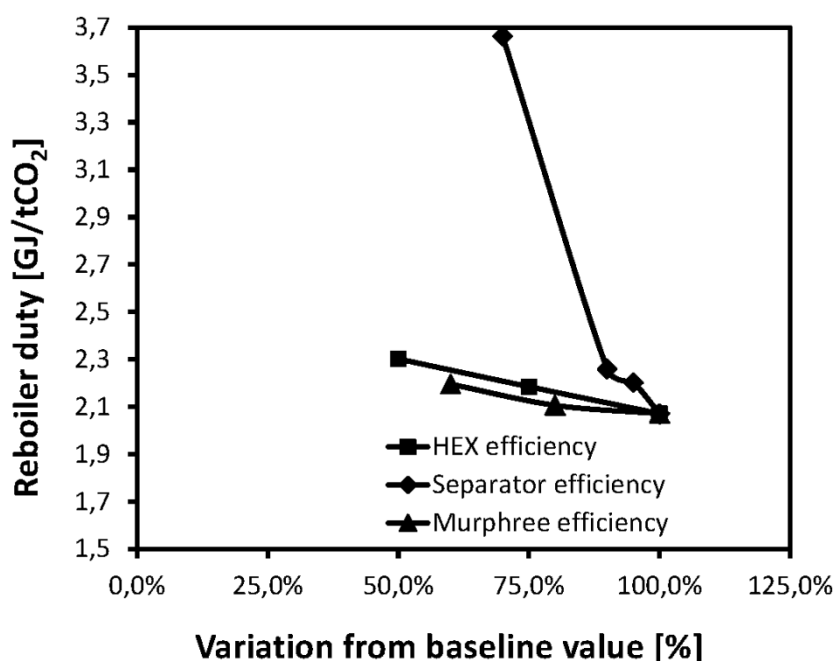


Figure 8.2. Analysis of risks per unit operation in the DECAB Plus process.

The results are presented in Figure 8.3. As shown in this figure, the loss of efficiency in each unit operation has a negative impact on the reboiler duty estimated in this work. However, from the three parameters, the separator efficiency has a drastic impact on the reboiler duty. Therefore, future research should include the design of a solid-liquid separator that has zero carry over of solids in the recycle stream.

### 8.3.1 Mass transfer characteristics of spray contactors

The absorption unit requires the use of alternative contactor types to conventional packed columns, due to severe clogging and raise in pressure drop when a solid phase is formed. Alternative contactor types suited for the contact of three phases (gas, liquid and solid) have been evaluated by Fernandez *et al.* [81] indicating the use of spray tower contactors (in combination with packed columns) as best option available for the DECAB and DECAB Plus processes. Nevertheless, the mass transfer characteristics of spray column with amino acid salt solutions are unknown at this stage and constitute the principal risks to the implementation of these processes.



**Figure 8.3.** Evaluation of the impact of Murphree efficiency, separator efficiency and heat exchanger (HEX) efficiency on the reboiler duty for the optimised DECAB Plus process with LVC (Chapter 7).

The mass transfer characteristics of spray contactors have been investigated for different conditions and absorption processes. To determine the possibility of using a spray tower contactor and, therefore, evaluate the risk associated with the implementation of a new contactor type in the DECAB and DECAB Plus processes, preliminary experiments were carried-out in a spray column of 12 cm diameter and 50 cm height. This was used to qualitatively compare the mass transfer coefficient obtained for potassium taurate with that of MEA. The experimental set-up and method used in these experiments are described in detail in Appendix 9.3.5. In this contactor type, the necessary contact area is created by spraying the liquid through a nozzle at the top of the column in the form of small droplets. The amount of droplets created and the size-distribution of the droplets depends on the spraying nozzle. This is also described in Appendix 9.3.5.

The experiments were performed batch-wise with respect to the liquid and continuously with respect to the gas phase. Figure 8.4 shows an example of the transient profiles obtained during an experiment. The figure shows the CO<sub>2</sub> content in the gas stream leaving the absorption column as a function of time for two experiments with MEA at different gas flow rates. Generally, upon liquid and gas contact (defined as time zero of the experiment) the CO<sub>2</sub> content in the gas stream leaving the column decreased drastically from the initial 12% v/v (representative of flue gas CO<sub>2</sub> concentration) to 4 to 6% v/v depending on the gas flow rate used. As soon as the liquid is loaded with CO<sub>2</sub>, the capacity decreases. Therefore, the CO<sub>2</sub> content in the absorption column exit starts to increase slowly until the initial concentration. At that point the solvent is fully saturated and equilibrium is reached.

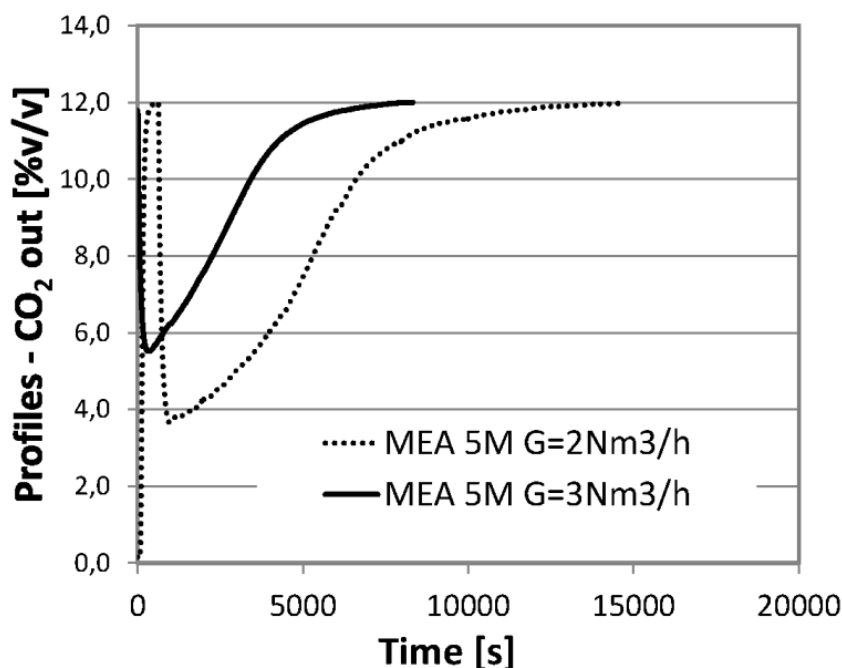


**Figure 8.4.** Transient profiles obtained for MEA in the evaluation of mass transfer in a spray-tower contactor. The CO<sub>2</sub> content in the absorption column outlet stream is plotted as a function of time. Experiments were done at 40°C and 40 kg/h of liquid flow. G represents the volumetric flow of the gas mixture (12 %v/v CO<sub>2</sub> in N<sub>2</sub>).

Mass transfer experiments have been performed for two solvents: (5 M MEA and 4 M potassium taurate) at different gas flows and constant liquid flow and temperature (40°C). The calculated mass transfer coefficients are shown in Figure 8.5 for both solvents. The overall mass transfer coefficient for MEA is higher than that of potassium taurate at same operating conditions. It is observed that the gas flow rate has no direct influence on the overall mass transfer coefficient for both solvents. This indicates that the overall mass transfer process is controlled by the mass transfer in the liquid phase. Moreover, the overall mass transfer coefficient for potassium taurate is 25% lower than the one for MEA. The MEA mass transfer coefficients in Figure 8.5 show substantial discrepancies with the data from Kuntz [242], who investigated the mass transfer for 5 M MEA in a spray tower of 10 cm diameter and 50 cm height using similar nozzles to this study. The overall mass transfer coefficient obtained by Kuntz under fairly similar conditions (with the temperature as exception) is substantially higher than the one obtained in this study (factor 7). One of the reasons for this discrepancy could be the lower effective area realised in the current experimental set-up due to the wall effect. This indicates the need to investigate the mass transfer characteristics of spray columns with nozzles of different angles in order to minimise wall effect.

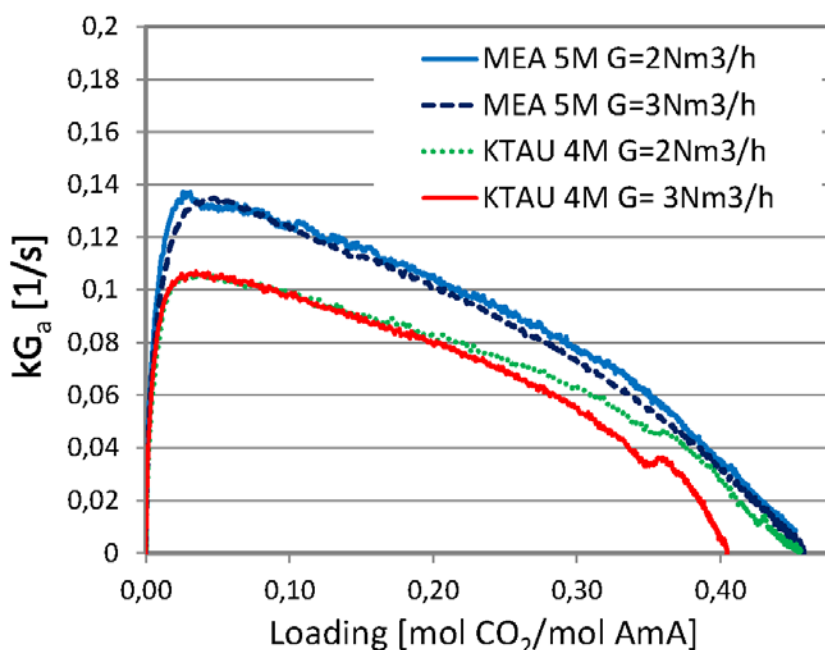


**Figure 8.5.** Overall mass transfer coefficient (volumetric) as a function of liquid loading. Experiments with 5 M MEA and 4 M KTAU (potassium taurate) at different gas flow rates (G). AmA represents the total concentration of amine or amino acid.

### 8.3.2 Solid-Liquid separator

Solid-liquid separation is crucial in the DECAB Plus process to induce the pH-shift effects analysed throughout this work. The characteristics of the slurry formed during absorption, such as solids shape and settling behaviour will determine the efficiency of the separation. Blockage and failure to separate efficiently solids from liquid are seen as the major risks of this operation. The impact on the process performance is high, therefore, a detailed technology study needs to be undertaken in order to understand this risk. Various methods and technologies are available to separate solids from liquids [243]. The two main categories are separation processes based on filtration and processes based on sedimentation. For the DECAB Plus process, the selected equipment needs to be suited for large scale (5-50 m<sup>3</sup>/h), continuously operated and the goal is to get a completely clear liquid. Based on this, the solid-liquid separation methods that could best be used are: Circular basin thickener, settling tank, hydrocyclones and low shear cross-flow micro-filters [244]. Of these, the low shear cross-flow micro-filter has the highest liquid product quality.

### 8.3.3 Heat transfer equipment

Heat exchange is important for the DECAB Plus process, and has, generally a large impact on the plant costs. Therefore, it is important to make a conscious choice for a suitable heat exchanger. Important properties for the process are the heat transfer coefficient, heat exchange area, operating conditions, and price. In the case of the phase changing solvent that is part of the DECAB Plus process, a crucial property for the heat exchanger is also the handling of solids.

## 8.4 Alternative process concepts

Alkaline salts can be used for acid gas removal due to their high basicity. For post-combustion application, alkali salts of weak acids offer many possibilities [39] and, similar to amino acid salts, there is no risk of emitting solvent molecules to the environment. An example of alkaline salt used for acid gas removal is potassium carbonate.

The applicability of potassium carbonate to CO<sub>2</sub> removal has been known for many years. The hot potassium carbonate process was developed in the 1950's for the removal of CO<sub>2</sub> and H<sub>2</sub>S. Potassium carbonate forms a buffer with the absorbed CO<sub>2</sub>, having generally higher capacity than primary amines [39] but substantially lower reaction rates. Increasing the absorption temperature to 75°C greatly increased the rate of absorption, resulting in the development of an economically commercial process to capture CO<sub>2</sub> from synthesis gas, where absorption takes place at temperatures near the atmospheric boiling point of the potassium carbonate solution and regeneration takes place by flashing and steam stripping [39].

The major drawbacks of the use of potassium carbonate for post combustion application are the absorption reaction kinetics, which are very slow for economical removal of CO<sub>2</sub>, and the high CO<sub>2</sub> content that remains in the treated flue gas. Moreover, the equilibrium partial pressures of CO<sub>2</sub> are relatively higher for potassium carbonate solutions than for amines [39]. Therefore, these solutions require deep regeneration in order to obtain 90% CO<sub>2</sub> removal in flue gas application. Promoters like DEA, glycine or piperazine have been tested for the enhancement of the absorption reaction rate of K<sub>2</sub>CO<sub>3</sub>, however, the regeneration of the solvent still constitutes an issue. A recent process from the University of Illinois, Hot-CAP, proposes the crystallisation of bicarbonate in the rich stream and desorption at temperatures at around 150°C [245]. In this case, the quality of the steam needed is higher than when amines are used, but the CO<sub>2</sub> stream is realised at high pressures, reducing the work required for compression.

The most promising process concepts developed in this thesis are based on a modest reduction of the pH in the rich solution prior to desorption. This pH-shift effect, which is brought about by concentrating a pure amino acid species in the rich stream, has been proven to enhance and promote the desorption of CO<sub>2</sub> (Chapter 6). Therefore, following the rationale of these concepts, a novel process idea can be derived, which uses amino acids to promote a pH-shift effect in alkali salt solutions such as potassium carbonate solutions. This process idea, here referred to as the SOPHIE process configuration, is a concept that aims at improving the potassium carbonate system by introducing amino acid salts into the process. The ideal pH for absorbing CO<sub>2</sub> is basic (since CO<sub>2</sub> is an acid gas) but, opposite conditions are desired for desorption (acidic). Most amines exhibit a substantial change in their dissociation constant when the temperature is increased from 40°C to 100 – 120°C creating a more favourable environment for the desorption of CO<sub>2</sub> [246]. This effect is not very relevant for alkali salts such as K<sub>2</sub>CO<sub>3</sub>, leading to more unfavourable desorption conditions, which results in higher CO<sub>2</sub> content of the regenerated solvent. The desorption of CO<sub>2</sub> can be enhanced by inducing a pH change in the system (Chapter 6), leading to lower regeneration energy. In the SOPHIE process concept (illustrated in Figure 8.6), this pH shift is achieved by mixing the reactive salt (*e.g.* K<sub>2</sub>CO<sub>3</sub>) with an amino acid with a relatively low pK<sub>a</sub> that will decrease the pH of the mixture. The “pH swinging” salt needs to be recovered from the process before the reactive mixture is fed back to the absorber, in order to

maintain a basic pH for absorption. For this purpose a separation based on precipitation is proposed. The amino acid has to be precipitated at relatively low temperatures ( $<40^{\circ}\text{C}$ ). Since the amino acid cannot be completely removed from the mixture, a low concentration of the amino acid will be present in the absorption mixture (equal to the solubility of the amino acid at the selected temperature for precipitation and pH of the solution). If the amino acid is, at the same time, selected with fast kinetics for  $\text{CO}_2$  reaction, it will promote the absorption rate and improve the absorption performance of the process.

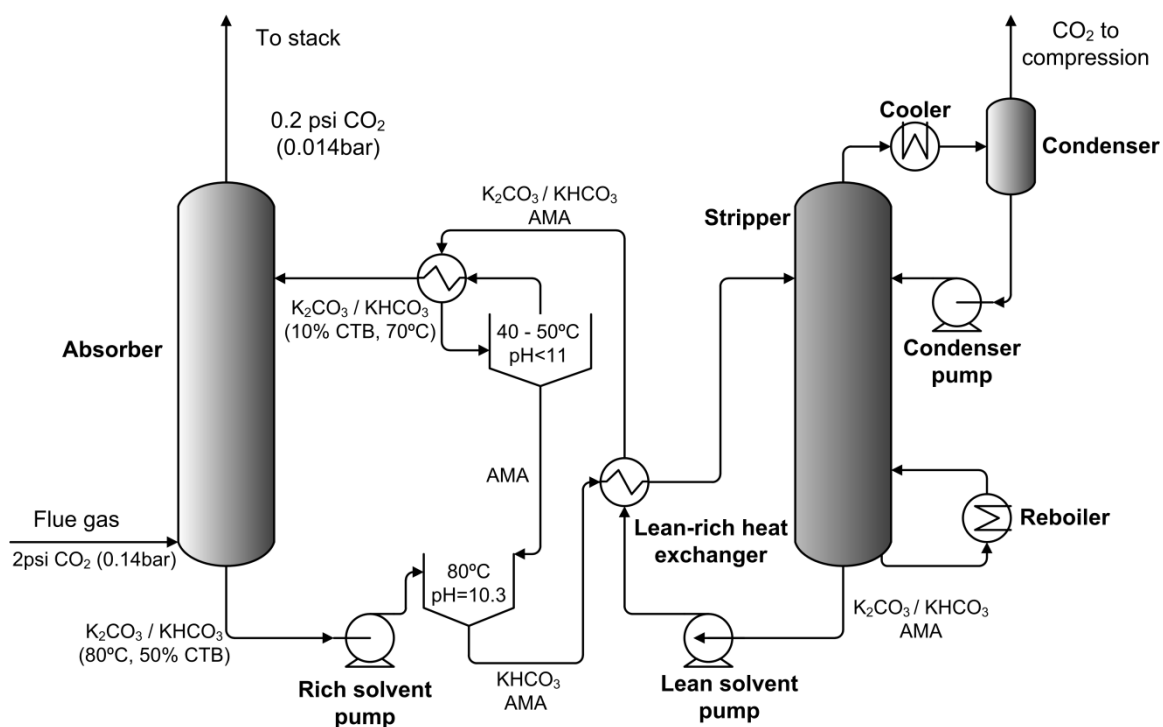


**Figure 8.6.** SOPHIE process configuration based on potassium carbonate and an hypothetical amino acid (AMA), which is present at higher concentrations in desorption, providing a low pH favourable for the realisation of  $\text{CO}_2$ , and at lower concentrations in absorption, promoting the reaction rates. CTB, represents the potassium carbonate conversion into potassium bicarbonate.

## 8.5 Future research

This thesis has addressed several aspects of current capture processes for post-combustion capture (Chapters 1 to 5). It has also evaluated novel capture process configurations based on precipitating amino acid solvents (Chapters 6 and 7). The evaluation has been provided at a conceptual level, based on an extensive number of experiments, which have provided first-hand knowledge on these process configurations. However, some assumptions had to be taken to cover various uncertainties in the evaluated process configurations. This chapter has analysed the main risks associated to the novel process concepts and the importance of the assumptions taken in the evaluation provided in Chapters 6 and 7. In this section, recommendations for future research are presented:

- 1) This thesis has shown that a reduction of the pH of the rich solution prior to desorption helps to reduce the energy use of the reboiler in the capture process (Chapter 6). Other process configurations, which have been just mentioned in this thesis as potential ideas, can also induce a pH-shift and provide improved performance. Future investigation on process concepts that can reduce the pH during desorption could lead to improvements in the capture process energy efficiency.
- 2) Scaling-up a contactor for the DECAB Plus process is crucial for its implementation. An extended experimental study is needed to evaluate the kinetics of the reaction between CO<sub>2</sub> and amino acid salts and the mass transfer characteristics of spray tower contactors.
- 3) The process concepts presented in this thesis were based on the potassium salt of taurine. This amino acid has a number of limitations. One major drawback of taurine is its high heat of dissolution. The evaluation of other amino acids presented in Chapter 7, has indicated the potential of alanine to solve this issue. Further investigation on the DECAB Plus process based on potassium alanate is highly recommended.

---

**APPENDIX**

## 9.1 EBTF summary of assumptions

The EBTF (European Benchmarking Task Force) report is the result of a joint effort of a team of members of the CAESAR, CESAR and DECARBit FP7 projects [21]. It presents a compilation of assumptions and parameters for Carbon Capture projects evaluation, including material related to the costs and economics of carbon capture. The document also provides three technical study cases of power plants without and with CO<sub>2</sub> capture. The evaluation of power plants with integrated post-combustion capture (Chapters 3 and 4) was based on two of the power plant cases presented in this document and the assumptions compiled in the Common Framework Document. The following sections provide a summary of the most relevant technical assumptions and parameters.

### 9.1.1 Air

Temperature (ISO), °C	15
Pressure (ISO), kPa	101.325
Composition, dry molar fraction [%]	
N <sub>2</sub>	78.08
CO <sub>2</sub>	0.04
Ar	0.93
O <sub>2</sub>	20.95
φ	60%

### 9.1.2 Natural gas

Temperature, °C	10
Pressure, bar	70
Molar mass, kg/kmol	18.0
Composition, molar fraction [%]	
CH <sub>4</sub>	89.00
C <sub>2</sub> H <sub>6</sub>	7.00
C <sub>3</sub> H <sub>8</sub>	1.00
C4-i	0.05
C4-n	0.05
C5-i	0.005
C5-n	0.004
CO <sub>2</sub>	2.00

---

N <sub>2</sub>	0.89
S	< 5 ppm
High heat value, MJ/kg	51.473
Low heat value (LHV), MJ/kg	46.502

### 9.1.3 Coal, Douglas premium

#### Proximate analysis, %

Moisture	8%
Ash	14.15%
Volatiles	22.9%
Fixed carbon	54.9%

#### Ultimate analysis, %

Carbon	66.52%,
Nitrogen	1.56%,
Hydrogen	3.78%,
Sulphur	0.52%,
Chlorine	0.009%,
Oxygen	5.46%,

High heat value (HHV), MJ/kg	26.23
Low heat value (LHV), MJ/kg	25.17

### 9.1.4 Technical parameters for power plants (ASC PC and NGCC)

#### **Boiler**

Pressure at boiler exit, bar	300
Temperature at boiler exit, °C	600
Single reheat pressure, bar	60
Single reheat temperature, °C	620
Boiler efficiency, %LHV	94.5
Temperature losses from boiler to turbine, °C	2

#### **Gas Turbine**

Pressure ratio,	18.1
Air flow rate, kg/s	650

TIT, °C	1360	
<b>Heat Recovery Steam Generator</b>		
Steam evaporation pressures, bar	130, 28, 4	
SH and RH temperature, °C	565	
Condensation pressure, bar	0.048	
Pinch point $\Delta T$ , °C	10	
Sub Cooling $\Delta T$ , °C	5	
Minimum approach $\Delta T$ in SH and RH, °C	25	
<b>Steam turbine</b>		
HP Steam turbine efficiency, %	92	
IP Steam turbine efficiency, %	94	
LP Steam turbine efficiency, %	88	
Electrical & Auxiliaries		
Generator efficiency, %	98.5	
Mechanical efficiency,	99.6	
Electric consumption for heat rejection, % of rejected thermal power	0.8	*

9.1.5 *Technical parameters for capture plants*

**CO<sub>2</sub> capture plant**

Booster fan pressure ratio	1.1
Booster fan isentropic efficiency, %	85
Booster fan driver efficiency, %	95
Lean-Rich Heat exchanger $\Delta T_{min}$ , °C	5
Absorption column pressure, bar	1.1
Absorption column number of stages	3
Absorption column pressure drop, mbar	50
Stripper column pressure (bottom), bar	1.8
Stripper column pressure drop, mbar	300

---

\* This value is taken by EBTF assuming natural draft cooling tower

---

Stripper column number of stages	8
Steam pressure for solvent regeneration, bar	3.2
Pumps Head, bar	10
Pumps Hydraulic efficiency, %	75
Pumps Driver efficiency, %	95
<b>CO<sub>2</sub> compression</b>	
Final delivery pressure, bar	110
Intercooled stages,	5
Compressor isentropic efficiency,%	85
Temperature for CO <sub>2</sub> liquefaction, °C	25
Pressure drop for intercooler and dryer,%	
Pump efficiency,%	75

## 9.2 Emission factors for air pollutants based on primary energy

The following tables are a compilation of the information on emission factors of different energy conversion technologies and the removal efficiency of selected Air Pollution control Systems. Based on this information, specific values were selected for quantitative evaluation of the emissions of the selected power plant cases in this work (Chapter 2). Table 11.1 shows the selected values for the Emission factors ( $E_i$ ) for use in equation (2.1). Table 11.2 shows the removal efficiencies ( $R_i$ ) for use in equation (2.1).

## Appendix

**Table 9.1. Emission factors, based on primary energy, for three selected energy conversion technologies: PC boiler, Gas turbine and IGCC gasification plant.**

Components		PC boiler <sup>a</sup>			Gas turbine <sup>b</sup>			IGCC plant <sup>c</sup>		
Pollutants	Units <sup>d</sup>	E <sub>i</sub>	Reference	Other sources	E <sub>i</sub>	Reference	Other sources	E <sub>i</sub>	Reference	Other sources
CO	kg/t	0.23	[103]		1.81	[103]				
SO <sub>2</sub>	kg/t S	17.10	[103]	[247]	0.08	[103]		0.13	[123]	[119, 248]
SO <sub>3</sub>				[249]						
NO <sub>x</sub>	kg/t	5.44	[103]	[104, 247, 250]	7.08	[103]	[109]	0.31	[123]	[248]
Chlorine ( HCl)	kg/t	0.544	[103]					0.02	[119]	
Fluorine (HF)	kg/t	0.068	[103]					0.00	[119]	
Dust (PM-10)	kg/t A	11.26	[103]	[247]	0.15	[103]		5.93·10 <sup>-3</sup>	[123]	
Antimony	kg/t	1.41·10 <sup>-4</sup>	[251]					1.20·10 <sup>-4</sup>	[119]	[100]
Arsenic	kg/t	1.32·10 <sup>-3</sup>	[103]					6.11·10 <sup>-5</sup>	[119]	[111]
Beryllium	kg/t	3.74·10 <sup>-5</sup>	[103]					2.73·10 <sup>-6</sup>	[119]	
Cadmium	kg/t	4.34·10 <sup>-5</sup>	[103]					8.51·10 <sup>-5</sup>	[119]	[111]
Chromium	kg/t	2.53·10 <sup>-4</sup>	[103]					7.96·10 <sup>-5</sup>	[119]	[252]
Cobalt	kg/t	7.85·10 <sup>-5</sup>	[103]					1.64·10 <sup>-5</sup>	[119]	
Lead	kg/t	1.32·10 <sup>-4</sup>	[103]					8.40·10 <sup>-5</sup>	[119]	[111, 253]
Manganese	kg/t	2.53·10 <sup>-4</sup>	[103]					9.05·10 <sup>-5</sup>	[119]	[252]
Nickel	kg/t	2.05·10 <sup>-4</sup>	[103]					1.20·10 <sup>-4</sup>	[119]	[254]
Selenium	kg/t	1.69·10 <sup>-3</sup>	[103]					8.73·10 <sup>-5</sup>	[119]	[111, 253]
Zn	kg/t	4.70·10 <sup>-2</sup>	[251]							[254]
Copper	kg/t	3.53·10 <sup>-4</sup>	[103]							[254]
Thalium	kg/t	5.88·10 <sup>-4</sup>	[251]							
Vanadium	kg/t	4.94·10 <sup>-4</sup>	[103]							[252]
Barium	kg/t	1.69E-03	[103]							
Silver	kg/t	5.88·10 <sup>-5</sup>	[251]							
Mercury	kg/t	5.81·10 <sup>-5</sup>	[103]					5.02·10 <sup>-5</sup>	[119]	[111]
VOC	kg/t				4.65·10 <sup>-2</sup>	[103]		1.53·10 <sup>-2</sup>	[248]	
Acetaldehyde	kg/t				8.85·10 <sup>-4</sup>	[103]		5.24·10 <sup>-5</sup>	[119]	
Formaldehyde	kg/t				1.57·10 <sup>-2</sup>	[103]		4.91·10 <sup>-4</sup>	[119]	
Benzene	kg/t				2.66·10 <sup>-4</sup>	[103]				
Methane	kg/t				1.90·10 <sup>-1</sup>	[103]				

<sup>a</sup> PC boiler, dry bottoms, tangential flow, bituminous coal.

<sup>b</sup> Stationary gas turbine with steam injection. Ash is normally not present or is carried over the pipes. Sulphur is generally not present depending on fuel quality. Factors are suggested by AP-42 [103] in the case of no information on fuel quality.

<sup>c</sup> Emission factors from Williams [119] are derived from LGTI plant in Luisiana for an entrainment flow gasifier, wet scrubber for PM control, Selexol and Selectamine for sulfur control (98% removal), dilution for NO<sub>x</sub> control. Based on sub-bituminous coal. Factors are used directly in equation (2.1) assuming no additional effect for APCS.

<sup>d</sup> For coal cases (kg/t coal dry). Sulphur and particulates emission factors are normalised to the sulphur and ash percentage in coal. *e.g.* for 0.95% sulphur content, emission factor is 17.10x0.95.

**Table 9.2. Matrix of Air Pollutants and removal efficiencies in Air Pollutant Control systems (APCS).**

Air Pollutant	APCS											
	ESP <sup>a</sup>			LNB&OFA&SCR <sup>b</sup>			FGD <sup>c</sup>			MEA based CO <sub>2</sub> capture unit <sup>d</sup>		
	Range	References	Ri	Range	References	Ri	Range	References	Ri	Range	References	Ri
PM-10	75% - 99.9%	[15, 103, 251, 255-257]	99.5%				50%	[103]	50.0%	50%	[103, 122]	50.0%
SO <sub>2</sub>							85%-95% (98%)	[103, 110, 174, 256]	95.0%	99.50%	[110, 139], [115]	99.5%
SO <sub>3</sub>	50%	[256]	50.0%				50%	[103, 110, 249]	50.0%	99.50%	[110, 139]	99.50%
NO <sub>2</sub>				85%-95%	[15, 103, 109]	95.0%				25%	[110, 139]	25.0%
Chlorine (HCl) Fluorine (HF)							95%	[103, 110]	95.0%	95%	[103, 110]	95.0%
Class 1 metals <sup>e</sup>	90%-99%	[93]	99% <sup>f</sup>					This study	50% <sup>g</sup>	>50%	[65, 122]	20.0%
Class 2 metals <sup>e</sup>	50%-76%	[93]	75.0%							>50%	[65, 122]	20.0%
Total Hg / Class 3 metals	97%-99%	[93]	99.0%				90%-95% (95%)	[103, 110]	90.0%			
Elemental mercury										8%	[120]	8.0%
Oxidized mercury							80%-95%	[110]		76%	[110, 171]	76.0%

Removal efficiencies (Ri) for use in equation (2.1)

<sup>a</sup> ESP (Electrostatic precipitator)

<sup>b</sup> LNB&OFA&SCR (combination of Low Nox Burners, Overfired air and Selective catalytic reduction)

<sup>c</sup> FGD (Flue Gas desulphurisation) Efficiencies depend on technology and alkali reagent. Values based on limestone with ratio limestone to sulphur of 1.03 - 1.04 molCa/molS

<sup>d</sup> Based on 30%wt MEA solution, 90% CO<sub>2</sub> removal

<sup>e</sup> Classification of metals based on volatility and condensability properties ([93], [101], [103]):

Class 1: Elements that are approximately equally concentrated in the fly ash and bottom ash. Examples include manganese, beryllium, cobalt, and chromium.

Class 2: Elements that are enriched in fly ash relative to bottom ash. Examples include arsenic, cadmium, lead, and antimony.

Class 3: Elements which are emitted in the gas phase (primarily mercury and, in some cases, selenium).

<sup>f</sup> Indications of trace metal removal is given in Sloss [93]. This study assumes removal metals adsorbed in particulates (Class 1) to be the same as the removal of PM-10.

<sup>g</sup> This study assumes removal metals adsorbed in particulates (Class 1) to be the same as the removal of PM-10 for a wet scrubber [103].

### 9.3 Experimental data and procedures

To develop the models used in Chapters 6 to 8 in this thesis, various data were measured experimentally. The following sections describe the experimental methods used and provide the detailed results of the experiments.

#### 9.3.1 Calibration of Taurine / KOH solutions

The pH of aqueous solutions of taurine and KOH has been measured to correlate the ratio of taurine to potassium [TAU/K] to the initial pH of the solution in the absence of CO<sub>2</sub> (pH<sub>0</sub>). This pH is used in the estimation of the vapour-liquid equilibrium of solutions with different [TAU/K] ratios, which is required by the model described in Chapter 6. The pH was measured in a well stirred vessel at different temperatures (21°C and 40°C) and Taurine concentration of 4 M with a pH-meter (Hach Lange). Solutions were prepared by dissolving Taurine (Sigma-Aldrich 99.8% purity) in deionized water. The concentration of taurine was checked by titration, with a standard deviation in the determination of multiple samples of 0.06M. Known amounts of KOH reagent (Sigma-Aldrich, > 86% purity) were added to the solution until full neutralisation of the amino acid. The exact purity of the KOH reagent was determined by titration with HCl. Purity was determined every time a new solution batch was prepared. The exact results of these experiments are presented in Table 9.3.

**Table 9.3. Measured  $\text{pH}_0$  for different solutions containing taurine (TAU) and KOH. The presence of taurine solids is indicated in grey.**

Temperature [K]	[TAU] [M]	[KOH] [M]	[TAU]/[K] [-]	$\text{pH}_0$ [-]
293.00	4.00	0.00	[-]	5.41
293.00	4.00	0.31	12.80	8.95
293.00	4.00	0.61	6.60	9.16
293.00	4.00	0.88	4.53	9.35
293.00	4.00	1.14	3.50	9.46
293.00	4.00	1.39	2.88	9.56
293.00	4.00	1.62	2.47	9.67
293.00	4.00	1.84	2.17	9.73
293.00	4.00	2.05	1.95	9.79
293.00	4.00	2.25	1.78	9.86
293.00	4.00	3.20	1.25	10.44
293.00	4.00	3.40	1.18	10.46
293.00	4.00	3.60	1.11	10.55
293.00	4.00	3.80	1.05	10.62
293.00	4.00	4.00	1.00	10.74
313.00	4.00	0.00	[-]	4.62
313.00	4.00	0.31	12.96	8.40
313.00	4.00	0.60	6.68	8.67
313.00	4.00	0.87	4.59	8.91
313.00	4.00	1.13	3.54	9.21
313.00	4.00	1.37	2.91	8.55
313.00	4.00	1.60	2.49	9.26
313.00	4.00	1.82	2.19	9.30
313.00	4.00	2.03	1.97	9.45
313.00	4.00	2.15	1.86	9.38
313.00	4.00	3.20	1.25	9.67
313.00	4.00	3.40	1.18	9.80
313.00	4.00	3.60	1.11	9.95
313.00	4.00	3.80	1.05	10.14
313.00	4.00	4.00	1.00	10.21

### 9.3.2 VLE data: Experimental set-up and procedures

Absorption of  $\text{CO}_2$  in potassium salt of amino acid solutions was measured in a well stirred jacketed autoclave (illustrated in Figure 9.1). The vessel is constructed in glass and has a nominal capacity of 0.965 L. The top flange is made of stainless steel and is bolted leaving an hermetic autoclave. The top flange is perforated to accommodate the stirrer, pH sensor (Hach Lange), pressure transducer (Keller PR-35XHTT-1, range up to 6 bar and deviation of 0.042% of the full scale), thermocouple and different pipelines. The temperature in the autoclave is controlled by controlling the temperature of the oil running in the vessel's jacket. The solvent solution is loaded and unloaded through the same pipeline. The dosing of  $\text{CO}_2$  is controlled with a mass flow controller from Bronkhorst (2  $\text{Nm}^3/\text{h}$ ) with a nominal accuracy of 1% of the full range.

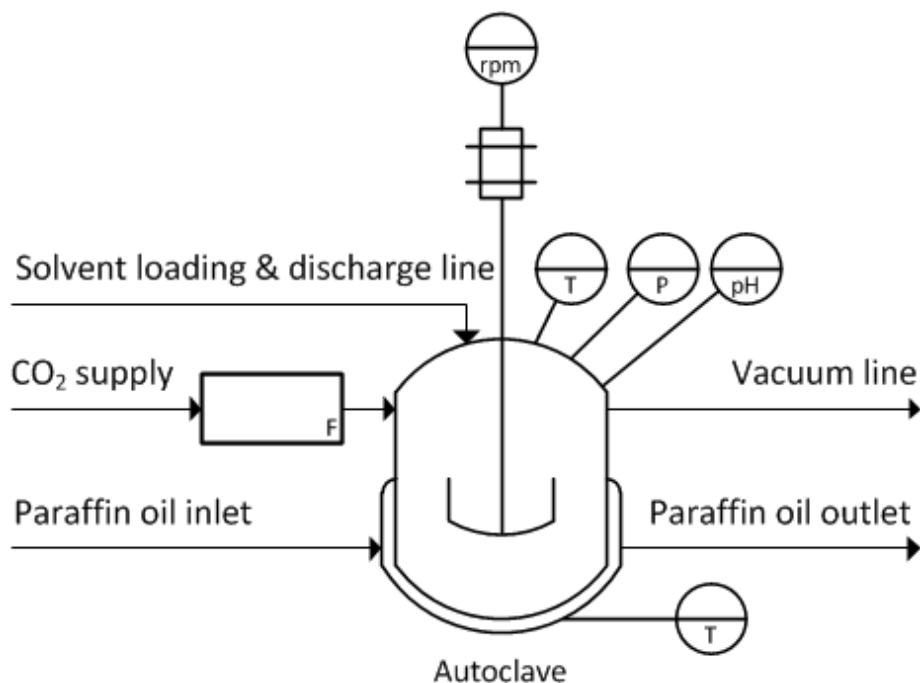


**Figure 9.1.** Schematic representation of the experimental set-up used in this work to measure the absorption of CO<sub>2</sub> in different types of solvents and the solvent's vapour pressure.

Absorption measurements were executed batch-wise. The solvent samples were prepared following the procedure described in Appendix 9.3.1. An exact amount of solvent (0.5L) was added for every experiment. At the beginning of each experiment, the vacuum line was used to establish a deep vacuum (ca -990 mbar) without boiling the solvent. The vessel was maintained at low pressure for a minimum of 10 minutes in order to discard air-in leakage. After this period, the autoclave was slowly heated up to the desired experimental temperature. During this process, both pressure and temperature were recorded in order to determine solvent's vapour pressure. Once the temperature was stabilised at the desired value, a small pulse of pure CO<sub>2</sub> gas was added to the autoclave. Temperature, pressure and pH were monitored online. When these variables were stable, a new CO<sub>2</sub> pulse was added. The criterion for steady state determination was pressure variation less than 6 mbar for at least 20 minutes. Since the solvents under investigation are alkaline salts, their vapour pressure is negligible and, therefore, the amount of CO<sub>2</sub> loaded in the solvent is determined by the difference between the CO<sub>2</sub> injected at a particular pulse ( $z$ ) and the CO<sub>2</sub> present in the gas phase after equilibrium has been reached, which is determined by subtracting the solvent's vapour pressure from the total autoclave pressure, according to:

$$n_{CO_2,L}^z = n_{CO_2,L}^{z-1} + V_{CO_2}^z \cdot \frac{P_{STP}}{R \cdot T_{STP}} - \frac{P_{CO_2,G}^z \cdot V_G}{R \cdot T^z} \quad 9.1$$

Where:

$n_{CO_2,L}^z$  is the amount of CO<sub>2</sub> loaded in the solvent at pulse number  $z$  [mol].

$n_{CO_2,L}^{z-1}$  is the amount of CO<sub>2</sub> loaded in the solvent at pulse number z-1 [mol].

$V_{CO_2}^z$  is the volume of CO<sub>2</sub> dosed by the mass flow controller, calculated as the volumetric flow times the dosing time [Nm<sup>3</sup>].

$P_{STP}$  is standard pressure 101335 Pa.

$T_{STP}$  is standard temperature 273.15K.

$P_{CO_2,G}^z$  is the partial pressure of CO<sub>2</sub> in the gas phase. Calculated as the difference between the autoclave pressure and the water vapour pressure at the autoclave temperature [Pa].

$V_G$  is the gas phase volume. Calculated as the autoclave volume minus the liquid volume.

$T^z$  is the autoclave temperature at pulse z, maintained constant [K].

The final solvent loading, after every pulse, is calculated as the ratio of CO<sub>2</sub> loaded in solution (equation 9.1) and the amount of amino acid present in solution:

$$\alpha_{CO_2}^z = \frac{n_{CO_2,L}^z}{C_A \cdot V_L} \quad 9.2$$

Where:

$\alpha_{CO_2}^z$  loading of the solvent at pulse z.

$C_A$  concentration of amino acid, checked by titration.

$V_L$  liquid volume in the autoclave.

This calculation method neglects the possible effect of the loaded CO<sub>2</sub> on the vapour pressure of the amino acid solution. This procedure was benchmarked with absorption experiments of CO<sub>2</sub> in 5 M MEA and compared to similar results published in the literature. Figure 9.2 shows the solubility results for 5 M MEA for two consecutive runs in the autoclave and its comparison to the data from the literature. The results indicate that the data obtained with our experimental set-up are as reliable as the given literature data. The results of the absorption of CO<sub>2</sub> in different amino acid salts are shown in Tables 9.4 to 9.9.

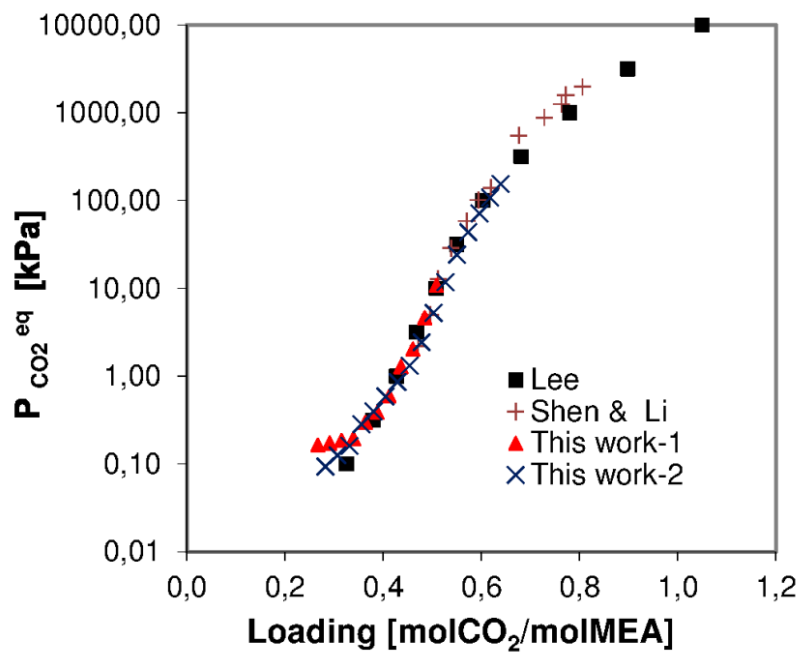


Figure 9.2. Comparison of two experiments with 5 M MEA at 40°C with the data (for the same conditions) of Lee [205] and Shen and Li [210].

**Table 9.4. VLE data for aqueous solutions of taurine (TAU) and potassium hydroxide (KOH) at different temperatures (1). The experiments where precipitation is observed are indicated in grey.**

T °C	TAU [M]	KOH [M]	$\alpha$ [mol/mol]	P <sup>CO2</sup> [kPa]	T °C	TAU [M]	KOH [M]	$\alpha$ [mol/mol]	P <sup>CO2</sup> [kPa]
40.2	4.0	4.0	0.252	0.180	100.0	4.0	4.0	0.051	1.470
40.2	4.0	4.0	0.303	0.280	100.0	4.0	4.0	0.077	0.559
40.2	4.0	4.0	0.355	0.440	100.0	4.0	4.0	0.102	1.139
40.2	4.0	4.0	0.406	0.740	100.0	4.0	4.0	0.127	1.434
40.2	4.0	4.0	0.458	2.430	100.0	4.0	4.0	0.153	2.078
40.2	4.0	4.0	0.508	5.700	100.0	4.0	4.0	0.178	2.733
40.2	4.0	4.0	0.553	19.020	100.0	4.0	4.0	0.204	3.910
40.2	4.0	4.0	0.593	47.120	100.0	4.0	4.0	0.229	5.481
40.2	4.0	4.0	0.625	85.840	100.0	4.0	4.0	0.255	7.617
40.2	4.0	4.0	0.632	96.050	100.0	4.0	4.0	0.280	10.514
60.1	4.0	4.0	0.219	0.570	100.0	4.0	4.0	0.306	14.485
60.1	4.0	4.0	0.263	0.830	100.0	4.0	4.0	0.330	21.212
60.1	4.0	4.0	0.306	1.240	100.0	4.0	4.0	0.356	28.820
60.1	4.0	4.0	0.350	2.050	100.0	4.0	4.0	0.380	41.642
60.1	4.0	4.0	0.393	3.960	100.0	4.0	4.0	0.404	62.202
60.1	4.0	4.0	0.435	9.390	100.0	4.0	4.0	0.428	90.657
60.1	4.0	4.0	0.473	25.370	100.0	4.0	4.0	0.450	132.181
60.1	4.0	4.0	0.505	56.000	100.0	4.0	4.0	0.471	189.766
60.1	4.0	4.0	0.524	89.240	100.0	4.0	4.0	0.491	264.240
80.0	4.0	4.0	0.229	1.862	120.0	4.0	4.0	0.509	352.957
80.0	4.0	4.0	0.255	2.172	120.0	4.0	4.0	0.092	0.868
80.0	4.0	4.0	0.280	2.908	120.0	4.0	4.0	0.108	1.719
80.0	4.0	4.0	0.305	3.772	120.0	4.0	4.0	0.123	3.059
80.0	4.0	4.0	0.330	5.203	120.0	4.0	4.0	0.138	4.224
80.0	4.0	4.0	0.356	5.794	120.0	4.0	4.0	0.154	5.769
80.0	4.0	4.0	0.381	8.510	120.0	4.0	4.0	0.169	8.088
80.0	4.0	4.0	0.406	12.848	120.0	4.0	4.0	0.184	10.120
80.0	4.0	4.0	0.430	20.055	120.0	4.0	4.0	0.199	12.731
80.0	4.0	4.0	0.451	32.444	120.0	4.0	4.0	0.215	15.858
80.0	4.0	4.0	0.474	53.709	120.0	4.0	4.0	0.230	19.704
					120.0	4.0	4.0	0.245	24.271
					120.0	4.0	4.0	0.260	29.348
					120.0	4.0	4.0	0.274	35.945
					120.0	4.0	4.0	0.289	43.193
					120.0	4.0	4.0	0.303	53.154
					120.0	4.0	4.0	0.318	62.201
					120.0	4.0	4.0	0.332	74.767
					120.0	4.0	4.0	0.346	88.589
					120.0	4.0	4.0	0.360	106.700
					120.0	4.0	4.0	0.374	125.127
					120.0	4.0	4.0	0.387	152.091
					120.0	4.0	4.0	0.401	180.512
					120.0	4.0	4.0	0.414	216.064
					120.0	4.0	4.0	0.426	256.183
					120.0	4.0	4.0	0.438	301.991

**Table 9.5. VLE data for aqueous solutions of taurine (TAU) and potassium hydroxide (KOH) at different temperatures (2).**

T °C	TAU [M]	KOH [M]	$\alpha$ [mol/mol]	P <sup>CO2</sup> [kPa]	T °C	TAU [M]	KOH [M]	$\alpha$ [mol/mol]	P <sup>CO2</sup> [kPa]
100.0	5.0	3.5	0.081	3.663	130.0	4.0	3.5	0.091	11.692
100.0	5.0	3.5	0.101	5.434	130.0	4.0	3.5	0.106	15.773
100.0	5.0	3.5	0.121	7.886	130.0	4.0	3.5	0.121	21.646
100.0	5.0	3.5	0.141	11.007	130.0	4.0	3.5	0.136	27.782
100.0	5.0	3.5	0.161	15.532	130.0	4.0	3.5	0.150	35.163
100.0	5.0	3.5	0.181	21.742	130.0	4.0	3.5	0.165	44.000
100.0	5.0	3.5	0.201	30.492	130.0	4.0	3.5	0.179	55.041
100.0	5.0	3.5	0.220	43.066	130.0	4.0	3.5	0.193	68.040
100.0	5.0	3.5	0.239	60.540	130.0	4.0	3.5	0.207	85.441
100.0	5.0	3.5	0.258	86.771	130.0	4.0	3.5	0.220	104.746
100.0	5.0	3.5	0.276	124.039	130.0	4.0	3.5	0.234	127.766
100.0	5.0	3.5	0.293	175.324	130.0	4.0	3.5	0.247	154.049
100.0	5.0	3.5	0.303	231.706	130.0	4.0	3.5	0.260	185.739
					130.0	4.0	3.5	0.272	221.979
120.0	4.0	3.8	0.015	1.915	120.0	4.0	3.5	0.015	1.131
120.0	4.0	3.8	0.031	3.168	120.0	4.0	3.5	0.030	2.341
120.0	4.0	3.8	0.046	5.655	120.0	4.0	3.5	0.046	3.481
120.0	4.0	3.8	0.061	7.843	120.0	4.0	3.5	0.061	4.735
120.0	4.0	3.8	0.076	10.776	120.0	4.0	3.5	0.076	6.512
120.0	4.0	3.8	0.091	13.561	120.0	4.0	3.5	0.091	8.746
120.0	4.0	3.8	0.105	21.432	120.0	4.0	3.5	0.107	11.448
					120.0	4.0	3.5	0.122	14.588
					120.0	4.0	3.5	0.137	18.652
					120.0	4.0	3.5	0.152	23.347
					120.0	4.0	3.5	0.167	29.106
					120.0	4.0	3.5	0.182	36.100
					120.0	4.0	3.5	0.197	44.761
					120.0	4.0	3.5	0.212	54.934
					120.0	4.0	3.5	0.226	67.756
					120.0	4.0	3.5	0.240	83.352
					120.0	4.0	3.5	0.254	101.928
					120.0	4.0	3.5	0.268	124.787
					120.0	4.0	3.5	0.282	151.340
					120.0	4.0	3.5	0.295	180.944
					120.0	4.0	3.5	0.308	217.334
					120.0	4.0	3.5	0.320	260.036

**Table 9.6. VLE data for aqueous solutions of taurine (TAU) and potassium hydroxide (KOH) at different temperatures (3).**

T °C	TAU [M]	KOH [M]	$\alpha$ [mol/mol]	$P^{CO_2}$ [kPa]	T °C	TAU [M]	KOH [M]	$\alpha$ [mol/mol]	$P^{CO_2}$ [kPa]
40.0	2.8	2.8	0.402	2.813	80.0	2.8	2.8	0.073	0.197
40.0	2.8	2.8	0.438	3.122	80.0	2.8	2.8	0.110	0.065
40.0	2.8	2.8	0.475	4.195	80.0	2.8	2.8	0.147	0.196
40.0	2.8	2.8	0.511	6.143	80.0	2.8	2.8	0.184	0.666
40.0	2.8	2.8	0.547	9.321	80.0	2.8	2.8	0.220	0.776
40.0	2.8	2.8	0.583	19.608	80.0	2.8	2.8	0.256	1.313
40.0	2.8	2.8	0.617	36.804	80.0	2.8	2.8	0.293	2.231
40.0	2.8	2.8	0.650	63.537	80.0	2.8	2.8	0.329	3.545
40.0	2.8	2.8	0.682	101.064	80.0	2.8	2.8	0.365	5.572
40.0	2.8	2.8	0.713	148.071	80.0	2.8	2.8	0.402	8.820
40.0	2.8	2.8	0.743	205.189	80.0	2.8	2.8	0.437	14.954
40.0	2.8	2.8	0.771	271.825	80.0	2.8	2.8	0.473	25.215
40.0	2.8	2.8	0.798	347.207	80.0	2.8	2.8	0.507	44.791
40.0	2.8	2.8	0.824	426.813	80.0	2.8	2.8	0.540	79.035
40.0	2.8	2.8	0.849	508.782	80.0	2.8	2.8	0.571	132.444
					80.0	2.8	2.8	0.599	212.702
					80.0	2.8	2.8	0.625	298.326
					80.0	2.8	2.8	0.655	407.258
50.0	2.8	2.8	0.435	4.152	110.0	2.8	2.8	0.073	0.267
50.0	2.8	2.8	0.472	5.786	110.0	2.8	2.8	0.110	1.200
50.0	2.8	2.8	0.508	8.516	110.0	2.8	2.8	0.146	2.715
50.0	2.8	2.8	0.543	15.030	110.0	2.8	2.8	0.183	4.453
50.0	2.8	2.8	0.578	28.550	110.0	2.8	2.8	0.219	7.796
50.0	2.8	2.8	0.611	55.295	110.0	2.8	2.8	0.255	12.530
50.0	2.8	2.8	0.643	90.506	110.0	2.8	2.8	0.291	19.883
50.0	2.8	2.8	0.673	142.812	110.0	2.8	2.8	0.327	31.119
50.0	2.8	2.8	0.702	207.548	110.0	2.8	2.8	0.362	47.153
50.0	2.8	2.8	0.729	285.273	110.0	2.8	2.8	0.397	72.551
50.0	2.8	2.8	0.756	367.481	110.0	2.8	2.8	0.430	108.903
50.0	2.8	2.8	0.780	455.485	110.0	2.8	2.8	0.462	160.491
					110.0	2.8	2.8	0.491	231.119
					110.0	2.8	2.8	0.518	320.029
					110.0	2.8	2.8	0.546	397.426

**Table 9.7. VLE Data for aqueous solutions of taurine (TAU) and potassium hydroxide (KOH) at different temperatures (4).**

T °C	TAU [M]	KOH [M]	$\alpha$ [mol/mol]	$P^{CO_2}$ [kPa]	T °C	TAU [M]	KOH [M]	$\alpha$ [mol/mol]	$P^{CO_2}$ [kPa]
120.0	2.8	2.8	0.073	1.877	120.0	2.8	2.8	0.323	63.387
120.0	2.8	2.8	0.109	3.538	120.0	2.8	2.8	0.357	92.406
120.0	2.8	2.8	0.146	6.294	120.0	2.8	2.8	0.390	134.093
120.0	2.8	2.8	0.182	10.024	120.0	2.8	2.8	0.421	190.664
120.0	2.8	2.8	0.218	17.485	120.0	2.8	2.8	0.450	264.277
120.0	2.8	2.8	0.253	26.761	120.0	2.8	2.8	0.477	350.711
120.0	2.8	2.8	0.289	42.320					

**Table 9.8. VLE data for aqueous solutions of 2 aminoisobutyric acid (AIB) and potassium hydroxide (KOH) at different temperatures. The experiments where precipitation is observed are indicated in grey.**

T °C	AIB [M]	KOH [M]	$\alpha$ [mol/mol]	P <sup>CO2</sup> [kPa]	T °C	AIB [M]	KOH [M]	$\alpha$ [mol/mol]	P <sup>CO2</sup> [kPa]
40.0	2.0	2.0	0.139	0.535	40.0	4.0	4.0	0.101	0.446
40.0	2.0	2.0	0.208	0.763	40.0	4.0	4.0	0.151	0.981
40.0	2.0	2.0	0.278	1.174	40.0	4.0	4.0	0.202	1.270
40.0	2.0	2.0	0.348	1.628	40.0	4.0	4.0	0.252	1.877
40.0	2.0	2.0	0.417	2.209	40.0	4.0	4.0	0.303	2.397
40.0	2.0	2.0	0.487	2.825	40.0	4.0	4.0	0.354	2.436
40.0	2.0	2.0	0.556	4.309	40.0	4.0	4.0	0.404	3.132
40.0	2.0	2.0	0.625	6.611	40.0	4.0	4.0	0.454	3.691
40.0	2.0	2.0	0.694	11.239	40.0	4.0	4.0	0.505	4.185
40.0	2.0	2.0	0.761	26.350	40.0	4.0	4.0	0.556	4.677
40.0	2.0	2.0	0.821	82.919	40.0	4.0	4.0	0.607	5.197
40.0	2.0	2.0	0.858	267.153	40.0	4.0	4.0	0.657	6.090
					40.0	4.0	4.0	0.708	7.653
					40.0	4.0	4.0	0.758	9.298
					40.0	4.0	4.0	0.809	11.236
					40.0	4.0	4.0	0.859	16.493
					40.0	4.0	4.0	0.909	25.964
120.0	2.0	2.0	0.070	2.121	130.0	4.0	4.0	0.051	1.574
120.0	2.0	2.0	0.139	10.135	130.0	4.0	4.0	0.076	2.810
120.0	2.0	2.0	0.207	22.274	130.0	4.0	4.0	0.101	6.474
120.0	2.0	2.0	0.275	40.932	130.0	4.0	4.0	0.126	7.190
120.0	2.0	2.0	0.341	66.271	130.0	4.0	4.0	0.152	11.857
120.0	2.0	2.0	0.405	101.480	130.0	4.0	4.0	0.177	13.763
120.0	2.0	2.0	0.466	151.302	130.0	4.0	4.0	0.202	18.559
120.0	2.0	2.0	0.526	219.296	130.0	4.0	4.0	0.227	24.631
120.0	2.0	2.0	0.581	312.596	130.0	4.0	4.0	0.252	32.232
					130.0	4.0	4.0	0.277	40.388
					130.0	4.0	4.0	0.302	49.845
					130.0	4.0	4.0	0.327	61.147
					130.0	4.0	4.0	0.351	74.930
					130.0	4.0	4.0	0.376	90.849
					130.0	4.0	4.0	0.400	104.384
					130.0	4.0	4.0	0.425	112.907

**Table 9.9.** VLE data for aqueous solutions of 6-amino hexanoic acid (6-AHA),  $\alpha$ -alanine ( $\alpha$ -ALA) and KOH at different temperatures. The experiments where precipitation is observed are indicated in grey.

T °C	ALA [M]	KOH [M]	$\alpha$ [mol/mol]	P <sup>CO2</sup> [kPa]	T °C	6-AHA [M]	KOH [M]	$\alpha$ [mol/mol]	P <sup>CO2</sup> [kPa]
40.0	4.0	4.0	0.202	0.384	40.0	3.0	3.0	0.138	0.340
40.0	4.0	4.0	0.231	0.384	40.0	3.0	3.0	0.207	0.786
40.0	4.0	4.0	0.262	0.455	40.0	3.0	3.0	0.277	0.994
40.0	4.0	4.0	0.318	0.635	40.0	3.0	3.0	0.346	1.659
40.0	4.0	4.0	0.348	0.746	40.0	3.0	3.0	0.416	2.020
40.0	4.0	4.0	0.377	0.887	40.0	3.0	3.0	0.485	4.915
40.0	4.0	4.0	0.437	1.037	40.0	3.0	3.0	0.553	15.043
40.0	4.0	4.0	0.497	1.881	40.0	3.0	3.0	0.620	32.011
40.0	4.0	4.0	0.556	4.594	40.0	3.0	3.0	0.686	57.150
40.0	4.0	4.0	0.615	10.958	40.0	3.0	3.0	0.746	134.806
40.0	4.0	4.0	0.673	20.616	40.0	3.0	3.0	0.798	270.910
40.0	4.0	4.0	0.707	28.058	40.0	3.0	3.0	0.839	496.692
40.0	4.0	4.0	0.757	47.236	40.0	3.0	3.0	0.842	529.893
40.0	4.0	4.0	0.803	80.337					
40.0	4.0	4.0	0.816	93.257					
40.0	4.0	4.0	0.821	100.236	120.0	3.0	3.0	0.102	0.536
					120.0	3.0	3.0	0.153	3.125
					120.0	3.0	3.0	0.204	0.015
120.0	4.0	4.0	0.053	0.850	120.0	3.0	3.0	0.254	1.627
120.0	4.0	4.0	0.097	3.083	120.0	3.0	3.0	0.305	8.323
120.0	4.0	4.0	0.187	6.333	120.0	3.0	3.0	0.355	16.893
120.0	4.0	4.0	0.215	9.178	120.0	3.0	3.0	0.403	38.256
120.0	4.0	4.0	0.247	16.293	120.0	3.0	3.0	0.450	76.969
120.0	4.0	4.0	0.273	23.107	120.0	3.0	3.0	0.494	143.699
120.0	4.0	4.0	0.298	28.501	120.0	3.0	3.0	0.535	242.659
120.0	4.0	4.0	0.336	44.599					
120.0	4.0	4.0	0.378	68.590					
120.0	4.0	4.0	0.415	110.688					
120.0	4.0	4.0	0.442	149.666					

### 9.3.3 *Slurry tests experimental procedure for samples loaded with $\text{KHCO}_3$*

This experimental procedure was used to measure the amount of solids formed at equilibrium in potassium taurate solutions loaded with  $\text{CO}_2$ . In this procedure, the loading of  $\text{CO}_2$  was mimicked by making a mixture of taurine, potassium carbonate, and potassium hydroxide in water. The amount of potassium carbonate added was determined by the desired loading and the remaining amount of potassium was added in the form of potassium hydroxide as the required molarity of potassium minus twice the added molar amount of potassium carbonate. The prepared slurry was heated up upon dissolution of all crystals, point at which temperature and pH were measured. The solution was then cooled to  $40^\circ\text{C}$ , and the solids were separated from the liquid with vacuum filtration. The solid to liquid ratio was determined by weight.

### 9.3.4 *Slurry tests experimental procedure for samples loaded with a $\text{CO}_2/\text{N}_2$ gas mixture*

This experimental procedure was used to measure the amount of solids formed at equilibrium in potassium taurate and potassium alanate solutions loaded with  $\text{CO}_2$ . For this purpose, a known amount of amino acid salt sample was placed in a beaker on a magnetic stirrer with integrated heating and temperature control. A mixture of 12% v/v of  $\text{CO}_2$  in  $\text{N}_2$  was flown into the solution at a constant flow controlled by a mass flow controller. The beaker and the stirrer were placed on a balance with accuracy of 0.01g in order to record the weight gain of the sample. Water evaporation was checked prior to the experiment by bubbling the same gas mixture in the amino acid salt solution at  $40^\circ\text{C}$ . Water losses were determined by following the weight loss with time.

The temperature was kept constant at  $40^\circ\text{C}$  with the heater-stirrer. Temperature and pH were measured and recorded online through all the experiment. Steady state was assumed when no change in temperature or pH was observed for 20 min. At that point the solids were separated from the liquid by vacuum filtration. The wet weight of the solid fraction was first measured. Then, the solids were dried in the furnace at  $180^\circ\text{C}$ . After drying the total weight of the solids was determined and a sample of the dried solids was redissolved in demineralised water. The  $\text{CO}_2$  content in this solution was determined by the phosphoric acid method. In this method, 5 ml of the solution is slowly injected into boiling phosphoric acid.  $\text{N}_2$  is used carrier gas, which transports the released  $\text{CO}_2$  to a Binos 200  $\text{CO}_2$  analyser from Emmerson with a controlled flow of 400 NL/hr. The  $\text{CO}_2$  concentration in 5 ml of solvent is calculated from the known flow of carrier gas and measured  $\text{CO}_2$  concentration. The results are expressed in  $\text{KHCO}_3$  mass, since this is the species commonly found in these amino acids [85].

The concentration of amino acid in the filtrate was determined by titration with HCl 0.1N in an automatic titrator TitrLab 965 from Radiometer. The concentration of  $\text{CO}_2$  in the filtrate was determined by the phosphoric acid method. Table 9.10 shows the results obtained with this procedure for potassium taurate and potassium alanate.

**Table 9.10. Results of the slurry tests for the determination of the solids formed in solutions of 4 M potassium taurate and 4 M potassium alanate in equilibrium with a CO<sub>2</sub>/N<sub>2</sub> gas mixture containing 12 v/v% of CO<sub>2</sub> at 40°C.**

		Total	Filtrate	Slurry
<i>Equilibrium with 12% v/v CO<sub>2</sub> at 40°C. 4M potassium taurate</i>				
Weight	g	125.00	108.82	16.18
TAU	g (dry)	50.00	37.64	12.16
KHCO <sub>3</sub>	g (dry)	7.87	7.60	0.27
Loading	mol/mol	0.45	0.57	0.06
Ws (dry)	%	10%		
<i>Equilibrium with 12% v/v CO<sub>2</sub> at 40°C. 4M potassium alanate</i>				
Weight	g	127.04	74.27	52.77
ALA	g (dry)	35.60	7.58	27.50
KHCO <sub>3</sub>	g (dry)	13.28	8.04	5.24
Loading	mol/mol	0.75	2.15	0.39
Ws (dry)	%	26%		

### 9.3.5 Mass transfer experiments

The experimental set-up used in these experiments is illustrated in Figure 9.3. The contactor is a jacketed column of 12 cm diameter and 50cm height. The necessary contact area is created by spraying the liquid through a nozzle at the top of the column in the form of small droplets. The amount of droplets created and the shape of the droplets' distribution depend on the characteristics of the nozzle. The most common outcome in contactors of this type is the formation of two different regions. One region is formed by a distribution of droplets that create a large contact area (region located close to the nozzle). The other region is formed when the droplets hit the column wall and fall along it as a thin film. In this set-up, the liquid is collected in two portions at the bottom of the column. The portion of the liquid that falls along the column wall is collected in a separate duct to the portion of the liquid that falls over the cross sectional area of the column, enabling the evaluation of the spray pattern by observing the liquid portions of the spray and falling film regions. The nozzle (P-40) selected for the set-up is provided by BETE and has a substantial tested wall effect in this column (up 60% of the liquid flow is collected in the wall duct). The gas flow is supplied at the base of the column and consists of a mixture of CO<sub>2</sub> and N<sub>2</sub>. The flow of each component is regulated by two independent mass flow controllers (Bronkhorst) with nominal flows of 2000 NI/h and 200 NI/h respectively). Prior to its injection in the column, the gas mixture is saturated with water at a temperature slightly above the experiment's temperature. After contact with the liquid, the gas flows through a flow meter and an IR analyser to determine the flow and composition of the gas leaving the column. There is a condenser used to dry the mixture before the IR analyser. The liquid collected at the column's base (both portions) falls to a tank from which is pumped again to the top of the column

via a filter, which retains the solids, and a heat exchanger (*Swagelok*) to control the liquid temperature. The column is maintained at constant temperature by circulating hot water in the jacket. The jacket temperature is controlled by a water bath. Temperature indicators are located at the inlets and outlets of the gas and liquid pipes to the absorption column. There is a pressure indicator in the gas stream leaving the column. Also, a pH-meter is located in the liquid line (*Hach Lange*). All variables mentioned are monitored online and recorded in a computer via a data acquisition card from Benchlink.

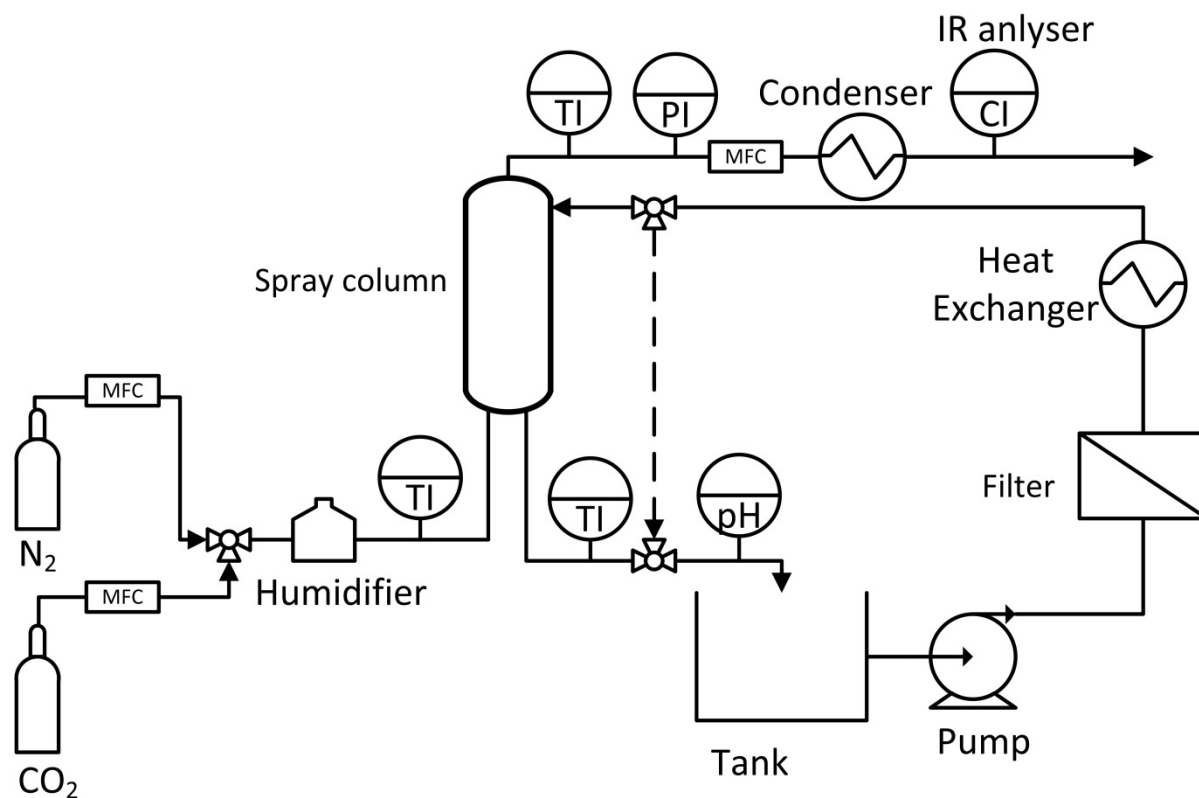


**Figure 9.3.** Illustration of the set-up to measure CO<sub>2</sub> absorption mass transfer in a spray column.

The transfer of CO<sub>2</sub> was measured in a dynamic experiment in which the gas flew once through the column while the liquid was recycled continuously through the column until saturation was achieved. It was considered that equilibrium had been reached when there was no change in the monitored variables (specially the CO<sub>2</sub> content in the gas stream leaving the column) for a period of 30 minutes. At the beginning of each experiment, the gas mixture was adjusted by the mass flow controllers and its composition was checked by connecting the column's gas inlet pipe to the CO<sub>2</sub> analyser. At the same time, the liquid was circulated through the tank and heat exchanger, by-passing the column, until the desired experimental temperature was reached. At that point, the gas mixture was connected to the column and subsequently the liquid flow was connected to the column, moment marked as initial time of the experiment. All variables were monitored online and liquid samples were taken at frequent time intervals in order to determine the CO<sub>2</sub> loading in the liquid as a function of time. The

CO<sub>2</sub> content in each sample was determined by the phosphoric acid method. The mass balance was checked by calculating the liquid loading from the gas side measurements and comparing it to the results of the analysis of liquid samples taken at different intervals during the experiments. Regarding the precipitation of taurine, solids were observed after a loading of 0.3 mol<sub>CO2</sub>/mol<sub>AmA</sub>, which corresponds to the findings of the equilibrium measurements (0.35 mol<sub>CO2</sub>/mol<sub>AmA</sub>).

The experimental results are presented in terms of the volumetric overall mass transfer coefficient ( $K_G a$ ) and are reported as function of liquid loading. The  $K_G a$  is calculated by using the following equation:

$$K_G a = \frac{F_{CO_2}}{\frac{\Delta P}{RT} V} \quad 9.3$$

Here,  $K_G a$  is the volumetric overall mass transfer coefficient (s<sup>-1</sup>),  $F_{CO_2}$  is the molar flow (mol/s) transferred from the gas phase to the liquid phase (calculated from the difference in CO<sub>2</sub> content between inlet and outlet, and the total inlet flow, which is assumed constant).  $\Delta P$  is the averaged driving force for mass transfer, calculated as the logarithmic mean between the inlet driving force (extra partial pressure of CO<sub>2</sub> over the equilibrium pressure at the inlet) and the outlet driving force (extra partial pressure of CO<sub>2</sub> over the equilibrium pressure at the outlet).  $V$  is the volume of the absorption column.

A total number of 6 experiments have been performed to measure the overall mass transfer coefficient (3 experiments with 5 M MEA and 3 experiments with 4 M KTAU). The operating conditions for each experiment and the results with MEA and KTAU are shown in Table 9.11.

**Table 9.11. Summary of mass transfer results. Experiments done with the P-40 nozzle at 40°C.**

Solvent	Concentration	Liquid flow rate		Gas flow rate		$K_G a$	Loading	$P_{CO_2}$
	M	kg/h	m <sup>3</sup> /m <sup>2</sup> h	nL/h	m/s	1/s	mol/mol	kPa
MEA	5	37.14	3.27	2000	0.049	0.136	0-0.02	12
MEA	5	40.01	3.52	2000	0.049	0.133	0-0.02	12
MEA	5	41.36	3.64	3000	0.074	0.133	0-0.03	12
KTAU	4	42.81	2.94	3000	0.074	0.102	0-0.03	12
KTAU	4	40.04	2.75	2000	0.049	0.103	0-0.02	12
KTAU	4	40.23	2.76	2000	0.049	0.103	0-0.02	12

## 9.4 VLEMS model basic calculations

In this work a model has been developed to estimate the performance of the DECAB Plus process based on equilibrium stages. The basic equations that the VLEMS model solves per stage are the MESH equations: Material balance, equilibrium expressions, summation equations and enthalpy

balance. An additional equation is added in each stage to calculate the initial pH of the solution ( $\text{pH}_0$ ) without considering the carbonated species. This variable is used as an input to the equilibrium expressions, empirically derived from experimental data, which allow the calculation of the equilibrium  $\text{CO}_2$  partial pressure at different temperatures.

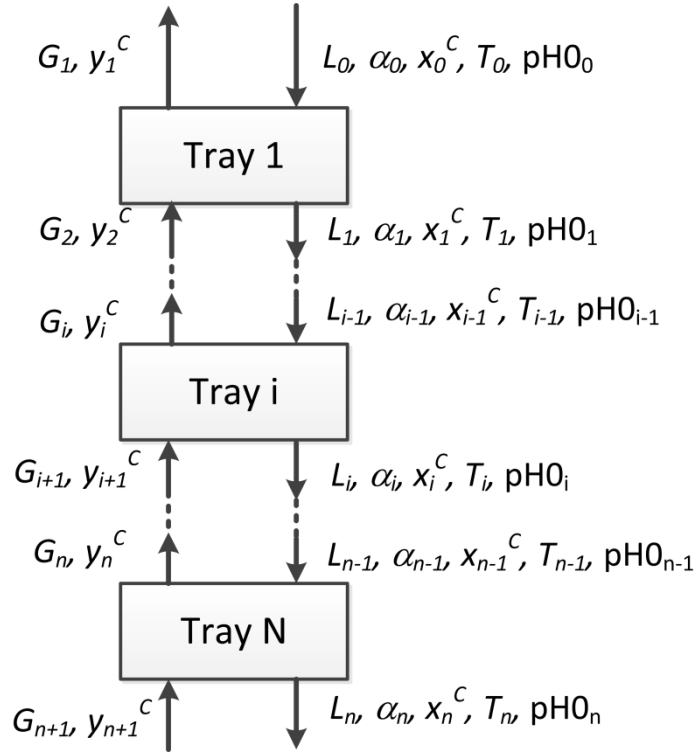


**Figure 9.4.** Illustration of a sequence of equilibrium stages in the VLEMS model. Stages are numbered from top to bottom (indicated by the sub-indexes).

As an example, Figure 9.4 illustrates a cascade of equilibrium stages for which, single stage calculations are presented in equations 9.4 to 9.15 for an intermediate stage. Table 9.12 shows the main input parameters to model MEA and potassium taurate capture processes.

Material balance over a stage, for  $\text{CO}_2$ , water, taurine and potassium:

$$L_{i-1} \cdot x_{i-1}^C + G_{i+1} \cdot y_{i+1}^C = L_i \cdot x_i^C + G_i \cdot y_i^C \quad (9.4)$$

Equilibrium expressions:

$$P_i^{CO_2^{eq}} = f^1(\alpha_i, T_i, \text{pH}_{0i}) \quad (9.5)$$

$$P_i^{H_2O^{eq}} = f^2(T_i, x_s) \quad (9.6)$$

$$P_i^{CO_2} = E_{mv} \cdot (P_i^{CO_2^{eq}}(\alpha_i, T_i, \text{pH}_{0i}) - P_{i+1}^{CO_2}) + P_{i+1}^{CO_2} \quad (9.7)$$

Summation equations:

$$\sum_c y_i^c = 1 \quad (9.8)$$

$$\sum_c x_i^c = 1 \quad (9.9)$$

Enthalpy balance per stage:

$$L_{i-1} \cdot h_{i-1}^L + G_{i+1} \cdot \left( \sum_c y_{i+1}^c \cdot h_{i+1}^c \right) = L_i \cdot h_i^L + G_i \cdot \left( \sum_c y_i^c \cdot h_i^c \right) + Q \quad (9.10)$$

Specific enthalpy calculations: The reference state adopted for enthalpy calculations is the temperature of the rich solvent entering the stripper column (liquid phase). The gas phase components enthalpy calculation, CO<sub>2</sub> and water, requires the heat of absorption of CO<sub>2</sub> and the heat of vaporization of water respectively.

$$h_i^c = Cp_i^c (T_i) \cdot (T_i - T_{ref}) + \Delta H_i^c \quad (9.11)$$

In the equation above C represents CO<sub>2</sub> or H<sub>2</sub>O.

Absorption enthalpy:

$$\Delta H_i^{CO_2} = f^3(\alpha_i, pH_{0i}) \quad (9.12)$$

Water heat of vaporization is considered constant (value given in Table 6.1)

$$\Delta H_i^{H_2O} = \text{Constant} \quad (9.13)$$

The liquid phase enthalpy is calculated considering a constant value of the liquid heat capacity (given in Table 1):

$$h_i^L = Cp^L \cdot (T_i - T_{ref}) \quad (9.14)$$

Electroneutrality:

$$\sum_i z_i \cdot C_i(pH_{0,i}) = 0 \quad (9.15)$$

**Table 9.12. Parameters used in the VLEMS model for two investigated solvents: MEA and potassium taurate.**

Variable	Unit	MEA	Potassium taurate
<b><u>Absorber</u></b>			
Flue Gas Flow Rate <sup>a</sup> :	Nm <sup>3</sup> /h	708581	
Flue Gas Temperature:	°C	40	
Flue Gas Pressure:	bar(a)	1.020	
CO <sub>2</sub> removal	%	90	
Number of Stages:	[-]	4	
Murphree efficiency CO <sub>2</sub> in absorber	[-]	1	
<b><u>Heat exchangers</u></b>			
Temperature Lean cooler:	°C	40	
Temperature approach in LRHX (hot side):	°C	10	
<b><u>Stripper</u></b>			
Reboiler Pressure <sup>b</sup> :	bar(a)	1.900	1.65-1.95
Reboiler Temperature:	°C	120	
Condenser temperature:	°C	40	
Pressure drop per stage stripper <sup>c</sup>	bar/stage	0.006	
Number of Stages <sup>d</sup> :	[-]	5	
Feed Stage:	[-]	2	
Murphree efficiency CO <sub>2</sub> in stripper <sup>e</sup>	[-]	0.8	
<b><u>Solid liquid separator</u></b>			
Recycle split fraction (RSF)	[-]	0.00	0-50%

<sup>a</sup> Based on ASC power plant 250 MW equivalent

<sup>b</sup> Optimal operating conditions from Knudsen <sup>34</sup>

<sup>c</sup> Adjusted for 30 mbar total pressure drop

<sup>d</sup> Excluding the reboiler

<sup>e</sup> Selected to fit the data from Knudsen <sup>34</sup>



---

# NOMENCLATURE

## Abbreviations

AGR	acid gas removal unit
6-AHA	6-aminohexanoic acid
AIB	2-aminoisobutyric acid
ALA	$\alpha$ -Alanine
AMA	Amino acid
AMAK <sup>+</sup>	Potassium salt of an amino acid
AMP	2-amino-2-methyl-1-propanol
APCS	Air pollution control systems
ARD%	Average relative deviation
ASC	Advanced supercritical
ASU	air separation unit
BU	bottom-up approach for capital investment estimation
CCQ	carbon capture quotient
CCS	Carbon capture and storage
CCTs	Carbon capture technologies
CESAR-1	amine based solvent (23% w/w AMP and 12% w/w PZ)
DCC	direct contact cooler
DCF	Discounted cash flow rate [%]
EBTF	European benchmarking task force
EDA	Ethylenediamine
ESP	electrostatic precipitator for particulates removal
FG	Flue gas
FGD	Flue gas desulphurisation
GECoS	Group of Energy Conversion Systems
GT	Gas turbine
HETP	Height equivalent to a theoretical plate
HRSG	Heat recovery steam generator

## Nomenclature

---

IGCC	Integrated gasification combined cycle
IP	Intermediate pressure (bar)
LHV	Low Heat Value of an specific fuel
LMTD	Logarithmic mean temperature difference [°C]
LP	low pressure (bar)
LNB	low NO <sub>x</sub> burners
LRHX	Lean-rich heat exchanger
LRHEX	Lean Rich Heat Exchanger
LVC	Lean vapour compression
KALA	Potassium $\alpha$ -alanate
KTAU	Potassium taurate
MDEA	Methy-di-ethyl-amine
MEA	Monoethanol amine
NGCC	Natural gas combined cycle
NPV	net present value
OFA	over fired air
PC	pulverised coal
PCC	Post combustion capture
PZ	Piperazine
RSF	Recycle split fraction [%]
SCR	selective catalytic reduction
S/L Separator	Solid-Liquid separator
SRU	sulphur recovery unit
SSE	Sum of Squared Errors
TAU	Total amount of taurine species [mol]
TD	top-down approach for capital investment estimation
USC PC	ultra supercritical pulverised coal
VLEMS	Vapour-Liquid Equilibrium MultiStage model
Symbols	
<i>CF</i>	cash flow in a given project year [M€]

---

$CCR$	$CO_2$ capture ratio (-)
$Cp^C$	specific heat of component C [kJ/molK]
$\Delta Depreciation$	depreciation difference between the reference case and any other given case
$\Delta H^{CO_2}$	enthalpy of absorption, desorption [kJ/mol $CO_2$ ]
$\Delta H^{H_2O}$	enthalpy of evaporation of water [kJ/mol $H_2O$ ]
$\Delta TC$	difference in total equipment cost between the reference case (at 1.8 bar), which is 2.72 M€ and any other given case
$\Delta T_{min}$	Minimum temperature approach in lean-rich heat exchanger (cold side) ( $^{\circ}C$ )
$COE$	break-even cost of electricity [€/MWh]
$COT$	Combustor outlet temperature ( $^{\circ}C$ )
$E$	emission rate (kg $CO_2$ /kWh <sub>e</sub> )
$EPC$	engineering and procurements cost [M€]
$G$	gas flow [kmol/s]
$h^{H_2O}$	enthalpy of water as vapour [kJ/mol $H_2O$ ]
$h^{CO_2}$	enthalpy of carbon dioxide [kJ/mol $CO_2$ ]
$h^L$	enthalpy of solvent solution in stage i [kJ/mol solution]
$HR$	Heat Rate (kJ <sub>LHV</sub> /kWh <sub>e</sub> )
$IC$	indirect cost factor [%]
$L$	solvent flow [kmol/s]
$P$	Pressure [bar]
$P^{CO_2}$	partial pressure of carbon dioxide [bar]
$P^{CO_2^{eq}}$	equilibrium partial pressure of carbon dioxide [bar]
$P^{H_2O}$	partial pressure of water [bar]
$pH_0$	pH of a solution containing taurine and KOH [-]
$P_{CO_2}$	Equilibrium partial pressure of $CO_2$ [kPa]
$P_s$	Steam pressure [bar]
$Q$	Specific thermal energy requirement [GJ/t $CO_2$ ]
$Q_r$	reboiler duty [GJth]
$Q_{duty}$	Heat input to the boiler [kW]

---

## Nomenclature

---

$r$	equipment performance rate [units depend on equipment type, <i>e.g.</i> for heat exchangers $r$ is heat transfer area [m <sup>2</sup> ])
$SPECCA$	specific primary energy consumption for CO <sub>2</sub> avoided (GJ/t CO <sub>2</sub> )
$T$	temperature [°C]
TAU	Total amount of taurine [mol]
[TAU/K]	molar ratio of total taurine to potassium ions [-]
$TDPC$	total direct plant cost [M€]
$TEC$	total equipment cost [M€]
$TIPC$	total indirect plant cost [M€]
$TIT$	turbine inlet temperature (°C)
$TPC$	Total plant cost [M€]
$W$	Specific work requirement [kWh/tCO <sub>2</sub> ]
$W_{eq}$	equivalent work necessary to separate CO <sub>2</sub> [GJ]
$w_s$	solid fraction [kg/kg]
$x^c$	liquid mol fraction of component c
$y^c$	gas mol fraction of component c in stage i
Greek symbols	
$\alpha$	liquid CO <sub>2</sub> loading [mol CO <sub>2</sub> / mol AMA]
$\beta$	factor accounting for owner's cost and contingency [%]
$\lambda$	turbine power loss to reboiler duty ratio [-]
$\eta$	Net electric efficiency of the power plant (%LHV)
$\sigma$	specific equipment cost as a function of equipment performance rate [M€]
$\varphi$	Relative air humidity (%)
Super indexes	
c	indicates a specific component: taurine, KOH, CO <sub>2</sub> , H <sub>2</sub> O
G	indicates the gas phase
L	indicates the solvent phase
s	total of amino acid and base species
Subscripts	
i	i-th year in cash flow calculations

i	indicates the stage number (stages are numbered from top to bottom)
k	indicates a specific equipment piece
HEX	heat exchangers
PUMP	pumps
VESSEL	vessel
REF	reference power plant
t	total
R	reboiler
LVC	LVC compressor
SEP	separator
COMP	CO <sub>2</sub> compressor

## REFERENCES

1. IPCC, *Carbon Dioxide Capture and Storage* 2005. Intergovernmental Panel on Climate Change. Bert Metz, et al. Available at: [http://www.ipcc.ch/pdf/special-reports/srccs/srccs\\_wholereport.pdf](http://www.ipcc.ch/pdf/special-reports/srccs/srccs_wholereport.pdf).
2. IPCC, *Climate Change 2007: Mitigation of climate change*. Fourth Assessment report (AR4). 2007. Intergovernmental Panel on Climate change. B. Metz, et al. Available at: [http://www.ipcc.ch/publications\\_and\\_data/publications\\_ipcc\\_fourth\\_assessment\\_report\\_wg3\\_report\\_mitigation\\_of\\_climate\\_change.htm](http://www.ipcc.ch/publications_and_data/publications_ipcc_fourth_assessment_report_wg3_report_mitigation_of_climate_change.htm).
3. Abu-Zahra, M.R., *Carbon Dioxide Capture from Flue Gas: Development and Evaluation of Existing and Novel Process Concepts* PhD Dissertation. Delft University of Technology. 2009. Delft, The Netherlands. Available at: <http://repository.tudelft.nl/>.
4. McKinsey & Company, *Carbon Capture and Storage: Assessing the Economics*. 2008. Available at: <http://www.mckinsey.com/client-service/ccsi/pdf/CCS-Assessing-the-Economics.pdf>.
5. Beér, J. and Obenshain, K., *Clean coal technologies in electric power generation: A brief overview*. EM: Air and Waste Management Association's Magazine for Environmental Managers, 2006(JUL).
6. Beér, J.M., *Combustion technology developments in power generation in response to environmental challenges*. Prog. Energy Combust. Sci., 2000. **26**(4): p. 301-327.
7. Beér, J.M., *High efficiency electric power generation: The environmental role*. Prog. Energy Combust. Sci., 2007. **33**(2): p. 107-134.
8. Franco, A. and Diaz, A.R., *The future challenges for "clean coal technologies": Joining efficiency increase and pollutant emission control*. Energy, 2009. **34**(3): p. 348-354.
9. EU, *A Roadmap for moving to a competitive low carbon economy in 2050*, 2011, EU COM/2011/0112 final
10. Rackley, S.A., *Carbon Capture and Storage* 2010, Burlington, MA, USA: Elsevier Inc.
11. Woodhead Publishing Ltd, *Developments and innovation in carbon dioxide (CO<sub>2</sub>) capture and storage technology*. Woodhead Publishing Series in Energy: Number 8. Vol. Volume 1: Carbon dioxide (CO<sub>2</sub>) capture, transport and industrial applications. 2010, Oxford: Woodhead publishing limited.
12. Miller, B.G., *Clean Coal Engineering Technology* 2011, Oxford, UK: Elsevier Inc.
13. Davison, J., *Performance and costs of power plants with capture and storage of CO<sub>2</sub>*. Energy, 2007. **32**(7): p. 1163-1176.
14. Davison, J. and Thambimuthu, K., *An overview of technologies and costs of carbon dioxide capture in power generation*. Proc. Inst. Mech. Eng., IMechE Conf. Part A: Journal of Power and Energy, 2009. **223**(3): p. 201-212.
15. NETL, *Cost and performance baseline for Fossil Energy plants, Volume 1: Bituminous Coal and Natural Gas to electricity* 2010. National Energy Technology Laboratory. Available at: [http://www.netl.doe.gov/energy-analyses/pubs/BitBase\\_FinRep\\_Rev2.pdf](http://www.netl.doe.gov/energy-analyses/pubs/BitBase_FinRep_Rev2.pdf).

16. Wang, M., et al., *Post-combustion CO<sub>2</sub> capture with chemical absorption: A state-of-the-art review*. Chem. Eng. Res. Des., 2011. **89**(9): p. 1609-1624.
17. Olajire, A.A., *CO<sub>2</sub> capture and separation technologies for end-of-pipe applications e A review*. Energy 2010. **35** p. 2610-2628.
18. Favre, E., *Membrane processes and postcombustion carbon dioxide capture: Challenges and prospects*. Chem. Eng. J., 2011. **171**(3): p. 782-793.
19. Yu, C.H., Huang, C.H., and Tan, C.S., *A review of CO<sub>2</sub> capture by absorption and adsorption*. Aerosol and Air Quality Research, 2012. **12**(5): p. 745-769.
20. Merkel, T.C., et al., *Power plant post-combustion carbon dioxide capture: An opportunity for membranes*. J. Membr. Sci., 2010. **359** p. 126-139.
21. EBTF, *European Best Practice Guidelines for Assessment of CO<sub>2</sub> Capture Technologies*. Collaborative Project– GA No. 213569. 2011. CESAR -project 7th FrameWork Programme. Available at: <http://www.co2cesar.eu/site/en/downloads.php>.
22. IEAGHG, *Water Usage and Power Loss Analysis of Bituminous Coal Fired Power Plants with CO<sub>2</sub> Capture*. 2010/05. 2011. IEA GHG R&D Programme. Available at: <http://cdn.globalccsinstitute.com/publications>.
23. Scholes, C.A., Kentish, S.E., and Stevens, G.W., *Effects of Minor Components in Carbon Dioxide Capture Using Polymeric Gas Separation Membranes* Sep. Purif. Rev., 2009. **38**(1): p. 1 — 44.
24. Manzolini, G., et al., *Integration of SEWGS for carbon capture in natural gas combined cycle. Part A: Thermodynamic performances*. Int. J. Greenhouse Gas Control, 2011. **5**(2): p. 200-213.
25. Manzolini, G., et al., *Integration of SEWGS for carbon capture in Natural Gas Combined Cycle. Part B: Reference case comparison*. Int. J. Greenhouse Gas Control, 2011. **5**(2): p. 214-225.
26. Buhre, B.J.P., et al., *Oxy-fuel combustion technology for coal-fired power generation*. Prog. Energy Combust. Sci., 2005. **31**(4): p. 283-307.
27. Wall, T., et al., *An overview on oxyfuel coal combustion-State of the art research and technology development*. Chem. Eng. Res. Des., 2009. **87**(8): p. 1003-1016.
28. Davison, R.M., *Post-combustion Carbon Capture from Coal fired plants - Solvent Scrubbing*. CCC/125. 2007. IEA Clean Coal Centre. Available at: <http://www.iea-coal.org.uk/>.
29. IEAGHG, *Leading options for the capture of CO<sub>2</sub> emissions at power stations*. Report PH3/14. 2000. IEA GHG R&D Programme. Available at: <http://www.ieaghg.org/>.
30. IEAGHG, *Potential for improvement in gasification combined cycle power generation with CO<sub>2</sub> capture*. Report PH4/19. 2003. IEA GHG R&D Programme. Available at: <http://www.ieaghg.org/>.
31. IEAGHG, *Improvement in power generation with post-combustion capture of CO<sub>2</sub>*. . Report PH4/33 2004. IEA GHG R&D Programme. Available at: <http://www.ieaghg.org/>.
32. Harmelen, T., et al., *The impacts of CO<sub>2</sub> capture technologies on transboundary air pollution in the Netherlands*. 2008. TNO and University of Utrecht. Available at: <http://igitur-archive.library.uu.nl/chem/2009-0310-203446/NWS-E-2008-30.pdf>.

33. Horsssen, A., et al., *The impacts of CO<sub>2</sub> capture technologies in power generation and industry on greenhouse gases emissions and air pollutants in the Netherlands*. 2009. Universiteit Utrecht, TNO. Available at: <http://igitur-archive.library.uu.nl>.
34. Koornneef, J., et al., *The impact of CO<sub>2</sub> capture in the power and heat sector on the emission of SO<sub>2</sub>, NO<sub>x</sub>, particulate matter, volatile organic compounds and NH<sub>3</sub> in the European Union*. *Atmos. Environ.*, 2010. **44**(11): p. 1369-1385.
35. Anderson, C., Schirmer, J., and Abjorensen, N., *Exploring CCS community acceptance and public participation from a human and social capital perspective*. *Mitigation and Adaptation Strategies for Global Change*, 2012. **17**(6): p. 687-706.
36. Ashworth, P., Pisarski, A., and Thambimuthu, K., *Public acceptance of carbon dioxide capture and storage in a proposed demonstration area*. *Proc. Inst. Mech. Eng., Part A*, 2009. **223**(3): p. 299-304.
37. de Coninck, H., et al., *The acceptability of CO<sub>2</sub> capture and storage (CCS) in Europe: An assessment of the key determining factors. Part 1. Scientific, technical and economic dimensions*. *Int. J. Greenhouse Gas Control*, 2009. **3**(3): p. 333-343.
38. Oltra, C., et al., *Lay perceptions of carbon capture and storage technology*. *Int. J. Greenhouse Gas Control*, 2010. **4**(4): p. 698-706.
39. Kohl, L. and Nielsen, R., *Gas Purification*. 5th ed, 1997, Houston, Texas: Gulf Publishing Company.
40. Versteeg, G.F., Van Dijck, L.A.J., and Van Swaaij, W.P.M., *On the kinetics between CO<sub>2</sub> and alkanolamines both in aqueous and non-aqueous solutions. An overview*. *Chem. Eng. Commun.*, 1996. **144**: p. 133-158.
41. Versteeg, G.F. and van Swaaij, W.P.M., *On the kinetics between CO<sub>2</sub> and alkanolamines both in aqueous and non-aqueous solutions-I. Primary and secondary amines*. *Chem. Eng. Sci.*, 1988. **43**(3): p. 573-585.
42. Versteeg, G.F. and van Swaaij, W.P.M., *On the kinetics between CO<sub>2</sub> and alkanolamines both in aqueous and non-aqueous solutions-II. Tertiary amines*. *Chem. Eng. Sci.*, 1988. **43**(3): p. 587-591.
43. Nguyen, T., Hilliard, M., and Rochelle, G.T., *Amine volatility in CO<sub>2</sub> capture*. *Int. J. Greenhouse Gas Control*, 2010. **4**(5): p. 707-715.
44. Supap, T., et al., *Part 2: Solvent management: Solvent stability and amine degradation in CO<sub>2</sub> capture processes*. *Carbon Management*, 2011. **2**(5): p. 551-566.
45. Gouedard, C., et al., *Amine degradation in CO<sub>2</sub> capture. I. A review*. *Int. J. Greenhouse Gas Control*, 2012. **10**: p. 244-270.
46. Saiwan, C., et al., *Part 3: Corrosion and prevention in post-combustion CO<sub>2</sub> capture systems*. *Carbon Management*, 2011. **2**(6): p. 659-675.
47. Pearson, P., Hollenkamp, A.F., and Meuleman, E., *Electrochemical investigation of corrosion in CO<sub>2</sub> capture plants-Influence of amines*. *Electrochimica Acta*, 2013.
48. Aaron, D. and Tsouris, C., *Separation of CO<sub>2</sub> from flue gas: A review*. *Sep. Sci. Technol.*, 2005. **40**(1-3): p. 321-348.
49. Chakma, A., Mehrotra, A.K., and Nielsen, B., *Comparison of chemical solvents for mitigating CO<sub>2</sub> emissions from coal-fired power plants*. *Heat Recovery Systems and CHP*, 1995. **15**(2): p. 231-240.

- 
50. Liang, Z.H., et al., *Part I: Design, modeling and simulation of post-combustion CO<sub>2</sub> capture systems using reactive solvents*. Carbon Management, 2011. **2**(3): p. 265-288.
  51. Mondal, M.K., Balsora, H.K., and Varshney, P., *Progress and trends in CO<sub>2</sub> capture/separation technologies: A review*. Energy, 2012. **46**(1): p. 431-441.
  52. Zhao, B., et al., *Post-combustion CO<sub>2</sub> capture by aqueous ammonia: A state-of-the-art review*. Int. J. Greenhouse Gas Control, 2012. **9**: p. 355-371.
  53. Reddy, S., Scherffius, J., and S., F., *Fluor's Econamine FG Plus Technology. An Enhanced Amine-based CO<sub>2</sub> capture Process*, in *2<sup>nd</sup> National Conference on Carbon Sequestration 2003*: National Energy Technology Laboratory/Department of Energy/Alexandria, VA /USA.
  54. Amrollahi, Z., Ertesvåg, I.S., and Bolland, O., *Optimized process configurations of post-combustion CO<sub>2</sub> capture for natural-gas-fired power plant-Exergy analysis*. Int. J. Greenhouse Gas Control, 2011. **5**(6): p. 1393-1405.
  55. Le Moullec, Y. and Kanniche, M., *Screening of flowsheet modifications for an efficient monoethanolamine (MEA) based post-combustion CO<sub>2</sub> capture*. Int. J. Greenhouse Gas Control, 2011. **5**(4): p. 727-740.
  56. Plaza, J.M., Van Wagener, D., and Rochelle, G.T., *Modeling CO<sub>2</sub> capture with aqueous monoethanolamine*. Int. J. Greenhouse Gas Control, 2010. **4**(2): p. 161-166.
  57. Kishimoto, S., et al., *Current status of MHI's CO<sub>2</sub> recovery technology and optimization of CO<sub>2</sub> recovery plant with a PC fired power plant*. Energy Procedia, 2009. **1**(1): p. 1091-1098.
  58. Idem, R., et al., *Pilot plant studies of the CO<sub>2</sub> capture performance of aqueous MEA and mixed MEA/MDEA solvents at the University of Regina CO<sub>2</sub> capture technology development plant and the boundary dam CO<sub>2</sub> capture demonstration plant*. Ind. Eng. Chem. Res., 2006. **45**(8): p. 2414-2420.
  59. Aroonwilas, A. and Veawab, A., *Characterization and Comparison of the CO<sub>2</sub> Absorption Performance into Single and Blended Alkanolamines in a Packed Column*. Ind. Eng. Chem. Res., 2004. **43**(9): p. 2228-2237.
  60. Aroonwilas, A. and Veawab, A., *Integration of CO<sub>2</sub> capture unit using single- and blended-amines into supercritical coal-fired power plants: Implications for emission and energy management*. Int. J. Greenhouse Gas Control, 2007. **1**(2): p. 143-150.
  61. Setameteekul, A., Aroonwilas, A., and Veawab, A., *Statistical factorial design analysis for parametric interaction and empirical correlations of CO<sub>2</sub> absorption performance in MEA and blended MEA/MDEA processes*. Sep. Purif. Technol., 2008. **64**(1): p. 16-25.
  62. Wilson, M., et al., *Test results from a CO<sub>2</sub> extraction pilot plant at boundary dam coal-fired power station*. Energy, 2004. **29**(9-10): p. 1259-1267.
  63. Rochelle, G., et al., *Aqueous piperazine as the new standard for CO<sub>2</sub> capture technology*. Chem. Eng. J., 2011. **171**(3): p. 725-733.
  64. Knudsen, J.N., et al., *Experience with CO<sub>2</sub> capture from coal flue gas in pilot-scale: testing of different amine solvents*. Energy Procedia, 2009. **1**: p. 783-790.
  65. Knudsen, J.N. *Results from test campaigns at the 1 t/h CO<sub>2</sub> post-combustion capture pilot-plant in Esbjerg under the EU FP7 CESAR project*. in *PCCCI 2011*. Abu Dhabi. Available at <http://ieaghg.org/conferences/pccc/52-conferences/pccc/245-technical-programme>.
-

## References

---

66. Eide-Haugmo, I., et al., *Marine biodegradability and ecotoxicity of solvents for CO<sub>2</sub>-capture of natural gas*. Int. J. Greenhouse Gas Control, 2012. **9**: p. 184-192.
67. Goetheer, E.L.V. and Nell, L., *First pilot results from TNO's solvent development workflow* Carbon Capture Journal 2009. **(8)**: p. 2–3.
68. Schneider, R. and Schramm, H., *Environmentally friendly and economic carbon capture from power plant flue gases: The SIEMENS PostCap technology.*, in *1st Post Combustion Capture Conference*. 2011: Abu Dhabi.
69. Aronu, U.E., et al., *Vapor-liquid equilibrium in amino acid salt system: Experiments and modeling*. Chem. Eng. Sci., 2011. **66**(10): p. 2191-2198.
70. Aronu, U.E., Hoff, K.A., and Svendsen, H.F., *CO<sub>2</sub> capture solvent selection by combined absorption-desorption analysis*. Chem. Eng. Res. Des., 2011. **89**(8): p. 1197-1203.
71. Kumar, P.S., et al., *Equilibrium solubility of CO<sub>2</sub> in aqueous potassium taurate solutions: Part 2. Experimental VLE data and model*. Ind. Eng. Chem. Res., 2003. **42**(12): p. 2841-2852.
72. Majchrowicz, M.E. and Brillman, D.W.F., *Solubility of CO<sub>2</sub> in aqueous potassium l-prolinate solutions-absorber conditions*. Chem. Eng. Sci., 2012. **72**: p. 35-44.
73. Portugal, A.F., et al., *Solubility of carbon dioxide in aqueous solutions of amino acid salts*. Chem. Eng. Sci., 2009. **64**: p. 1993-2002.
74. Aronu, U.E., Hartono, A., and Svendsen, H.F., *Density, viscosity, and N<sub>2</sub>O solubility of aqueous amino acid salt and amine amino acid salt solutions*. J. Chem. Thermodyn., 2012. **45**(1): p. 90-99.
75. Kumar, P.S., et al., *Density, viscosity, solubility, and diffusivity of N<sub>2</sub>O in aqueous amino acid salt solutions*. J Chem. Eng. Data, 2001. **46**(6): p. 1357-1361.
76. Hamborg, E.S., Van Swaaij, W.P.M., and Versteeg, G.F., *Diffusivities in aqueous solutions of the potassium salt of amino acids*. J Chem. Eng. Data, 2008. **53**(5): p. 1141-1145.
77. Aronu, U.E., et al., *Kinetics of carbon dioxide absorption into aqueous amino acid salt: Potassium salt of sarcosine solution*. Ind. Eng. Chem. Res., 2011. **50**(18): p. 10465-10475.
78. Holst, J.v., et al., *Kinetic study of CO<sub>2</sub> with various amino acid salts in aqueous solution*. Chem. Eng. Sci., 2009. **64**(1): p. 59-68.
79. Vaidya, P.D., et al., *Kinetics of carbon dioxide removal by aqueous alkaline amino acid salts*. Ind. Eng. Chem. Res., 2010. **49**(21): p. 11067-11072.
80. Misiak, K., et al. *Next Generation Post-Combustion capture: Combined CO<sub>2</sub> and SO<sub>2</sub> removal*. in *GHGT-11*. 2012. Kyoto. Available at <http://www.ghgt.info/index.php/Content-GHGT11/ghgt-11-overview.html>.
81. Fernandez, E.S. and Goetheer, E.L.V., *DECAB: Process development of a phase change absorption process*. Energy Procedia, 2011. **4**: p. 868-875.
82. Kumar, P.S., *Development and Design of Membrane Gas Absorption Processes*. PhD Thesis. University of Twente. 2002. The Netherlands. Available at: <http://www.tup.utwente.nl/catalogue/book/index.jsp?isbn=9036517486>.

- 
83. Li, L. and Rochelle, G. *Amino acid solvents for CO<sub>2</sub> absorption*. in *PCCC1*. 2011. Abu Dhabi. Available at <http://ieaghg.org/conferences/pccc/52-conferences/pccc/245-technical-programme>.
  84. Kumar, P.S., et al., *Equilibrium solubility of CO<sub>2</sub> in aqueous potassium taurate solutions: Part I. Crystallization in carbon dioxide loaded aqueous salt solutions of amino acids*. *Ind. Eng. Chem. Res.*, 2003. **42**(12): p. 2832-2840.
  85. Majchrowicz, M.E., Brilman, D.W.F., and Groeneveld, M.J., *Precipitation regime for selected amino acid salts for CO<sub>2</sub> capture from flue gases*. *Energy Procedia*, 2009. **1**(1): p. 979-984.
  86. Goetheer, E.L.V. and Sanchez Fernandez, E., *Method for depleting a flue gas of a gaseous acid compound* TNO. 2012. WO2012144898 (A1).
  87. Goetheer, E.L.V., Sanchez Fernandez, E., and Roelands, C.P.M., *Method for absorption of acid gases using amino acids*. TNO. 2009. EP2311545 (A1).
  88. Versteeg, G.F., et al., *Method for absorption of acid gases*. TNO. 2003. WO03095071 (A1)
  89. Fernandez, E.S. and Goetheer, E.L.V. *DECAB: Process development of a phase change absorption process*. 2011. *Energy Procedia*. 4: p.868-875.
  90. CESAR. *Cesar FP7 Project*. <http://www.co2cesar.eu> 2011 september 2011]; Available from: <http://www.co2cesar.eu>.
  91. CATO-2. *CO<sub>2</sub> afvang en-opslag (CATO)*. 2012; Available from: [www.co2-cato.nl](http://www.co2-cato.nl).
  92. EEA, *Air Pollution Impacts from Carbon Capture and Storage (CCS)*. 2011. European Environmental Agency. Available at:
  93. Sloss, L.L. and Smith, I.M., *Trace elements emissions*. 2000. Clean Coal Centre report number CCC/34, 2000.
  94. Kehlhofer, R., et al., *Combined-Cycle Gas and Steam Turbine Power Plants*, 2009, Tulsa, Oklahoma, USA: Pennwell Cooperation.
  95. Kotowicz, J., Skorek-Osikowska, A., and Bartela, L., *Economic and environmental evaluation of selected advanced power generation technologies*. *Proc. Inst. Mech. Eng., Part A*, 2011. **225**(3): p. 221-232.
  96. Zhao, M., Minett, A.I., and Harris, A.T., *A review of techno-economic models for the retrofitting of conventional pulverised-coal power plants for post-combustion capture (PCC) of CO<sub>2</sub>*. *Energy Environ. Sci.*, 2013. **6**(1): p. 25-40.
  97. Samanta, A., et al., *Post-combustion CO<sub>2</sub> capture using solid sorbents: A review*. *Industrial and Engineering Chemistry Research*, 2012. **51**(4): p. 1438-1463.
  98. Higman, *Gasification processes and synthesis gas treatment technologies for carbon dioxide (CO<sub>2</sub>) capture*, in *Developments and innovation in carbon dioxide (CO<sub>2</sub>) capture and storage technology 2010*, Woodhead publishing Limited: Cambridge, UK.
  99. Scheffknecht, G., et al., *Oxy-fuel coal combustion-A review of the current state-of-the-art*. *International Journal of Greenhouse Gas Control*, 2011. **5**(SUPPL. 1): p. S16-S35.
  100. Apps, J.A., *A review of Hazardous Chemical species Associated with CO<sub>2</sub> Capture from Coal-fired power plants and their potential fate during CO<sub>2</sub> geologic storage*. . 2006. Ernesto Orlando Lawrence Berkeley National Laboratory. Available at: <http://www.escholarship.org/uc/item/2162k9tn>.
-

## References

---

101. Reddy, M.S., et al., *Evaluation of the emission characteristics of trace metals from coal and fuel oil fired power plants and their fate during combustion*. Journal of Hazardous Materials, 2005. **123**(1-3): p. 242-249.
102. Liu, H. and Shao, Y., *Predictions of the impurities in the CO<sub>2</sub> stream of an oxy-coal combustion plant*. Appl. Energy, 2010. **87**(10): p. 3162-3170.
103. AP-42, *Compilation of Air Pollutant Emission factors*. Us Environmental protection Agency; Office of Air quality Planning and Standards and office of Research and Development: Washington, DC, 2009. Volume 1: Stationary Point and Area Sources.
104. Srivastava, R.K., et al., *Nitrogen oxides emission control options for coal-fired electric utility boilers*. J. Air Waste Manage. Assoc., 2005. **55**(9): p. 1367-1388.
105. Srivastava, R.K., et al., *Controlling NO<sub>x</sub> emission from industrial sources*. Environmental Progress, 2005. **24**(2): p. 181-197.
106. Le Moulec, Y. and Kanniche, M., *Description and evaluation of flowsheet modifications and their interaction for an efficient monoethanolamine based post-combustion CO<sub>2</sub> capture*. Chemical Engineering transactions, 2010. **21**: p. 175-180.
107. White, V., et al., *Purification of oxyfuel-derived CO<sub>2</sub>*. Int. J. Greenhouse Gas Control, 2010. **4**(2): p. 137-142.
108. Allan, R.J., White, V., and Miller, E.J., *Purification of carbon dioxide*. 2006.
109. Tzimas, E., et al., *Trade-off in emissions of acid gas pollutants and of carbon dioxide in fossil fuel power plants with carbon capture*. Energy Policy, 2007. **35**(8): p. 3991-3998.
110. Lee, J.Y., Keerner, T.C., and Tang, Y., *Potential Flue Gas Impurities in Carbon Dioxide Streams Separated from Coal-fired Power Plants*. Journal of the Air & Waste Management Association, 2009. **59**: p. 725-732.
111. Bunt, J.R. and Waanders, F.B., *Trace element behaviour in the Sasol-Lurgi MK IV FBDB gasifier. Part 1 - The volatile elements: Hg, As, Se, Cd and Pb*. Fuel, 2008. **87**(12): p. 2374-2387.
112. Cummings, A.L., Smith, G.D., Nelsen, D.K., *Advances in Amine Reclaiming - Why There is No Excuse To Operate a dirty Amine System*. , in Laurence Reid Gas Conditioning Conference.2007.
113. Goff, G.S. and Rochelle, G.T., *Monoethanolamine degradation: O<sub>2</sub> mass transfer effects under CO<sub>2</sub> capture conditions*. Ind. Eng. Chem. Res., 2004. **43**(20): p. 6400-6408.
114. Goff, G.S. and Rochelle, G.T., *Oxidation inhibitors for copper and iron catalyzed degradation of monoethanolamine in CO<sub>2</sub> capture processes*. Ind. Eng. Chem. Res., 2006. **45**(8): p. 2513-2521.
115. Thitakamol, B., Veawab, A., and Aroonwilas, A., *Environmental impacts of absorption-based CO<sub>2</sub> capture unit for post-combustion treatment of flue gas from coal-fired power plant*. Int. J. Greenhouse Gas Control, 2007. **1**(3): p. 318-342.
116. Uyanga, I.J. and Idem, R.O., *Studies of SO<sub>2</sub>- and O<sub>2</sub>-induced degradation of aqueous MEA during CO<sub>2</sub> capture from power plant flue gas streams*. Industrial and Engineering Chemistry Research, 2007. **46**(8): p. 2558-2566.
117. Veltman, K., Singh, B., and Hertwich, E.G., *Human and Environmental Impact Assessment of Postcombustion CO<sub>2</sub> Capture Focusing on Emissions from Amine-Based Scrubbing Solvents to Air*. Environmental Science & Technology, 2010. **44**(4): p. 1496-1502.

- 
118. Cameron, E.D., et al., *Demonstration of an oxyfuel combustion system*. 2010. HFCCAT Demonstration programme. Available at:
  119. Williams, A., Wetherold, B., and Maxwell, D., *Trace Substance Emissions from a Coal-fired Gasification Plant*. 1996. Available at:
  120. Cui, Z., Aroonwilas, A., and Veawab, A., *Simultaneous Capture of Mercury and CO<sub>2</sub> in Amine-Based CO<sub>2</sub> Absorption Process*. *Industrial & Engineering Chemistry Research*, 2010. **49**(24): p. 12576-12586.
  121. EU, *Integrated Pollution Prevention and Control Reference Document on Best Available Techniques for Large Combustion Plants*. , 2006, European IPPC Bureau.
  122. Huizeling, E. and Weijde, G., *Non-confidential FEED study report. Special report for the global Carbon Capture and Storage Institute*. 2011. Global carbon capture and storage Institute. Available at:
  123. Weeks, A., *Advanced coal technology Development Can Be Supported under Existing Clean Air act Permitting Frameworks: why IGCC, for example, is BACT for new coal-fueled EGUs*. . 2007. U.S. EPA's Advanced Coal Technologies Working Group. Available at:
  124. Mertens, J., et al., *Understanding ethanolamine (MEA) and ammonia emissions from amine based post combustion carbon capture: Lessons learned from field tests*. *Int. J. Greenhouse Gas Control*, 2013. **13**: p. 72-77.
  125. Vevelstad, S.J., et al., *Degradation of MEA; a theoretical study*. *Energy Procedia*, 2011. **4**(0): p. 1608-1615.
  126. IEA, *Chapter 3: Technology roadmaps, in Energy Technology Perspectives 2008 -- Scenarios and Strategies to 2050*2008, International Energy Agency, ISBN 978-92-64-04142-4.
  127. IEA, *CO<sub>2</sub> Capture and Storage -- A Key Carbon Abatement Option 2008*: International Energy Agency, ISBN 978-92-64-041400.
  128. Gazzani, M., Macchi, E., and Manzolini, G., *CO<sub>2</sub> capture in integrated gasification combined cycle with SEWGS - Part A: Thermodynamic performances*. *Fuel*, 2013. **105**: p. 206-219.
  129. Gazzani, M., Macchi, E., and Manzolini, G., *CO<sub>2</sub> capture in natural gas combined cycle with SEWGS - Part A: Thermodynamic performances*. *International Journal of Greenhouse Gas Control*, 2013. **Article in press**.
  130. ROAD. *Road project*. <http://www.road2020.nl> 2011.
  131. Braitsch, J., *CCS Projects are Becoming Reality - the USA Demonstration Program. Keynote talk, in GHGT-11*, <http://www.ghgt.info/docs/GHGT-11/GHGT11%20Plenary%20Presentations/GHGT-11%202012-11-19%20Jay%20Braitsch%20USDOE.pdf>, Editor 2012: Kyoto.
  132. NGC, <http://www.newgencoal.com.au/post-combustion.html>. Accessed 2012.
  133. Chapel, D., Ernst, J., and Maritz, C. *Recovery of CO<sub>2</sub> from flue gases: commercial trends*. in *Canadian Society of Chemical. Engineering Annual Meeting*. 1999. Saskatoon (Canada).
  134. Hamilton, M.R., Herzog, H.J., and Parsons, J.E. *Cost and U.S. public policy for new coal power plants with carbon capture and sequestration*. 2009. *Energy Procedia*, 2009. 1 (1): p. 4487-4494.
-

135. Abu-Zahra, M.R., et al., *CO<sub>2</sub> capture from power plants: Part II. A parametric study of the economical performance based on mono-ethanolamine*. Int. J. Greenhouse Gas Control, 2007. **1**(2): p. 135-142.
136. Abu-Zahra, M.R.M., et al., *CO<sub>2</sub> capture from power plants: Part I. A parametric study of the technical performance based on monoethanolamine*. Int. J. Greenhouse Gas Control, 2007. **1**(1): p. 37-46.
137. Karimi, M., Hillestad, M., and Svendsen, H.F., *Capital costs and energy considerations of different alternative stripper configurations for post combustion CO<sub>2</sub> capture*. Chem. Eng. Res. Des., 2011. **89**(8): p. 1229-1236.
138. Oexmann, J. and Kather, A., *Post-combustion CO<sub>2</sub> capture in coal-fired power plants: Comparison of integrated chemical absorption processes with piperazine promoted potassium carbonate and MEA*. Energy Procedia, 2009. **1**(1): p. 799-806.
139. Rao, A.B. and Rubin, E.S., *A Technical, Economic, and Environmental Assessment of Amine-Based CO<sub>2</sub> Capture Technology for Power Plant Greenhouse Gas Control*. Environmental Science & Technology, 2002. **36**(20): p. 4467-4475.
140. CAESAR. *Caesar FP7 Project*. <http://caesar.ecn.nl> 2011 september 2011]; Available from: <http://caesar.ecn.nl>.
141. Decarbit. *Decarbit FP7 Project*. <http://www.sintef.no/Projectweb/DECARBit> 2011 september 2011]; Available from: <http://caesar.ecn.nl>.
142. Pequot, *Gas Turbine world " GTW Handbook"*. Vol. 27.2009: Pequot Publication.
143. Herzog, H.J., *An Introduction to CO<sub>2</sub> Separation and Capture Technologies*. MIT Laboratory, 1999.
144. Milano, P.d. *Software presentation: GS (Gas-Steam Cycles)*. . 2009.
145. Consonni, S., et al., *Gas turbine-based cycles for power generation. Part A: calculation model*. 1991.
146. Lozza, G., *Bottoming steam cycles for combined gas-steam power plants: a theoretical estimation of steam turbine performance and cycle analysis*. , in *ASME Cogen-Turbo*, 1990: New Orleans, USA
147. Manzolini, G., et al. *Technical economic evaluation of a system for electricity production with CO<sub>2</sub> capture using a membrane reformer with permeate side combustion*. 2006. Barcelona.
148. Chiesa, P. and Macchi, E., *A thermodynamic analysis of different options to break 60% electric efficiency in combined cycle power plants*. Journal of Engineering for Gas Turbines and Power, 2004. **126**(4): p. 770-785.
149. Fukuda, M., et al. *Advanced USC technology development in Japan*. in *Advances in Materials Technology for Fossil Power Plants-6<sup>th</sup> International conference*. 2011.
150. Amrollahi, Z., Ertesvåg, I.S., and Bolland, O., *Thermodynamic analysis on post-combustion CO<sub>2</sub> capture of natural-gas-fired power plant*. Int. J. Greenhouse Gas Control, 2011. **5**(3): p. 422-426.
151. Darde, V., et al., *Comparison of two electrolyte models for the carbon capture with aqueous ammonia*. Int. J. Greenhouse Gas Control, 2012. **8**: p. 61-72.
152. Li, B., et al., *Advances in CO<sub>2</sub> capture technology: A patent review*. Appl. Energy, 2013. **102**(0): p. 1439-1447.

- 
153. GCCSI, G.C.I., *Global CCS Institute*, 2011.
  154. Hoffmann, B.S. and Szklo, A., *Integrated gasification combined cycle and carbon capture: A risky option to mitigate CO<sub>2</sub> emissions of coal-fired power plants*. Appl. Energy, 2011. **88**(11): p. 3917-3929.
  155. Herzog, H.J., *Scaling up carbon dioxide capture and storage: From megatons to gigatons*. Energy Economics, 2011. **33**(4): p. 597-604.
  156. Finkenrath, M., *Cost performance of carbon dioxide capture from power generation*. International Energy Agency, 2010. **OECD/IEA**.
  157. Huang, B., et al., *Industrial test and techno-economic analysis of CO<sub>2</sub> capture in Huaneng Beijing coal-fired power station*. Appl. Energy, 2010. **87**(11): p. 3347-3354.
  158. ECOFYS, *Financing renewable energy in the European market*. PECPNL084659. 2010. Available at: <http://www.ecofys.com/>.
  159. Artanto, Y., et al., *Performance of MEA and amine-blends in the CSIRO PCC pilot plant at Loy Yang Power in Australia*. Fuel, 2012. **101**: p. 264-275.
  160. Sanchez Fernandez, E., et al., *Comparison of amine based CO<sub>2</sub> capture technologies in Power plants based on European Benchmarking Task Force. Part A: Thermodynamic assessment - Submitted for publication*, 2012.
  161. Rubin, E.S., *Understanding the pitfalls of CCS cost estimates*. Int. J. Greenhouse Gas Control, 2012. **10**: p. 9.
  162. Bhattacharyya, S.C., *Energy Economics, Concepts, Issues, Markets and Governance*, 2011: Springer-Verlag, London
  163. Konstantin, P., *Praxisbuch Energiewirtschaft 2009*: Springer-Verlag, Berlin Heidelberg.
  164. Peters, M.S. and Timmerhaus, K.D., *Plant Design and economics for Chemical Engineers*. 5th ed, 2003: McGraw-Hill, New York.
  165. Towler, G. and Sinnott, R., *Chemical Engineering Design, Principles, Practice and Economics of Plant and Process Design*, 2008: Elsevier.
  166. AspenTech, <http://www.aspentech.com>, 2011.
  167. Thermoflow Inc, <http://www.thermoflow.com>, 2011.
  168. Ulster University, <http://www.cst.ulster.ac.uk/ccf.php>, 2011.
  169. Fostås, B., et al., *Effects of NO<sub>x</sub> in the flue gas degradation of MEA*. Energy Procedia, 2011. **4**: p. 1566-1573.
  170. Strazisar, B.R., Anderson, R.R., and White, C.M., *Degradation of monoethanolamine used in CO<sub>2</sub> capture from flue gas of a coal-fired electric power generating station*. Fuel chemistry Division Preprints, 2002. **47**(1): p. 55.
  171. Strazisar, B.R., Anderson, R.R., and White, C.M., *Degradation Pathways for monoethanolamine in a CO<sub>2</sub> Capture Facility*. Energy Fuels, 2003. **17**: p. 1034-1039.
  172. Lepaumier, H., et al., *Comparison of MEA degradation in pilot-scale with lab-scale experiments*. Energy Procedia, 2011. **4**(0): p. 1652-1659.
  173. Freeman, S.A., et al., *Carbon dioxide capture with concentrated, aqueous piperazine*. Int. J. Greenhouse Gas Control, 2010. **4**(2): p. 119-124.
  174. Bozzuto, C.R., et al., *Engineering Feasibility And Economics Of CO<sub>2</sub> Capture On An Existing Coal-Fired Power Plant*. . 2001. Available at:
-

## References

---

- [http://www.netl.doe.gov/technologies/carbon\\_seq/refshelf/analysis/pubs/AlstomReport.pdf](http://www.netl.doe.gov/technologies/carbon_seq/refshelf/analysis/pubs/AlstomReport.pdf).
175. EBTF, *Personal communication with L. Robinson (Eon Engineering) and M. Rost (Siemens) during EBTF discussions.*, 2011.
176. Cousins, A., Feron, P. *Analysis of combined process flow sheet modifications for energy efficient CO<sub>2</sub> capture from flue gases using chemical absorption in GHGT-10.* 2010. Amsterdam. Available at.
177. Cousins, A., Wardhaugh, L.T., and Feron, P.H.M., *Preliminary analysis of process flow sheet modifications for energy efficient CO<sub>2</sub> capture from flue gases using chemical absorption.* Chem. Eng. Res. Des., 2011. **89**(8): p. 1237-1251.
178. Bergsma, E.J. and Goetheer, E.L.V. *AMP emissions: pilot plant measurements and Aspen Plus modeling* in *1st Post combustion capture conference.* . 2011. Abu Dhabi. Proceedings available at <http://www.ieaghg.org/index.php/?technical-programme.html>
179. Sulzer, <http://www.sulzer.com/en/Products-and-Services/Separation-Technology/Structured-Packings>, 2011.
180. Alfa Laval, <http://www.alfalaval.com/solution-finder/products/packinox/pages/documentation.aspx>, 2011.
181. AACE, *AACE International Recommended Practice No. 16R-90, "Conducting Technical and Economic Evaluations – As Applied for the Process and Utility Industries," TCM Framework: 3.2 – Asset Planning, 3.3 – Investment Decision Making.*, 2003: American Association of Cost Engineers, USA.
182. Pettinau, A., Ferrara, F., and Amorino, C., *Techno-economic comparison between different technologies for a CCS power generation plant integrated with a sub-bituminous coal mine in Italy.* Appl. Energy, 2012. **99**(0): p. 32-39.
183. Rezvani, S., et al., *Comparative assessment of sub-critical versus advanced super-critical oxyfuel fired PF boilers with CO<sub>2</sub> sequestration facilities.* Fuel, 2007. **86**(14 SPEC. ISS.): p. 2134-2143.
184. Viebahn, P., Daniel, V., and Samuel, H., *Integrated assessment of carbon capture and storage (CCS) in the German power sector and comparison with the deployment of renewable energies.* Appl. Energy, 2012. **97**(0): p. 238-248.
185. GTW, in *Gas Turbine World* March-April 2012, Pequot pub. Inc.
186. GTW, *Gas Turbine World Handbook (GTW)*, 2007: Pequot Publishing, Inc.
187. EBTF, *Personal communication with M Rost (Siemens) in the European Benchmarking Task Force framework*, 2011.
188. Melien, T. and Brown-Roijen, S., *Carbon dioxide capture for storage in deep geologic formations.* Vol. Volume 3. 2009: Lars Ingolf, Eide, CPLPress.
189. Rezvani, S., et al., *Natural gas oxy-fuel cycles-Part 3: Economic evaluation.* Energy Procedia, 2009. **1**(1): p. 565-572.
190. Gibbins, J., et al., *Techno-economic assessment of CO<sub>2</sub> capture retrofit to existing power plants.* Energy Procedia, 2011. **4**: p. 1835-1842.
191. Rubin, E.S., Chen, C., and Rao, A.B., *Cost and performance of fossil fuel power plants with CO<sub>2</sub> capture and storage.* Energy Policy, 2007. **35**(9): p. 4444-4454.

- 
192. Van Wagener, D.H. and Rochelle, G.T., *Stripper configurations for CO<sub>2</sub> capture by aqueous monoethanolamine*. Chem. Eng. Res. Des., 2011. **89**(9): p. 1639-1646.
193. Bolland, O., *Common framework of the modelling basis*. ENCAP report D6.1.1 / D4.1.1. 2004. Available at: [www.co2-cato.org](http://www.co2-cato.org).
194. Bergsma, E.J., *CATO-2 Deliverable WP 1.1A – D01D*. 2011. Available at: <http://www.co2-cato.org/publications>.
195. Oexmann, J., et al., *Post-combustion CO<sub>2</sub> capture: Chemical absorption processes in coal-fired steam power plants*. Greenhouse Gases: Science and Technology, 2012. **2**(2): p. 80-98.
196. Siemens, *Personal communication with M. Rost*, 2010.
197. Karimi, S., H.F. *Investigation of effect of intercooling in CO<sub>2</sub> capture energy consumption*. in *GHGT10*. 2010. Amsterdam. Available at <http://www.ghgt.info/index.php/Content-GHGT10/overview.html>.
198. Rochelle, G.T., *Thermal degradation of amines for CO<sub>2</sub> capture*. Curr. Opin. Chem. Eng., 2012. **1**(2): p. 183-190.
199. Hamborg, E.S., Niederer, J.P.M., and Versteeg, G.F., *Dissociation constants and thermodynamic properties of amino acids used in CO<sub>2</sub> absorption from (293 to 353) K*. J. Chem. Eng. Data, 2007. **52**(6): p. 2491-2502.
200. Kumar, P.S., et al., *Kinetics of the reaction of CO<sub>2</sub> with aqueous potassium salt of taurine and glycine*. AIChE Journal, 2003. **49**(1): p. 203-213.
201. King, E.J., *The ionisation constant of Taurine and its activity coefficient in hydrochloric acid solutions from electromotive force measurements*. J. Am. Chem. Soc., 1953. **75**: p. 2204-2209.
202. Dalton, J.B., Schmidt, C.L.A., *The solubilities of certain amino acids in water, the densities of their solutions at twenty-five degrees, and the calculated heats of solution and partial molal volumes* J. Biol. Chem., 1933. **103**: p. 549-578.
203. Benoit, R.L., Beoulet, D., and Frechette, M., *Solvent effect on the solution, ionization, and structure of aminosulfonic acids*. Can. J. Chem., 1988. **66**, : p. 3038.
204. Cheng, S., Meisen, A., and Chakma, A., *Predict amine solutions properties accurately*. Hydrocarbon Process., Int. Ed., 1996: p. 81-84.
205. Lee, J.I., Otto, F.D., Mather, A.E., *Equilibrium between carbon dioxide and monoethanolamine solutions*. J. appl. Chem. Biotechnol., 1976. **26**: p. 541-549.
206. Wagner, W. and Kretzschmar, H., *International Steam Tables - Properties of Water and Steam based on the Industrial Formulation IAPWS-IF97*, 2008, Germany: Springer.
207. Posey, M.L. and Rochelle, G.T., *A Thermodynamic Model of Methyldiethanolamine-CO<sub>2</sub>-H<sub>2</sub>S-Water*. Ind. Eng. Chem. Res., 1997. **36**(9): p. 3944-3953.
208. Oyenekan, B.A. and Rochelle, G.T., *Energy performance of stripper configurations for CO<sub>2</sub> capture by aqueous amines*. Ind. Eng. Chem. Res., 2006. **45**(8): p. 2457-2464.
209. Oyenekan, B.A. and Rochelle, G.T., *Alternative stripper configurations for CO<sub>2</sub> capture by aqueous amines*. AIChE J., 2007. **53**(12): p. 3144-3154.
210. Shen, K.P. and Li, M.H., *Solubility of carbon dioxide in aqueous mixtures of monoethanolamine with methyldiethanolamine*. J. Chem. Eng. Data, 1992. **37**: p. 96-100.
211. Kister, H.Z., *Distillation design*, 1992, New York: McGraw-Hill, Inc.
-

## References

---

212. NIST, *NIST Chemistry WebBook*, <http://webbook.nist.gov/chemistry/>.
213. Gibbins, J.R. and Crane, R.I., *Scope for reductions in the cost of CO<sub>2</sub> capture using flue gas scrubbing with amine solvents*. Proc. Inst. Mech. Eng., Part A, 2004. **218**(4): p. 231-239.
214. Oexmann, J. and Kather, A., *Post-Combustion CO<sub>2</sub>-Capture from Coal-fired Power Plants - Wet Chemical Absorption Processes*. Post-Combustion CO<sub>2</sub>-Abtrennung in Kohlekraftwerken Rauchgaswäschen mit chemischen Lösungsmitteln, 2009. **89**(1-2): p. 92-103.
215. Romeo, L.M., Bolea, I., and Escosa, J.M., *Integration of power plant and amine scrubbing to reduce CO<sub>2</sub> capture costs*. Appl. Therm. Eng., 2008. **28**(8-9): p. 1039-1046.
216. Pellegrini, G., Strube, R., and Manfrida, G., *Comparative study of chemical absorbents in postcombustion CO<sub>2</sub> capture*. Energy, 2010. **35**(2): p. 851-857.
217. Gibbins, J.R. and Crane, R.I., *Preliminary assessment of electricity costs for existing pulverized fuel plant retrofitted with an advanced supercritical boiler and turbine and solvent CO<sub>2</sub> capture*. Proc. Inst. Mech. Eng., Part A, 2004. **218**(7): p. 551-555.
218. Puxty, G., et al., *Carbon dioxide postcombustion capture: A novel screening study of the carbon dioxide absorption performance of 76 amines*. Environ. Sci. Technol., 2009. **43**(16): p. 6427-6433.
219. Shen, S., et al., *Kinetic study of carbon dioxide absorption with aqueous potassium carbonate promoted by arginine*. Chem. Eng. J. , 2013. **222**: p. 478-487.
220. Cullinane, J.T. and Rochelle, G.R., *Carbon dioxide absorption with aqueous potassium carbonate promoted by piperazine*. Chem. Eng. Sci., 2004. **59**(17): p. 3619-3630.
221. NETL. *Bench-Scale Development of a Hot Carbonate Absorption Process with Crystallization-Enabled High Pressure Stripping for Post-Combustion CO<sub>2</sub> Capture*. Project No.: DE-FE0004360. 2013 2013]; Available from: <http://www.netl.doe.gov/>.
222. Raynal, L., et al., *From MEA to demixing solvents and future steps, a roadmap for lowering the cost of post-combustion carbon capture*. Chem. Eng. J. , 2011. **171**(3): p. 742-752.
223. Cousins, A., Wardhaugh, L.T., and Feron, P.H.M., *A survey of process flow sheet modifications for energy efficient CO<sub>2</sub> capture from flue gases using chemical absorption*. Int. J. Greenhouse Gas Control, 2011. **5**(4): p. 605-619.
224. Ahn, H., et al., *Process configuration studies of the amine capture process for coal-fired power plants*. Int. J. Greenhouse Gas Control, 2013. **16**: p. 29-40.
225. de Miguel Mercader, F., et al., *Integration between a demo size post-combustion CO<sub>2</sub> capture and full size power plant. An integral approach on energy penalty for different process options*. Int. J. Greenhouse Gas Control, 2012. **11**(SUPPL): p. 102-113.
226. Sanchez Fernandez, E., et al., *Optimisation of lean vapour compression (LVC) as an option for post-combustion CO<sub>2</sub> capture: Net present value maximisation*. Int. J. Greenhouse Gas Control, 2012. **11**(SUPPL): p. 114-121.
227. Sanchez Fernandez, E., et al. *New process concepts for CO<sub>2</sub> capture based on precipitating amino acids*. in *GHGT-11*. 2012. Kyoto. Available at <http://www.ghgt.info/index.php/Content-GHGT11/ghgt-11-overview.html>.

- 
228. Ahn, S., et al., *Characterization of metal corrosion by aqueous amino acid salts for the capture of CO<sub>2</sub>*. Korean J. Chem. Eng., 2010. **27**(5): p. 1576-1580.
229. Paul, S. and Thomsen, K., *Kinetics of absorption of carbon dioxide into aqueous potassium salt of proline*. Int. J. Greenhouse Gas Control, 2012. **8**: p. 169-179.
230. Sanchez Fernandez, E., et al., *Conceptual design of a novel CO<sub>2</sub> capture process based on precipitating amino acid solvents*. Ind. Eng. Chem. Res., 2013. **52**: p. 12223-12235.
231. Aronu, U.E., et al. *Understanding precipitation in amino acid salt systems at process conditions*. in *GHGT-11*. 2012. Kyoto. Available at <http://www.ghgt.info/index.php/Content-GHGT11/ghgt-11-overview.html>.
232. Yalkowsky, S.H. and Yan, H., *Handbook of Aqueous solubility data*, 2006, Florida: CRC Press LLC.
233. Gucker, F.T. and Allen, T.W., *The Densities and Specific Heats of Aqueous Solutions of dl- $\alpha$ -Alanine,  $\beta$ -Alanine and Lactamide 1,2*. J. Am. Chem. Soc., 1942. **64**(2): p. 191-199.
234. Korolev, V.P., Antonova, O.A., and Smirnova, N.L., *Thermal properties and interpartical interactions of l-proline, glycine, and l-alanine in aqueous urea solutions at 288-318 K*. J. Therm. Anal. Calorim., 2012. **108**(1): p. 1-7.
235. Korolev, V.P., et al., *Amino acids in aqueous solution. Effect of molecular structure and temperature on thermodynamics of dissolution*. Russian Chemical Bulletin, 2007. **56**(4): p. 739-742.
236. Eide-Haugmo, I., et al., *Chemical stability and biodegradability of new solvents for CO<sub>2</sub> capture*. Energy Procedia, 2011. **4**(0): p. 1631-1636.
237. Portugal, A.F., Magalhães, F.D., and Mendes, A., *Carbon dioxide absorption kinetics in potassium threonate*. Chem. Eng. Sci., 2008. **63**(13): p. 3493-3503.
238. Guo, D., et al., *Amino acids as carbon capture solvents: Chemical kinetics and mechanism of the glycine + CO<sub>2</sub> reaction*. Energy Fuels, 2013. **27**(7): p. 3898-3904.
239. Goetheer, E.L.V., et al., *Depleting exhaust gas stream in gaseous acid compound comprises contacting stream with absorbent solution lean, subjecting absorbent solution rich to thermal stripping, subjecting absorbent solution semi-lean to air stripping and recycling*. Netherlands Organisation for Applied Scientific Research. 2013. WO2013081460-A1
240. Kim, M., et al., *Kinetics and steric hindrance effects of carbon dioxide absorption into aqueous potassium alaninate solutions*. Ind. Eng. Chem. Res., 2012. **51**(6): p. 2570-2577.
241. Lim, J.A., et al., *Absorption of CO<sub>2</sub> into aqueous potassium salt solutions of l-alanine and l-proline*. Energy Fuels, 2012. **26**(6): p. 3910-3918.
242. Kuntz, J. and Aroonwilas, A., *Performance of spray column for CO<sub>2</sub> capture application*. Ind. Eng. Chem. Res., 2008. **47**(1): p. 145-153.
243. Wakeman, R. and Tarleton, S., *Solid liquid separation - Scale-up of industrial equipment*, 2005, Oxford: Elsevier Advanced Technology.
244. Tarleton, E.S. and Wakeman, R.J., *Solid/Liquid separation: equipment selection and process design* 2007, Burlington Elsevier Ltd.
245. Lu, Y., et al. *Experimental Studies of a Carbonate-Based Absorption Process with High Pressure Stripping for Post-combustion CO<sub>2</sub> Capture*. in *Clearwater Clean coal conference*. 2013. Florida. Available at <http://www.netl.doe.gov>.
-

## References

---

246. Hamborg, E.S. and Versteeg, G.F., *Dissociation constants and thermodynamic properties of amines and alkanolamines from 293 to 353 K*. J. Chem. Eng. Data, 2009. **54**(4): p. 1318-1328.
247. Zhao, Y., et al., *Establishment of a database of emission factors for atmospheric pollutants from Chinese coal-fired power plants*. Atmos. Environ., 2010. **44**(12): p. 1515-1523.
248. Chaney, R., Van Bibber, L., and Sheets, B., *Beluga Coal Gasification Feasibility Study*. DOE/NETL-2006/1248. 2006. NETL. Available at: [www.netl.doe.gov](http://www.netl.doe.gov).
249. Srivastava, R.K., et al., *Emissions of sulfur trioxide from coal-fired power plants*. J. Air Waste Manage. Assoc., 2004. **54**(6): p. 750-762.
250. Srivastava, R.K., et al., *Control of mercury emissions from coal-fired electric utility boilers*. Environ. Sci. Technol., 2006. **40**(5): p. 1385-1393.
251. Korre, A., Nie, Z., and Durucan, S., *Life cycle modelling of fossil fuel power generation with post-combustion CO<sub>2</sub> capture*. Int. J. Greenhouse Gas Control, 2010. **4**(2): p. 289-300.
252. Bunt, J.R. and Waanders, F.B., *Trace element behaviour in the Sasol-Lurgi fixed-bed dry-bottom gasifier. Part 3 - The non-volatile elements: Ba, Co, Cr, Mn, and V*. Fuel, 2010. **89**(3): p. 537-548.
253. Yoshiie, R., et al., *Emissions of particles and trace elements from coal gasification*. Fuel, 2013. **108**: p. 67-72.
254. Bunt, J.R. and Waanders, F.B., *Trace element behaviour in the Sasol-Lurgi MK IV FBDB gasifier. Part 2 - The semi-volatile elements: Cu, Mo, Ni and Zn*. Fuel, 2009. **88**(6): p. 961-969.
255. Lind, T., et al., *Electrostatic precipitator performance and trace element emissions from two kraft recovery boilers*. Environ. Sci. Technol., 2006. **40**(2): p. 584-589.
256. Odeh, N.A. and Cockerill, T.T., *Life cycle GHG assessment of fossil fuel power plants with carbon capture and storage*. Energy Policy, 2008. **36**(1): p. 367-380.
257. Shanthakumar, S., Singh, D.N., and Phadke, R.C., *Flue gas conditioning for reducing suspended particulate matter from thermal power stations*. Prog. Energy Combust. Sci., 2008. **34**(6): p. 685-695.

---

# SUMMARY

The environmental impact of CO<sub>2</sub> emissions and its contribution to the greenhouse gas effect is a matter of global concern. Although there are uncertainties on the quantitative relationship between atmospheric CO<sub>2</sub> concentration and global warming, it is expected that the CO<sub>2</sub> emissions will be closely regulated in the future as a precautionary action. This implies a substantial change in the energy sector, a large CO<sub>2</sub> emitter, that will have to drastically reduce the use of fossil fuels to meet the emission targets. One of the possibilities to mitigate carbon emissions is capturing the CO<sub>2</sub> contained in flue gas from power plants for ultimate long term storage in suitable deep reservoirs or saline formations. This alternative, known as post-combustion capture, is one of the technologies collectively termed CO<sub>2</sub> capture and storage (CCS), which will permit the continuation on fossil fuel based electricity while the sector moves to a low carbon based electricity.

The technology readiness and know-how of post-combustion capture are relatively mature for implementation, however, there are issues that prevent the energy sector from making a step forward. Specific research indicates that power plants with integrated post-combustion capture have lower net power plant efficiency than conventional power plants, which results from the energy demands for CO<sub>2</sub> removal and compression to disposal conditions (Chapter 1). The reduction in thermal plant efficiency, which depends on the CO<sub>2</sub> capture technology and power plant type, increases fuel use and has a direct effect on electricity costs and the emissions of the power plant. This thesis focusses on the mitigation of this impact by introducing and investigating novel process designs for CO<sub>2</sub> capture.

The current state-of-the-art in post combustion capture is a chemical absorption process that uses an aqueous solution of monoethanolamine (MEA). The characteristics of this process and its integration into two types of power plants, advanced supercritical pulverized coal (ASC PC) and natural gas combined cycle (NGCC), have been analysed in chapters 2 to 5 in this thesis. The deployment of this technology into power plants reduces the net thermal efficiency from 45% LHV to 34% LHV in the case of the ASC PC power plant and from 58% LHV to 50% LHV in the case of the NGCC power plant (Chapter 3). This reduction in efficiency, which is mainly related to the necessary energy to regenerate the solvent, has consequences for the electricity cost that increases from 56 €/MWh to 87 €/MWh for the ASC PC power plant and from 55 €/MWh to 71 €/MWh for the NGCC power plant (Chapter 4). The emissions of other air pollutants are also affected. For instance, the emissions of NO<sub>x</sub> increase 30% per unit electricity basis for both power plant types due to the reduction in power plant efficiency (Chapter 2). In the coal power plant case, this is accompanied by a drastic reduction in SO<sub>x</sub> emissions, virtually 100%, due to the amine process requirements. Another important impact derived from the use of amines is the increase in ammonia emissions, result of amine degradation, and the possibility of amine emissions due to amine evaporation and amine carry over in the form of aerosols (Chapter 2).

One research line to improve the performance of CO<sub>2</sub> capture is the development of solvents better than the state-of-the-art. A tertiary amine or hindered amine is generally blended with a primary or secondary amine. The goal with respect the use of these blends is to reduce the

---

regeneration energy while maintaining solvent reactivity (Chapter 1). CESAR-1 is an example of amine blend, consisting of AMP (hindered amine) and piperazine (secondary amine). This solvent has also been evaluated in chapters 3 and 4, using the same assumptions and methods as conventional MEA. In this case, the final net efficiencies of the coal and natural gas plants are 36%LHV and 51%LHV respectively. Despite the improvement in net plant efficiency, other issues related to solvent management and environmental impact were revealed during the evaluation. The toxicity of piperazine and AMP is higher than for MEA and the volatility of AMP is substantially higher than MEA (Chapter 3). This has consequences for the solvent replenishment costs and for the emissions of these substances to the atmosphere, which will be strictly regulated (Chapter 3). The development of process designs and configurations that contribute to decrease the energy required for solvent regeneration is an alternative research line to improve the performance of CO<sub>2</sub> capture processes. One example of process configuration is the lean vapour compression (LVC), which consists in flashing the hot lean stream leaving the stripper column, re-compressing the steam generated and recycling it back to the stripper column. The application of this configuration to the state-of-the-art MEA process, will reduce the required energy for regeneration by 7-9% (Chapter 5).

This work has investigated the application of novel capture processes to the post-combustion capture of CO<sub>2</sub> from flue gas, which are based on alternative solvents and process configurations to the state-of-the-art post combustion capture process. A novel concept for CO<sub>2</sub> capture based on amino acid salts is introduced in Chapter 6 of this thesis. Amino acids are more biodegradable and less toxic than amines and have negligible vapour pressure. Therefore, a capture process based on amino acid salts will have, generally, a lower environmental impact than amines. CO<sub>2</sub> absorption on aqueous amino acid solutions can lead to the formation of precipitates, depending on the particular amino acid and the concentration in solution. This phase change can influence the equilibrium reactions in CO<sub>2</sub> absorption and desorption contributing to decrease the energy consumption of the conventional absorption-desorption capture process. The identified effects related to the precipitation of amino acids are; (1) the enhancement of the specific CO<sub>2</sub> capacity of amino acid salt solutions; (2) the acidification of the rich solution, which is not a direct effect of precipitation but is brought about by introducing a phase separation after precipitation (liquid from solid) that modifies the amino acid to counter-ion molar ratio in solution, concentrating the amino acid in the rich solution.

The first effect, enhancement of CO<sub>2</sub> absorption, occurs when precipitates are formed during absorption as a result of the chemical reaction of CO<sub>2</sub> with the amino acid solvent, due to its limited solubility. The removal from the liquid phase of the solid reaction product shifts the reaction equilibrium towards the production of more products. The result is a rich stream in the form of slurry that contains mainly amino acid in the solid phase and carbamate, bicarbonate, potassium and remaining amino acid species in the liquid phase. Absorption takes place in a suitable contactor that can handle solids. This can be a spray tower contactor or a sequence of spray tower contactor and packed column. The slurry that results from the absorption of CO<sub>2</sub> can be directly regenerated in the stripper, via the lean-rich heat exchanger, in a process concept known as DECAB. The second effect, acidification of the rich stream, requires the processing of the slurry in a solid-liquid separator to partially separate the supernatant from the solids. This forms a concentrated slurry, enriched in the pure amino acid species. This stream is further processed in the stripper for desorption. By re-dissolving the amino acid crystals, the pH of the

---

new rich solution is decreased before thermal desorption, which results in higher partial pressures of CO<sub>2</sub> at stripper conditions that facilitate desorption. The recycle stream is the supernatant excess, enriched in the amino acid salt counter-ion, which is fed back to the absorber without passing through the stripper. This process alternative is known as DECAB Plus.

Chapters 6 and 7 in this thesis provide new data and modelling to evaluate the two process concepts, DECAB and DECAB Plus, based on the potassium salt of taurine. The evaluation relies on an equilibrium based model, which includes all the necessary unit operations of the processes to capture CO<sub>2</sub> from coal fired power plant flue gas containing circa 13 %v/v CO<sub>2</sub>. The model uses an approximate thermodynamic representation of the solvents investigated based on empirical correlations that have been derived from experimental data. The results show a 35% reduction in the solvent regeneration energy with respect to conventional MEA. The specific reboiler energy is reduced from 3.7 GJ/ t CO<sub>2</sub>, which corresponds to the MEA baseline, to 2.4 GJ/ t CO<sub>2</sub>, which corresponds to the DECAB Plus process. This value can be further decreased by optimisation of the process configuration. Several additions to the DECAB and DECAB Plus process configurations are investigated in Chapter 7. These include the lean vapour compression option, multiple feeds to the absorber and the effect of potassium alanate in the DECAB process configuration. The best process configuration in this analysis, with respect to energy efficiency, is the DECAB Plus process with lean vapour compression based on potassium taurate with a reboiler temperature of 120°C and solid-liquid separation at 40°C, which reduces the specific reboiler duty to 2.07 GJ/t CO<sub>2</sub>.

The developed process configurations also require low grade energy to dissolve the precipitates formed during absorption. The estimated reductions in reboiler duty are accompanied by an increase in the energy required by the separator to dissolve the precipitates having a moderate impact to the overall energy penalty. Under the assumptions considered for the retrofit of these processes into power plants, all the DECAB Plus configurations analysed reduce the overall energy consumption of the capture process with respect to the MEA baseline. The integration of the optimal process configuration in this study (DECAB Plus with lean vapour compression) into the ASC PC power plant reduces the total parasitic load by 15% compared to conventional MEA, resulting in 2 percentage points higher plant efficiency. This reduction in energy penalty encourages further investment in the research of this process alternative.

For future development of this process, it would be beneficial to direct the research efforts towards the scale up of a suitable contactor for the absorption unit. For this purpose the mass transfer characteristics of the precipitating amino acid solvents need to be further investigated (Chapter 8). In addition, the implementation of efficient solid-liquid separation is crucial for the performance of the process. After investigating these aspects it can be expected that the process concepts presented in this thesis will be demonstrated at pilot scale.



---

# SAMENVATTING

De impact van CO<sub>2</sub> emissies op het milieu en de bijhorende bijdrage tot het broeikaseffect is een wereldwijd probleem. Alhoewel er onzekerheden zijn over de kwantitatieve relatie tussen de atmosferische CO<sub>2</sub> concentratie en het broeikaseffect, valt te verwachten dat de CO<sub>2</sub> emissies in de toekomst uit voorzorg streng gereguleerd zullen worden. Dit zal leiden tot aanzienlijke veranderingen in de energie sector (een grote uitstoter van CO<sub>2</sub>), die zullen leiden tot een drastische afname in het gebruik van fossiele brandstoffen met als doel de emissie doelen te halen. Een van de mogelijkheden om CO<sub>2</sub> emissies te verminderen is het afvangen van CO<sub>2</sub> uit uitlaatgassen van energiecentrales om het daarna voor lange tijd op te slaan in geschikte diepe reservoirs of zoutformaties. Deze mogelijkheid, bekend als “post-combustion capture” (PCC), is één van de technologieën die geschaard kan worden onder de verzamelnaam “CO<sub>2</sub> capture and storage” (CCS). Hierdoor blijft het mogelijk om fossiele brandstoffen te gebruiken om elektriciteit op te wekken gedurende een periode waarin de sector zich omvormt naar een vorm van elektriciteit die minder afhankelijk van koolstof is.

De “readiness” van de technologie en de “know-how” van PCC zijn in principe voldoende ontwikkeld voor implementatie. Er zijn echter zaken die de energie sector ervan weerhouden een stap voorwaarts te zetten. Specifiek onderzoek toont aan dat energiecentrales met geïntegreerde PCC een lagere netto efficiëntie hebben dan conventionele energiecentrales. Dit komt door de energiebehoefte voor het verwijderen van CO<sub>2</sub> en de compressie naar condities voor opslag (Hoofdstuk 1). De lagere efficiëntie, die afhangt van de technologie voor CO<sub>2</sub> afvang en het type energiecentrale, leidt tot een groter brandstofgebruik en heeft een direct effect op de elektriciteitskosten en de emissies van de centrale. Dit proefschrift is gericht op het verkleinen van dit probleem door het introduceren en onderzoeken van nieuwe procesontwerpen voor CO<sub>2</sub> afvang.

De huidige state-of-the-art in PCC is een chemische absorptieproces dat gebruik maakt van een waterige oplossing van monoethanolamine (MEA). De karakteristieken van dit proces en de integratie ervan in twee type energiecentrales, de zogenaamde “advanced supercritical pulverized coal” (ASC PC) en “natural gas combined cycle” (NGCC) worden geanalyseerd in Hoofdstukken 2 tot en met 5 van dit proefschrift. Het gebruik van deze technologie in energiecentrales vermindert de netto thermische efficiëntie van 45% LHV naar 34% LHV in het geval van de ASC PC energiecentrale, en van 58% LHV naar 50% LHV in het geval van de NGCC energiecentrale (Hoofdstuk 3). Deze reductie in efficiëntie, die vooral gerelateerd is aan de benodigde energie voor het regenereren van het oplosmiddel, heeft grote consequenties voor de elektriciteitskosten, die toenemen van 46 €/MWh naar 87 €/MWh voor de ASC PC energiecentrale, en van 55 €/MWh naar 71 €/MWh voor de NGCC energiecentrale (Hoofdstuk 4). De emissies van andere schadelijke stoffen worden ook beïnvloed. De emissie van NO<sub>x</sub> neemt bijvoorbeeld toe met 30% per basiseenheid elektriciteit voor beide type energiecentrales; een gevolg van de verlaagde efficiëntie van de centrales (Hoofdstuk 2). In het geval van de kolencentrale resulteert dit ook in een drastische afname van SO<sub>x</sub> emissies (bijna 100%), als gevolg van het amine proces. Een ander belangrijk effect van het gebruik van amines is de

---

toename in ammonia emissies. Dit komt door de degradatie van amines en het verdampen van amines en aminedragers in de vorm van aerosolen (Hoofdstuk 2).

Eén lijn van onderzoek om de prestaties van CO<sub>2</sub> afvang te verbeteren is het ontwikkelen van betere oplosmiddelen. Een ternaire amine, of sterisch gehinderde amine, wordt normaal gesproken gemengd met een primaire of secundaire amine. Het doel van het gebruik van deze mengsels is het reduceren van de energie voor regeneratie, waarbij de reactiviteit van het oplosmiddel behouden blijft (Hoofdstuk 1). CESAR-1 is een voorbeeld van een amine mengsel, bestaande uit AMP (een sterisch gehinderd amine) en piperazine (een secundaire amine). Dit oplosmiddel is ook geëvalueerd in Hoofdstukken 3 en 4, door gebruik te maken van dezelfde aannames en methodes als voor het conventionele MEA oplosmiddel. In dit geval zijn de uiteindelijke netto efficiëntie van de kool- en aardgascentrales respectievelijk 36% LHV en 51% LHV. Ondanks de verbeterde netto efficiëntie zijn andere zaken gerelateerd tot “solvent management” en impact op het milieu tot ontdekking gekomen tijdens de evaluatie. De toxiciteit van piperazine en AMP is hoger dan die van MEA en de vluchtigheid van AMP is substantieel hoger dan die van MEA (Hoofdstuk 3). Dit heeft consequenties voor de kosten voor aanvulling van het oplosmiddel en voor de emissies van deze stoffen in de atmosfeer, welke naar verwachting streng gereguleerd zullen worden (Hoofdstuk 3). De ontwikkeling van procesontwerp en –configuraties die bijdragen aan een vermindering van de energiebehoefte voor de regeneratie van het oplosmiddel is een alternatieve onderzoekslijn om de prestaties van CO<sub>2</sub> afvang te verbeteren. Een voorbeeld van zo’n procesconfiguratie is de zogenaamde “lean vapour compression” (LVC), die bestaat uit het flashen van de hete stroom met lage concentratie CO<sub>2</sub> die de stripperkolom verlaat, het opnieuw comprimeren van de gegenereerde stoom en het terugvoeren van de stoom naar de stripperkolom. De toepassing van deze configuratie in het state-of-the-art MEA proces zal de benodigde energie voor regeneratie verminderen met 7-9% (Hoofdstuk 5).

Dit werk heeft de toepassing van nieuwe processen voor PCC van CO<sub>2</sub> uit uitlaatgassen onderzocht, die gebaseerd zijn op alternatieve oplosmiddelen en procesconfiguraties van het state-of-the-art proces. Een nieuw concept voor CO<sub>2</sub> afvang gebaseerd op zouten van aminozuren is geïntroduceerd in Hoofdstuk 6 van dit proefschrift. Aminozuren zijn beter biologisch afbreekbaar en minder toxisch dan amines en hebben een te verwaarlozen dampspanning. Hierdoor zal een afvang proces gebaseerd op aminozuren over het algemeen een lagere impact op het milieu hebben dan een proces gebaseerd op amines. Absorptie van CO<sub>2</sub> in waterige oplossingen van aminozuur kan leiden tot vorming van precipitaten, afhankelijk van het specifieke aminozuur en de concentratie van de oplossing. Deze faseovergang kan de evenwichtsreacties van CO<sub>2</sub> absorptie en desorptie veranderen, wat resulteert in een afname van de energieconsumptie in vergelijking tot het conventionele absorptie-desorptie proces. De geïdentificeerde effecten gerelateerd tot de precipitatie van aminozuren zijn; (1) De verhoging van de specifieke CO<sub>2</sub> capaciteit van aminozuur oplossingen; (2) Verzuring van de CO<sub>2</sub> rijke oplossing, wat geen direct effect van precipitatie is maar tot stand komt door het introduceren van een faseovergang na de precipitatie (vloeistof vanuit vast) dat de aminozuur-zuurrestion ratio verandert, leidend tot een verhoogde concentratie van aminozuur in de CO<sub>2</sub> rijke oplossing.

Het eerste effect (verbetering van CO<sub>2</sub> absorptie) treedt op wanneer precipitaten gevormd worden tijdens absorptie ten gevolge van de chemische reactie van CO<sub>2</sub> met het aminozuur. De

---

verwijdering van het vaste reactieproduct uit de vloeistoffase verschuift het reactie-evenwicht naar de kant van het product. Het resultaat is een CO<sub>2</sub> rijke stroom in de vorm van slurry die vooral aminozuur bevat in de vaste fase en carbamaat, bicarbonaat, kalium en overblijvende aminozuren in de vloeistoffase. Absorptie vindt plaats in een geschikte contactor die vaste stoffen kan verwerken. Dit kan een sproeitoren-contactator of een serie van een sproeitoren-contactator met een gepakte kolom zijn. De slurry kan direct geregenereerd worden in de stripper, via een “lean-rich” warmtewisselaar. Dit procesconcept staat bekend als DECAB. Het tweede effect (verzuring van de CO<sub>2</sub> rijke stroom) vereist een verwerking van de slurry in een vast-vloeistof scheider om de vaste stof deels te scheiden van het “supernatant”. Dit vormt een geconcentreerde slurry die verrijkt is in de pure aminozuren. Deze stroom wordt verder bewerkt in de stripper voor desorptie. Door de aminozuurkristallen opnieuw op te lossen wordt de pH van die nieuwe CO<sub>2</sub> rijke oplossing verlaagd voor de desorptie, wat resulteert in hoger partiële drukken van CO<sub>2</sub> bij strippercondities die desorptie faciliteren. De gerecyclede stroom is het “supernatant” exces, verrijkt in het aminozuurrestion, die wordt teruggevoerd aan de absorber zonder door de stripper te gaan. Dit alternatieve proces staat bekend als DECAB Plus.

Hoofdstuk 6 en 7 van dit proefschrift beschrijven nieuwe data en modellering om de twee procesconcepten DECAB en DECAB Plus te evalueren, gebaseerd op het kaliumzout van taurine. De evaluatie gebruikt een op chemisch evenwicht gebaseerd model, dat alle benodigde unit operaties bevat voor het afvangen van CO<sub>2</sub> uit het uitlaatgas van een kolencentrale (13% v/v CO<sub>2</sub>). Het model gebruikt een benaderde thermodynamische representatie van de onderzochte oplosmiddelen die gebaseerd is op empirische correlaties afgeleid uit experimentele data. De resultaten tonen een 35% reductie in de energie nodig voor regeneratie van het oplosmiddel in vergelijking tot conventioneel MEA. De specifieke reboiler energie is gereduceerd van 3.7 GJ/t CO<sub>2</sub> (voor de MEA standaard) naar 2.4 GJ/t CO<sub>2</sub> (voor het DECAB Plus proces). Deze waarde kan verder verlaagd worden door verdere optimalisatie van de procesconfiguratie. Enkele toevoegingen aan de DECAB en DECAB Plus procesconfiguraties zijn onderzocht in Hoofdstuk 7, waaronder de LVC optie, meerdere feeds naar de absorber, en het effect van kaliumaanaat in de DECAB procesconfiguratie. De beste procesconfiguratie in deze analyse, wat betreft energie-efficiëntie, is het DECAB Plus proces met LVC gebaseerd op kaliumtauraat, met een reboiler temperatuur van 120 °C en een vast-vloeistof scheiding bij 40 °C. Hierdoor wordt de specifieke reboiler duty vermindert tot 2.07 GJ/t CO<sub>2</sub>.

De ontwikkelde procesconfiguraties hebben energie van lage kwaliteit nodig om de precipitaten die ontstaan tijdens absorptie op te lossen. De geschatte reductie in reboiler duty wordt vergezeld met een verhoging in de energiebehoefte voor de scheider om de precipitaten op te lossen, wat een gemiddelde impact heeft op de totale energie penalty. Gebruik makend van de aannames voor de retrofit van deze processen in bestaande energiecentrales, reduceren alle geanalyseerde DECAB Plus configuraties de energiebehoefte van het afvang proces ten opzichte van de MEA standaard. De integratie van de optimale proces configuratie in deze studie (DECAB Plus met LVC) in de ASC PC energiecentrales reduceren de totale “parasitic load” met 15% vergeleken met conventioneel MEA, resulterende in een 2% hogere efficiëntie van de centrale. Deze reductie in energie penalty moedigt verdere investering in het onderzoek naar dit alternatieve proces aan.

Voor de verdere ontwikkeling van dit proces zou het raadzaam zijn om het onderzoek te richten op de opschaling van een gepaste contactor voor de absorptie unit. Om dit te bewerkstelligen dient het massatransport van de precipiterende aminozuren verder onderzocht te worden

---

(Hoofdstuk 8). Daarnaast is de implementatie van een efficiënte vast-vloeistof scheidingsmethode cruciaal voor de toepassing van dit proces. Na onderzoek van deze aspecten kan verwacht worden dat de procesconcepten gepresenteerd in dit proefschrift gedemonstreerd kunnen worden op pilot schaal.

---

# ACKNOWLEDGEMENTS

This thesis has been realised with the contribution and input of many people who have supported me and guided me through all these years of work. I would like to show my appreciation to them.

I am very thankful to my promoter professor Thijs Vlugt. His guidance and support through all the phases of this project have been vital in finalising this work. I have learnt from him almost everything I know about research and scientific publications. His corrections, comments and guidelines have been crucial to publish this work. Moreover, he is one of the fastest readers I have ever encountered in my life and I have to admit I am very impressed at the speed, accuracy and background of his corrections.

I am very thankful to the promotion committee members for reviewing this work.

The work covered in this thesis has been done at TNO (The Netherlands Organisation for Applied Scientific Research) under the co-supervision of Dr. Earl Goetheer. I would like to express my gratitude to Dr. Goetheer for many years of learning and collaboration. I also need to extend this gratitude to everyone at TNO that helped to organise and finance this thesis: Sven van der Gijp, Erwin Gilling and Marco Linders.

Also the members of the DECAB team at TNO, Kasia Heffernan and Leen van der Ham, have had a very important involvement in this thesis. Thanks to our discussions we have been able to develop the ideas investigated in this work.

Kasia Heffernan and Cristina Sanchez Sanchez thank you for being my “paranimfen” and supporting me in my defence.

Finally, I would like to give special thanks to my parents and to my husband, Derry, for encouraging me to finish this PhD.

Thank you very much,



Eva Sanchez

October 2013

---

## CURRICULUM VITAE

Eva Sanchez Fernandez was born in Madrid, Spain, on the 17<sup>th</sup> of August 1978. She obtained her MSc. in Chemical Engineering from Madrid Complutense University in 2004. She graduated with a project on pH control based on Artificial Neural Networks. In the Netherlands, she joined the Professional Doctorate in engineering program in the University of Delft, where she obtained her P. D. Eng. diploma in 2007 with a project contracted by Unilever R&D that studied the feasibility of the extraction of a natural taste enhancer. The same year, she started her job as an innovator and later as a research scientist within TNO Separation Technology, that later became TNO Gas Treatment. She has contributed in her work in multiple projects related to gas treatment, specially the purification of flue gas and syngas. Within this area, she has been involved in developing and evaluating CO<sub>2</sub> capture processes. This work has been done in different European projects, CESAR and Decarbit, and national projects, CATO-2, which have resulted in this PhD thesis. As a result from her work at TNO, She is co-inventor of several patents, two of which protect the new processes presented in this thesis. In 2012, she established herself as a research contractor in Dubai (UAE) working in an assignment for TNO on the precipitating amino acid processes. Currently she works as a Researcher at the University of Edinburgh in Scotland working of flexible design of carbon capture processes.

---

## Publications

- E. Sanchez Fernandez, E. J. Bergsma, F. de Miguel Mercader, E. L.V. Goetheer and T. J.H. Vlugt. "Optimisation of lean vapour compression (LVC) as an option for post-combustion CO<sub>2</sub> capture: Net present value maximisation". *International Journal of Greenhouse Gas control* 11S, S114-S121. 2012.
- E. Sanchez Fernandez, K. Heffernan, L. V. van der Ham, M. J.G. Linders, E. Eggink, F. N.H. Schrama, D.W.F. Brillman, E. L.V. Goetheer and T. J.H.Vlugt. "Conceptual design of a novel CO<sub>2</sub> capture process based on precipitating amino acid solvents". *Industrial & Engineering Chemistry Research* 2013, 52, 12223-12235.
- E. Sanchez Fernandez, K. Heffernan, L. van der Ham, M.J.G. Linders, D.W.F. Brillman, E. L.V. Goetheer, T. J.H.Vlugt. "Analysis of process configurations for CO<sub>2</sub> capture based on precipitating amino acid salts". Submitted to the *Industrial & Engineering Chemical Research Journal*.
- E. Sanchez Fernandez, E.L.V. Goetheer, M. Juzvicka, T. van Harmelen, A. van Horsen, M. Oldenburg and M. R. M. Abu-Zahra. "Emissions of Substances other than CO<sub>2</sub> from Power Plants with CCS". IEAGHG report NO. 2012/03. Available at [http://ieaghg.org/docs/General\\_Docs/Reports/](http://ieaghg.org/docs/General_Docs/Reports/)
- E. Sanchez Fernandez, E.L.V. Goetheer, G. Manzolini, E. Macchi, S. Rezvani and T.J.H. Vlugt. "Thermodynamic evaluation of amine based CO<sub>2</sub> capture technologies in power plants based on European Benchmarking Task Force methodology". Submitted to the *Chemical Engineering Journal*.
- G. Manzolini, E. Sanchez Fernandez, S.Rezvani, E. Macchi, E. L.V. Goetheer and T. J.H. Vlugt. "Economic evaluation of novel amine based CO<sub>2</sub> capture technologies in power plants based on European Benchmarking Task Force methodology". Submitted to *Applied Energy*.
- F. de Miguel Mercader, G. Magneschi, Eva Sanchez Fernandez, G. J. Stienstra and E. L.V. Goetheer. "Integration between a demo size post-combustion CO<sub>2</sub> capture and full size power plant. An integral approach on energy penalty for different process options". *International Journal of Greenhouse Gas Control*, 11S, S102-S113. 2012
- E. Sanchez Fernandez, P. Geerdink and E. L.V. Goetheer. "Thermo Pervap: The next step in energy efficient pervaporation". *Desalination* 250 (3) 1053-1055, 2010.

## Patents

- E. L. V. Goetheer and E. Sanchez Fernandez. "Method for depleting a flue gas of a gaseous acid compound." World Patent WO2012144898 (A1). 2012
- E. L. V. Goetheer, E. Sanchez Fernandez and C. P. M. Roelands. "Method for absorption of acid gases using amino acids". World Patent WO2011046441 (A1). 2009
- E. E. B. Meuleman, P. Geerdink, E. L. V. Goetheer and E. Sanchez Fernandez. "Process for separating liquid mixtures. European Patent" EP2156880 (A1). 2008

---

### **Presentations at conferences**

New process concepts for CO<sub>2</sub> capture based on precipitating amino acids. International Conference on Greenhouse Gas Technologies 2012. November 2012, Kyoto, Japan. [www.ghgt.info](http://www.ghgt.info)

FT-IR: suitable process analytical technique for Post Combustion Capture. 1st Post-Combustion capture conference. Abu Dhabi. UAE. 2010. <http://www.ieaghg.org>

Evaluation of emissions of substances other than CO<sub>2</sub> from Power Plants with Post Combustion Capture. 1st Post-Combustion capture conference. Abu Dhabi. UAE. 2010. <http://www.ieaghg.org>

DECAB: Process Development of a Phase Change Absorption Process. International Conference on Greenhouse Gas Technologies. September 2010, Amsterdam, The Netherlands. [www.ghgt.info](http://www.ghgt.info).

Advances in Membrane Slurry Reactors for Heterogeneous Catalytic Reactions. 8th World Congress of Chemical Engineering. August 2009, Montreal, Canada. [www.wcce8.org](http://www.wcce8.org)

MEMFRAC – A New Approach to Membrane Distillation. International Conference on Membranes and Membrane Processes. July 2008, Honolulu, Hawaii, USA. [www.icom2008.org](http://www.icom2008.org)